



AFRL-RZ-WP-TR-2011-2030

**EVALUATION OF TRIETHYLENE GLYCOL
MONOMETHYL ETHER (TRIEGME) AS AN
ALTERNATIVE FUEL SYSTEM ICING INHIBITOR FOR
JP-8 FUEL**

S. Zabarnick, M.J. DeWitt, R. Adams, Z.J. West, L.M. Shafer, T.F. Williams,
R. Cook, R. Striebich, and L.M. Balster

University of Dayton Research Institute

C.L. Delaney

Encore Support Systems

D.K. Phelps

**Fuels and Energy Branch
Energy/Power/Thermal Division**

**AUGUST 2010
Interim Report**

Approved for public release; distribution unlimited.

See additional restrictions described on inside pages

STINFO COPY

**AIR FORCE RESEARCH LABORATORY
PROPELLION DIRECTORATE
WRIGHT-PATTERSON AIR FORCE BASE, OH 45433-7251
AIR FORCE MATERIEL COMMAND
UNITED STATES AIR FORCE**

NOTICE AND SIGNATURE PAGE

Using Government drawings, specifications, or other data included in this document for any purpose other than Government procurement does not in any way obligate the U.S. Government. The fact that the Government formulated or supplied the drawings, specifications, or other data does not license the holder or any other person or corporation; or convey any rights or permission to manufacture, use, or sell any patented invention that may relate to them.

This report was cleared for public release by the USAF 88th Air Base Wing (88 ABW) Public Affairs (AFRL/PA) Office and is available to the general public, including foreign nationals. Copies may be obtained from the Defense Technical Information Center (DTIC) (<http://www.dtic.mil>).

AFRL-RZ-WP-TR-2011-2030 HAS BEEN REVIEWED AND IS APPROVED FOR PUBLICATION IN ACCORDANCE WITH THE ASSIGNED DISTRIBUTION STATEMENT.

/*Signature//

ROBERT W. MORRIS, JR.
Project Manager
Fuels and Energy Branch
Energy/Power/Thermal Division

//Signature//

JOHN T. DATKO, Acting Chief
Fuels and Energy Branch
Energy/Power/Thermal Division
Propulsion Directorate

//Signature//

KIRK L. YERKES
Deputy for Science
Energy/Power/Thermal Division
Propulsion Directorate

This report is published in the interest of scientific and technical information exchange, and its publication does not constitute the Government's approval or disapproval of its ideas or findings.

*Disseminated copies will show “//Signature//” stamped or typed above the signature blocks.

REPORT DOCUMENTATION PAGE

Form Approved
OMB No. 0704-0188

The public reporting burden for this collection of information is estimated to average 1 hour per response, including the time for reviewing instructions, searching existing data sources, gathering and maintaining the data needed, and completing and reviewing the collection of information. Send comments regarding this burden estimate or any other aspect of this collection of information, including suggestions for reducing this burden, to Department of Defense, Washington Headquarters Services, Directorate for Information Operations and Reports (0704-0188), 1215 Jefferson Davis Highway, Suite 1204, Arlington, VA 22202-4302. Respondents should be aware that notwithstanding any other provision of law, no person shall be subject to any penalty for failing to comply with a collection of information if it does not display a currently valid OMB control number. PLEASE DO NOT RETURN YOUR FORM TO THE ABOVE ADDRESS.

1. REPORT DATE (DD-MM-YY)			2. REPORT TYPE		3. DATES COVERED (From - To)	
August 2010			Interim		01 March 2006 – 27 August 2010	
4. TITLE AND SUBTITLE EVALUATION OF TRIETHYLENE GLYCOL MONOMETHYL ETHER (TRIEGME) AS AN ALTERNATIVE FUEL SYSTEM ICING INHIBITOR FOR JP-8 FUEL					5a. CONTRACT NUMBER F33615-03-2-2347	
					5b. GRANT NUMBER	
					5c. PROGRAM ELEMENT NUMBER 62203F	
6. AUTHOR(S) S. Zabarnick, M.J. DeWitt, R. Adams, Z.J. West, L.M. Shafer, T.F. Williams, R. Cook, R. Striebich, and L.M. Balster (University of Dayton Research Institute) C.L. Delaney (Encore Support Systems) D.K. Phelps (AFRL/RZPF)					5d. PROJECT NUMBER 3048	
					5e. TASK NUMBER 04	
					5f. WORK UNIT NUMBER 304804AK	
7. PERFORMING ORGANIZATION NAME(S) AND ADDRESS(ES)					8. PERFORMING ORGANIZATION	
University of Dayton Research Institute 300 College Park Avenue Dayton, OH 45469-0170		Fuels and Energy Branch (AFRL/RZPF) Energy/Power/Thermal Division Air Force Research Laboratory, Propulsion Directorate Wright-Patterson Air Force Base, OH 45433-7251			REPORT NUMBER	
Encore Support Systems 303 Clarence Tinker Drive San Antonio, TX 78226		Air Force Materiel Command, United States Air Force				
9. SPONSORING/MONITORING AGENCY NAME(S) AND ADDRESS(ES)					10. SPONSORING/MONITORING	
Air Force Research Laboratory Propulsion Directorate Wright-Patterson Air Force Base, OH 45433-7251 Air Force Materiel Command United States Air Force					AGENCY ACRONYM(S) AFRL/RZPF	
					11. SPONSORING/MONITORING AGENCY REPORT NUMBER(S) AFRL-RZ-WP-TR-2011-2030	
12. DISTRIBUTION/AVAILABILITY STATEMENT Approved for public release; distribution unlimited.						
13. SUPPLEMENTARY NOTES Report contains color. PA Case Number: 88ABW-2011-0251; Clearance Date: 21 Jan 2011.						
14. ABSTRACT In recent years there has been an increasing incidence of reports of the peeling of topcoat material in the ullage space of integral wing tanks in B-52 aircraft. Recent work indicates that with the JP-8/DiEGME combination, the icing inhibitor additive can concentrate in the tank ullage and condense at high concentrations on the upper tank walls. High concentrations of DiEGME cause swelling and subsequent peeling of the epoxy-based topcoat. In this work, we report on the identification and evaluation of alternative icing inhibitor additives that do not cause topcoat delamination in fuel tank upper surfaces. The selection process identified triethylene glycol monomethyl ether (TriEGME) as the most promising candidate for replacement of DiEGME. TriEGME was shown to exhibit equivalent icing inhibition performance to DiEGME, but also exhibits a much lower tendency to negatively impact BMS 10-39 topcoat on aircraft fuel tank ullage surfaces. Subsequent testing was performed to determine the impact of TriEGME on compatibility with other fuel system materials and its effect on fuel properties.						
15. SUBJECT TERMS jet fuel, DiEGME, TriEGME, icing inhibitor, fuel tank topcoat peeling						
16. SECURITY CLASSIFICATION OF:			17. LIMITATION OF ABSTRACT: SAR	18. NUMBER OF PAGES 336	19a. NAME OF RESPONSIBLE PERSON (Monitor) Robert W. Morris, Jr.	
a. REPORT Unclassified	b. ABSTRACT Unclassified	c. THIS PAGE Unclassified				19b. TELEPHONE NUMBER (Include Area Code) N/A

INTENTIONALLY LEFT BLANK

Table of Contents

<u>Section</u>	<u>Page</u>
List of Figures	iii
List of Tables	iv
Acknowledgements	v
1. Summary	1
2. Introduction	3
2.1 Fuel Specification Properties	5
2.2 Fit-for-Purpose Properties	5
3. Fit-for-Purpose Results for Evaluation of TriEGME	9
3.1 Topcoat Compatibility Evaluations	9
3.2 Materials Compatibility Evaluation	11
3.3 Thermal Stability	11
3.4 Biostat Evaluation	16
3.5 Fuel Tank Gauging	17
3.6 Additive Compatibility	19
3.7 Specific Heat vs. Temperature	19
3.8 Autoignition Temperature	20
3.9 Filter-Coalescer Compatibility	20
3.10 Toxicity Evaluation	21
3.11 Hot Gas Path Evaluation of Compatibility with Turbine Engine Materials	21
3.12 Kinematic Viscosity vs. Temperature	21
3.13 Density	22
3.14 Conductivity	23
3.15 Seal Swell Characteristics	24
3.16 Surface Tension	25
3.17 Icing Inhibition Evaluations	26
4. Conclusions	35
5. References	37
Appendix A. Compatibility of TriEGME with Fuel Tank Coatings (AFRL Coatings Technology Integration Office Study)	39
Appendix B. Compatibility of DiEGME and TriEGME Fuel System Icing Inhibitor Additives with BMS 10-39 Aircraft Tank Topcoat Material (AFRL Fuels and Energy Branch Study)	83

Table of Contents (continued)

<u>Section</u>	<u>Page</u>
Appendix C. Fuel Systems Materials Compatibility	123
Appendix D. Biostat Evaluation	161
Appendix E. SwRI Filter-Coalescer Compatibility	213
Appendix F. Toxicity Evaluation.....	245
Appendix G. Hot Gas Path Evaluation of Compatibility with Turbine Engine Materials	259
LIST OF ACRONYMS, ABBREVIATION, AND SYMBOLS.....	325

List of Figures

<u>Figure</u>	<u>Page</u>
1. EDTST Preheater Tube Carbon Deposits for DiEGME and TriEGME at 0.15 vol%	13
2. EDTST Heater Tube Carbon Deposits for DiEGME and TriEGME at 0.15 vol%.....	13
3. EDTST Preheater Carbon Tube Deposits for DiEGME and TriEGME at 0.60 vol%	14
4. EDTST Heater Carbon Tube Deposits for DiEGME and TriEGME at 0.60 vol%.....	15
5. EDTST Preheater Carbon Tube Deposits at JP-8+100 Conditions (DiEGME and TriEGME at 0.15 vol%)	15
6. EDTST Heater Carbon Tube Deposits at JP-8+100 Conditions (DiEGME and TriEGME at 0.15 vol%)	16
7. Plots of Dielectric Constant vs. Temperature with 0.12 vol% TriEGME	18
8. Plots of Velocity of Sound vs. Temperature with 0.12 vol% TriEGME.....	18
9. Specific Heat Measurements vs. Temperature for Fuels containing DiEGME and TriEGME	19
10. Kinematic Viscosity Measurements for DiEGME and TriEGME in Fuel over a Range of Temperatures	22
11. Plots of Density vs. Temperature for a Jet A-1 Fuel with DiEGME and TriEGME.....	23
12. Conductivity Results for Fuels containing DiEGME and TriEGME	24
13. Plots of Volume Swell vs. FSII concentration	25
14. Schematic of the Small-Scale Icing Simulator	28
15. Failure Temperature vs. Additive Concentration for Various FSII Candidates using the SSIS at 288 ppmv of Total Water.....	28
16. Schematic of B-52 Fuel Strainer Housing.....	29
17. Process Flow Diagram of Fuel Conditioning and Test System for Component Level Testing at Parker Aerospace.....	30

List of Tables

<u>Table</u>	<u>Page</u>
1. Comparison of Physical and Chemical Properties of DiEGME and TriEGME	4
2. Comparison of the Impact of DiEGME or TriEGME on JP-8 Specification Properties on a Baseline Jet A-1 Fuel.....	6
3. Fit-for-Purpose Properties of FSII/Fuel Mixtures Evaluated by Similarity	7
4. EDTST Results.....	14
5. Autoignition Temperature Results for a Jet A Fuel with DiEGME and TriEGME	20
6. Surface Tension Measurements.....	26
7. TriEGME Results from B-52 Fuel Strainer FSII Testing at Parker Aerospace	33

Acknowledgements

This material is based on research sponsored by Air Force Research Laboratory under agreement numbers F33615-03-2-2347 and FA8650-10-2-2934. The U.S. Government is authorized to reproduce and distribute reprints for Governmental purposes notwithstanding any copyright notation thereon. The views and conclusions contained herein are those of the authors and should not be interpreted as necessarily representing the official policies or endorsements, either expressed or implied, of Air Force Research Laboratory or the U.S. Government.

The authors would like to acknowledge funding support from the DoD Reduction of Total Ownership Cost program through Ed Wells of ASC/ENFA. Help is gratefully acknowledged for experimental measurements by the Air Force Petroleum Agency, the Air Force Research Laboratory Coatings Technology Integration Office, AFRL Materials Directorate, and Goodrich, Parker Aerospace, Southwest Research Institute, and Pratt & Whitney. The following individuals contributed substantially to the success of this program: Rex Cash of the 540 ACSS/GFLBB, Travis Whitmer of Boeing IDS, Tedd Biddle of Pratt & Whitney, Doug Hufnagle and Dave Barrington of UDRI, Al Fletcher, Larry Butkus and Joe Leone of the AFRL Materials Directorate, John Passmore-Strong of Parker Aerospace, Ryan Osysko of UDRI, Ed Wells and Jolene Bouton formerly of ASC/ENFA, and Gary Bessee of SwRI.

Thanks are also due to the following individuals: Bill Stevenson of Wichita State University, Margaret Adamson of Pratt & Whitney, Steven Shaeffer and Mel Regoli of AFPET, Philip Chang of NAVAIR, and Cliff Cunningham of 95 MSG.

INTENTIONALLY LEFT BLANK

1. SUMMARY

In recent years there has been an increasing incidence of reports of the peeling of topcoat material (Boeing Material Specification 10-39, aka BMS 10-39) in the ullage space of integral wing tanks in B-52 aircraft. This increase in delamination phenomena coincides with the change from JP-4 to JP-8 as the primary U.S. Air Force fuel and also the change in primary icing inhibitor additive from ethylene glycol monomethyl ether (EGME) to diethylene glycol monomethyl ether (DiEGME). Recent work indicates that with the JP-8/DiEGME combination, the icing inhibitor additive can concentrate in the tank ullage and condense at these high concentrations on the upper tank walls. These high concentrations of DiEGME cause swelling and subsequent peeling of the epoxy-based topcoat. In this work, we report on the identification and evaluation of alternative icing inhibitor additives that do not cause topcoat delamination in fuel tank upper surfaces.

Initially, prospective additives need to be evaluated for their ability to inhibit the formation of ice in aircraft fuel systems. Additives which perform well as icing inhibitors then need to be evaluated for their compatibility with fuel tank topcoat material. The initial group of additive candidates evaluated consisted of glycol ether species with decreased volatility. These low volatility species should be less able to concentrate in the ullage and cause topcoat failure. The selection process identified triethylene glycol monomethyl ether (TriEGME) as the most promising candidate for replacement of DiEGME. TriEGME was shown to exhibit equivalent icing inhibition performance to DiEGME, but also exhibits a much lower tendency to negatively impact BMS 10-39 topcoat on aircraft fuel tank ullage surfaces at typical use concentrations (≤ 0.15 vol%). Subsequent testing was performed to determine the impact of TriEGME on compatibility with other fuel system materials, evaluation of the effect on fuel properties such as thermal stability, impact on fuel filtration, impact on functionality of other additives, and testing of the biostat capabilities of the additive. Where practical this testing was performed at both 1x and 4x concentrations of the additives. In all cases TriEGME was found to compare favorably with DiEGME in these properties.

INTENTIONALLY LEFT BLANK

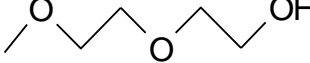
2. INTRODUCTION

Diethylene glycol monomethyl ether (DiEGME) is a required additive in the JP-8 and JP-5 fuel specifications, where it is used to inhibit free water from freezing. The DiEGME concentration in the fuel at procurement is required to be in the range 0.10 to 0.15 vol%. Fuel system icing inhibitors (FSII) were originally added to military fuels in the early 1960's as a result of several malfunctions and accidents attributed to fuel system plugging caused by icing. The current FSII additive, and the previously used ethylene glycol monomethyl ether (EGME) additive, performed successfully in inhibiting ice formation over many decades without significant problems. But in recent years, DiEGME has been implicated in causing a number of problems in aircraft fuel systems, particularly the peeling of integral fuel tank topcoats (BMS 10-39) in certain bomber and tanker systems. This peeling, which occurs primarily in the fuel tank ullage surfaces, has been attributed to DiEGME which can concentrate in the vapor of kerosene fuels and condense at relatively high concentrations onto the topcoat surfaces (Aliband et al., 2006). Topcoat peeling is a serious issue as the resulting paint chips and flakes can plug fuel system filters and screens and the exposed metal surfaces are left unprotected from corrosion. The peeling which has occurred to date has resulted in significant increases in scheduled and unscheduled maintenance costs and decreased aircraft mission capabilities.

The U.S. Air Force, with funds provided by the Reduction in Total Ownership Cost (RTOC) program of the Department of Defense, has undertaken the task of finding a replacement FSII which does not cause fuel tank topcoat peeling. This program consisted of four phases: additive development, safety of flight certification, specification development, and field implementation/logistics. The initial additive development process which consisted of studies on additive selection/screening, icing inhibition evaluation, topcoat compatibility, and fit-for-purpose testing is being reported separately (Zabarnick et al., 2007; Zabarnick et al., 2009). The additive selection process and subsequent testing identified Triethylene Glycol Monomethyl Ether (TriEGME) as the candidate icing inhibitor additive which exhibited the desired properties for replacing DiEGME. These properties included equivalent icing inhibition performance to DiEGME and a lower vapor pressure which greatly decreases the likelihood fuel tank topcoat peeling on the ullage surfaces of integral wing tanks of military aircraft. The current report is a compilation of all of the specification and fit-for-purpose properties evaluations performed for the approval of the additive for use in JP-8 fuel. This approval process closely follows the new ASTM D4054 "Standard Practice for Qualification and Approval of New Aviation Turbine Fuels and Fuel Additive," which was developed by gas turbine engine Original Equipment Manufacturers (OEMs) and ASTM International members to provide a framework for the qualification and approval of new fuels and additives for use in commercial and military aviation gas turbine engines. Following the D4054 standard practice guidelines, the additive was evaluated in jet fuel for its effect on both specification (MIL-DTL-83133) and fit-for-purpose properties. In these evaluations, the effect of TriEGME on fuel properties was evaluated in comparison with DiEGME, as many years of operation in numerous military aircraft platforms has provided confidence in the ability of DiEGME to perform well in inhibiting icing, as well as in not negatively impacting jet fuel performance and properties (except for topcoat compatibility which was evaluated both in comparison with DiEGME and for its ability to not degrade topcoat under realistic conditions).

Fuel specifications do not define all properties and characteristics that are required for proper operation of aircraft fuel systems, engines, storage and delivery systems, and ground handling systems. ASTM Standard Practice D4054 defines both a framework for qualification and approval of new fuels and additives, and also a list of other properties and characteristics (fit-for-purpose properties) that fuels and additives may be required to display to be considered acceptable for use in these systems. These fit-for-purpose properties are divided into the following categories: chemistry, bulk physical and performance properties, electrical properties, ground handling properties and safety, and compatibility. The chemical similarity between TriEGME and the currently approved FSII, DiEGME, results in a number of similar properties and characteristics of these additives. The selection of required fit-for-purpose properties reflects these known similarities in chemistry and properties, and thus a number of fit-for-purpose properties have not been evaluated experimentally, but rather, evaluated by comparison of these similar chemistry and properties. A comparison of some physical and chemical properties of DiEGME and TriEGME are shown in Table 1.

Table 1. Comparison of Physical and Chemical Properties of DiEGME and TriEGME

	DiEGME	TriEGME
Chemical Type	Glycol Ether	Glycol Ether
Chemical Structure		
Molecular Weight	120.15	164.20
Boiling Point (°C)	194	249
Vapor Pressure at 20°C (Torr)	0.19	0.008
Density at 25°C (g/mL)	1.023	1.026
Physical State	Liquid	Liquid
Color	Colorless	Colorless
Common Impurities	EGME, TriEGME, TetraEGME	DiEGME, TetraEGME, and PentaEGME

The DiEGME employed in the testing reported here is a Dow Chemical product obtained from Univar USA as “Glycol Ether DM Fuel Additive Grade.” The TriEGME employed in the testing reported here is also a Dow Chemical product obtained from Univar USA as “Methoxytriglycol.”

2.1 Fuel Specification Properties

Evaluation of the specification tests required for JP-8 fuel (MIL-DTL-83133) were performed for a baseline Jet A-1 fuel and the same fuel with 0.15 and 0.60 vol% DiEGME or TriEGME. These concentrations follow the 1x and 4x suggested concentrations in the ASTM D4054 Standard Practice. This testing was performed to determine the effect of TriEGME on the specification properties in comparison with DiEGME. The Jet A-1 fuel was used, rather than a JP-8 fuel, as it did not contain FSII, which would interfere with the measurements. The Jet A-1 fuel was treated with specification levels of corrosion inhibitor and static dissipater additives. In addition, a Jet A-1 fuel sample was selected which exhibited a freeze point meeting the JP-8 specification (i.e., -47°C max). The results of this testing is shown in Table 2. The table shows that both additives have very little effect on the specification properties. The only values outside the specification limits were the FSII vol% measurements. These results are expected as greater than specification levels of FSII were employed in some tests, and the test method, ASTM D5006 which uses the refractive index method, is not calibrated for the refraction index of TriEGME. Due to the difference in refractive index between DiEGME and TriEGME, implementation of TriEGME as a fuel system icing inhibitor will require the modification or development of a standard test method for measurement of its concentration in aviation fuel.

Also shown in Table 2 are some fit-for-purpose properties including Jet Fuel Thermal Oxidation Test (JFTOT®) breakpoint, dissolved water content, and lubricity. The results shown for these properties are all within acceptable levels.

2.2 Fit-for-Purpose Properties

A wide range of fit-for-purpose properties were examined for the effect of TriEGME on the properties of the baseline fuel, fuel system, and aircraft/engine materials. These include materials compatibility, thermal stability, microbiological growth, autoignition temperature, filter-coalescer and filter monitor compatibility, toxicity, turbine hot section erosion and corrosion, viscosity, conductivity, response to SDA, density, seal swell, solubility, surface tension, and lubricity. In addition, some properties unique to icing inhibitors were also examined including icing inhibition and detailed studies of aircraft fuel topcoat material compatibility. A number of fit-for-purpose properties that are listed in ASTM D4054 were not evaluated experimentally. These properties were evaluated based on previous experience with icing inhibitor additives and their effect on fuel properties, along with the chemical and physical characteristic similarities between TriEGME and DiEGME. A list of fit-for-purpose properties that were not evaluated experimentally is shown in Table 3.

Table 2. Comparison of the Impact of DiEGME or TriEGME on JP-8 Specification Properties on a Baseline Jet A-1 Fuel

50% recovered, °C		201	201	201	201	201
90% recovered, °C		227	226	227	226	226
EP, °C	≤300	249	248	248	250	248
Residue, % vol	≤1.5	1.2	1.3	1.3	1.3	1.2
Loss, % vol	≤1.5	1.0	0.7	1.3	0.3	0.6
Flash point, °C	≥38	60	60	60	60	60
Cetane Index (calculated)		50.8	50.6	50.7	50.3	50.5
Freeze Point, °C	≤-47	-53	-53	-53	-53	-53
Viscosity @ -20°C, cSt	≤8.0	4.1	4.2	4.2	4.4	4.2
Viscosity @ -40°C, cSt		8.9	9.0	8.9	8.9	9.1
Heat of Combustion (calculated), BTU/lb	≥18,400	18615	18617	18612	18617	18613
Hydrogen Content, % mass	≥13.4	13.8	13.9	13.8	13.9	13.8
Smoke Point, mm	≥25.0	25.0	25.0	25.0	25.0	25.0
Copper Strip Corrosion	≤1	1a	1a	1a	1a	1a
Thermal Stability @ 260°C:						
Tube Deposit Rating	≤3	<1	1	1	1	1
Change in Pressure, mm Hg	≤25	0	0	0	0	3
Existent Gum, mg/100mL	≤7.0	0.4	0.2	1.6	0	1.4
Particulate Matter, mg/mL	≤1.0	0.3	0.2	0.8	0.1	0
Filtration Time, minutes	≤15	5	4	4	15	14
Water Reaction	≤1b	1b	1	1	1	1
FSII, % vol	0.10 to 0.15	0*	0.14	0.20*	0.68*	0.64*
Conductivity, pS/m	150 to 600	545	447	457	378	359
API Gravity @ 60°F	37.0 to 51.0	46.1	46.1	46.1	45.9	45.9
Density @ 15C	0.775 to 0.840	0.797	0.797	0.797	0.798	0.798
Lubricity (BOCLE), wear scar mm		0.60	0.56	0.56	0.55	0.54
JFTOT® Breakpoint, °C		290	285	295	330	>380
Dissolved Water, ppmV		14	15	24	28	36

Table 3. Fit-for-Purpose Properties of FSII/Fuel Mixtures Evaluated by Similarity

Property	Evaluation
Hydrocarbon type, aromatics, hydrogen, trace materials, organics, inorganics, and trace elements	The TriEGME additive will not affect the bulk fuel components. The chemical synthesis process for production of TriEGME is identical to DiEGME so the identity of trace materials will be similar (e.g., other glycol ethers- see Table 1), and no problems are anticipated from these materials.
Boiling point distribution	The volatility of TriEGME is well known. The fuel specification boiling distribution is sufficient for evaluation
Simulated distillation	The volatility of TriEGME is well known. The fuel specification boiling distribution is sufficient for evaluation.
True Vapor Pressure vs. Temperature	The volatility of TriEGME is well known. The fuel specification boiling distribution is sufficient for evaluation.
Bulk Modulus vs. Temperature & Pressure	Based on similarity of TriEGME to DiEGME.
Thermal Conductivity vs. Temperature	Based on similarity of TriEGME to DiEGME.
Effect on Clay Filtration	Based on similarity of TriEGME to DiEGME.
Storage Stability	Based on similarity of TriEGME to DiEGME.
Flammability Limits	Based on similarity of TriEGME to DiEGME.
Hot Surface Ignition Temperature	Based on similarity of TriEGME to DiEGME.
Compatibility with Other Approved Fuels	Based on similarity of TriEGME to DiEGME.

INTENTIONALLY LEFT BLANK

3. FIT-FOR-PURPOSE RESULTS FOR EVALUATION OF TRIEGME

3.1 Topcoat Compatibility Evaluation

Two studies were performed that assessed the compatibility of TriEGME with fuel tank topcoat material. The first study was performed by the AFRL Coatings Technology Integration Office (CTIO) and evaluated liquid and vapor exposure of TriEGME and DiEGME in fuel and aqueous solutions under extreme temperature and time exposure regimes, with the primary intent of comparing the behavior between the two additives in liquid/surface interactions between the additive and topcoat material.

The second study, performed by the AFRL Fuels and Energy Branch, evaluated the compatibility of DiEGME and TriEGME with BMS 10-39 topcoat material with both liquid and vapor phases under realistic temperature and concentration regimes with the intent of reproducing topcoat degradation in the laboratory and determining conditions which cause compatibility issues.

3.1.1 Compatibility of TriEGME with Fuel Tank Coatings (AFRL Coatings Technology Integration Office Study)

This study primarily evaluated the compatibility of liquid phase exposure of DiEGME and TriEGME with BMS 10-39 and AMS-C-27725A topcoat panels. The details of the study are reported in Appendix A. The relative effects that the additives had on the two different aircraft fuel tank coatings were evaluated in side-by-side laboratory comparisons. The testing indicated that for exposures which simulate liquid fuel or water/fuel interactions with topcoat the two FSII's exhibited very similar behavior in degrading the topcoat materials tested. In contrast, for testing which simulates exposure of vapor condensates the results indicated that TriEGME exhibited significantly less softening of the BMS 10-39 coating due to the lower concentrations expected for this species in the headspace area, which results from its lower vapor pressure. However, the test protocols were not sufficiently robust to replicate the damage currently being experienced in aircraft fuel tanks (due to DiEGME) to draw definitive conclusions.

3.1.2 Compatibility of DiEGME and TriEGME Fuel System Icing Inhibitor Additives with BMS 10-39 Aircraft Tank Topcoat Material (AFRL Fuels and Energy Branch Study)

In this study the compatibility of DiEGME and FSII replacement candidate TriEGME with BMS 10-39 fuel tank topcoat material was evaluated (Zabarnick et al., 2010). The details of the study are reported in Appendix B. Tests were designed to simulate fuel tank wall exposures with subsequent topcoat degradation measured by icing inhibitor uptake analyses and pencil hardness evaluations. The results show that the lower volatility of TriEGME relative to the JP-8 fuel components results in it being less able to concentrate in the tank ullage and promote topcoat failure, as compared to DiEGME. This was confirmed with lower additive levels measured in the ullage, condensed vapors, and the exposed topcoat material. The pencil hardness of topcoat material exposed to fuel vapors was significantly improved upon changing from DiEGME to TriEGME exposure. Simulation experiments were able to reproduce the fuel tank topcoat peeling observed in the field, as well as determine the conditions (concentration and temperature) required for topcoat degradation.

The compatibility of DiEGME and TriEGME with BMS 10-39 topcoat material was studied to provide a better understanding of the fuel tank topcoat peeling mechanisms, to determine the requisite conditions for degradation to occur, and to determine the conditions under which degradation can be prevented. Under liquid exposure conditions, both fuel system icing inhibitor additives were found to partition equally, on a molar basis, into the topcoat over a wide range of concentrations. This was demonstrated for aqueous, fuel, and fuel surrogate solution exposures for both old and new topcoat panels. The absorption of FSII was found to increase dramatically for old panels relative to new panels. The old panels are considered to be representative of topcoat surfaces of real fuel tank walls in the current USAF fleet. The new panels studied are likely more resistant to FSII absorption than what is currently present in B-52 aircraft.

The desorption rate of FSII out of the topcoat differed between DiEGME and TriEGME. Initially, TriEGME showed a slower desorption rate than DiEGME, which can be explained by its lower vapor pressure and greater molecular size. After two hours, the DiEGME and TriEGME concentrations in the panel began to reach similar levels, and eventually reached a final concentration of approximately 0.7 mol FSII/L topcoat after aqueous exposures of 80 vol% FSII or greater. This concentration was similar to that from failed topcoat flakes, which suggests that the FSII component in the topcoat will not completely desorb or evaporate after exposure to high concentrations. In the pencil hardness study, both DiEGME and TriEGME performed identically within experimental error. There was a large difference between the new and old panels, with the old panels falling below the passing hardness lead of "B" when exposed to FSII concentrations as low as 0.40 vol% in the fuel surrogate, while the new panels required concentrations of 1.0 vol% for failure. In pencil hardness measurements of FSII desorption, the hardness of the topcoat was found to increase as desorption occurs. This hardening effect is indicative of relamination of the topcoat after FSII exposure and topcoat softening.

The experimental simulation that was developed to re-create FTTP in a controlled setting was the first laboratory system able to reproduce the entire FTTP process and to determine the requisite conditions for topcoat failure. DiEGME was found to concentrate in the ullage vapor by a factor of two to seven times the initial concentration in the fuel. These high condensate concentrations resulted in severe degradation of the topcoat. The highest concentration in the bulk fuel that did not cause a failure, as rated by the pencil hardness of the coating, was at ~0.07 vol% DiEGME. However, TriEGME proved very effective as it did not lower the pencil hardness of the topcoat panel up to approximately 0.14 vol% TriEGME. The resulting TriEGME condensate concentration did increase on average by a factor of 1.2, although this small increase did not prove detrimental to the BMS 10-39 panel. The lower vapor pressure of TriEGME was determined to be the major reason in its improved topcoat compatibility for fuel tank ullage surfaces. Based upon these results, TriEGME has been shown to be an excellent FSII replacement in terms of BMS 10-39 topcoat material compatibility. During the scenarios analyzed in these studies, TriEGME would not cause degradation to the topcoat at the current concentrations employed for DiEGME in JP-8. If DiEGME continues to be used as the specification FSII additive, it is recommended that the maximum concentration in aircraft tanks be no more than 0.07 vol% to prevent topcoat degradation. This should prevent high concentrations of DiEGME vaporizing and condensing on topcoat surfaces. Adherence to required maintenance practices, such as sumping of fuel tanks, is essential to the prevention of FTTP in water bottoms when either FSII additive is used.

The occurrence of FTTP in the simulated fuel tank box was dependent on the temperatures of the fuel and condensing surfaces. Fuel temperatures of 60°C were able to selectively vaporize levels of DiEGME sufficient to cause swelling and blistering. Lower temperatures were unable to provide condensate concentrations that were sufficient to cause degradation of the coating during the test period. The optimum cooled surface temperature for selective condensation of DiEGME and topcoat degradation is near 20°C. At higher temperatures the surface condensate had reduced DiEGME concentrations, and below 20°C an aqueous phase condensed on the topcoat surface, which decreased the concentration of DiEGME in contact with the polymer.

3.2 Materials Compatibility Evaluation

A comparison of the compatibility of TriEGME with fuel system materials compared with DiEGME was performed by Materials Integrity Branch of AFRL in collaboration with the University of Dayton Research Institute. Both metals and non-metal materials interactions with fuel containing these additives were conducted by aging the materials at elevated temperatures. A representative sample of thirty (30) metallic and thirty-five (35) non-metallic materials were aged in Jet A-1 fuel containing four times (4x) the maximum concentration of the additives by specification. Thus, FSII concentrations of 0.60 vol% mixtures were used in Phase I of testing for both metals and non-metals. Evaluation of all materials after aging was performed and comparison made to the evaluation of materials which were aged in the same base fuel containing the current, approved, FSII additive – diethylene glycol monomethyl ether (DiEGME). Metallic results showed no differences between the two additives except for 7075-T6 Chromate Conversion Coated Class 1A, which was reexamined at the 4x concentration (0.60 vol%) and subsequently passed. Results for non-metallic materials showed that eight (8) non-metallic materials (adhesives, bladder coating and sealant materials) needed to be re-evaluated due to failures for both DiEGME and TriEGME. These re-evaluations were conducted at lower, more realistic additive concentrations of 0.225 vol% FSII (1.5x of the maximum specification concentration). Results at this level showed no significant differences in material degradation between TriEGME and the current approved additive DiEGME. One of these materials, the MIL-27725 coating, showed an unusual discoloration of fuel and materials during testing at 1.5x; this result was repeated and showed greatly reduced discoloration in the retest and no hardness or adhesion issues.

A report of the complete study is attached as Appendix C. The report concludes that:

“Results from both metals and non-metals indicated that in liquid phase exposure studies, the TriEGME additive is no more aggressive towards metallic and nonmetallic materials than the current DiEGME additive. In general, when TriEGME and DiEGME degraded materials, they did so in a similar fashion. Also, the lower vapor pressure characteristics of TriEGME should make this additive less aggressive to materials exposed to fuel vapor than DiEGME.”

3.3 Thermal Stability

A thermal stability evaluation of the use of TriEGME in place of DiEGME as an icing inhibitor for JP-8 fuels was conducted in the Extended Duration Thermal Stability Test (EDTST) system. The purpose of the EDTST is to simulate the fuel flow and heat cycle characteristics of a typical aircraft fuel system and to evaluate fuels and additives under these conditions. Since this test does not operate at conditions that accelerate thermal degradation (high temperature, long

residence times), longer test times are necessary to evaluate fuels and additives. The EDTST subjects the fuels to specified bulk fuel and wetted wall temperatures at residence times related to those occurring in gas turbine fuel systems. A fuel bypass line is incorporated to represent military aircraft designs for thermal management that recirculate fuel from the engine back to the airframe tanks. Also, the fuel is exposed to the specified wetted wall temperatures for very short durations and then is scrapped. This is representative of the fuel exposed to the engine injection nozzles. The EDTST system consists of a 60 gallon feed tank, an electrical motor driven gear pump, two clamshell furnace heaters, and a scrap tank. The first furnace heater (preheater) in the system is used to establish the desired fuel bulk temperature into the second heater and to establish the desired fuel bypass temperature. The fuel bulk temperature represents the temperature that results from aircraft and engine heat loads. The experimental system has been described in detail previously (Morris et al., 2002).

A series of back to back tests were conducted on TriEGME and DiEGME additives in POSF-4877 (Jet A-1) fuel at two concentrations. The first series of tests were conducted at 325°F bulk (with active recirculation) and 425°F wetted wall temperature conditions. A test of POSF-4877 fuel was conducted with no additives for baseline purposes. A test period of 96 hours was used for all tests in this report. The carbon deposits in the pre-heater and heater tubes for tests with 0.15 vol% of the additives are shown in Figures 1 and 2. There was very little difference in deposits between the additives or the baseline fuel in the pre-heater and heater tubes. All witness strips also had no significant deposits. Also shown in Figures 3 and 4 are the results for both additives at a concentration of 0.6 vol%. These results also show no significant differences between the two additives in affecting the thermal stability of the fuel. A summary of the results of these tests are shown in Table 4. The acceptable limits were established previously for JP-8+100 additive evaluations.

Tests of the two additives were also conducted in the presence of JP-8+100 additives. The JP-8+100 additive tests were conducted at the temperatures used previously for evaluating the JP-8+100 additives. These tests were conducted to insure that there were no adverse effects of TriEGME with the JP-8+100 additive package at these higher temperatures. Specifically these tests were conducted at bulk temperature out of the preheater of 375°F and a maximum wetted wall temperature of 500°F in the heater. The carbon deposits in the preheater and heater tubes for these tests are shown in Figures 5 and 6, respectively. There were also very little difference in deposits between the additives in the pre-heater and heater tubes for these tests. The TriEGME additive heater deposit was slightly higher than DiEGME in the JP-8+100 test. This was likely caused by an interaction between the polar JP-8+100 additive molecules and this very high concentration of polar TriEGME. The deposit increase was very small relative to the 1000 $\mu\text{g}/\text{cm}^2$ peak heater deposit maximum for JP-8+100, and the result was still within the JP-8+100 thermal stability requirement. Also, the witness strips showed no significant deposits. Based on the tests, there is no thermal stability impact for substituting TriEGME for DiEGME in JP-8 or JP-8+100 fuels.

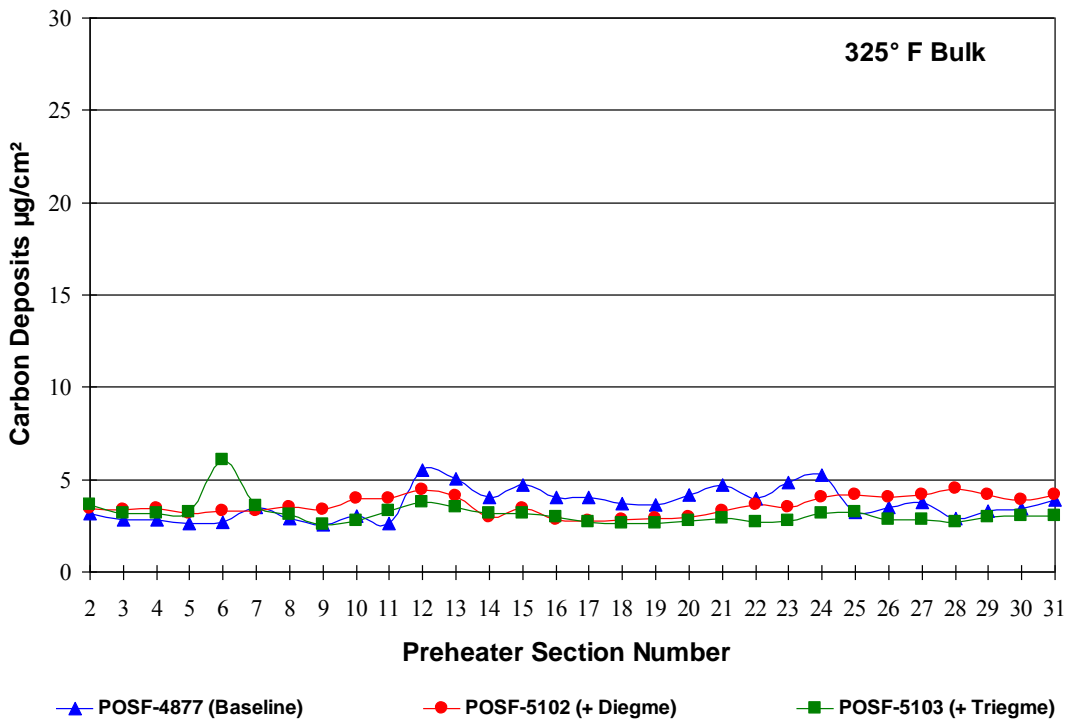


Figure 1. EDTST Preheater Tube Carbon Deposits for DiEGME and TriEGME at 0.15 vol%

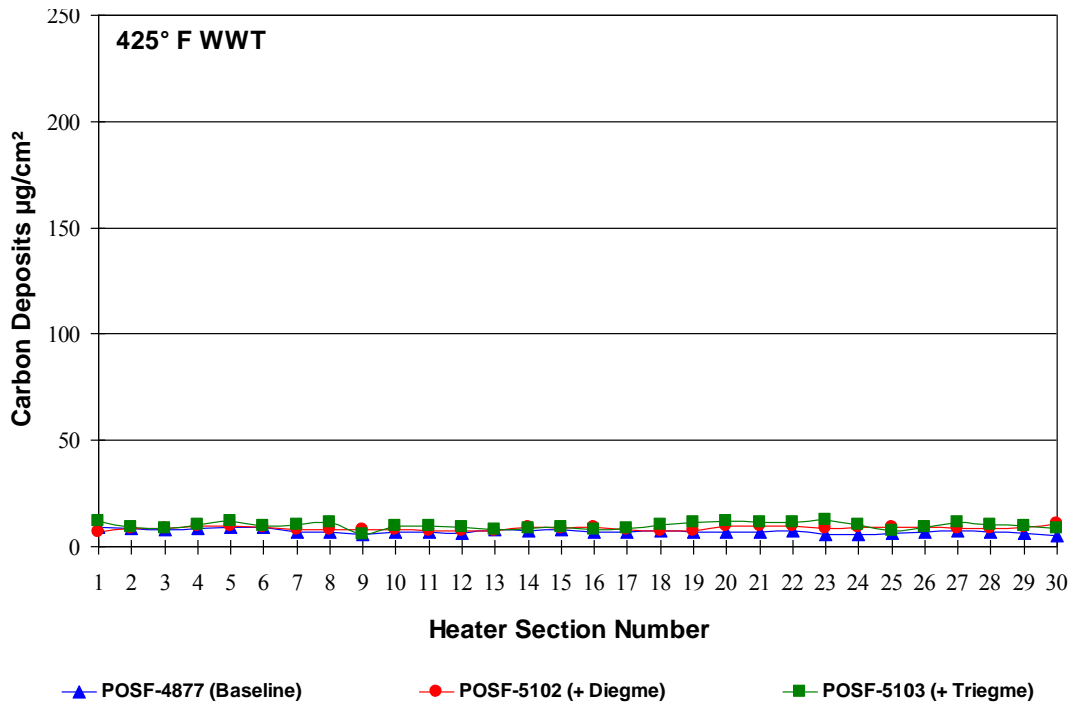
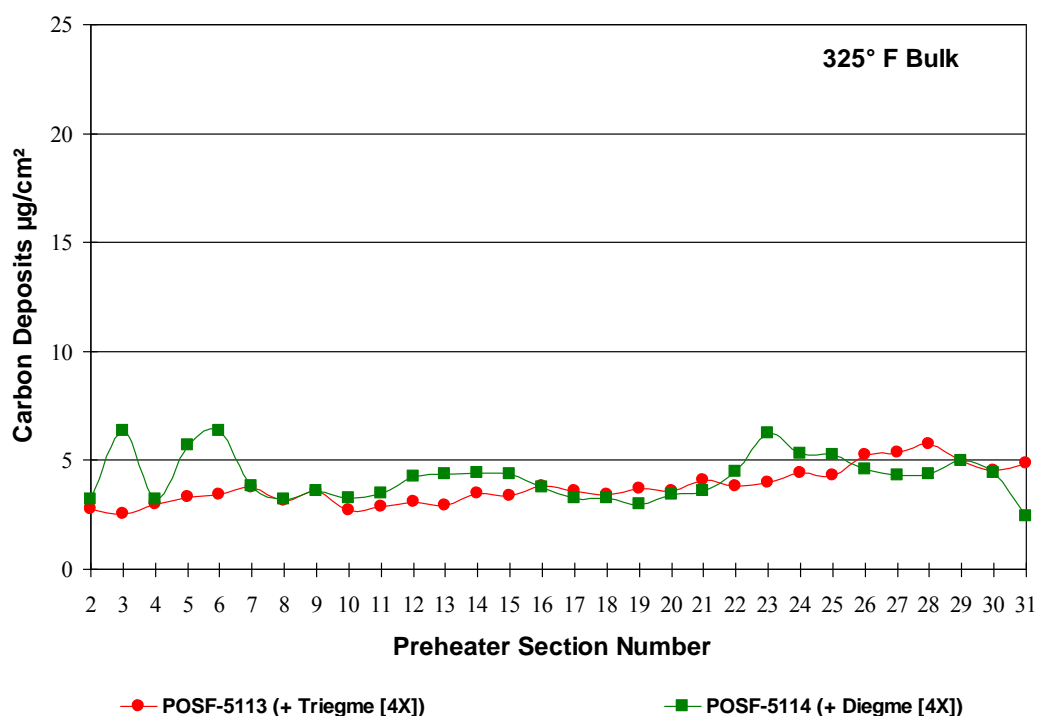


Figure 2. EDTST Heater Tube Carbon Deposits for DiEGME and TriEGME at 0.15 vol%

Table 4. EDTST Results

Additive ID (Fuel ID)	Max Segment Deposit, $\mu\text{g}/\text{cm}^2$			Filter (μg)		Strips (Visual)	
	Heater	Preheater	Heat Exchanger	2 μ	7 μ	Cold	Hot
POSF-4877	8	5	6	140	1340	Slight	slight
DiEGME 0.15 vol%	9	4	10	250	4950	Slight	Slight
TriEGME 0.15 vol%	10	3	19	1070	1310	Slight	slight
DiEGME 0.60 vol%	14	6	14	1320	1020	Slight	slight
TriEGME 0.60 vol%	17	6	15	3320	1073	Slight	slight
JP-8+100 DiEGME 0.15 vol%	13	6	13	260	677	Slight	slight
JP-8+100 TriEGME 0.15 vol%	74	3	10	221	509	Slight	slight
Acceptable Limits	250	8	Report	Report	Report	Clean to Slight	Report

**Figure 3. EDTST Preheater Carbon Tube Deposits for DiEGME and TriEGME at 0.60 vol%**

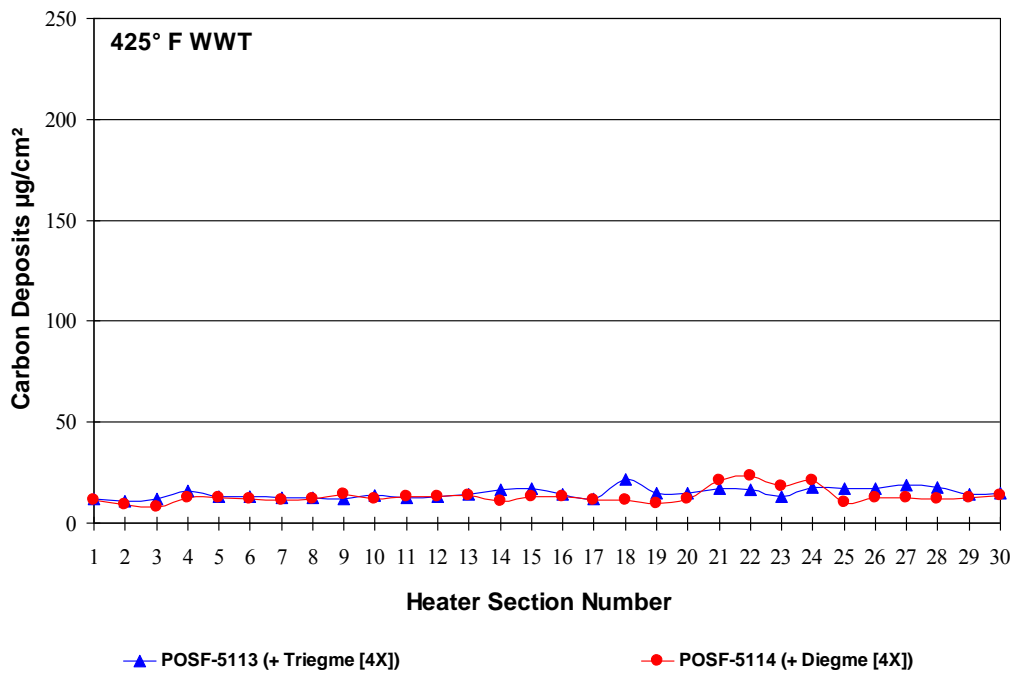


Figure 4. EDTST Heater Carbon Tube Deposits for DiEGME and TriEGME at 0.60 vol%

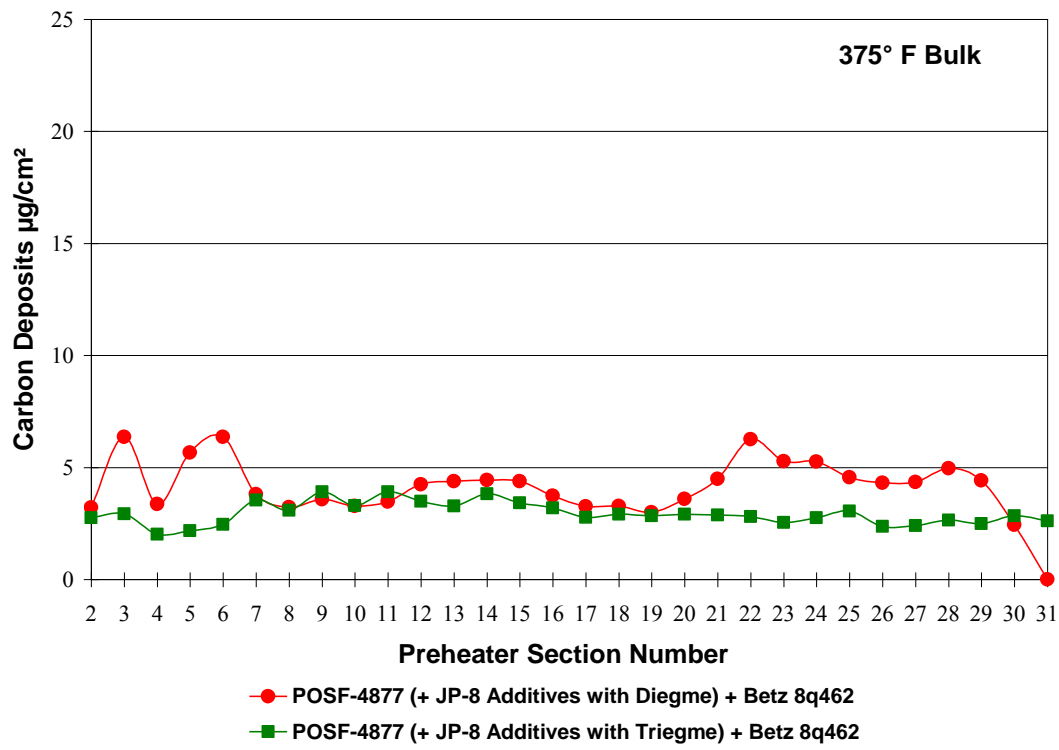


Figure 5. EDTST Preheater Carbon Tube Deposits at JP-8+100 Conditions (DiEGME and TriEGME at 0.15 vol%)

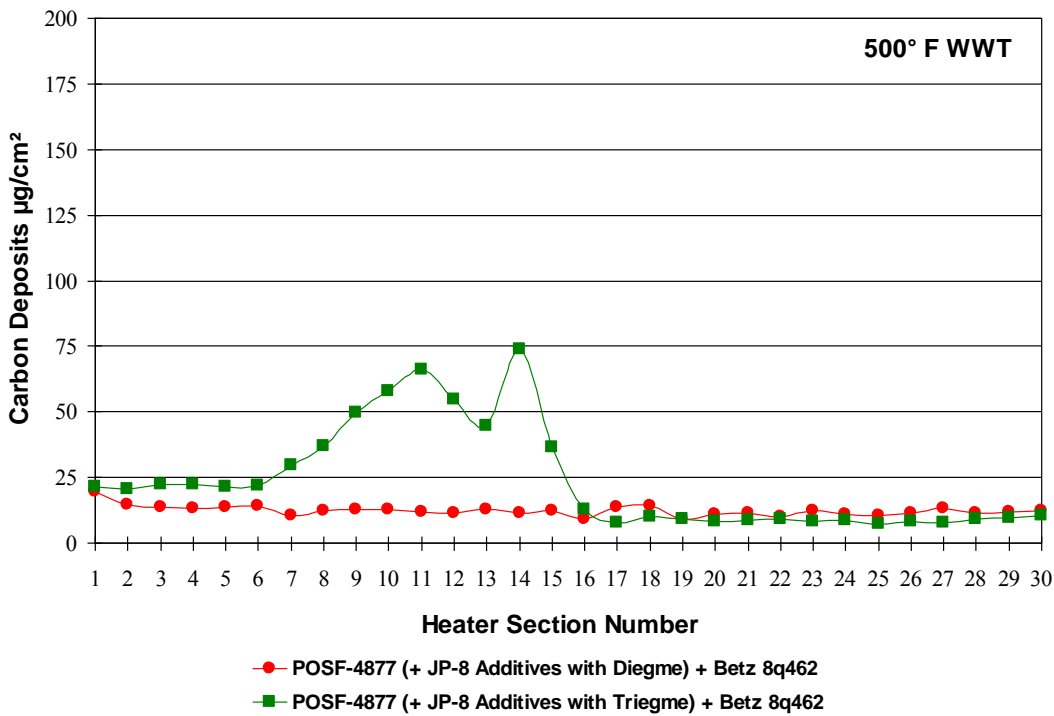


Figure 6. EDTST Heater Carbon Tube Deposits at JP-8+100 Conditions (DiEGME and TriEGME at 0.15 vol%)

3.4 Biostat Evaluation

Fuel system icing inhibitors are primarily added to jet fuel to suppress ice formation, but these additives have also been found to suppress growth of microbial contaminants in fuel storage tanks and aircraft. Over the years military jet fuels have come to depend upon this inhibition to prevent the detrimental effects of microbial growth including biofilm fouling and corrosion. As DiEGME is effective in limiting biological growth in fuel system, a replacement candidate such as TriEGME also needs to exhibit an equivalent ability to prevent excess biological growth. A study was performed to determine the ability of TriEGME to suppress biological growth in fuel tanks and systems and is detailed in Appendix D. The study compares the effectiveness of TriEGME and DiEGME in suppressing growth of lab and field cultured microorganisms, including various samples of fungi, bacteria, and yeast. The study was performed on samples containing fuel and water which were inoculated with the microorganisms and incubated at 28°C for 46 days. During this period, the mixtures were sampled and concentrations of colony forming units were determined by standard agar plate culture and colony counting techniques. The study concludes the following:

“The current study provides valuable information regarding potential effects of adding DiEGME or TriEGME to fuel systems, and it also provides a better understanding of the current role of DiEGME and TriEGME with respect to microbial contamination. This study of the biocidal/biostatic effects of TriEGME at reduced levels, similar to the levels targeted for the reduced FSII (DiEGME) program, was conducted in support of an RTOC program aimed at replacing DiEGME with TriEGME. TriEGME has preferential vapor properties that would

prevent topcoat peeling problems in the B-52 and also has a partition coefficient which would make possible similar additive dosage rates compared to DiEGME. This study explored the biological impact of replacing DiEGME with TriEGME at the reduced levels expected to be implemented for DiEGME, i.e. from ~30-60% by volume in the aqueous phase to 0-30%. In this study, where field microorganisms were included, in addition to lab cultured ATCC microbes, it was found that TriEGME levels of 15% by volume in the water phase or greater were sufficient to eliminate microbial growth of all three lab cultured, ATCC microorganisms tested and were sufficient to significantly limit the growth of the field microorganisms. The results of this study suggest that DiEGME levels of 10% and above and TriEGME levels of 15% and above in the aqueous phase (~0.01-0.02% in the fuel phase) are beneficial for controlling microbial growth in aircraft fuel systems. Additional tests at higher DiEGME levels suggest that even 30%-60% DiEGME in the aqueous phase did not completely eliminate field consortia growth. The field *Bacillus* and *Clostridium* strains tested were shown to be viable, even at these high concentrations. However, TriEGME levels of 40% and above were sufficient to eliminate all field microbes tested here, but only after 30-40 days of exposure. Examination of post-test liquid setups suggests that the presence of DiEGME or TriEGME can dramatically curtail active microbial growth and/or biofilm formation in fuel/water liquid samples. Overall, it appears that DiEGME or TriEGME would still act beneficially, even at reduced levels, to control microbial growth in current fuel systems. It is expected that a reduction in dosage to the minimum levels indicated would result in the same performance as is currently seen at the higher additive levels used in the field today.”

3.5 Fuel Tank Gauging

Two fuel properties related to fuel tank gauging systems were measured by Bruce Kline of Goodrich. These properties were dielectric constant vs. temperature and velocity of sound vs. temperature. The results for a Jet A-1 fuel (POSF-4877) with 0.12 vol% TriEGME are shown below compared with typical values for various fuels as a function of temperature. Dielectric constant vs. temperature was measured with a Goodrich “K” cell and the results are shown in Figure 7. At 22.1°C the value was 2.11368. Speed of Sound was measured with a NuSonics meter and the results are shown in Figure 8. At 22.2C the value was 1304.0 m/s, and the dissipation factor was 0.00173, a typical value. Density also effects fuel tank gauging and density measurements are reported separately. The results indicate that all properties of the TriEGME containing fuel pertaining to fuel tank gauging are within normal limits. Thus, TriEGME should not negatively impact fuel tank gauging systems.

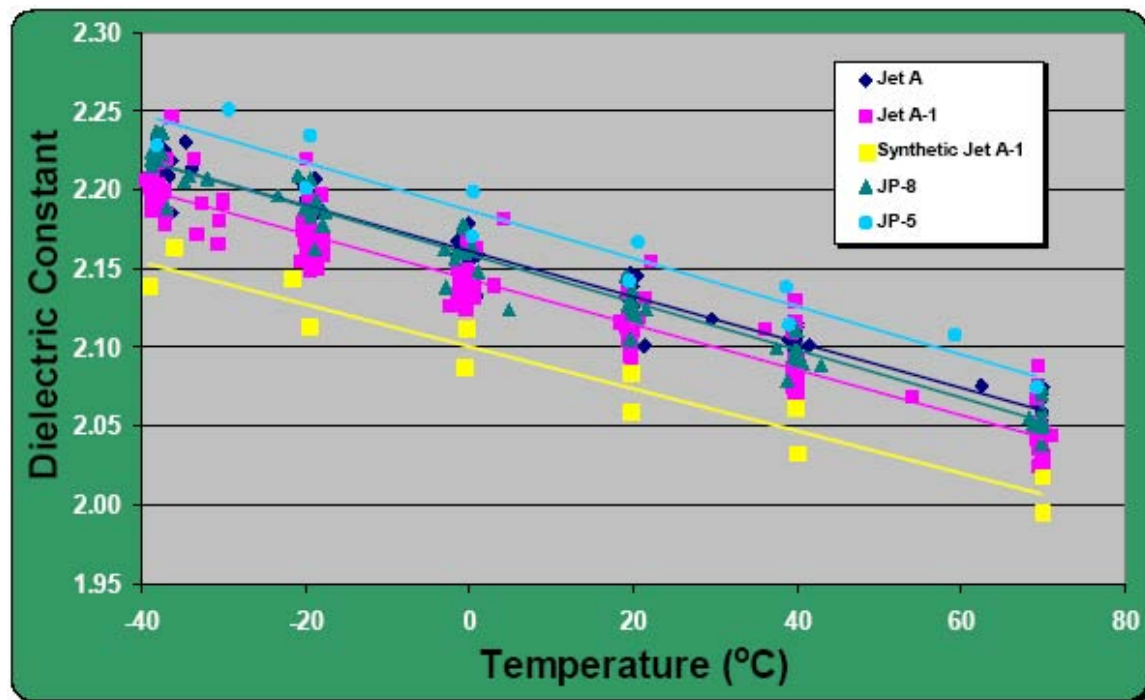


Figure 7. Plots of Dielectric Constant vs Temperature with 0.12 vol% TriEGME

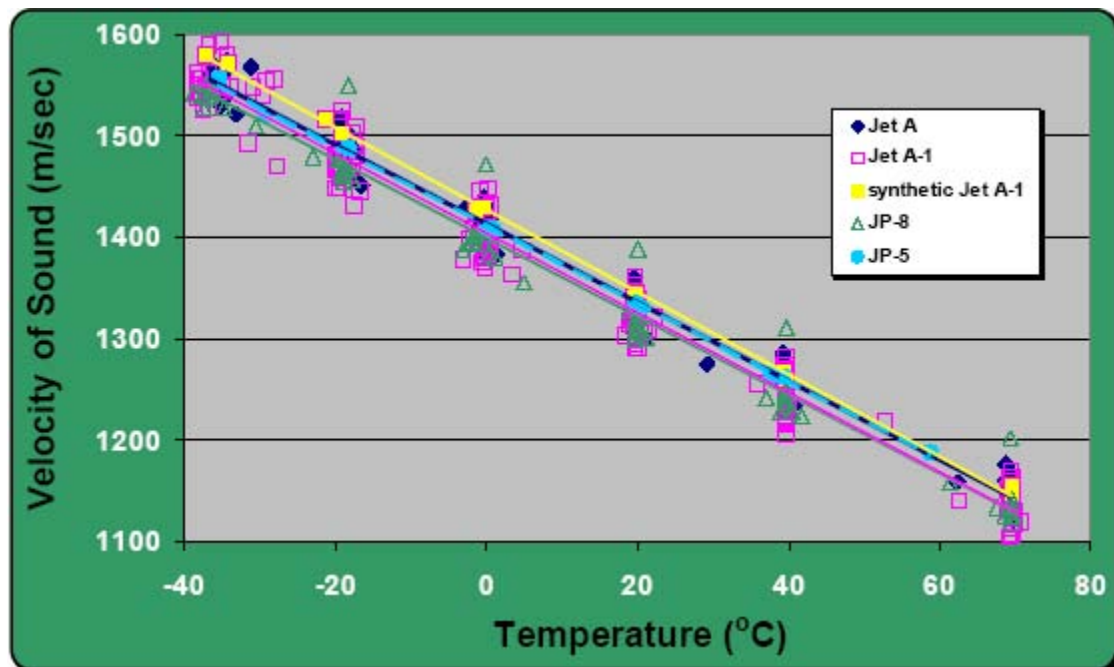


Figure 8. Plots of Velocity of Sound vs. Temperature with 0.12 vol% TriEGME

3.6 Additive Compatibility

The compatibility of TriEGME with other approved jet fuel additives was evaluated via ASTM D4054 Annex A2. Four Jet A-1 fuel samples were treated with two times (2x) concentrations of TriEGME (0.30 vol%) and 2x concentration of each individual JP-8 additives (static dissipater additive Stadis 450, corrosion inhibitor/ lubricity improver Unicor J, and DiEGME) and the Spec-Aid 8Q462 JP-8+100 thermal stability additive. These samples, along with a sample of the fuel with no additional additives, were cooled to 0°F (-17.8°C) for 24 hours in an environmental chamber followed by heating to 100°F (38°C) for 24 hours. The samples were inspected after each 24 hour period and were found to contain no visible indications of incompatibility, i.e, no solids, cloudiness or darkening in color.

3.7 Specific Heat vs Temperature

The specific heat of fuel containing DiEGME and TriEGME were evaluated via differential scanning calorimetry over the temperature range -40 to 150°C and the results are shown in Figure 9. The results show that the additives do not change the fuel specific heat significantly over the entire temperature range.

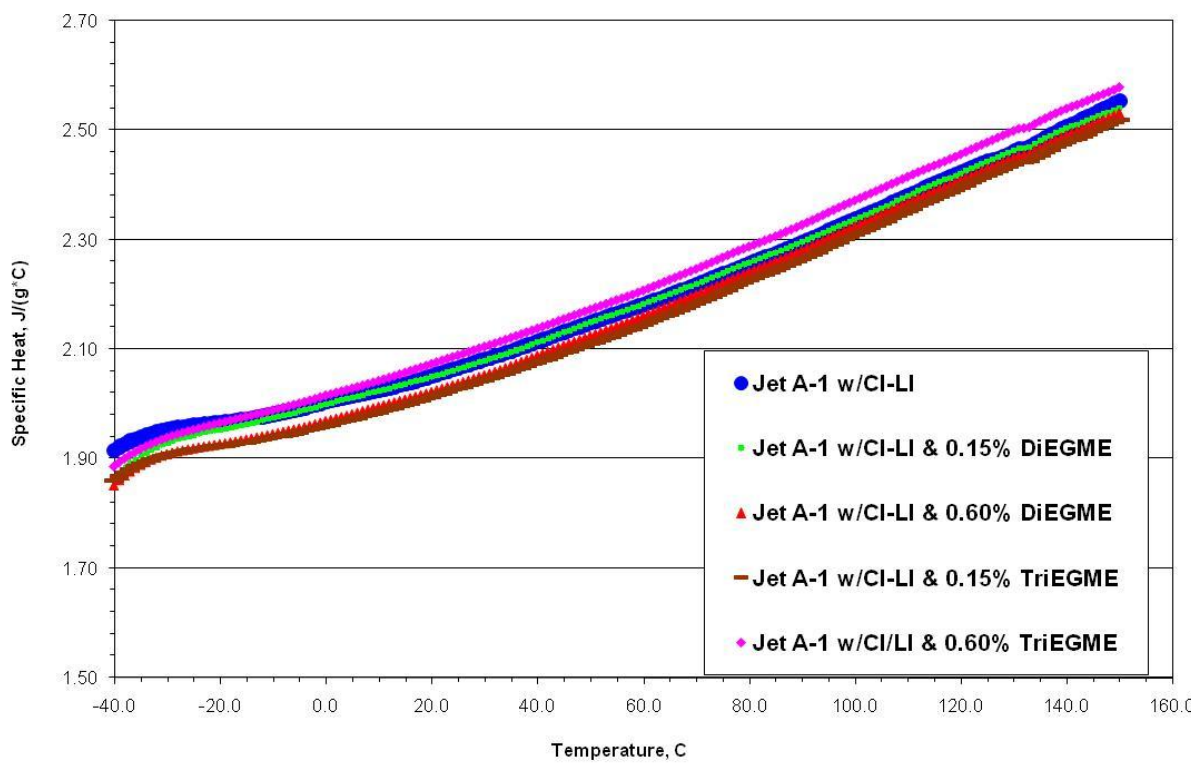


Figure 9. Specific Heat Measurements vs Temperature for Fuels containing DiEGME and TriEGME

3.8 Autoignition Temperature

Southwest Research Institute was tasked with performing autoignition temperature measurements on fuels treated with both TriEGME and DiEGME. The results are shown in Table 5. The tests were performed using ASTM E659-78 (Reapproved 2005) Standard Test Method for Autoignition Temperature of Liquid Chemicals. The tests were conducted using the same Jet A fuel sample, so that the effects of the two additives can be compared. The results are within the 5% reproducibility claimed in the specification, and thus TriEGME appears to have the same effect on autoignition temperature as DiEGME.

Table 5. Autoignition Temperature Results for a Jet A Fuel with DiEGME and TriEGME

Sample	Autoignition Temperature (°C)
Jet Fuel with 0.6 vol% DiEGME	227
Jet Fuel with 0.6 vol% TriEGME	222

3.9 Filter-Coalescer Compatibility

The Southwest Research Institute performed a program to determine the impact of the replacement FSII additive on the water separation and filterability of JP-8 and JP-8+100 fuel. This was performed by comparison of the performance of TriEGME in a base fuel with DiEGME in the same fuel. The program performed is detailed in Appendix E. The study concludes that:

“A variety of filtration and fuel property evaluations were performed on JP-8 and JP-8+100 fuels containing Di-EGME and Tri-EGME fuel system icing inhibitors. Both the gravimetric and water results for the API/IP 1581 5th Edition evaluations suggest there is no difference in performance between the two fuel system icing inhibitors. Additional particle counting and turbidity measurements agree with the gravimetric and standard water measurements. The API/IP 1583 evaluations substantiated the poor performance of water absorbent monitors in fuels containing FSII. All fuels containing FSII performed poorly with the fuels containing TriEGME performing worse than the fuels containing Di-EGME. For the water slug evaluations, all fuels (even those containing FSII) passed with less than 1% of the rated flow passing through the monitor. The material compatibility evaluations show no indications of compatibility issues up to 4X the concentration of the FSII. The resultant fuel properties were similar between the Di- and Tri-EGME fuels. As a result of the accumulated data comparing Di-EGME and Tri-EGME performance and physical properties, there is no indication there is any difference in performance.”

3.10 Toxicity Evaluation

An evaluation of the toxicity of TriEGME relative to DiEGME was performed by the Applied Biotechnology Branch of AFRL via a review of existing toxicity information from the scientific literature. A letter listing the main results of this evaluation is included in Appendix F. To aid in the comparison, the former FSII additive, EGME, was added to the review. Evaluations of the following measurements were compared: inhalation studies, oral LD₅₀ values (dose that is lethal to 50% of the test population), skin and eye irritation, diffusion across the skin, drinking water studies, nervous system toxicity, reproductive and developmental effects, and mutagenicity. The evaluation concludes that:

“A review of the toxicity of the past, current and potential FSIIIs indicates that TriEGME has less or equal toxicity to the current FSII. Use of TriEGME should not pose any additional hazard than the current FSII, DiEGME, and may pose less of a reproductive hazard. Based on this toxicological review, TriEGME should be an acceptable replacement for DiEGME as a FSII. An exposure assessment of JP-8 with TriEGME should be conducted to ensure that there are no conditions under which TriEGME as an additive to the JP-8 fuel mixture might pose a greater exposure or hazard.”

3.11 Hot Gas Path Evaluation of Compatibility with Turbine Engine Materials

Pratt & Whitney performed hot path gas tests to determine the compatibility of TriEGME with hot section turbine engine materials using burner rigs. The results are detailed in Appendix G. The report provides the following conclusion:

“The objective of this program was to perform oxidation and corrosion hot gas-path testing to determine the compatibility of triethylene glycol monomethyl ether (TriEGME) fuel additive on turbine engine alloys and coatings. The hot gas-path tests are part of the approval process set forth by jet engine manufacturers for the use of the TriEGME additive in fuels used by military and commercial aircraft. In this program the hot gas-path testing was accomplished using burner rigs. The 1850°F cyclic oxidation tests were carried out on six different alloy/coating combinations. The isothermal 1600°F, 3.5 ppm salt, hot corrosion tests were conducted on seven different alloy/coating combinations. Oxidation and corrosion samples were tested using a TriEGME/Jet A additive blend and compared to a DiEGME/Jet A baseline blend. Test samples were evaluated by mass, dimensional and visual change. Only minor differences were found between the additive packages thus the TriEGME additive was deemed to be comparable to the DiEGME additive.”

3.12 Kinematic Viscosity vs. Temperature

Kinematic viscosity was measured versus temperature via ASTM D445, Standard Test Method for Kinematic Viscosity of Transparent and Opaque Liquids, by measuring the time for a volume of liquid to flow under gravity through a calibrated glass capillary viscometer. Measurements were performed at four temperatures, -40, -20, 40, and 90 C, using a Jet A-1 fuel with added Stadis 450 and corrosion inhibitor additives. DiEGME and TriEGME additives were employed

at 0.15 and 0.60 vol%. The results are shown in Figure 10. The figure shows that the additives have little effect on the viscosity of the base fuel and that there are no measurable differences between DiEGME and TriEGME on the temperature dependent viscosity of the fuel.

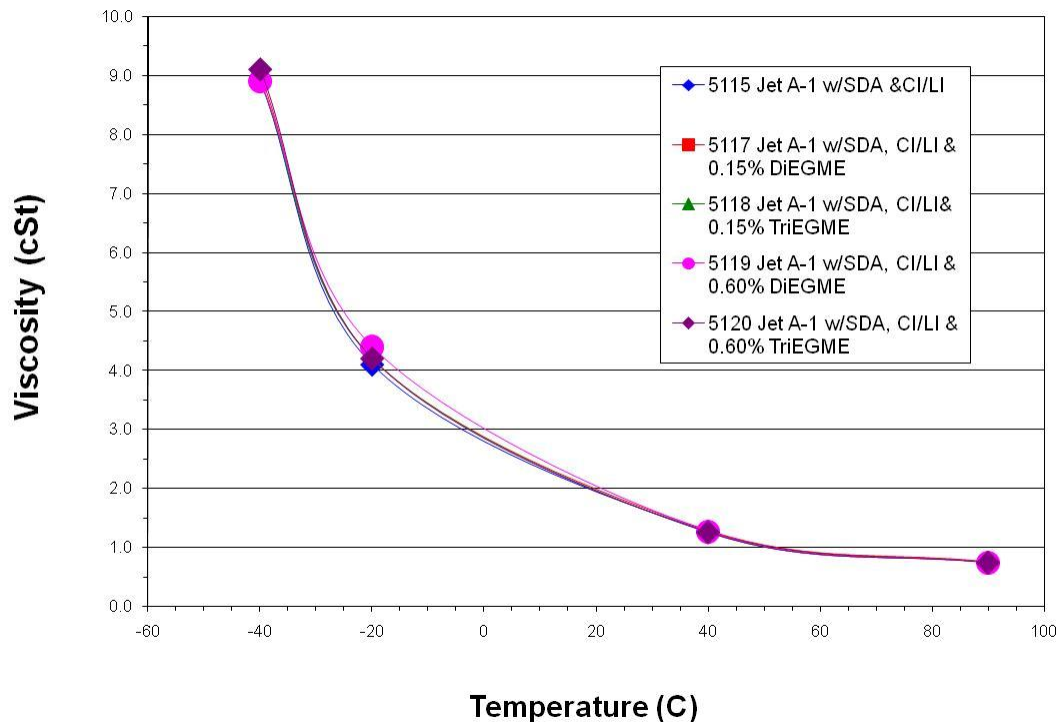


Figure 10. Kinematic Viscosity Measurements for DiEGME and TriEGME in Fuel over a Range of Temperatures

3.13 Density

The effect of DiEGME and TriEGME on the density of Jet A-1 fuel was measured over the temperature range -40 to 90°C. Specification levels of static dissipating additive and corrosion inhibitor were added to the base Jet A-1 fuel to satisfy the JP-8 specification. The results are shown in Figure 11. The figure shows that the additives have no measurable effect on the density of the fuel over this temperature range and concentrations of 0.15 vol% for DiEGME and TriEGME. DiEGME and TriEGME are also shown at the 4x concentration (0.60 vol%) and no change in density is observed even at this high concentration.

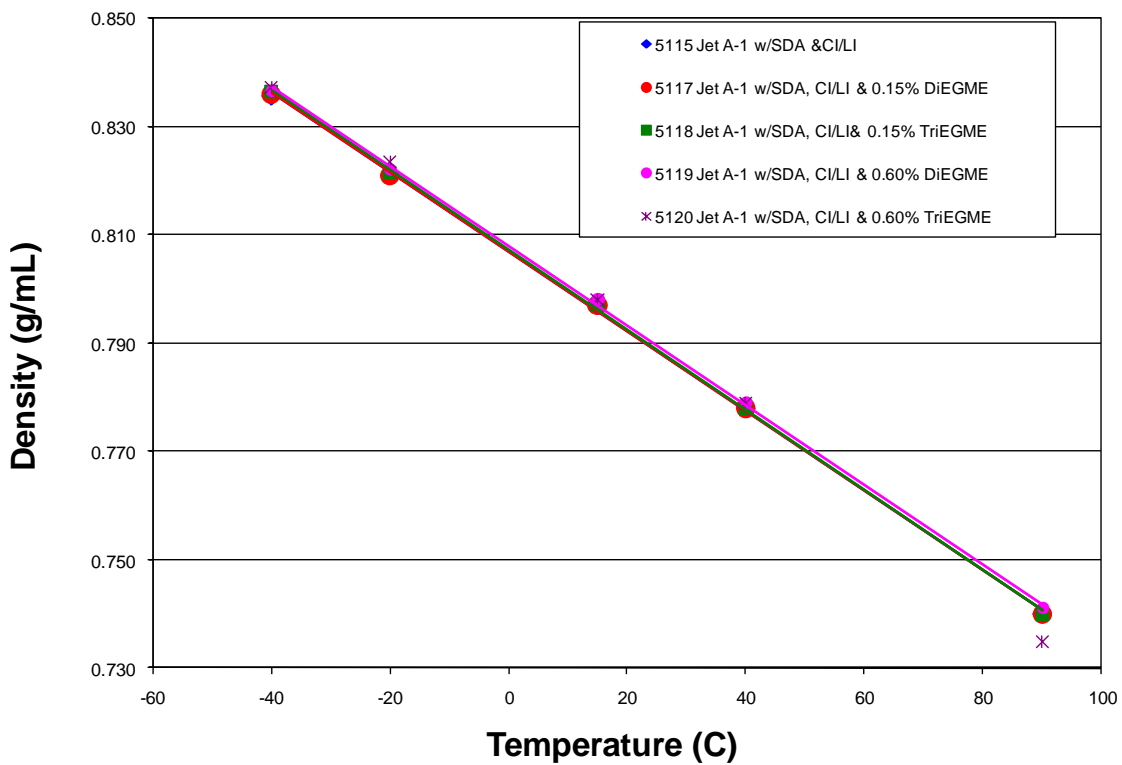


Figure 11. Plots of Density vs. Temperature for a Jet A-1 fuel with DiEGME and TriEGME

3.14 Conductivity

The effect of DiEGME and TriEGME on fuel conductivity and the effectiveness of Stadis 450 static dissipating additive were evaluated. Conductivity was measured by ASTM D2624. DiEGME and TriEGME were evaluated at two concentrations, 0.15 and 0.60 vol%, and compared in three fuels: Jet A-1 fuel POSF-4877, Jet A fuel POSF-4658, and Jet A fuel POSF-3084. Before adding the FSII additives, the fuels were treated with Stadis 450 to obtain a conductivity of ~360 pS/m. The results are shown in Figure 12. The results indicate that while the effect of these FSII additives varies between fuels, DiEGME and TriEGME show very similar effects on a given fuel. In particular, fuel POSF-4877 shows a decrease in conductivity for both additives, while the other two fuels show an increase. The amounts of increase and decrease are nearly identical for the two FSII additives, except at the 0.15 vol% level, where TriEGME reduces the conductivity of POSF-4877 fuel significantly more than DiEGME.

Changes in conductivity upon addition of polar additives such as DiEGME and TriEGME is likely a function of the polar constituents present in the fuels, their concentrations, and their interactions with the FSII additives and Stadis 450. These interactions are poorly understood. In general, the similar behavior exhibited by DiEGME and TriEGME, along with the long history

of safe handling of DiEGME-containing fuels, leads to the conclusion that the no significant undesirable behavior will be expected for fuels treated with TriEGME.

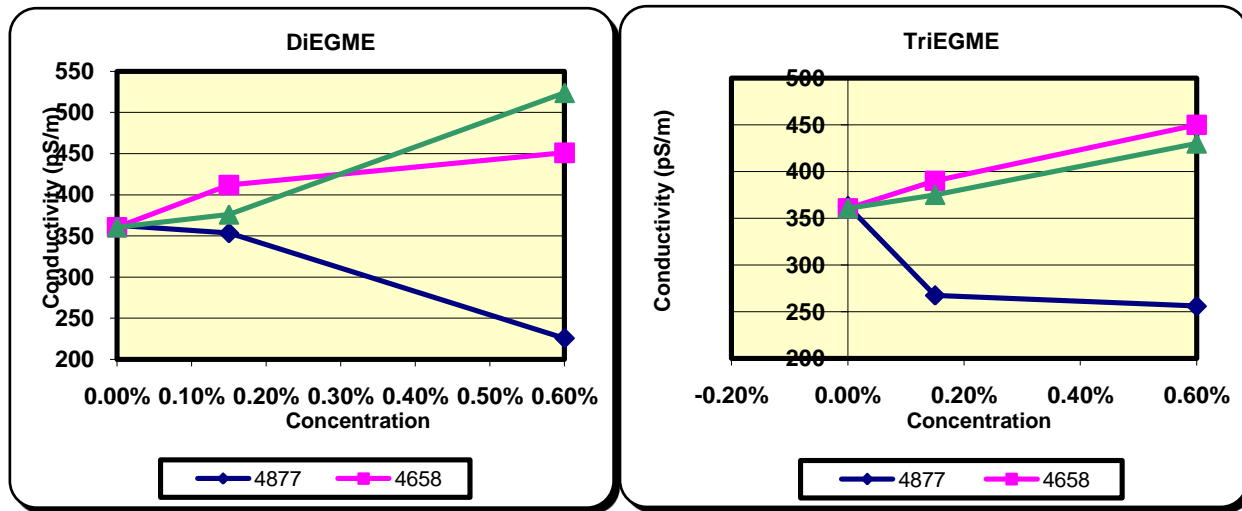


Figure 12. Conductivity Results for Fuels containing DiEGME and TriEGME

3.15 Seal Swell Characteristics

Some jet fuel components, e.g., aromatics, are known to migrate into elastomer sealing materials such as o-rings, resulting in a swelling of these seals. Ordinarily, the sealing fixtures are designed to incorporate this swell, and thus fuels which do not swell these materials, e.g., low aromatic fuels, can cause seal failure and fuel leakage. The ability of DiEGME and TriEGME to swell nitrile, fluorosilicon, and fluorocarbon elastomer materials was evaluated to determine the effect of TriEGME on these seals. DiEGME and TriEGME were investigated at 0.15 and 0.6 vol% in a baseline Jet A-1 fuel (POSF-4877) containing 2 mg/L of Stadis 450.

The volume swell of each sample was determined using optical dilatometry at room temperature. The volume swell results are summarized in Figure 13. These results show that the volume swell of the nitrile rubber (N0602), fluorosilicone (L1120), and fluorocarbon (V0747) increased with increasing FSII concentration. Furthermore, the increase in volume for the nitrile rubber and the fluorocarbon was greater for the TriEGME than DiEGME, while the volume swell of the fluorosilicone was not significantly different between these two species. Note that the volume swell data for the N0602 and L1120 was found to vary linearly with FSII concentration and therefore replicate analysis were not conducted. In contrast, the volume swell of V0747 was found to be non-linear with respect to the FSII concentration, therefore replicate analyses were performed to verify this behavior and the results shown are the average of three independent samples.

The volume swell of typical O-ring materials as represented by nitrile rubber, fluorosilicone, and fluorocarbon is a function of the FSII type and concentration to varying degrees. The volume swell of fluorosilicone was found to be a weak function of FSII concentration and not to be a function of the type of FSII (DiEGME versus TriEGME). The volume swell of nitrile rubber was found to be a moderate function of FSII concentration and to respond somewhat stronger to

TriEGME versus DiEGME. The volume swell of fluorocarbon was found to be a strong function of FSII concentration and also to respond somewhat stronger to TriEGME versus DiEGME. The overall result is that at nominal treatment levels (on the order of 0.15%v/v) the effect of DiEGME versus TriEGME on the volume swell of typical O-rings materials is relatively small. This indicates that the performance of DiEGME and TriEGME should be similar with respect to their compatibility with elastomers at nominal treatment levels. However, at elevated treatment levels, the effect of the FSII concentration can be significant and the TriEGME will be more aggressive towards nitrile rubber and fluorocarbon elastomers than DiEGME. In contrast, there was no significant difference between the behavior of DiEGME and TriEGME towards the volume swell of fluorosilicone within the concentration range used in this study.

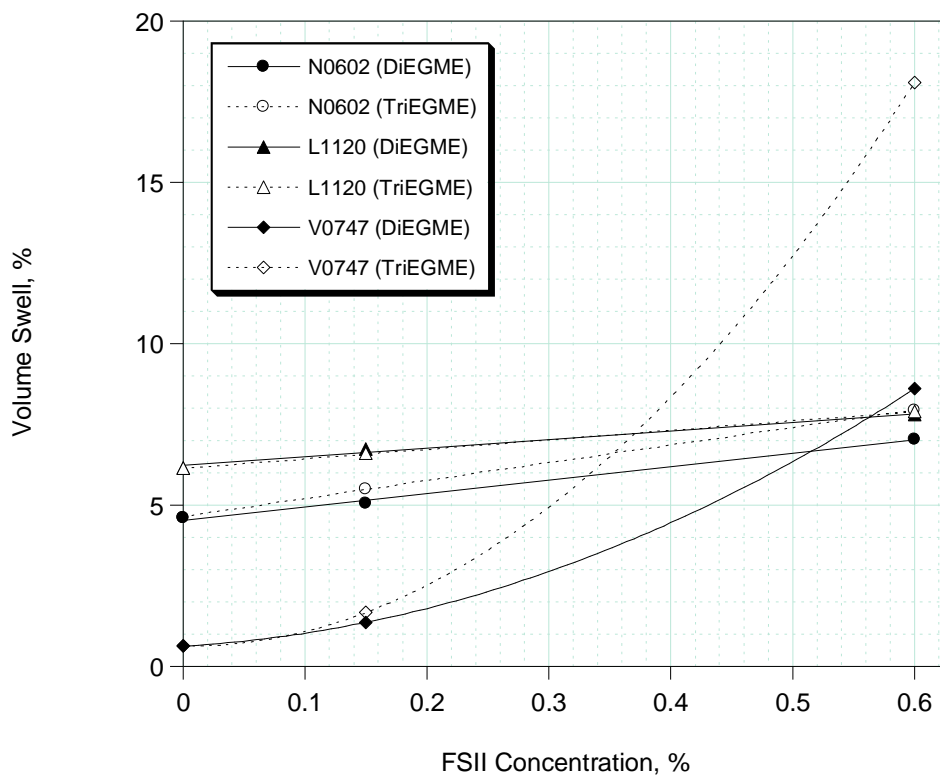


Figure 13. Plots of Volume Swell vs. FSII Concentration

3.16 Surface Tension

Table 6 shows results of surface tension measurements obtained using a Fisher Surface Tensiomat, Model 21. Both liquid/liquid and liquid/air surface tensions were evaluated in comparison. A platinum-iridium ring of known dimensions is suspended from a counterbalanced lever-arm. The arm is clamped to a stainless steel wire that holds it horizontal by torsion. The ring is initially immersed in a liquid. The arm and ring are raised by increasing the torsion in the wire. The tensiometer measures the surface tension in dynes/centimeter required to pull the ring free from the surface film of the liquid. Interfacial surface tension of two liquids is measured by either pulling the ring from the more dense liquid into the less dense liquid, or

pushing the ring from the less dense liquid into the more dense liquid. The instrument measures apparent surface tension. Absolute surface tension is calculated by multiplying apparent surface tension by a correction factor. The tensiometer is factory calibrated, and the calibration is checked by analyzing a liquid of known surface tension. (e.g., water). The accuracy of the method is approximately $\pm 10\%$ and the precision between duplicate measurements is $<10\%$ relative.

The results indicate that, within the experimental uncertainty, TriEGME and DiEGME have essentially identical effects on interfacial surface tension for both liquid/air and liquid/liquid interfaces using fuel and water at various concentrations.

Table 6. Surface Tension Measurements

Test Fluid 1	Test Fluid 2	Liquid/Air Surface Tension (dynes/cm)		Liquid/Liquid Surface Tension (dynes/cm)	
		Test Fluid 1 (DiEGME)/Air	Test Fluid 1 (TriEGME)/Air	Test Fluid 1 (DiEGME)/Test Fluid 2	Test Fluid 1 (TriEGME)/Test Fluid 2
Jet A	DI water	25.4	25.6	25.7	26.0
10% DiEGME or TriEGME in water	Jet A	58.4	56.8	21.8	27.1
20% DiEGME or TriEGME in water	Jet A	52.7	49.2	18.3	20.6
30% DiEGME or TriEGME in water	Jet A	48.1	46.3	16.2	17.5
40% DiEGME or TriEGME in water	Jet A	45.5	43.9	14.8	15.3
50% DiEGME or TriEGME in water	Jet A	44.4	42	13.6	13.9
50% DiEGME or TriEGME in water	Jet A w/ 256 mg/L +JP-8+100			12.3	14.2
50% DiEGME or TriEGME in water	Jet A w/ 1024 mg/L JP-8+100			10.3	9.6
100 % DiEGME or TriEGME		34.7	33.6		

3.17 Icing Inhibition Evaluations

Potential candidate additives must display icing inhibition properties equivalent to DiEGME under realistic aircraft conditions; however, there are currently no performance requirements for FSII additives. Thus evaluation of icing inhibition performance is not standardized and methods for evaluation are open to interpretation. Ideally these methods should reflect actual aircraft conditions; however, the wide variety of temperatures, fuel samples, water levels, etc., make this impractical. Regardless of the experimental conditions, any potential replacement FSII candidate should perform as well or better than DiEGME based upon the selected evaluation criteria. Both small-scale studies, using low fuel volumes and simulated fuel system components, and large-scale studies, using large fuel volumes and actual aircraft fuel system components, have been pursued for this work. Both small and large scale icing evaluations are reported below.

3.17.1 Small-Scale Icing Testing

An experimental system was developed to evaluate FSII candidates under the dynamic effects of water freezing in a flowing fuel line. The design has many similarities to the U.S. Navy Fuel System Icing Simulator (Mushrush et al., 1999). A general schematic of the small-scale icing simulator (SSIS) is shown in Figure 14. Two and one half gallons of fuel is continuously circulated at 1 L/min in a closed loop while the system temperature is slowly decreased by means of a heat exchanger and environmental chamber. The total water and additive concentration is adjusted prior to cooling. The test section consists of a custom metal housing that contains a segment of B-52 aircraft fuel filter material. Icing is evaluated by monitoring the pressure drop and flow rate across the test section. When ice begins to block the filter the pressure drop across the filter increases sharply and the flow rate decreases, thus indicating a freezing event. The system is outfitted with four sample/drain valves (not shown in Figure 14) located before the reservoir, pump, heat exchanger, and test section to monitor dissolved water levels. Thermocouples are spaced throughout the system to monitor fluid temperatures at various points of interest.

Experiments were begun with a Jet A-1 fuel with 288 ppm total water; incremental amounts of the candidate FSII additive were then added (typically 0.005 vol% increments). Between each incremental additive addition the experiment was run until a failure occurred (or minimum temperature reached), then warmed back to ambient temperature before adding the next additive increment. Figure 15 shows the results of these experiments for some select FSII candidates. The figure shows that for DiEGME the failure temperature decreased rapidly as the additive was added to a concentration of 0.03 vol%, at which concentration no freezing event was observed down to the test temperature limit of -45°C. Other candidate additives that behaved similarly to DiEGME in these tests were DPG and TriEGME. Due to its high viscosity, DPG was not considered a viable replacement additive. Thus TriEGME was found to be the most promising candidate based upon the experiments performed. The overall efficacy ranking of additives based upon SSIS studies is as follows:

$$\text{TriEGME} \approx \text{DPG} \approx \text{DiEGME} > \text{TriEGEE} > \text{GF} > \text{DiEGEE}$$

Additional experiments were conducted at a total water level of 600 ppmv (results not shown). While higher additive concentrations were required to inhibit icing at this higher water level, the overall efficacy ranking of the additives remained unchanged. Due to these results, TriEGME was selected as the most attractive replacement additive candidate.

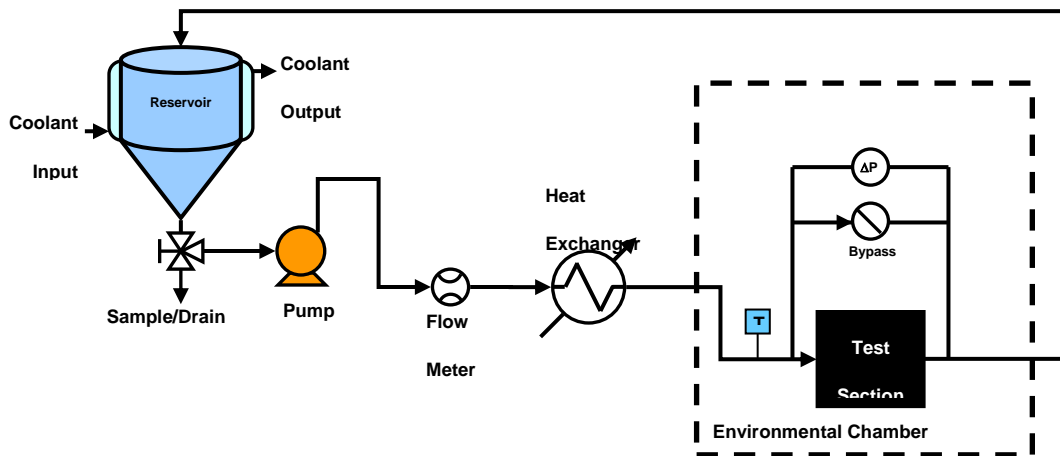


Figure 14. Schematic of the Small-Scale Icing Simulator

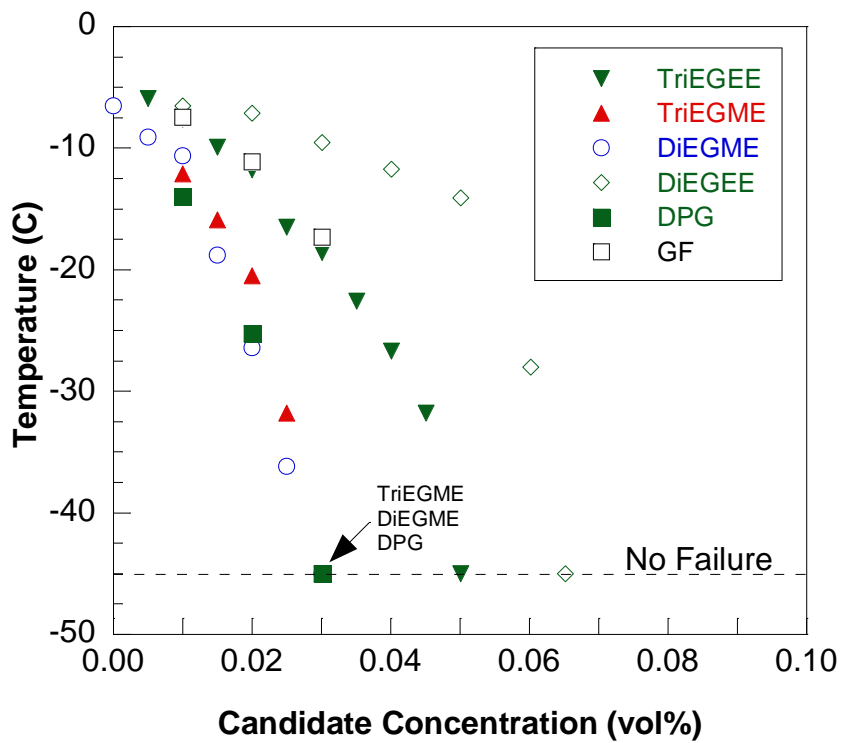


Figure 15. Failure Temperature vs. Additive Concentration for Various FSII Candidates using the SSIS at 288 ppmv of Total Water

3.17.2 Parker Icing Testing

Large-scale evaluation of the effectiveness of TriEGME as an icing inhibitor was performed in comparison with DiEGME to validate the results from the small-scale flow testing under more representative conditions. Ideally, a detailed review of all USAF platforms would be performed and available which would identify components prone to blockage due to icing and relevant

conditions (e.g., temperatures, flow rates) experienced. Unfortunately, a detailed review of all USAF aircraft was not available, and therefore as in the related “minimum FSII program” (Phelps et al., 2009), the approach implemented was evaluation on a platform/component which could represent a “worst-case” operational condition, would provide a conservative estimate of reduced FSII efficacy, and be applicable to other platforms. The B-52 aircraft fuel system was used for this basis for several reasons. The B-52 was the original driving force for the FSII requirement as aircraft crashes in the 1950s were attributed to excessive ice build-up in the fuel system. The B-52 typically has high-altitude/long-duration missions and large volumes of fuel, which can result in low fuel temperatures. Also the aircraft has no specific hardware within the fuel tanks and fuel transfer system to prevent water accumulation (e.g., water scavenge rakes or OBIGGS) or solidification (e.g., fuel heaters).

An independent effort was performed by Boeing and the B-52 Flight/Mechanical Systems Office to review the B-52 fuel system for locations and conditions that were most prone to icing vulnerability during operation. Several components in the fuel system upstream of the engines were identified for potential icing concern. However, it was determined that the fuel strainer housing between the main fuel boost pumps and the engine-driven fuel pump would be most prone to blockage due to ice formation. The fuel strainer is the first fine-flow passage after the fuel is transferred from the fuel tanks and is not actively heated. Therefore, it is rational to use this component for evaluation of candidate FSII additives since proper operation of this component will indicate that down-stream problems would be improbable. A schematic of the strainer housing is shown in Figure 16. During standard operation, the housing has a built-in bypass which can allow flow if the pressure drop across the filter element becomes too high. This could potentially allow ice particles to flow to downstream components during standard operation. It should be noted that this component has passed icing qualification during FSII-free testing, most likely due to the bypass actuation.

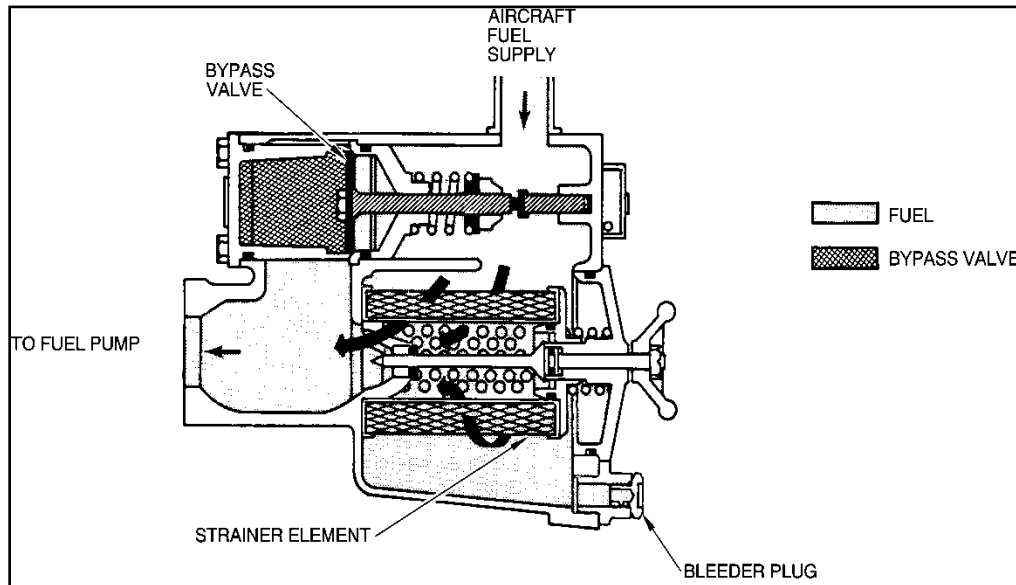


Figure 16. Schematic of B-52 Fuel Strainer Housing

The evaluation of reduced FSII effectiveness was performed using a modified B-52 strainer housing; the internal bypass valve was wired shut to prevent opening during testing. The

primary goal during testing with the B-52 strainer was to identify the minimum TriEGME concentration which would provide for safe operation without any appreciable solid formation. Performing this testing with fuel conditioned with precise quantities of total water and FSII was critical to provide a valid basis for evaluation. In addition, testing under representative fuel flow rates, temperatures and durations were required. These overall constraints required that a large-volume of conditioned fuel and appropriate test facilities be available for the evaluation. It was determined that the testing would be performed by Parker Aerospace, Irvine California; Parker Aerospace has extensive test facilities and experience performing large-scale icing studies. A process flow diagram of the fuel conditioning and test system at the Parker Facilities is shown in Figure 17.

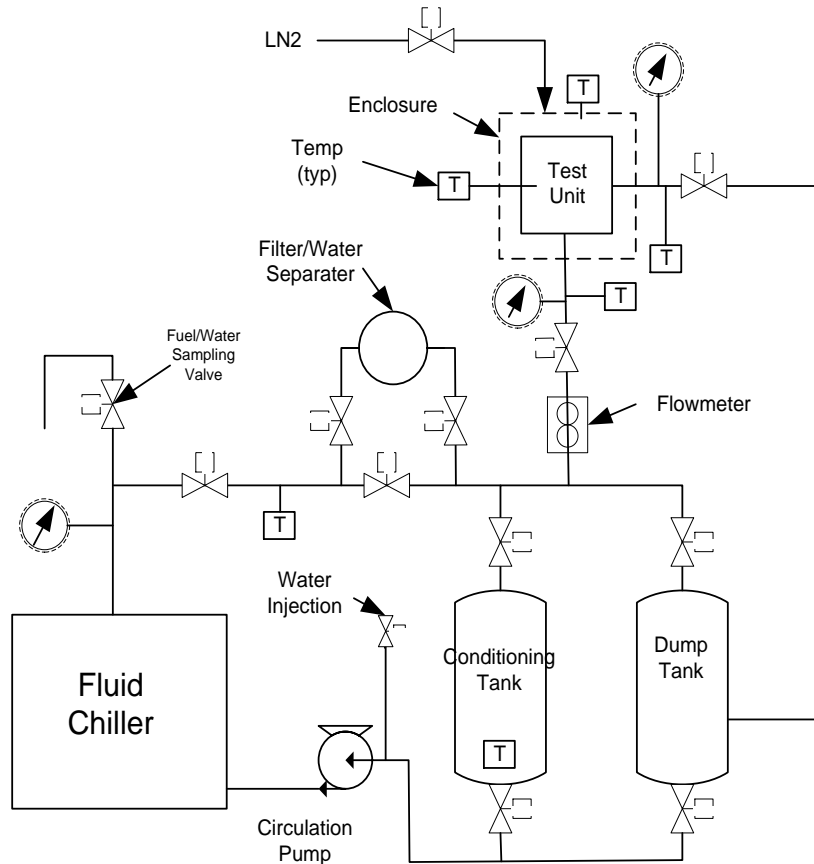


Figure 17. Process Flow Diagram of Fuel Conditioning and Test System for Component Level Testing at Parker Aerospace

The basic test methodology is comprised of pre-conditioning the test fuel to the water saturation limit at 80°F via continuous recirculation of the condition tank through the fluid chiller followed by removal of excess water via the coalescer (Filter/Water Separator in Figure 17). Once achieved, the required additional water volume and FSII are sequentially added to the recirculating system to achieve the target values. The fuel temperature is then set to the target value via recirculation through the chiller; once achieved, the desired flow rate to the test unit is initiated while fuel continually recirculates to the conditioning tank to prevent water settling. The external temperature of the test unit is independently maintained via cooling with liquid

nitrogen. Determination of ice formation and blockage of the test unit is made by monitoring the differential pressure across the unit and the overall fuel flow rate. Significant changes in these metrics are indicative of ice formation and blockage of the respective flow path.

Testing was performed with the B-52 strainer housing using a fuel flow rate of 6 gallons/minute, which is similar to the required flow rate during aircraft cruise at altitude (Cash, 2004). Testing was performed while varying the total FSII and water contents and test temperature. Initially, the attempt was made to perform the testing similar to that prescribed in the SAE ARPs. The first test was performed with FSII-free fuel with 288 ppm total water while passing half of the fuel volume through the component at test temperatures of -9°C (+15°F) and -40°C, respectively. Testing showed complete failures (significant pressure rise and loss of fuel flow) after approximately 25-30 minutes for the FSII-free testing at -9°C (+15°F), indicating that the test set-up was capable of reliably indicating failure due to icing. Visual inspection of the test filter showed significant ice with complete coverage of the filter element. Testing was then performed using 0.07% DiEGME with 288 ppm total water to represent current FSII efficacy. This testing showed no decrease in measurable component fuel flow or increase in pressure differential. However, it was determined that with the presence of FSII, performing the test at -9°C (+15°F) (critical icing temperature) is not a relevant condition since even low concentrations and partitioning would prevent solidification under this condition. Therefore, subsequent testing was performed at a single test temperature.

Several difficulties were encountered during the following FSII-efficacy testing with the B-52 fuel strainer. It was determined that the majority of these were a result of attempting to perform detailed quantitative evaluation of the effectiveness of varying FSII concentration on a large-scale using the ARPs for standard icing evaluation. It was determined that the recommended methodologies for fuel conditioning and component testing for FSII-free evaluations can introduce experimental artifacts during FSII-efficacy testing. This resulted in several modifications and improvements to the testing methodology, which significantly improved the overall quality control and applicability of the testing. A detailed discussion on all studies performed, modifications to the test methodology and improvements will be provided in subsequent reporting; major comments and primary test results will be provided below.

During large-scale evaluation of a reduced FSII concentration, several experimental parameters were determined to be critical to control for quantitative evaluations to be performed. These parameters included:

- Precise control of total water and FSII concentration
- Sufficient contacting time for FSII partitioning
- Testing at single condition with entire volume of test fuel

As previously discussed, there is no established methodology for “FSII-evaluations” or a “FSII-performance” specification. Icing qualifications are typically performed without FSII in the fuel. The consequence of this is that solid ice is most likely present (and probably desired) in the fuel conditioning system during testing. A standard icing test will determine if a component can function properly with ice accumulation; slight variations ($\pm 10\text{-}20\%$) in the total water content will most likely not affect the final test results. However, a goal of the current program is to define a reduced FSII concentration where there will not be any solid formation in the fuel.

Therefore, precise control of the total water and FSII content is vital for quantitative evaluations to be performed, especially when operating near the icing transitional regime for FSII/water mixtures. It was determined that the recommended practice of over-saturating the fuel with excess water at 80°F and filtering with a coalescer could allow for excess water to exist in the fuel system which is not readily detected. In particular, if the fuel is at the saturation limit, it is not possible to determine if excess free water is present in the system. Therefore, a modification of the initial fuel conditioning was made to first chill the fuel to 35-40°F, remove free water by passing through the coalescer, and then heating the fuel to 80°F. Samples at the elevated temperature were then analyzed for the total water content. The benefit of this approach is that if the measured total water content is below the saturation limit at 80°F, all water in the fuel system should be dissolved and there is higher confidence in the total water content.

High-precision analytical methods are required to verify total water and FSII content of the treated fuel due to the effect of potential inaccuracies while attempting to precisely condition a large-volume of fuel. Analytical difficulties were experienced during this large-scale component testing; ultimately, all sample analyses were performed at the AFRL/RZPF laboratory for quality control. Due to the design of the fuel conditioning system, only a small portion of the fuel volume is actively chilled during the cool-down segment of the test. This can result in a significant temperature differential between fuel in the chiller as compared to that in the conditioning tank. As previously discussed, the partitioning of FSII from the fuel to free water is highly dependent on temperature. In the event that the fuel (or portion of) is cooled more quickly than the FSII can partition, the potential exists that the freeze point of the existing water/FSII mixture will be exceeded and solidification will occur, even though there is sufficient overall FSII in the tank to prevent freezing. Therefore, a modification to the method was made to cool-down the fuel using sequential temperature steps with equilibration time to allow for adequate contacting and to prevent undercooling and solidification. The final modification was to pass the entire fuel volume through the strainer at a single test condition. This was performed since once excess water has been added to the fuel, the overall fuel/FSII/water mixture will not be homogenous. Passing the entire fuel volume through the component will ensure that the component is exposed to the entire volume of water during testing.

Several TriEGME evaluation tests were performed using the modified test procedures and compared with identical evaluations performed with DiEGME. All tests were performed with a total water concentration of 125 ± 10 ppm and reduced FSII concentrations based on the minimum required levels from the preceding bench- and small-scale testing. Temperatures of -40 and -44°C were evaluated. The temperature of -44°C was selected as the minimum temperature that JP-8 fuel (with a specification freeze point of -47°C) should see during use due to the minimum of a 3°C operational temperature margin above the specification freeze point for most aircraft. A summary of the results from the testing is shown in Table 7. The results indicates that, for a conservative total water content of 125 ppm, a DiEGME concentration of 0.040 vol% is a conservative lower level that is able to prevent ice formation for fuel temperatures down to -44°C. A separate, concurrent study has used this evaluation and others to recommend a minimum use level of 0.040 vol% for DiEGME (DeWitt et al., 2009). Table 7 also shows that TriEGME performance is identical to DiEGME at both -40 and -44 °C, successfully preventing ice formation at a concentration of 0.040 vol%.

Table 7. DiEGME and TriEGME Results from B-52 Fuel Strainer FSII Testing at Parker Aerospace

FSII	Temperature	FSII Concentration (vol%)	Total Water Concentration (ppm)	Test Result
DiEGME	-40 °C (-40 °F)	0.040	125	Pass
DiEGME	-40 °C (-40 °F)	0.031	125	Fail
DiEGME	-44 °C (-47°F)	0.041	125	Pass
TriEGME	-40 °C (-40 °F)	0.040	125	Pass
TriEGME	-44 °C (-47 °F)	0.041	125	Pass

INTENTIONALLY LEFT BLANK

4. CONCLUSIONS

This report has described a program, funded by the DoD RTOC office, in which the U.S. Air Force has developed a new fuel system icing inhibitor which does not cause fuel tank topcoat peeling of aircraft fuel tank ullage surfaces. Glycol and glycol ether additive candidates, and other additive candidates, with low vapor pressures were targeted and screened for the ability to lower aqueous freeze points and selectively partition from the fuel phase into the aqueous phase. Promising candidates were then evaluated in a small-scale icing simulator for the ability to inhibit icing in a flowing system through aircraft fuel filter material. TriEGME was the additive that showed the most promise and was selected for further testing after these evaluations. TriEGME was evaluated for its effect on fuel specification properties, fit-for-purpose properties, and its compatibility with aircraft fuel tank topcoat materials. The extensive fit-for-purpose studies included evaluation of additive-additive compatibility, biostat capability, thermal stability, filter-coalescer and filter monitor compatibility, fuel system materials compatibility, autoignition temperature, toxicity, turbine hot section erosion and corrosion, viscosity, conductivity, response to SDA, density, seal swell, solubility, surface tension, and lubricity. TriEGME has successfully passed all evaluations performed. Large scale testing of the icing inhibition capability of TriEGME shows that at a use concentration of 0.040 vol% in the fuel, it will prevent ice formation down to a temperature of -44°C. This program provides the military with an alternate fuel system icing inhibitor which provides adequate icing inhibition but does not negatively impact fuel tank ullage topcoat surfaces, with resulting savings in maintenance costs.

INTENTIONALLY LEFT BLANK

5. REFERENCES

Aliband, A., Lenz, D., Dupois, J., Alliston, K., Sorhaug, V., Stevenson, L., Whitmer, T., Burns, D., and Stevenson, W., "Epoxy Paint Failure in B-52 Fuel Tanks, Part 1 – Preliminary Development of a Model for the Process," *Progress in Organic Coatings*, Vol. 56, pp. 285-296, 2006.

DeWitt, M.J., Zabarnick, S., Williams, T.F., West, Z., Shafer, L., Striebich, R., Breitfield, S., Adams, R., Cook, R., Phelps, D.K., and Delaney, C.L., "Determination of the Minimum Use Level of Fuel System Icing Inhibitor (FSII) in JP-8 That Will Provide Adequate Icing Inhibition and Biostatic Protection for Air Force Aircraft," AFRL-RZ-WP-TR-2009-2217, Propulsion Directorate, Air Force Research Laboratory, 2009.

Morris, R.W., Minus, D., Zabarnick, S., Balster, L., Binns, K.E., Dieterle, G., and Biddle, T., "Protocol of Test Methods for Evaluating High Heat Sink Fuel Thermal Stability Additives for Aviation Turbine Fuel: JP-8+100," Technical Report No. AFRL-PR-WP-TR-2002-2037, Propulsion Directorate, Air Force Research Laboratory, 2002.

Mushrush, G.W., Beal, E.J., Hardy, D.R., Hughes, J.M. and Cummings, J.C., "Jet Fuel System Icing Inhibitors," *Industrial & Engineering Chemistry Research*, Vol. 38, pp. 2497-2502, 1999.

Zabarnick S., West Z., DeWitt M., Shafer L., Striebich R., Adams R., Delaney C., and Phelps D., "Development of Alternative Fuel System Icing Inhibitor Additives That Are Compatible with Aircraft Tank Topcoat Material" *IASH 2007, the 10th International Conference on Stability, Handling and Use of Liquid Fuel*, October 2007.

Zabarnick, S., Adams, R., West, Z., DeWitt, M.J., Shafer, L., Striebich, R., Delaney, C.L., and Phelps, D.K., "Compatibility of DiEGME and TriEGME Fuel System Icing Inhibitor Additives with BMS 10-39 Aircraft Tank Topcoat Material," *Energy & Fuels*, Vol. 24, pp. 2614-2627, 2010.

INTENTIONALLY LEFT BLANK

Appendix A. Topcoat Compatibility

INTENTIONALLY LEFT BLANK

COMPATIBILITY OF TRIEGME WITH FUEL TANK COATINGS

Douglas Hufnagle
University of Dayton Research Institute
300 College Park
Dayton, OH 45469-0146

EXECUTIVE SUMMARY

The US Air Force uses diethylene glycol monomethyl ether (DiEGME) as a fuel system icing inhibitor (FSII) to prevent icing in the fuel system of jet aircraft. Recently, it has been found to cause delamination of the coating applied to the inner surface of the fuel tanks. The delaminations are occurring in two locations in the fuel tanks. One is in the water bottom area, where DiEGME has been found to concentrate in the water to about 50 vol%. The other location, which is a more significant problem, is in the headspace above the fuel layer that is exposed to vapors and condensate from the fuel mixture, where DiEGME is concentrated to 1 to 1.5 vol%. The delamination in the water bottom can be controlled to a great extent by frequently draining out the water from the fuel tank, but the headspace area has no easy solution. Triethylene glycol monomethyl ether (TriEGME) is a promising candidate for replacing DiEGME as a FSII because it has a much lower volatility than DiEGME.

This project investigated the relative effects of both materials had on two different aircraft fuel tank coatings in a side-by-side laboratory comparison. The testing indicated that for exposures which simulate liquid fuel or water/fuel interactions with topcoat that the two FSII's exhibited very similar behavior in degrading the topcoat materials tested. In contrast, for the testing which simulates exposure of vapor condensates the results indicated that TriEGME exhibited significantly less softening of one of the coatings (BMS 10-39) due to the lower concentrations expected for this species in the headspace area, which results from its relatively low vapor pressure. However, the test protocols were not sufficiently robust to replicate the damage currently being experienced in aircraft fuel tanks with DiEGME to draw definitive conclusions.

1.0 PURPOSE

This project investigated the effects of triethylene glycol monomethyl ether (TriEGME) on the adhesion of USAF aircraft fuel tank coatings relative to the effects of diethylene glycol monomethyl ether (DiEGME). DiEGME is the current fuel system icing inhibitor used in military jet fuel to prevent icing in the fuel systems of aircraft and is known to cause fuel tank coating adhesion failures. TriEGME has been identified by the Air Force Research Laboratory's Fuels Branch as a possible candidate to replace DiEGME because of its excellent anti-icing properties and low volatility.

2.0 BACKGROUND

In recent years, failures over large areas in the fuel tank coatings of US military aircraft have been observed. The coating failure being experienced is delamination, and has been observed in the fuel tanks of B-52, KC-135, C-17, and P-3 aircraft. Recent laboratory investigations into the cause of the delaminations have identified the fuel system icing inhibitor (FSII) as the most probable cause¹. The current FSII is DiEGME, and is added to the fuel in low concentrations (approximately 0.1% by volume) to prevent icing in the fuel system.

The fuel tank coating is a protective organic polymer coating applied to the inner surfaces of aircraft fuel tanks, and it is delaminating in two distinct zones of the fuel tanks. The most serious delamination occurs in the headspace area which is usually above the fuel layer. That is, where only vapors are present. The other zone is the sump areas where liquid water that separates from the fuel collects. In the intermediate zone, where only liquid fuel is in contact with the coating, no delamination has been observed.

It is believed that the reason the delaminations only occur in the headspace and the sump zones is the high concentrations of DiEGME in these zones. It is speculated that DiEGME at high concentrations causes the fuel tank coating to swell and eventually peel away from the substrate. DiEGME concentrates in the headspace zone because it is more volatile than the jet fuel (JP-8). DiEGME concentrates in the sump area because it is only partially soluble in jet fuel, whereas it is highly soluble in water. Therefore, when fuel containing DiEGME is in contact with water, the DiEGME preferentially partitions out of the fuel and into the water layer. Lab and field

testing has shown that DiEGME will partition into the water to a typical concentration of 50% by volume¹.

3.0 TECHNICAL APPROACH

Two fuel system icing inhibitors (FSII) were tested for compatibility with two US Air Force fuel tank coatings. One FSII was diethylene glycol monomethyl ether (DiEGME), which is the standard FSII currently in use in USAF jet fuel. The other FSII was triethylene glycol monomethyl ether (TriEGME), which is under study by the Air Force Research Laboratory's Fuels Branch as a possible replacement for DiEGME. One coating was formulated to meet the requirements of AMS-C-27725A, and the other was formulated to meet the requirements of BMS 10-39. Test panels were prepared by spray applying each coating onto 3" x 6" aluminum 2024 T-3 panels to a dry film thickness of 1 mil. Prior to coating application, the aluminum panels were cleaned, acid etched with an alcoholic phosphoric acid solution, and chemically treated with Alodine 1200S, which is a chromium chemical conversion coating surface treatment.

Compatibility was tested by immersing sets of three 3" x 6" coated panels in sealed glass containers with the solutions containing various concentrations of FSIIs and exposure conditions. Only one-half of each panel was submerged. This was done to assess the effects of the FSII in both the liquid phase and the vapor phase. In addition, a set of panels were exposed dry, in empty containers to the same environmental conditions as the immersed panels. The testing was conducted in six phases to address the various types of exposures expected in aircraft fuel tanks. Phases 1 and 2 involve exposure of FSII/water mixtures at high concentrations to simulate topcoat exposure in situations where water has collected in tank bottoms. Phases 3 and 4 involve exposure to a bottom layer of FSII/water and a top layer of fuel to simulate both water bottom and fuel exposure. Phases 5 and 6 involve exposure of vapor condensate surrogates with various concentrations of FSII to simulate exposure of topcoat in fuel tank ullage areas. The odd-numbered phases are high temperature exposures, while the even numbered phases are high/low temperature cycling exposures. The details of the six phases are as follows:

1. Phase 1 involved immersion in an 80/20 v/v solution of FSII/water at a constant temperature of 90° C for three different time periods: 1 week, 2 weeks, and 60 days. The solution concentration and exposure temperature were selected to match previous FSII compatibility testing conducted at the AFRL/RXSSO Coatings Technology Integration Office (CTIO), which represented the most severe exposure regime.

¹ W. Stevenson, et. al., Epoxy Paint Failure in B-52 Fuel Tanks Part I – Preliminary Development of a Model for the

2. Phase 2 involved immersions in a solution of the same concentration as Phase 1, but using a 24-hour exposure cycle: 16 hours at 90°C, then 2 hours at ambient, then 4 hours at -20°C, and finally, 2 hours at ambient before beginning the cycle again. The exposure length was 60 days. This exposure cycle was selected to simulate the cyclic nature of temperatures that an aircraft fuel tank would experience from being parked in the hot sun and then flying at altitude.
3. Phase 3 involved immersions in a mixture of jet fuel (Jet A1) with a 50/50 v/v solution of FSII/water. The jet fuel and FSII/water solution were added to the glass container such that one quarter of the panel was in the FSII/water phase, one quarter was in the fuel phase, and one half was in the vapor phase. The exposure was held constant at 60° C for a period of 60 days. This solution was selected to mimic the mixture of water and fuel contained in aircraft fuel tanks, where the water bottom contains a maximum concentration of 50% FSII. The temperature was reduced from the 90°C Phase 1 condition to 60°C because of safety concerns for the jet fuel. In addition, a small pinhole was made through the sealed lids of the containers as an additional safety concern for the jet fuel present. The pinholes did not appear to have caused any observable fluid loss from the containers after the 60-day exposure.
4. Phase 4 involved immersions in a mixture of the same make-up as Phase 3, using lids with pinholes, but used the following 24-hour cyclic exposure: 16 hours at 60°C, then 2 hours at ambient, then 4 hours at -20°C, and finally, 2 hours at ambient before beginning the cycle again. The exposure length was 60 days.
5. Phase 5 involved immersions in six different solutions containing different concentrations of FSII in a surrogate jet fuel, which approximated the fuel volatiles in the vapor phase, with no water present for 60 days at 60° C, using lids with pinholes. The concentrations of FSII that were selected were provided by the Air Force Research Laboratory's Fuels Branch as being the typical range of concentrations of each FSII that were found in the condensate from vapor over jet fuel that contained the prescribed level of FSII. The larger concentrations used for DiEGME are a reflection of its much higher volatility than TriEGME. The following FSII/jet fuel concentrations were tested:
 - a. 0.01% TriEGME
 - b. 0.05% TriEGME
 - c. 0.10% TriEGME
 - d. 0.10% DiEGME
 - e. 0.80% DiEGME
 - f. 1.50% DiEGME

6. Phase 6 involved testing the medium range FSII concentration from Phase 5 using the cyclic exposure conditions used for Phase 4. The solutions tested for Phase 6 were:

- a. 0.05% TriEGME
- b. 0.80% DiEGME

After each exposure period was completed, the panels were removed from the containers, visually evaluated for coating defects, and then gently cleaned with 10% Brulin 815GD, then thoroughly rinsed with warm tap water, followed by a final rinse in DI water, then blotted dry with a clean cloth, then allowed to dry for 2 hours at room temperature. After two hours, the coatings were tested for color change, softening, and loss of adhesion.

Color change was tested in accordance with ASTM E 1311 *Standard Test Method for Reflectance Factor and Color by Spectrophotometer Using Hemispherical Geometry*. Prior to immersion, the color of each panel in both the vapor phase area and the fluid phase area was measured using a Gretag-Macbeth ColorEye 1700A spectrophotometer with a 10° observer, a D65 light source, and specular component included. Then after exposure and cleaning, the same areas were measured for final color. The color measurements were made using the tri-coordinate CIELAB color system in which L* is a measure of lightness/darkness, a* is a measure of greenness/redness, and b* is a measure of blueness/yellowness. Deltas for each value were calculated by subtracting each initial measurement from the final measurements. These deltas were then used to calculate the total overall color difference which is referred to as ΔE and is calculated as the square root of the sum of the squares of the L*, a*, and b* color differences. It is generally accepted that a ΔE of 1.0 represents the smallest change in color that the human eye can discern. For fluid exposure testing of Air Force coatings, acceptable performance is a color change ≤ 3 .

Softening was tested in accordance with ASTM D 3363 *Standard Test Method for Film Hardness by Pencil Test*, using a set of calibrated Turquoise pencil leads. The set contains a series of 14 pencil leads in which each lead is said to differ from the next one in the series by “one pencil lead”. The pencil leads are ranked from softest to hardest according to the following scale:

6B - 5B - 4B - 3B - 2B - B - HB - F - H - 2H - 3H - 4H - 5H - 6H
Softest → → Hardest

To facilitate graphing, the pencil hardness data was converted to numbers, using an analogous 0-14 number scale where 6B equals 0, and 6H equals 14. Because this is a destructive test, the

hardness of the immersed panels was compared to the hardness of the dry panels to assess softening. Because the repeatability of the hardness test is ± 1 pencil lead, a difference of ≥ 2 pencil leads was used as the criterion for softening.

Loss of Adhesion was tested in accordance with Method B of ASTM D 3359 *Standard Test Methods for Measuring Adhesion by Tape Test*. Because this is a destructive test, the adhesion of the dry exposed panels was used as the initial adhesion value and was compared to the exposed panel to assess any adhesion losses. Method B of ASTM D 3359 uses the rating scale shown in **Figure 1** to quantify adhesion.

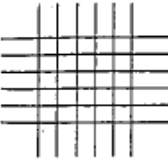
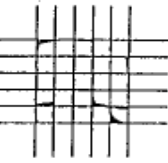
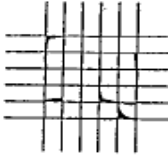
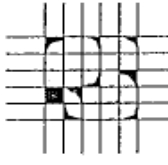
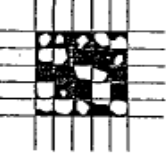
CLASSIFICATION OF ADHESION TEST RESULTS		
CLASSIFICATION	PERCENT AREA REMOVED	SURFACE OF CROSS-CUT AREA FROM WHICH FLAKING HAS OCCURRED FOR SIX PARALLEL CUTS AND ADHESION RANGE BY PERCENT
5B	0% None	
4B	Less than 5%	
3B	5 - 15%	
2B	15 - 35%	
1B	35 - 65%	
0B	Greater than 65%	

Figure 1: ASTM D 3359 Adhesion Rating Scale.

4.0 RESULTS

4.1 Phase 1 Results

As described above, Phase 1 involved exposing panels to an 80/20 (by volume) mixture of FSII/water at 90°C for periods of 1 week, 2 weeks, and 60 days.

4.1.1 Phase 1 Visual Examinations (Figures A3-A14; Appendix)

Photos of the control panels are shown in the Appendix (Figures A1, A2).

4.1.1.1 Visual Examination of 7-Day Exposures (Figures A3, A4, A9, A10; Appendix)

Control Panels: The dry control panels were visually unchanged after the 7-day exposure period with no delamination or other film defects noticed.

BMS 10-39 Coating: Both DiEGME and TriEGME caused the complete removal of the BMS 10-39 in both the vapor phase, and the liquid phase. However, the manner of coating removal was different. The DiEGME appeared to cause the depolymerization of the epoxy polymer because there was no evidence of delaminated coating pieces in the solution in the jar, and the solution was cloudy with a powdery substance on the bottom. TriEGME, on the other hand, caused delamination of the coating as evidenced by a clear solution with pieces of intact film in the jar. In addition, both FSIIIs caused corrosion pitting on the panels. The corrosion occurred only on the vapor-exposed sides of the test panels, and only on the side that was coated. The uncoated backs of the panels had no corrosion. The extent of the corrosion pitting was slightly greater on the DiEGME exposed panels than on the TriEGME exposed panels (Figures A3-A8).

AMS-C-27725A Coating: The effects that both FSIIIs had on the AMS-C-27725A coating were less severe.

Effects on the vapor-exposed part of the panels: Neither FSII caused any coating loss, but the DiEGME caused a small amount of blistering over about 25% of the exposed area. There was no coating loss or blistering on the TriEGME exposed panels. Both FSIIIs caused a color change with the color of the DiEGME exposed panels appearing to have yellowed with some areas having lightened and some areas having darkened. The color of the TriEGME exposed panels appeared to have slightly darkened. Neither FSII caused any corrosion.

Effects on the liquid-exposed part of the panels: DiEGME caused about a 25% coating loss and had moderate blistering over about 40% of the exposed surface. There was no coating loss

and no blistering on the TriEGME exposed panels. Both FSIIIs also caused a color change with the DiEGME panels appearing to have yellowed, while the TriEGME exposed panels darkened and shifted toward a light tan color. Neither FSII caused any corrosion.

4.1.1.2 Visual Examination of 14-Day Exposures (Figures A5, A6, A11, & A12; Appendix)

Control Panels: The dry control panels were visually unchanged after the 14-day exposure period with no delamination or other film defects noticed.

Effects on the BMS 10-39 Coating: Both DiEGME and TriEGME caused the complete removal of the BMS 10-39 in both the vapor phase and the liquid phase. As with the 7-day immersion panels, DiEGME appeared to have caused the depolymerization of the epoxy polymer, while TriEGME caused simple delamination. Both FSIIIs also caused corrosion pitting which only occurred on the coated side of the vapor-exposed part of the panels. The corrosion pitting was greater for the 14-day exposure than the 7-day exposure, and the extent was equivalent for both FSIIIs.

Effects on AMS-C-27725A coating:

Effects on the vapor-exposed part of the panels: Neither FSII caused any film loss. DiEGME caused blistering over about 50% of the exposed surface; whereas TriEGME caused no blistering. Both FSIIIs caused the same apparent color changes which were a change to light tan. Both FSIIIs also caused corrosion pitting, with the more corrosion on the TriEGME exposed panels than on the DiEGME exposed panels.

Effects on the liquid-exposed part of the panels: Neither FSII caused any film losses or blistering. Both FSIIIs caused the same color change which was a change to a medium tan color that was noticeably darker than the vapor-exposed color change. Neither FSII caused any corrosion in the liquid-exposed area.

4.1.1.3 Visual Examination of 60-Day Exposures (Figures A7, A8, A13, & A14; Appendix)

Control Panels: The dry control panels were visually unchanged after the 60-day exposure period with no delamination or other film defects noticed.

Effects on the BMS 10-39 Coating: Both DiEGME and TriEGME caused the complete removal of the BMS 10-39 in both the vapor phase, and the liquid phase. As with the 7-day and 14-day immersion panels, DiEGME appeared to have caused the depolymerization of the epoxy polymer, while TriEGME appeared to have caused simple delamination. Both FSIIIs also caused

extensive corrosion pitting which only occurred on the coated side of the vapor-exposed part of the panels. The corrosion pitting was much greater than for the 7-day and 14-day exposures, and the extent of the corrosion was greater for DiEGME.

Effects on AMS-C-27725A coating:

Effects on the vapor-exposed part of the panels: TriEGME caused a 70% coating loss, and DiEGME caused a 50% coating loss. Both FSIIIs darkened the color of the coating to a deep tan, with the DiEGME panels being significantly darker. Both FSIIIs also caused corrosion pitting, which was more extensive than for the 14-day exposures. DiEGME caused the greatest extent of corrosion, with the pitting being so concentrated as to appear to be general corrosion over large areas of the panels.

Effects on the liquid-exposed part of the panels: TriEGME caused a 50% coating loss, and DiEGME caused a 10% coating loss. Both FSIIIs caused similar color changes as noted above for the vapor-exposed side. TriEGME did not cause any corrosion; however, DiEGME caused corrosion pitting over about 10% of the panel area.

4.1.2 Phase 1 Color Measurement Results

Color changes for the 7-day and 14-day exposures for the AMS-C-27725A coated panels are presented in **Figure 2**, and summarized in **Tables 1** and **2**. No data are available for the BMS 10-39 test panels due to complete removal of that coating. Also, no data were measured for the 60-day AMS-C-27725A panels due to coating removal and extensive corrosion. Both FSIIIs caused about the same total color change (ΔE) in the AMS-C-27725A coating at 7-days and 14-days exposures. The largest color changes occurred in the liquid phases, and the 14-day exposures produced the largest color changes, as expected. The only notable difference between the DiEGME exposed panels and the TriEGME exposed panels occurred in the 7-day exposure panels with the DiEGME showing a strong yellow shift that was not matched in the TriEGME panels. The magnitude of the recorded color changes is very large, being 3-5 times larger than the accepted color change for fluid immersions of Air Force coatings which is a ΔE of 3.0.

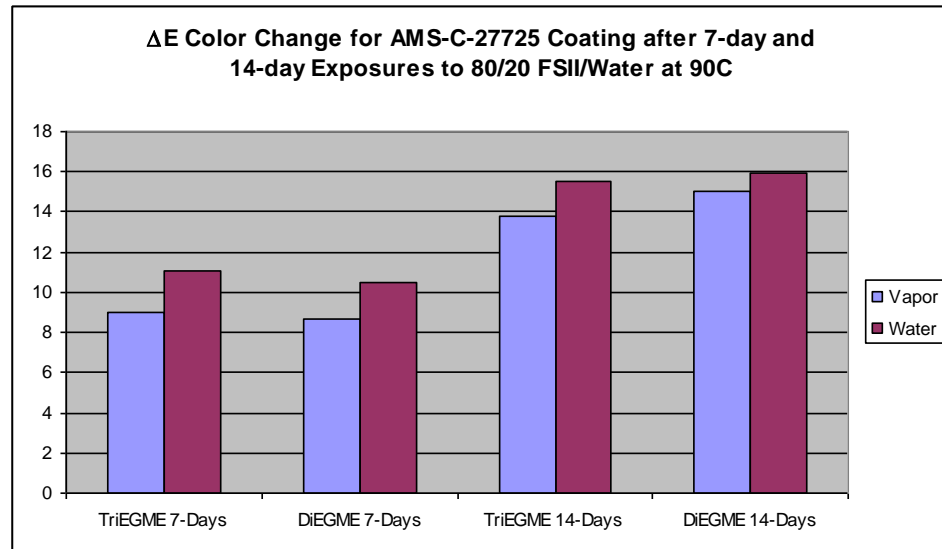


Figure 2: Phase 1 Color Change.

Table 1: Color Change after 7-Days Exposure.

Panel Location	FSII	ΔL^*	Δa^*	Δb^*	ΔE
Vapor	DiEGME	3.4	5.9	5.4	8.7
Vapor	TriEGME	-5.3	7.3	0.4	9.0
Liquid	DiEGME	1.9	8.8	5.4	10.5
Liquid	TriEGME	-7.2	8.2	-2.5	11.1

Table 2: Color Change after 14-Days Exposure.

Panel Location	FSII	ΔL^*	Δa^*	Δb^*	ΔE
Vapor	DiEGME	-9.1	12.0	-0.1	15.0
Vapor	TriEGME	-8.0	11.1	-2.0	13.8
Liquid	DiEGME	-10.0	12.2	-1.7	15.9
Liquid	TriEGME	-9.3	11.8	-3.8	15.5

4.1.3 Phase 1 Softening Results

The softening data for the 7-day and 14-day exposures for the AMS-C-27725A coated panels are presented in **Figure 3**, and summarized in **Tables 3** and **4**. No data were obtained from the BMS 10-39 test panels due to complete removal of that coating. Also, no data were measured for the 60-day AMS-C-27725A panels due to coating removal and extensive corrosion. For each exposure period and for each panel position, DiEGME produced significantly more softening than TriEGME. The 7-day DiEGME exposures had the greatest softening and were softer than

the softest pencil lead in the set. It is unknown why these panels would soften more than the 14-day panels.

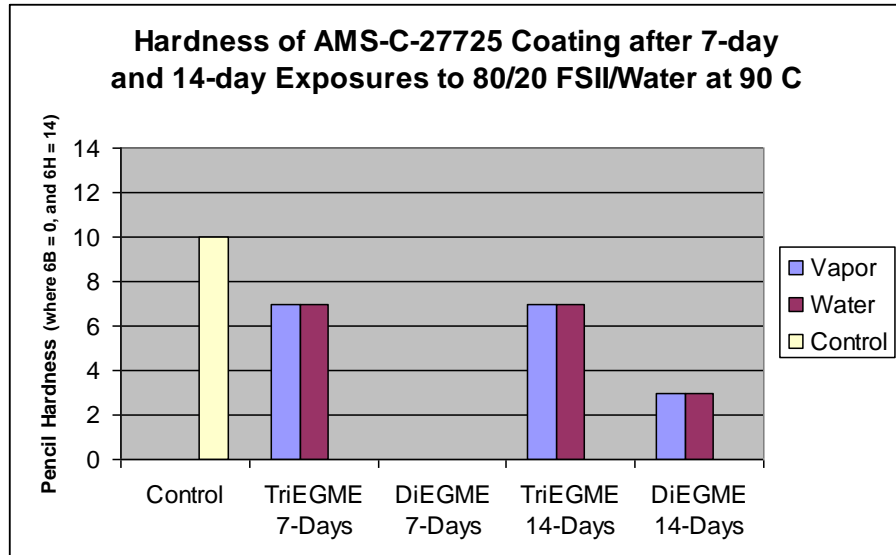


Figure 3: Phase 1 Softening.

Table 3: Phase 1 Softening after 7 Days.

Panel Location	FSII	Hardness	Softening
N/A	Control	2H	N/A
Vapor	DiEGME	< 6B	> 9 leads
Vapor	TriEGME	HB	3 leads
Liquid	DiEGME	< 6B	> 9 leads
Liquid	TriEGME	HB	3 leads

Table 4: Phase 1 Softening after 14 Days.

Panel Location	FSII	Hardness	Softening
N/A	Control	2H	N/A
Vapor	DiEGME	4B	7 leads
Vapor	TriEGME	HB	3 leads
Liquid	DiEGME	4B	7 leads
Liquid	TriEGME	HB	3 leads

4.1.4 Phase 1 Adhesion Loss Results

The adhesion loss data for the 7-day and 14-day exposures of the AMS-C-27725A coated panels are presented in **Figure 4**, and summarized in **Tables 5** and **6**. No data are available for any of the BMS 10-39 test panels due to complete removal of that coating. Also, no data were obtained for the 60-day AMS-C-27725A panels due to coating removal and extensive corrosion. Adhesion is rated on a scale of 5B to 0B with 5B representing the highest adhesion. As can be seen from the data, DiEGME caused an adhesion loss in both the vapor-exposed side and the liquid-exposed side after 7-days exposure; whereas, TriEGME panels had no adhesion losses. For the 14-day exposure, both FSIIIs caused an adhesion loss on the vapor-exposed side, and no adhesion loss on the immersed sides.

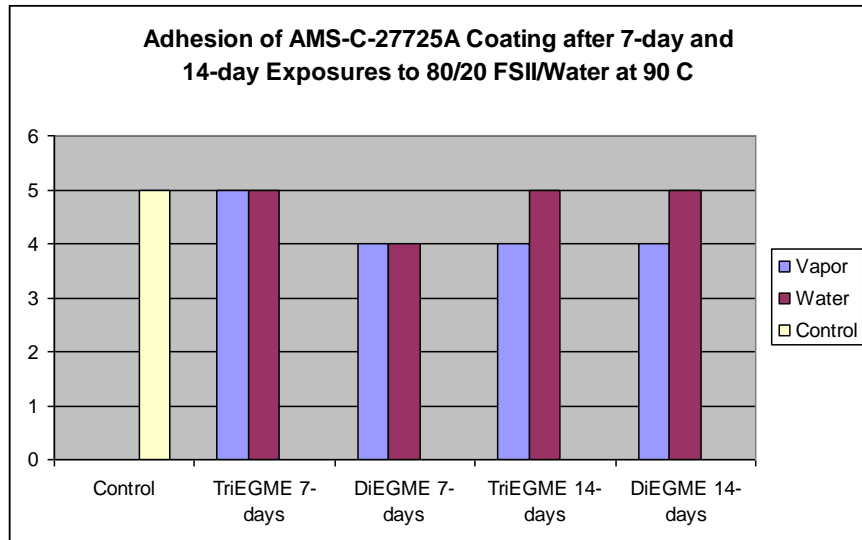


Figure 4: Phase 1 Adhesion Loss.

Table 5: Adhesion Loss after 7-Day Exposure.

Panel Location	FSII	Adhesion Rating	Adhesion Loss?
N/A	Control	5B	N/A
Vapor	DiEGME	4B	Slight
Vapor	TriEGME	5B	No
Liquid	DiEGME	4B	Slight
Liquid	TriEGME	5B	No

Table 6: Adhesion Loss after 14-Day Exposure.

Panel Location	FSII	Adhesion Rating	Adhesion Loss?
N/A	Control	5B	N/A
Vapor	DiEGME	4B	Slight
Vapor	TriEGME	4B	Slight
Liquid	DiEGME	5B	No
Liquid	TriEGME	5B	No

4.2 Phase 2 Results

As described above, Phase 2 involved exposing panels to an 80/20 (by volume) mixture of FSII/water in a cyclic environment (16 hours @ 90°C/2 hours ambient/4 hours at -20°C/2 hours ambient) for 60 days.

4.2.1 Phase 2 Visual Examinations (Figures A15-A18; Appendix)

Control Panels: The dry control panels were visually unchanged after the 60-day exposure period with no delamination or other film defects noticed.

Effects on the BMS 10-39 Coating: Both DiEGME and TriEGME completely removed the BMS 10-39 in both the vapor phase, and the liquid phase. As with the coating losses observed in Phase 1, DiEGME appeared to have caused the depolymerization of the epoxy polymer, while TriEGME appeared to have caused simple delamination. Both FSII's also caused corrosion

pitting which, as in Phase 1, only occurred on the coated side of the vapor-exposed part of the panels. The corrosion pitting was greater for DiEGME than for TriEGME.

Effects on AMS-C-27725A Coating:

Effects on the vapor-exposed part of the panels: Both FSIIIs caused about a 5% coating loss, and darkened the coating to a deep tan. Both FSIIIs also caused corrosion pitting, which was not as severe as the 60-day exposure from Phase 1. DiEGME caused significantly more corrosion than TriEGME.

Effects on the liquid-exposed part of the panels: Both FSIIIs caused about a 5% coating loss, and darkened the coating to a deep tan color. There was no corrosion on the TriEGME panels, but the DiEGME panels had considerable corrosion pitting.

4.2.2 Phase 2 Color Measurement Results

No color data were taken due to complete removal of the BMS 10-39 coating, and extensive corrosion on the AMS-C-27725A test panels.

4.2.3 Phase 2 Softening Results

No hardness data were taken due to complete removal of the BMS 10-39 coating, and extensive corrosion on the AMS-C-27725A test panels.

4.2.4 Phase 2 Adhesion Loss Results

No adhesion data were taken due to complete removal of the BMS 10-39 coating, and extensive corrosion on the AMS-C-27725A test panels.

4.3 Phase 3 Results

As described above, Phase 3 involved exposing panels to a 25/25/50 (by volume) mixture of FSII/water/jet fuel at 60°C for 60 days.

4.3.1 Phase 3 Visual Examinations (Figures A19-A22; Appendix)

Control Panels: The dry control panels were visually unchanged after the 60-day exposure period with no delamination or other film defects noticed.

Effects on the BMS 10-39 Coating: No coating loss was observed for either FSII. Both FSIIIs caused a slight color change in the water bottom area of the test panels, with the color change

being more pronounced in coatings that had been exposed to the TriEGME mixture. TriEGME caused the fuel exposed area and the vapor exposed area to slightly darken to a tan coloration; whereas, DiEGME had no effect in these areas. Neither FSII caused any corrosion or blistering.

Effects on AMS-C-27725A Coating: No coating loss was observed for either FSII. Both FSII caused a slight color change in the water bottom area of the test panels with the color change by TriEGME being more pronounced. Neither FSII affected the fuel exposed areas nor the vapor exposed areas. Neither FSII caused any corrosion or blistering.

4.3.2 Phase 3 Color Measurement Results

TriEGME caused a greater color change in the BMS 10-39 coating than DiEGME, with an average ΔE of 2.9 in the three exposure areas (water bottom, jet fuel, vapor) compared to an average ΔE of 0.6 for DiEGME. Both were below the generally accepted color change of 3.0. TriEGME also caused a greater color change in the AMS-C-27725A coating with an average ΔE of 2.6 compared to a ΔE of 1.8 for DiEGME. The data are presented in **Figure 5** and **Table 7**.

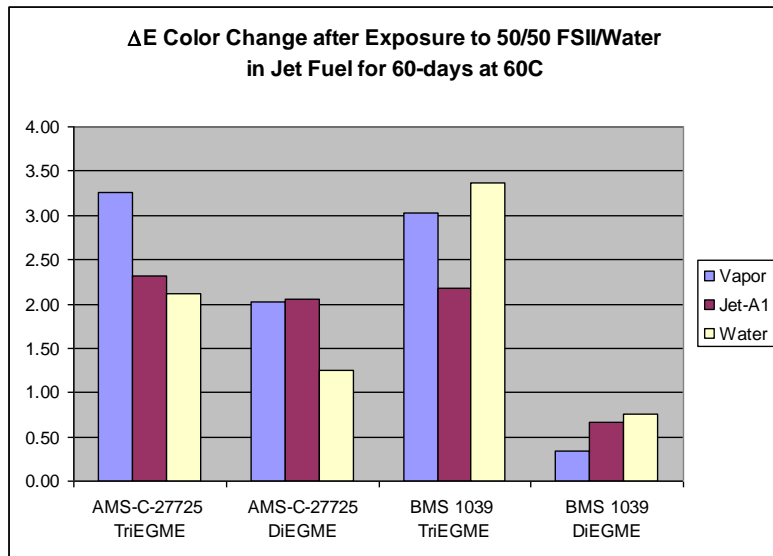


Figure 5: Phase 3 Color Change.

Table 7: Phase 3 Color Change.

Coating	FSII	ΔE Color Change		
		Vapor	Jet Fuel	Water Bottom
AMS-C-27725A	TriEGME	3.25	2.32	2.12
AMS-C-27725A	DiEGME	2.02	2.05	1.24
BMS 10-39	TriEGME	3.03	2.17	3.37
BMS 10-39	DiEGME	0.33	0.67	0.75

4.3.3 Phase 3 Softening Results

Effects on the BMS 10-39 Coating: Both FSIIIs softened the BMS 10-39 coating. TriEGME caused a little more softening (two pencil leads) in the section of coating that was exposed to vapor or fuel, while DiEGME caused more softening (two pencil leads) in the water bottom exposed area.

Effects on AMS-C-27725A Coating: TriEGME did not soften the AMS-C-27725A coating (based on the criterion that softening is represented by a change in pencil hardness of two or more pencil leads). DiEGME caused some softening on the water bottom exposed area, but did not cause any softening in the other two areas.

The data for both coatings are presented in **Figure 6** and **Tables 8-9**.

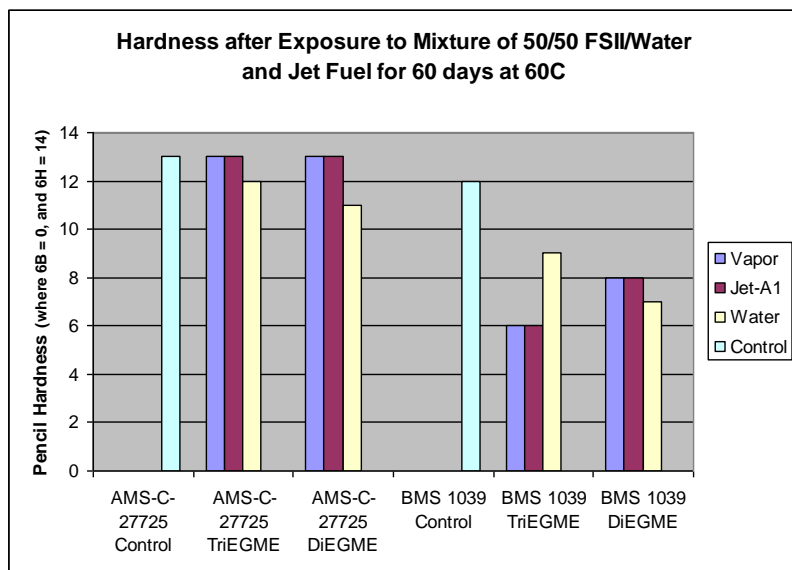


Figure 6: Phase 3 Softening.

Table 8: Phase 3 Softening for BMS 10-39

Panel Location	FSII	Pencil Hardness	Softening
N/A	Control	4H	N/A
Vapor	DiEGME	F	4 leads
Vapor	TriEGME	B	6 leads
Jet Fuel	DiEGME	F	4 leads
Jet Fuel	TriEGME	B	6 leads
Water	DiEGME	HB	5 leads
Water	TriEGME	H	3 leads

Table 9: Phase 3 Softening for AMS-C-27725

Panel Location	FSII	Pencil Hardness	Softening
N/A	Control	5H	N/A
Vapor	DiEGME	5H	none
Vapor	TriEGME	5H	none
Jet Fuel	DiEGME	5H	none
Jet Fuel	TriEGME	5H	none
Water	DiEGME	3H	2 leads
Water	TriEGME	4H	none

4.3.4 Phase 3 Adhesion Loss Results

Neither FSII reduced the adhesion of the coatings. The data are presented in **Figure 7** and **Tables 10-11**.

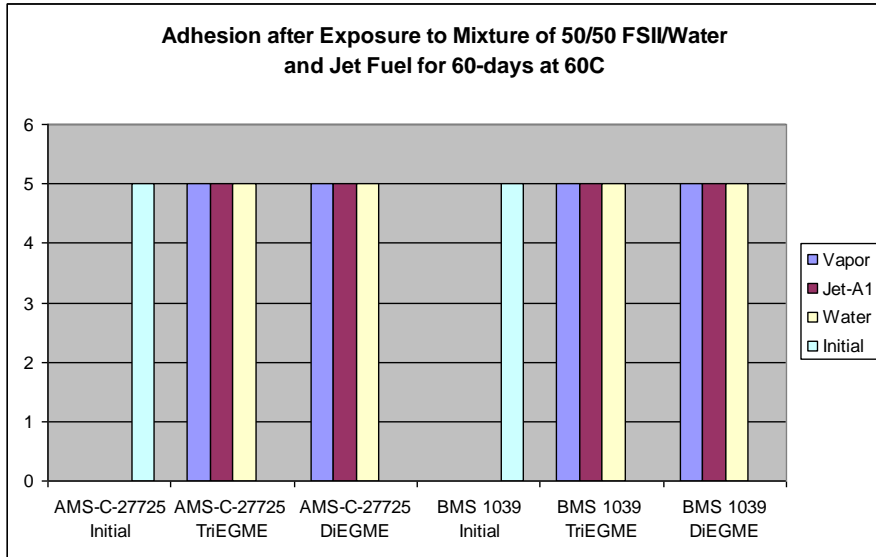


Figure 7: Phase 3 Adhesion Loss

Table 10: Phase 3 Adhesion Loss - BMS 10-39.

Panel Location	FSII	Adhesion Rating	Adhesion Loss?
N/A	Control	5B	N/A
Vapor	DiEGME	5B	No
Vapor	TriEGME	5B	No
Jet Fuel	DiEGME	5B	No
Jet Fuel	TriEGME	5B	No
Water	DiEGME	5B	No
Water	TriEGME	5B	No

Table 11: Phase 3 Adhesion Loss - AMS-C-27725.

Panel Location	FSII	Adhesion Rating	Adhesion Loss?
N/A	Control	5B	N/A
Vapor	DiEGME	5B	No
Vapor	TriEGME	5B	No
Jet Fuel	DiEGME	5B	No
Jet Fuel	TriEGME	5B	No
Water	DiEGME	5B	No
Water	TriEGME	5B	No

4.4 Phase 4 Results

As described above, Phase 4 involved exposing panels to a 25/25/50 (by volume) mixture of FSII/water/jet fuel in a cyclic environment (16 hours @ 60°C/2 hours ambient/4 hours at -20°C/2 hours ambient) for 60 days.

4.4.1 Phase 4 Visual Examinations (Figures A23-A26; Appendix)

Control Panels: The dry control panels were visually unchanged after the 60-day exposure period with no delamination or other film defects noticed.

Effects on the BMS 10-39 Coating: No coating loss was observed for either FSII. Both FSIIIs caused a slight color change in the water bottom area of the test panels, with the color change of coatings exposed to the TriEGME mixture being more pronounced. TriEGME caused the fuel exposed area and the vapor exposed area to slightly darken to a tan color; whereas DiEGME had no effect in these areas. Neither FSII caused any corrosion or blistering.

Effects on AMS-C-27725A Coating: No coating loss was observed for either FSII. Both FSIIIs caused a slight color change in the water bottom area of the test panels with the color change more pronounced in the TriEGME solution. Neither FSII affected the fuel exposed areas nor the vapor exposed areas. Neither FSII caused any corrosion or blistering.

4.4.2 Phase 4 Color Measurement Results

The color data for both coatings are presented in **Figure 8** and **Table 12**.

Effects on the BMS 10-39 Coating: Neither FSII caused a color change on the BMS 10-39 coating greater than the allowable limit of 3.0. TriEGME caused a greater color change in all of the exposure areas, averaging a ΔE of 1.6 compared to an average ΔE of 0.4 for DiEGME.

Effects on AMS-C-27725A Coating: The effects of both FSIIIs were greater on the AMS-C-27725A coating, but were still less than the allowable limit of 3.0. TriEGME caused a greater color change in all of the exposure areas, averaging a ΔE of 2.3 compared to an average ΔE of 1.0 for DiEGME.

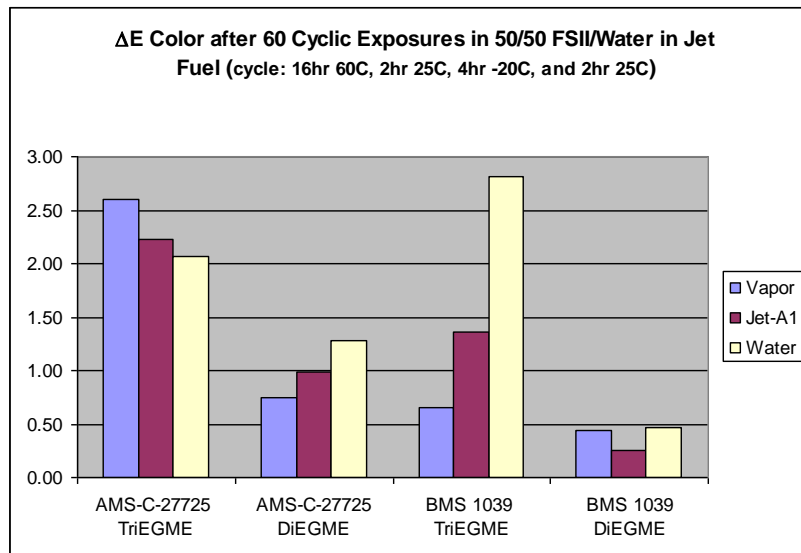


Figure 8: Phase 4 Color Change.

Table 12: Phase 4 Color Change.

Coating	FSII	ΔE Color Change		
		Vapor	Jet Fuel	Water Bottom
AMS-C-27725A	TriEGME	2.6	2.2	2.1
AMS-C-27725A	DiEGME	0.7	1.0	1.3
BMS 10-39	TriEGME	0.7	1.4	2.8
BMS 10-39	DiEGME	0.4	0.3	0.5

4.4.3 Phase 4 Softening Results

The data for both coatings are presented in **Figure 9** and **Tables 13-14**.

Effects on the BMS 10-39 Coating: Both FSII's caused a softening of three pencil leads for the BMS 10-39 coating. The hardness reduced from a rating of H to a rating of HB.

Effects on AMS-C-27725A Coating: Neither FSII caused softening of the AMS-C-27725A coating.

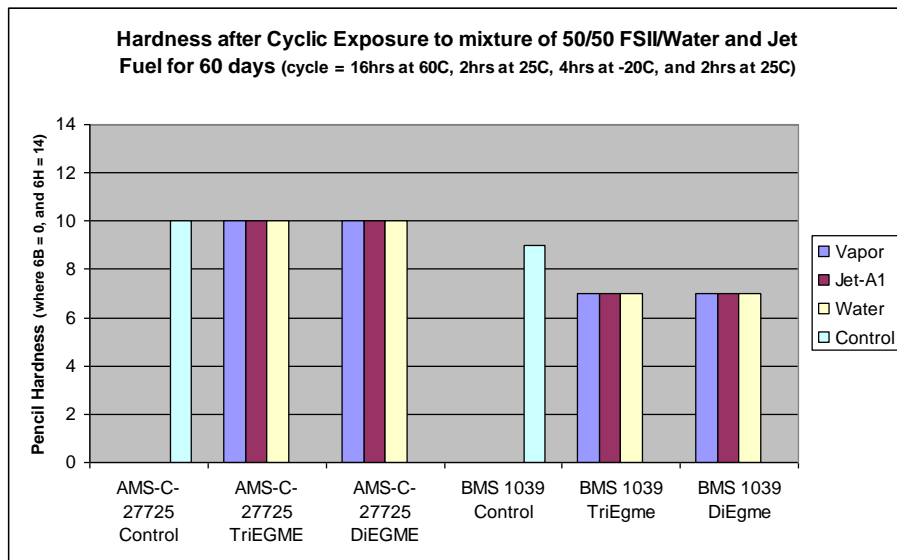


Figure 9: Phase 4 Softening.

Table 13: Phase 4 Softening for BMS 10-39.

Panel Location	FSII	Pencil Hardness	Softening
N/A	Control	H	N/A
Vapor	DiEGME	HB	3 leads
Vapor	TriEGME	HB	3 leads
Jet Fuel	DiEGME	HB	3 leads
Jet Fuel	TriEGME	HB	3 leads
Water	DiEGME	HB	3 leads
Water	TriEGME	HB	3 leads

Table 14: Phase 4 Softening for AMS-27725A.

Panel Location	FSII	Pencil Hardness	Softening
N/A	Control	2H	N/A
Vapor	DiEGME	2H	none
Vapor	TriEGME	2H	none
Jet Fuel	DiEGME	2H	none
Jet Fuel	TriEGME	2H	none
Water	DiEGME	2H	none
Water	TriEGME	2H	none

4.4.4 Phase 4 Adhesion Loss Results

Neither FSII caused any adhesion losses on the test coatings. The data are presented in **Figure 10** and **Tables 15-16**.

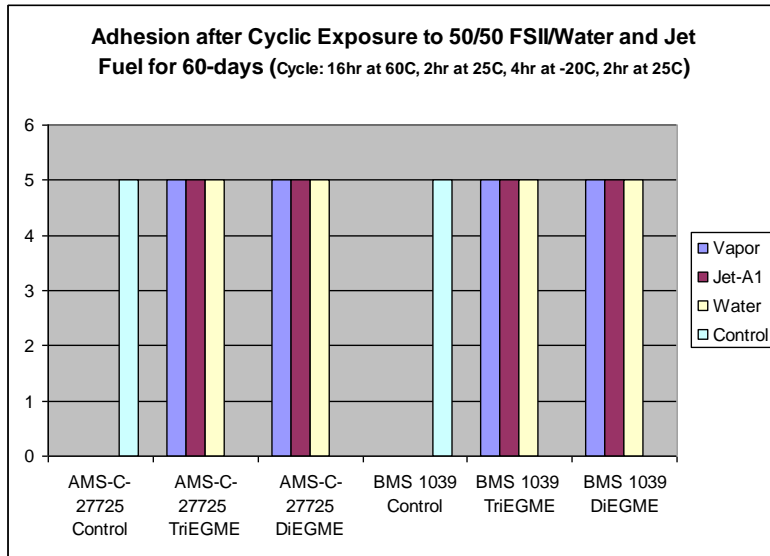


Figure 10: Phase 4 Adhesion Loss.

Table 15: Phase 4 Adhesion Loss - BMS 10-39.

Panel Location	FSII	Adhesion Rating	Adhesion Loss?
N/A	Control	5B	N/A
Vapor	DiEGME	5B	no
Vapor	TriEGME	5B	no
Jet Fuel	DiEGME	5B	no
Jet Fuel	TriEGME	5B	no
Water	DiEGME	5B	no
Water	TriEGME	5B	no

Table 16: Phase 4 Adhesion Loss AMS-C-27725A.

Panel Location	FSII	Adhesion Rating	Adhesion Loss?
N/A	Control	5B	N/A
Vapor	DiEGME	5B	no
Vapor	TriEGME	5B	no
Jet Fuel	DiEGME	5B	no
Jet Fuel	TriEGME	5B	no
Water	DiEGME	5B	no
Water	TriEGME	5B	no

4.5 Phase 5 Results

As described previously, Phase 5 involved exposing panels to mixtures of FSII and water at 60°C for 60 days

4.5.1 Phase 5 Visual Examinations (Figures A27-A38; Appendix)

Control Panels: The dry control panels were visually unchanged after the 60-day exposure period with no delamination or other film defects noticed.

Effects on the BMS 10-39 Coating: No coating loss, corrosion, or blistering was observed for either FSII. Neither FSII caused any noticeable color changes on the test panels.

Effects on AMS-C-27725A Coating: No coating loss, corrosion, or blistering was observed for either FSII. Neither FSII caused any noticeable color changes on the test panels.

4.5.2 Phase 5 Color Measurement Results

The data for both coatings are presented in Figures 11-12 and Tables 17-18.

Effects on the BMS 10-39 Coating: Neither FSII caused a significant color change for any of the six solution concentrations used to test the BMS 10-39 coating. All of the measured color changes were significantly below a ΔE of 3.0. The largest ΔE for TriEGME was 0.3 and the largest ΔE for DiEGME was 0.5.

Effects on AMS-C-27725A Coating: Both FSII caused greater color changes for the AMS-C-27725A coating, but the ΔE values were always below the allowable limit of 3.0. At a FSII concentration level of 0.10%, the average ΔE for TriEGME was 2.0 while the average ΔE for DiEGME was 1.5.

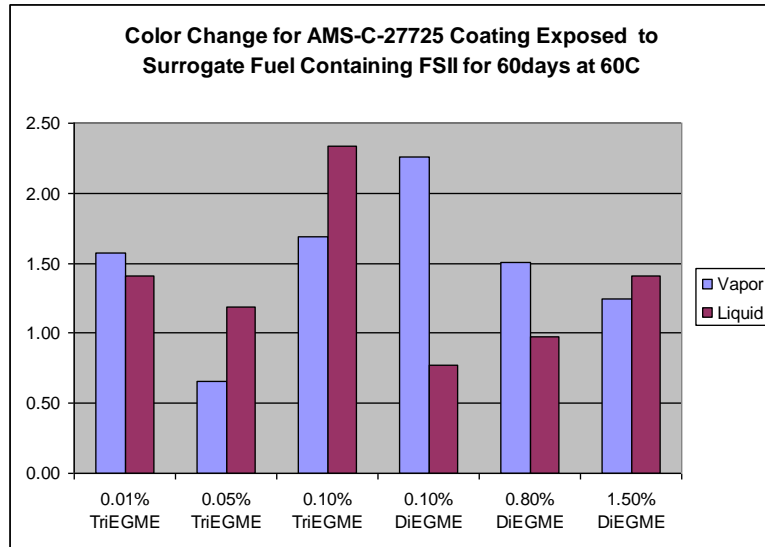


Figure 11: Phase 5 Color Change for BMS 10-39.

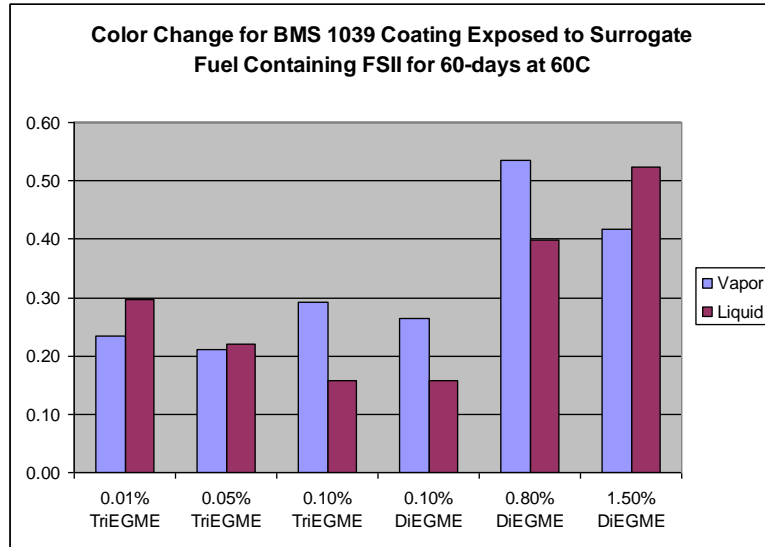


Figure 12: Phase 5 Color Change for AMS-C-27725A.

Table 17: Phase 5 Color Change - BMS 10-39.

Coating	FSII	ΔE Color Change	
		Vapor	Fuel
BMS 10-39	0.01% TriEGME	0.2	0.3
BMS 10-39	0.05% TriEGME	0.2	0.2
BMS 10-39	0.10% TriEGME	0.3	0.2
BMS 10-39	0.10% DiEGME	0.3	0.2
BMS 10-39	0.80% DiEGME	0.5	0.4
BMS 10-39	1.50% DiEGME	0.4	0.5

Table 18: Phase 5 Color Change - AMS-C-27725A.

Coating	FSII	ΔE Color Change	
		Vapor	Fuel
AMS-C-27725A	0.01% TriEGME	1.6	1.4
AMS-C-27725A	0.05% TriEGME	0.6	1.2
AMS-C-27725A	0.10% TriEGME	1.7	2.3
AMS-C-27725A	0.10% DiEGME	2.3	0.8
AMS-C-27725A	0.80% DiEGME	1.5	1.0
AMS-C-27725A	1.50% DiEGME	1.3	1.4

4.5.3 Phase 5 Softening Results

The data for both coatings are presented in **Figures 13-14** and **Tables 19-20**.

Effects on the BMS 10-39 Coating: All of the FSII solutions softened the BMS 10-39 coating. The three TriEGME concentrations caused a softening of two pencil leads. The 0.10% DiEGME solution also caused a two-pencil lead softening, but the other two DiEGME concentrations caused greater softening, with the 0.80% solution causing softening of four pencil leads, and the 1.50% solution causing softening of five pencil leads.

Effects on AMS-C-27725A Coating: All of the FSII solutions caused the same level of softening of the AMS-C-27725A coating, which was three pencil leads.

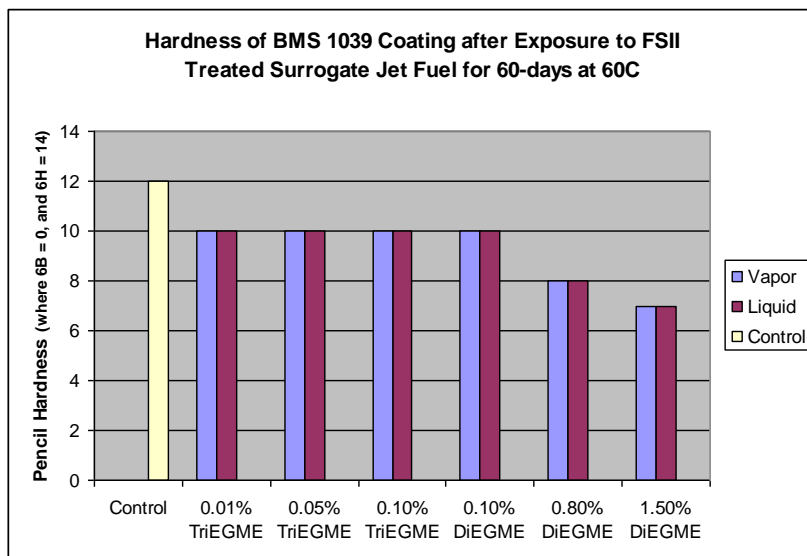


Figure 13: Phase 5 Softening for BMS 10-39.

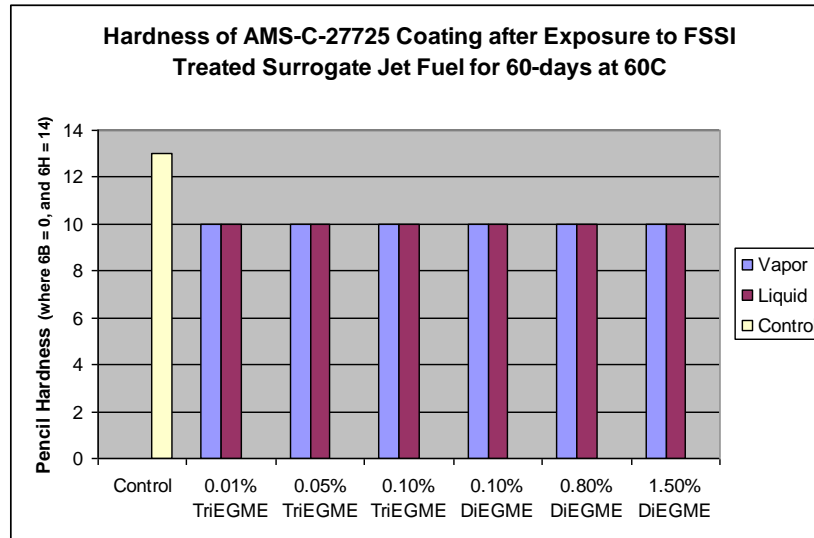


Figure 14: Phase 5 Softening for AMS-C-27725A.

Table 19: Phase 5 Softening - BMS 10-39.

FSII	Vapor Phase		Fuel Phase	
	Hardness	Softening	Hardness	Softening
Control	4H	N/A	4H	N/A
0.01% TriEGME	2H	2 leads	2H	yes
0.05% TriEGME	2H	2 leads	2H	yes
0.10% TriEGME	2H	2 leads	2H	yes
0.10% DiEGME	2H	2 leads	2H	yes
0.80% DiEGME	F	4 leads	F	yes
1.50% DiEGME	HB	5 leads	HB	yes

Table 20: Phase 5 Softening - AMS-C-27725A.

FSII	Vapor Phase		Fuel Phase	
	Hardness	Softening	Hardness	Softening
Control	5H	N/A	5H	N/A
0.01% TriEGME	2H	3 leads	2H	3 leads
0.05% TriEGME	2H	3 leads	2H	3 leads
0.10% TriEGME	2H	3 leads	2H	3 leads
0.10% DiEGME	2H	3 leads	2H	3 leads
0.80% DiEGME	2H	3 leads	2H	3 leads
1.50% DiEGME	2H	3 leads	2H	3 leads

4.5.4 Phase 5 Adhesion Loss Results

Neither of the FSII caused any adhesion losses on the test coatings. The data are presented in **Figures 15-16** and **Tables 21-22**.

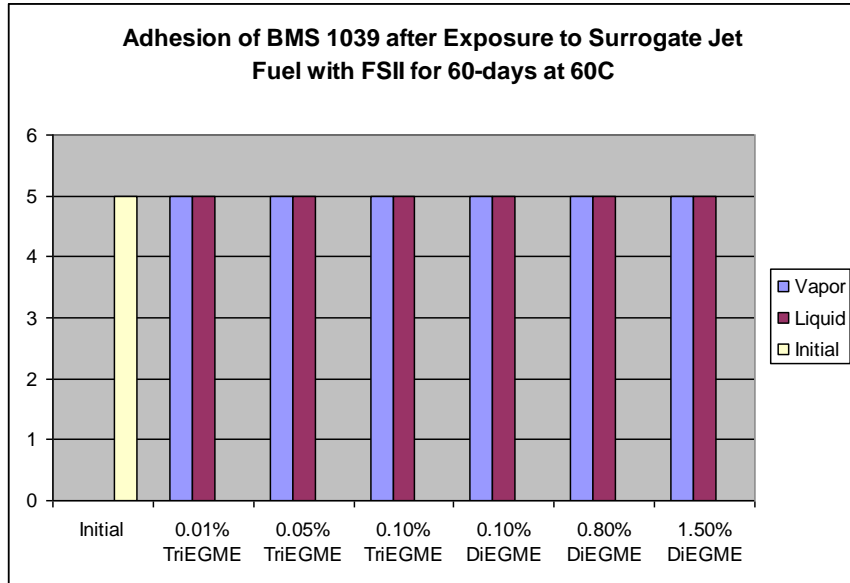


Figure 15: Phase 5 Adhesion Loss for BMS 10-39.

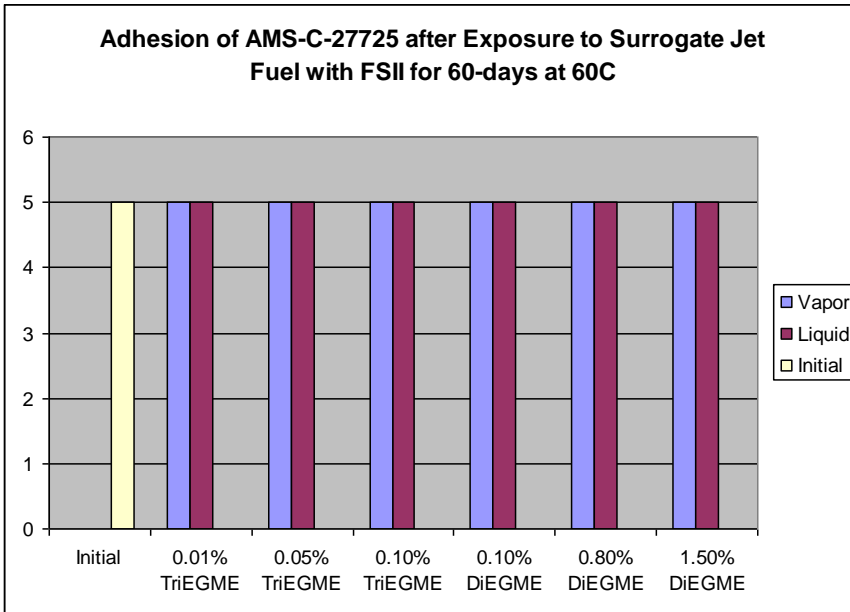


Figure 16: Phase 5 Adhesion Loss for AMS-C-27725A.

Table 21: Phase 5 Adhesion Loss - BMS 10-39.

FSII	Vapor Phase		Fuel Phase	
	Adhesion	Loss?	Adhesion	Loss?
Control	5B	N/A	5B	N/A
0.01% TriEGME	5B	none	5B	none
0.05% TriEGME	5B	none	5B	none
0.10% TriEGME	5B	none	5B	none
0.10% DiEGME	5B	none	5B	none
0.80% DiEGME	5B	none	5B	none
1.50% DiEGME	5B	none	5B	none

Table 22: Phase 5 Adhesion Loss - AMS-C-27725A.

FSII	Vapor Phase		Fuel Phase	
	Adhesion	Loss?	Adhesion	Loss?
Control	5B	N/A	5B	N/A
0.01% TriEGME	5B	none	5B	none
0.05% TriEGME	5B	none	5B	none
0.10% TriEGME	5B	none	5B	none
0.10% DiEGME	5B	none	5B	none
0.80% DiEGME	5B	none	5B	none
1.50% DiEGME	5B	none	5B	none

4.6 Phase 6 Results

As described above, Phase 6 involved exposing panels to mixtures of FSII and water in a cyclic environment (16 hours @ 60°C/2 hours ambient/4 hours at -20°C/2 hours ambient) for 60 days.

4.6.1 Phase 6 Visual Examinations (Figures A39-A42; Appendix)

Control Panels: The dry control panels were visually unchanged after the 60-day exposure period with no delamination or other film defects noticed.

Effects on the BMS 10-39 Coating: No coating loss, corrosion, or blistering was observed for either FSII. Neither FSII caused any noticeable color changes on the test panels.

Effects on AMS-C-27725A coating: No coating loss, corrosion, or blistering was observed for either FSII. Neither FSII caused any noticeable color changes on the test panels.

4.6.2 Phase 6 Color Measurement Results

Effects on the BMS 10-39 Coating: Both FSIIIs had little effect on the color of the BMS 10-39 coating. The 0.05% TriEGME solution had the least effect with an average ΔE of only 0.1, while the 0.80% DiEGME solution had an average ΔE of 0.45

Effects on AMS-C-27725A Coating: Both FSIIIs had little effect on the color of the AMS-C-27725A coating. The 0.05% TriEGME solution had the least effect with an average ΔE of only 0.15, while the 0.80% DiEGME solution had an average ΔE of 0.4. The data for both coatings are presented in **Figure 17** and **Table 23**.

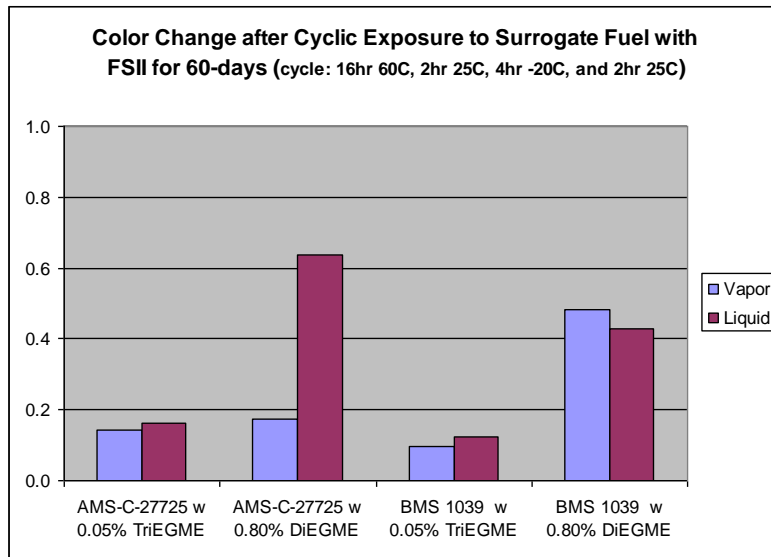


Figure 17: Phase 6 Color Change.

Table 23: Phase 6 Color Change.

Coating	FSII	ΔE Color Change	
		Vapor	Fuel
BMS 10-39	0.05% TriEGME	0.1	0.1
BMS 10-39	0.80% DiEGME	0.5	0.4
AMS-C-27725A	0.05% TriEGME	0.1	0.2
AMS-C-27725A	0.80% DiEGME	0.2	0.6

4.6.3 Phase 6 Softening Results

Effects on the BMS 10-39 Coating: Neither FSII caused any softening of the BMS 10-39 coating. While TriEGME appeared to have hardened the coating by one pencil lead, and DiEGME appeared to have softened the coating by one pencil lead, these ratings are within the experimental accuracy of the pencil hardness test, which is \pm one pencil lead.

Effects on AMS-C-27725A Coating: Neither FSII softened the AMS-C-27725A coating. The data for both coatings are presented in **Figure 18** and **Tables 24-25**.

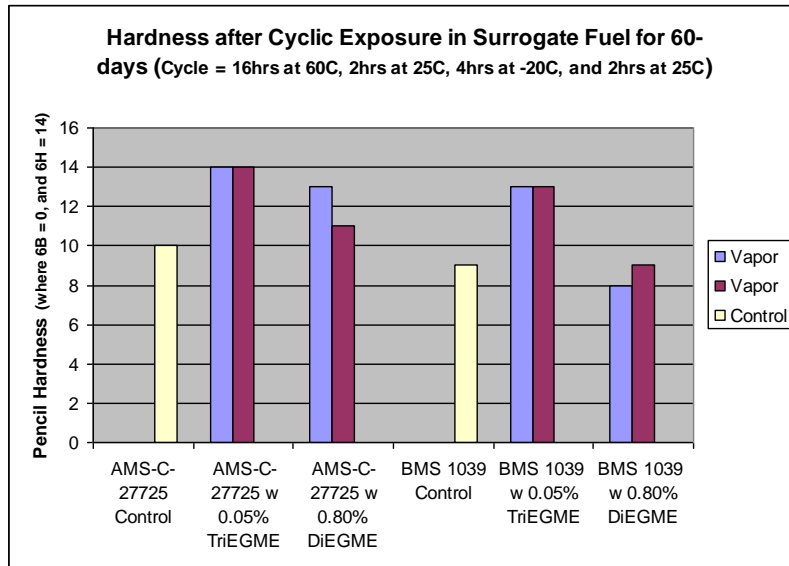


Figure 18: Phase 6 Softening.

Table 24: Phase 6 Softening - BMS 10-39.

Panel Location	FSII	Pencil Hardness	Softening
N/A	Dry Control	H	N/A
Vapor	0.05% TriEGME	2H	none
Vapor	0.80% DiEGME	F	none
Fuel	0.05% TriEGME	2H	none
Fuel	0.80% DiEGME	F	none

Table 25: Phase 6 Softening - AMS-C-27725A.

Panel Location	FSII	Pencil Hardness	Softening
N/A	Dry Control	2H	N/A
Vapor	0.05% TriEGME	2H	none
Vapor	0.80% DiEGME	2H	none
Fuel	0.05% TriEGME	2H	none

Fuel	0.80% DiEGME	2H	none
------	--------------	----	------

4.6.4 Phase 6 Adhesion Loss Results

Neither FSII caused any adhesion loss on the test coatings. The data are presented in **Figure 19** and **Tables 26-27**.

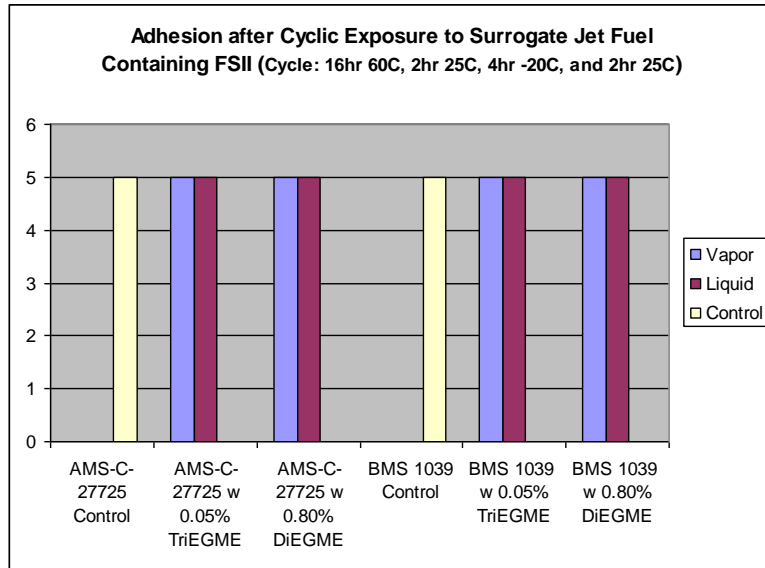


Figure 19: Phase 6 Adhesion Loss.

Table 26: Phase 6 Adhesion Loss - BMS 10-39

Panel Location	FSII	Adhesion Rating	Adhesion Loss?
N/A	Control	5B	N/A
Vapor	0.05% TriEGME	5B	no
Vapor	0.80% DiEGME	5B	no
Jet Fuel	0.05% TriEGME	5B	no
Jet Fuel	0.80% DiEGME	5B	no

Table 27: Phase 6 Adhesion Loss - AMS-C-27725A

Panel Location	FSII	Adhesion Rating	Adhesion Loss?
N/A	Control	5B	N/A
Vapor	0.05% TriEGME	5B	no
Vapor	0.80% DiEGME	5B	no
Jet Fuel	0.05% TriEGME	5B	no
Jet Fuel	0.80% DiEGME	5B	no

5.0 CONCLUSIONS

5.1 Phase 1

Exposure Solution: 80% FSII and 20% water v/v

Exposure Condition: Constant temperature of 90° C for 7 days, 14 days, and 60 days.

The 7-day and 14-day exposures showed that DiEGME softened the AMS-C-27725A coating more than TriEGME, while the color changes and adhesion loss were essentially the same for both FSIIIs. Another difference between the two FSIIIs is that while both coatings completely removed the BMS 10-39 coating, TriEGME caused a simple delamination, whereas, DiEGME caused a depolymerization of the coating. These results indicate that TriEGME was less destructive than DiEGME.

However, the exposure condition may have been excessively severe, because it caused excessive color changes and corrosion pitting (excessively in the 60-day exposure), which are not commonly observed in aircraft currently experiencing fuel tank delaminations. It is believed that this exposure regime may have produced results of questionable value, especially considering that the FSII exposure solution concentration of 80/20 does not occur in fuel tanks, where the maximum concentration is found to be a 50/50 mixture of FSII to water. The Phase 1 exposure condition was adopted from a CTIO project, which is trying to develop a test method to investigate a replacement coating for fuel tanks. Unfortunately, the test method is still under development, and the CTIO project did not include the test coatings used in this project so direct comparisons of data are not possible.

5.2 Phase 2

Exposure Solution: 80% FSII and 20% water v/v

Exposure Condition: Cyclic 24-hr temperature program of 16 hours at 90°C, 2 hours at ambient, 4 hours at -20°C, and finally, 2 hours at ambient, running for a total of 60 days.

The results were similar to the 60-day exposure for Phase 1, albeit with less corrosion. It is hypothesized that this difference is due to the lower average temperature.

5.3 Phase 3

Exposure Solution: 50% FSII and 50% water v/v with an equal volume of Jet A-1 jet fuel.

Exposure Condition: Constant temperature of 60° C for 60 days.

TriEGME caused a larger color change than DiEGME in both coatings; however, the color changes were below the acceptable limit. Neither FSII caused a loss of adhesion and the small differences seen in softening were considered negligible. This exposure regime did not appear to elicit any meaningful differences between the two FSIIIs.

5.4 Phase 4

Exposure Solution: 50% FSII and 50% water v/v with an equal volume of Jet A-1 jet fuel.

Exposure Condition: Cyclic 24-hr temperature program of 16 hours at 60°C, 2 hours at ambient, 4 hours at -20°C, and finally, 2 hours at ambient, running for a total of 60 days.

The only difference seen between the two FSIIIs was that TriEGME caused a larger color change than DiEGME; however, the color change was below the acceptable limit. This exposure regime did not appear to elicit any meaningful differences between the two FSIIIs.

5.5 Phase 5

Exposure Solution: The following six exposure solutions were used:

1. 0.01% TriEGME in surrogate jet fuel
2. 0.05% TriEGME in surrogate jet fuel
3. 0.10% TriEGME in surrogate jet fuel
4. 0.10% DiEGME in surrogate jet fuel
5. 0.80% DiEGME in surrogate jet fuel
6. 1.50% DiEGME in surrogate jet fuel

Exposure Condition: Constant temperature of 60° C for 60 days.

DiEGME softened the BMS 10-39 coating more than TriEGME. The softening of the AMS-C-27725A coating was the same for both FSIIIs. No significant differences were seen in color or adhesion. Based on the softening data, TriEGME performed a little better than DiEGME. It is believed that if this exposure regime were continued longer and/or conducted at a higher temperature more coating defects may have become apparent and perhaps elicited more differentiation between the FSIIIs.

5.6 Phase 6

Exposure Solution: The following two exposure solutions were used:

1. 0.05% TriEGME in surrogate jet fuel
2. 0.80% DiEGME in surrogate jet fuel

Exposure Condition: Cyclic 24-hr temperature program of 16 hours at 60°C, 2 hours at ambient, 4 hours at -20°C, and finally, 2 hours at ambient, running for a total of 60 days.

Neither FSII caused any defects, and the color changes noted were significantly lower than the changes seen in Phase 5, which would seem to indicate that the cyclic exposure regime was much more benign than the constant temperature regime.

6.0 OVERALL CONCLUSION

The compatibility of DiEGME and TriEGME with two commonly used fuel tank topcoat materials over a range of conditions was tested. The results indicate that for exposures which simulate liquid fuel or water/fuel interactions with topcoat (Phases 1 through 4) that the two FSIIIs exhibit similar effects on the topcoat tested. In contrast, exposure to vapor condensates (Phases 5 and 6) did differ, with TriEGME causing significantly less softening of BMS 10-39 (**Figure 13**). This is believed to be due to the lower vapor phase concentrations that result from

its relatively low vapor pressure. However, the test protocols were not sufficiently robust to replicate the damage currently being experienced in aircraft fuel tanks with DiEGME to draw definitive conclusions.

7.0 RECOMMENDATIONS

The data suggest that there are differences between TriEGME and DiEGME, and that TriEGME does less damage to coatings. However, it is believed that the exposure regimes selected did not fully establish this. It is recommended that a follow-on effort be planned using the following recommendations:

1. Do not perform the testing exposure testing seen in Phases 2, 4, and 6, because in all exposure fluids, cyclic exposures represented a much more benign environment than the constant temperature exposures.
2. Eliminate the 80/20 FSII/water exposure solution because this FSII concentration level is much higher than is naturally occurring and caused coating and substrate damages not commonly seen in operational aircraft.
3. Consider dropping the 50/50 FSII/water exposure solution. While this concentration is seen in aircraft, the water bottom in aircraft fuel tank is a very small percentage of the total fuel tank volume, but in the lab test jars it represented the 50% of the liquid volume, and is such, makes for an unrealistic test.
4. Raise the temperature of the fuel exposures. The reduced temperature of 60° C was done because of safety concerns, but others have safely tested the jet fuel at higher temperatures. The higher temperature is more likely to elicit performance differences being sought. It is believed that the fuel/FSII solutions could be safely tested at 90° C.
5. Eliminate the color test. It was not predictive of physical defects, and eliminating it will allow the softening and adhesion loss tests to be performed much sooner after removal from the fluids, which should detect film damages before they can self-heal.
6. Add a dry film thickness test. The test is rapid and non-destructive and would detect any swelling or thinning of the coating caused by the FSII.

APPENDIX



Figure A1: Unexposed BMS 10-39 Coating.



Figure A2: Unexposed AMS-C-27725 Coating.



Figure A3: Phase 1 BMS 10-39 7-days DiEGME.

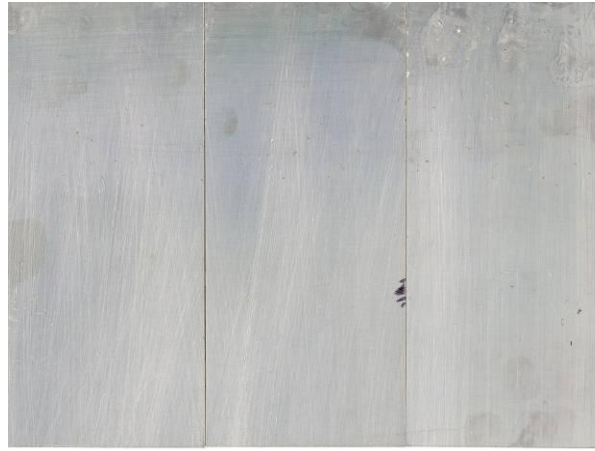


Figure A4: Phase 1 BMS 10-39 7-days TriEGME.

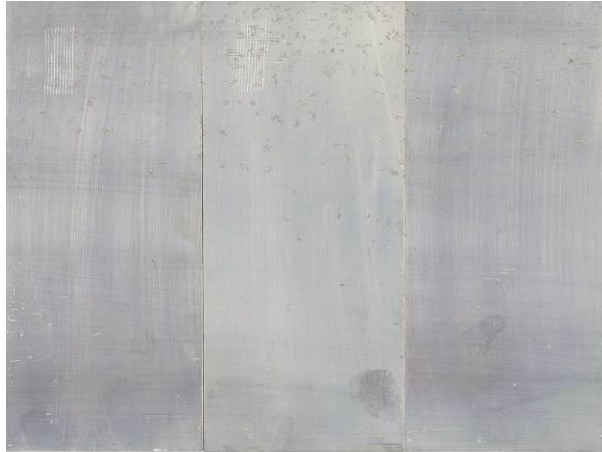


Figure A5: Phase 1 BMS 10-39 14-days DiEGME.



Figure A6: Phase 1 BMS 10-39 14-days TriEGME.

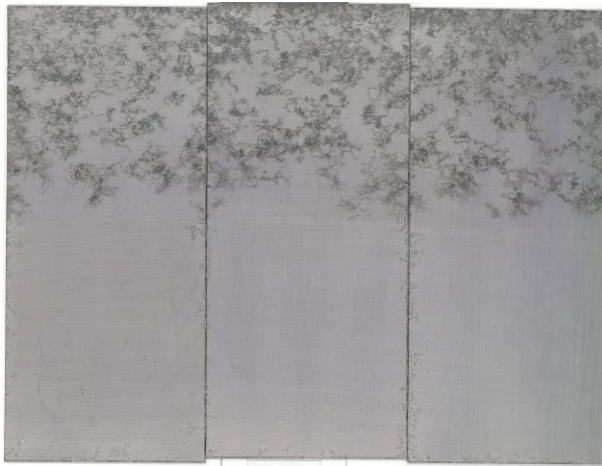


Figure A7: Phase 1 BMS 10-39 60-days DiEGME.



Figure A8: Phase 1 BMS 10-39 60-days TriEGME.



Figure A9: Phase 1 AMS-C-27725 7-days DiEGME.



Figure A10: Phase 1 AMS-C-27725 7-days TriEGME.



Figure A11: Phase 1 AMS-C-27725 14-days DiEGME.



Figure A12: Phase 1 AMS-C-27725 14-days TriEGME.



Figure A13: Phase 1 AMS-C-27725 60-days DiEGME.



Figure A14: Phase-1 AMS-C-27725 60-days TriEGME.

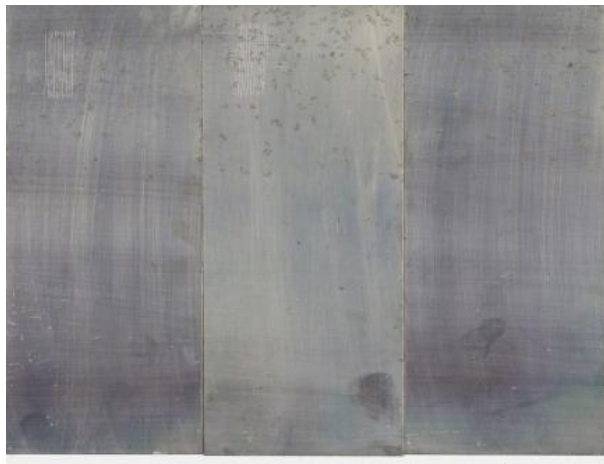


Figure A15: Phase 2 BMS 10-39 DiEGME.



Figure A16: Phase 2 BMS 10-39 TriEGME.



Figure A17: Phase 2 AMS-C-27725 DiEGME.

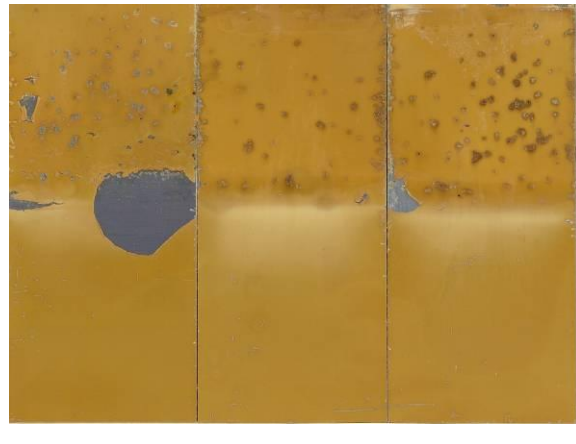


Figure A18: Phase 2 AMS-C-27725 TriEGME.



Figure A19: Phase 3 BMS 10-39 DiEGME.



Figure A20: Phase 3 BMS 10-39 TriEGME.



Figure A21: Phase 3 AMS-C-27725 DiEGME.



Figure A22: Phase-3 AMS-C-27725 TriEGME.



Figure A23: Phase 4 BMS 10-39 DiEGME.



Figure A24: Phase 4 BMS 10-39 TriEGME.



Figure A25: Phase 4 AMS-C-27725 DiEGME.



Figure A26: Phase 4 AMS-C-27725 TriEGME.



Figure A27: Phase 5 BMS 10-39 (0.10% DiEGME).



Figure A28: Phase 5 BMS 10-39 (0.01% TriEGME).



Figure A29: Phase 5 BMS 10-39 (0.80% DiEGME).



Figure A30: Phase 5 BMS 10-39 (0.05% TriEGME).



Figure A31: Phase 5 BMS 10-39 (1.50% DiEGME).



Figure A32: Phase 5 BMS 10-39 (0.10% TriEGME).



Figure A33: Phase 5 AMS-C-27725 (0.10% DiEGME).



Figure A34: Phase 5 AMS-C-27725 (0.01% TriEGME).



Figure A35: Phase 5 AMS-C-27725 (0.80% DiEGME).



Figure A36: Phase 5 AMS-C-27725 (0.05% TriEGME).



Figure A37: Phase 5 AMS-C-27725 (1.50% DiEGME).



Figure A38: Phase 5 AMS-C-27725 (0.10% TriEGME).



Figure A39: Phase 6 BMS 10-39 (0.80% DiEGME).



Figure A40: Phase 6 BMS 10-39 (0.05% TriEGME).



Figure A41: Phase 6 AMS-C-27725 (0.80% DiEGME).



Figure A42: Phase 6 AMS-C-27725 (0.05% TriEGME).

Appendix B.

**Compatibility of DiEGME and TriEGME Fuel System Icing Inhibitor Additives with
BMS 10-39 Aircraft Tank Topcoat Material
(AFRL Fuels and Energy Branch Study)**

INTENTIONALLY LEFT BLANK

COMPATIBILITY OF DiEGME AND TriEGME FUEL SYSTEM ICING INHIBITOR ADDITIVES WITH BMS 10-39 AIRCRAFT TANK TOPCOAT MATERIAL

Steven Zabarnick,^{*1} Ryan Adams,¹ Zachary West,¹ Matthew J. DeWitt,¹ Linda Shafer,¹ Richard Striebich,¹ Charles L. Delaney,² and Donald K. Phelps³

¹University of Dayton Research Institute, Dayton, OH 45469 USA

²Consultant, 10011 Bennington Drive, Cincinnati, OH 45241 USA

³Air Force Research Laboratory, Fuels and Energy Branch AFRL/RZPF,
Wright-Patterson AFB, OH 45433 USA

ABSTRACT

In recent years, the fuel system icing inhibitor (FSII) diethylene glycol monomethyl ether (DiEGME) has been implicated in an increasing incidence of peeling of topcoat material in the ullage space of integral wing tanks in the B-52 and other military aircraft. Work has indicated that for the combination of DiEGME in JP-8 fuel, the icing inhibitor additive can concentrate in the tank ullage and condense at elevated concentrations on cooled tank walls. These high concentrations of DiEGME cause swelling and subsequent peeling of the epoxy-based topcoat. Here we report on detailed studies of the compatibility of DiEGME and FSII replacement candidate triethylene glycol monomethyl ether (TriEGME) with BMS 10-39 fuel tank topcoat material. Tests were designed to simulate fuel tank wall exposures with subsequent topcoat degradation measured by icing inhibitor uptake analyses and pencil hardness evaluations. The lower volatility of TriEGME relative to the JP-8 fuel components results in it being less able to concentrate in the tank ullage and promote topcoat failure, as compared to DiEGME. This was confirmed with lower additive levels measured in the ullage, condensed vapors, and the exposed topcoat material. The pencil hardness of topcoat material exposed to fuel vapors was significantly improved upon changing from DiEGME to TriEGME exposure. Simulation experiments were able to reproduce the fuel tank topcoat peeling observed in the field, as well as determine the conditions (concentration and temperature) required for topcoat degradation.

Keywords: fuel system icing inhibitor, DiEGME, TriEGME, topcoat peeling, compatibility

INTRODUCTION

At high altitudes, the exterior of aircraft are subjected to cold temperatures ($<-60^{\circ}\text{C}$) from the surrounding environment. While the current USAF fuel, JP-8, has a low freezing point (-47°C maximum), any free water within the fuel will readily freeze at altitude. To remedy this situation, a fuel system icing inhibitor (FSII) was developed and introduced as a fuel additive to selectively partition into any free water present and suppress the freezing point of the aqueous mixture. This additive became required by the US military in 1961 after a B-52 Stratofortress crash, which was attributed to ice formation that caused fuel line blockages. Initially, ethylene glycol monomethyl ether (EGME)/glycerol mixtures were employed as the FSII additive during the period JP-4 was used by the United States Air Force (USAF). However, EGME was subsequently shown to have a relatively high toxicity and problems arose with the volatility of JP-5, the fuel used by the Navy, as it became difficult for EGME-containing fuels to meet the flashpoint specification ($\geq 60^{\circ}\text{C}$).¹ Diethylene glycol monomethyl ether (DiEGME) was found to be an acceptable alternative FSII additive, and transition to this species began in 1987 for JP-5, and was authorized for use in JP-8 in 1992. DiEGME is currently required in both JP-5 and JP-8 fuels, with a specification procurement level of 0.10 – 0.15 vol% for both fuels. The current aircraft use limits for DiEGME are currently 0.03 vol% for the US Navy and 0.07 vol% for the US Air Force.

Recently, DiEGME has been implicated in causing degradation and peeling of the protective fuel tank topcoat layer in B-52 aircraft, a process referred to as fuel tank topcoat peeling (FTTP).^{2,3} This epoxy topcoat layer is Boeing Material Specification (BMS) 10-39, and serves as a physical barrier between the fuel/air environment and the aluminum tank wall. Peeled surfaces are more likely to support corrosion and pitting of the aluminum substrate. Also, the topcoat flakes that have lost adhesion can cause blockages in fuel filters and valves resulting in catastrophic failure of the aircraft. Figure 1 shows examples of fuel tank topcoat peeling and the problems it causes.



Figure 1. (a) Fuel tank topcoat peeling in a B-52 wing fuel tank,² and (b) a B-52 boost pump intake screen (4-mesh) clogged with BMS 10-39 flakes.

The BMS 10-39 epoxy topcoat was originally formulated to resist degradation from prolonged exposure to JP-4 fuel. Despite this formulation, FTTP has occurred in fuel containing DiEGME and high concentrations of DiEGME in fuel and water have been shown to promote swelling and peeling of the topcoat layer.^{2,3} FTTP has primarily been observed above the fuel level on the tank walls in the headspace (ullage) of the tank and at the bottom of the tank where water accumulates (Figure 1). Mechanisms of deterioration have been proposed for both of these peeling areas. For the ullage space above the fuel level, DiEGME concentrates in the vapor phase due to its high vapor pressure relative to the JP-8 fuel.² This DiEGME rich vapor phase can then condense on cold topcoat surfaces, resulting in a wall wetted with condensate that has a DiEGME concentration which is significantly higher than the base fuel. The presence of relatively warm bulk fuel and vapor along with a cold fuel tank wall encourages this process, as demonstrated graphically in Figure 2.

The conditions of relatively warm bulk fuel and a cold wall to promote selective condensation are possible under several scenarios during aircraft operation. For example, after takeoff the fuel tank walls will cool down quickly due to the low outside air temperature at altitude, while the large thermal mass of bulk fuel will result in the fuel cooling down significantly more slowly. These conditions will be repeated for each flight, resulting in continued exposure of DiEGME rich condensate in contact with the topcoat. Another scenario

involves aircraft on the ground in warm climates. If the aircraft is left exposed to the sun throughout a hot day, the bulk fuel temperature in the aircraft fuel tanks can rise substantially. In studies of the temperature of refueling tankers, it was found that the tanker trucks showed fuel temperatures above 55⁰C during the middle of the day in a desert location.⁴ As the sun sets, the outside air temperature will decrease quickly, especially in arid climates, while the wall will cool more quickly due to the differences in thermal mass and promote surface condensation. These conditions can be repeated daily if the ambient temperature is sufficiently warm to vaporize the lighter fuel components, such as DiEGME.

Simulated Fuel Tank

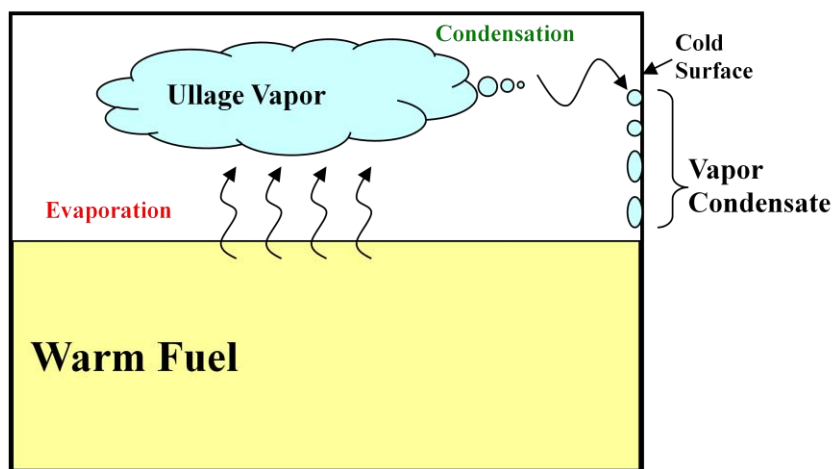


Figure 2. The FTTP phenomenon initiated by a DiEGME rich ullage vapor and condensation on a cold topcoat surface.

Topcoat degradation at lower fuel tank surfaces is likely initiated by high concentrations of DiEGME in water bottoms. The specific gravity of water and DiEGME (1.00 and 1.023, respectively) are higher than JP-8 (~0.8), and thus free water that phase separates will collect at the bottom of the tank. DiEGME and water are completely miscible, and DiEGME typically concentrates in water to the range of 30 to 50 vol% within the fuel tank. Higher concentrations of DiEGME in aqueous solutions have been shown to cause FTTP with seven day liquid exposures.⁵ Severe swelling of topcoat flakes have also been shown to occur at similar exposure concentrations.²

The chemical and physical mechanisms which result in FTTP are still not fully understood, and thus it is difficult to eliminate or minimize future occurrences. More information needs to be obtained on the required concentrations, temperatures, and time of exposure to induce FTTP. Along with attempting to confirm the mechanisms which cause FTTP, a number of solutions have been proposed to prevent future problems. To reduce the occurrence of peeling in water bottom areas, regular sumping of aircraft tanks ensures that water/FSII mixtures do not accumulate in the fuel tanks and high concentrations of FSII are not in contact with the topcoat for extended periods of time. For the issue of FTTP on the tank ullage surfaces, one solution is to reduce the concentration of DiEGME in JP-8. Decreasing the concentration of DiEGME in the fuel would reduce the concentration in the vapor phase and lower the concentration in the condensate which collects on the ullage topcoat. This approach would also lower the DiEGME levels in tank water bottoms. However, the DiEGME concentration still needs to be high enough to provide the required anti-icing performance. Ideally, a proper balance between reducing the occurrence of FTTP and retaining the inhibiting icing performance of the additive would be found.

Another approach is to replace DiEGME with an alternative FSII additive which does not promote FTTP. With the current hypothesized mechanisms for FTTP on the tank ullage walls, a suitable replacement would provide equivalent anti-icing efficacy, but exhibit a lower vapor pressure. One such species that may fit these requirements is triethylene glycol monomethyl ether (TriEGME) which has a vapor pressure that is more than an order of magnitude lower than DiEGME as shown in Table 1.⁶ TriEGME should not volatilize as readily from the bulk fuel, resulting in a lower effective concentration in any condensate in contact with the topcoat surfaces. Table 1 also shows other selected property differences between DiEGME and TriEGME.

It is apparent that further investigation of the requisite conditions for the occurrence of FTTP in aircraft is required. A comparison of the topcoat compatibility between DiEGME and TriEGME is also essential to assess TriEGME as an alternative icing inhibitor additive. Determination of the anti-icing efficacy of DiEGME and TriEGME at lower concentrations is being evaluated separately.^{6,7} The experiments in this study were designed to assess the effects of DiEGME and TriEGME on BMS 10-39 topcoat degradation using the most probable scenarios

relating to FTTP. The absorption of FSII into BMS 10-39 was quantified to analyze the effects of concentration in aqueous or fuel solutions under various exposure conditions. This work also studied differences between DiEGME and TriEGME using topcoat panels that were recently fabricated and those that were exposed to fuel for many years, as well as the conditions which will reduce the topcoat integrity below the minimum specification requirement. After being softened due to DiEGME exposure, BMS 10-39 topcoat has been observed to „re-harden”,² which is most likely due to FSII molecules desorbing from the coating. Thus, preliminary studies were also performed to investigate the desorption rates of FSII from the topcoat. An ultimate goal of this work was to reproduce FTTP in a controlled laboratory setting to assess the differences between DiEGME and TriEGME, as well as to investigate the degradation process and to provide a knowledgebase of the conditions necessary for FTTP.

Table 1. Selected Properties of DiEGME and TriEGME

FSII Additive	Vapor Pressure (mmHg) @ 20°C	Density (g/mL @ 20°C)	Molecular weight (g/mol)	Freezing Point (°C)
DiEGME	0.19	1.023	120	-85
TriEGME	<0.01	1.026	164	-47

EXPERIMENTAL SECTION

BMS 10-39 Panels

Experimental studies were performed to investigate the compatibility of FSII additives with both aged and new BMS 10-39 topcoat panels. The AFRL Coatings Technology Integration Office fabricated 1-sided topcoat panels on 1/32 inch aluminum (2024-T3) to meet the 1 mil thickness specification of BMS 10-39. Prior to coating, the aluminum panels were cleaned, acid etched with an alcoholic phosphoric acid solution, and chemically treated with Alodine 1200S, which is a chromium chemical conversion coating surface treatment. These manufactured panels are referred to as “new” panels, as they have not been exposed to fuel or FSII before these studies. The “old” BMS 10-39 panels were obtained from a scrapped B-52G aircraft from Boeing Wichita which had been operated for many years with JP-4 and JP-5/EGME and/or JP-5/DiEGME fuels.

FSII Exposure Solutions

Interactions with the BMS 10-39 topcoat can occur with FSII in solution with various liquids. Three different bulk solutions were used in the experimental studies while varying the FSII concentrations: water, fuel, and a surrogate fuel condensate. Aqueous solutions were used for many of the studies to evaluate the required concentrations for FTTP to occur in water bottoms. The water used to create the solutions was purified via reverse osmosis. A clay treated Jet A-1 (POSF-4877) was used as the base fuel in the experimental studies. The clay treatment was necessary to remove any FSII contamination in the fuel that may have occurred during transportation and storage. Finally, a surrogate fuel was developed to simulate the fuel condensate which would be in contact with the BMS 10-39 coating in the ullage of aircraft tanks. This surrogate was comprised of Exxsol D40 (85% by volume), Aromatic 100 (9%), and Aromatic 150 (6%). The mixture closely simulates the lighter components that are initially vaporized from the bulk fuel and subsequently condense on cold surfaces.⁶

FSII Absorption Study

The uptake study investigated the liquid-solid interactions between FSII and the BMS 10-39 layer by quantifying the FSII absorbed into the topcoat. Aluminum topcoat panels squares (0.25 in²) are submerged in 20 mL of fuel or water with specific concentrations of DiEGME or TriEGME in 30 mL capped vials. This volume of liquid was used to ensure there would not be a significant change in the FSII concentration of the liquid phase due to partitioning into the topcoat. This was verified by analyzing the concentration of the solution before and after exposure to a BMS 10-39 panel.

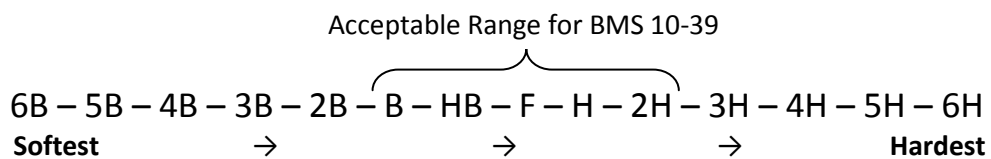
The aqueous solutions ranged from 0 to 100% of DiEGME or TriEGME, while the fuel or surrogate solutions ranged from 0 to 2%. This difference in concentration ranges resulted from the typical concentrations expected in these phases. Initially, the solutions were placed into a shaker to be agitated throughout the exposure period; however, further studies revealed that agitation was unnecessary due to the short time required for the FSII in the liquid and topcoat layer to equilibrate. The initial exposure time used was five days, as further time did not increase the absorption of FSII in the topcoat. Later, this was shortened based upon the absorption study discussed below. After the exposure period, the panels were removed from the vials and cleaned

to remove any liquid droplets by rinsing with a small volume of hexane (1-2 mL) and then blotted dry with Kimwipes. The panel was then submerged in 2 mL of acetone for one hour to extract the absorbed FSII component from the topcoat. Consecutive acetone extractions on the same panel failed to yield detectable levels of FSII, showing that all of the extractable FSII was removed. The acetone extract was collected and analyzed by GC-MS to obtain the total mass of absorbed FSII. The FSII absorption quantity was normalized by the topcoat volume, measured via thickness measurements, and reported as moles of FSII absorbed per liter of topcoat. Each experimental condition was performed in triplicate to obtain a measure of reproducibility.

This basic approach was modified to investigate the rate of FSII absorption and desorption. To evaluate the absorption rate, the exposure time of the topcoat in contact with a FSII solution was varied to determine when the uptake concentrations reached a plateau. A plateau in the uptake absorption vs time suggests that the topcoat no longer absorbs FSII and equilibrium is reached with the FSII in solution. The panels were removed from the solutions at varying times between 10 seconds and 144 hours. This was performed with new panels and 50% aqueous solutions of DiEGME and TriEGME. The results indicated that equilibrium was reached in less than 24 hours. This data was used to validate reducing the exposure time for the absorption study to one day for later experiments from the initial five days. Alternatively, the desorption rate was qualitatively analyzed by varying the time between the cleaning of the panel (after removal from the solution) and the acetone extraction.

Pencil Hardness Study

To correlate the quantity of FSII absorbed with the integrity of the coating after exposure, pencil hardness tests were performed. These were performed according to ASTM D3363 procedures. The pencil leads used for this analysis along with the range of acceptable hardness for BMS 10-39 are shown below.



The pencil hardness study was performed on 1" x 2" panels of new and old BMS 10-39 on aluminum. The panel size was chosen to allow the use of all leads required to determine the hardness. Two such panels were submerged in 100 mL beakers with 80 mL of a FSII solution for two days. This exposure time permitted two data sets to be collected per week while maintaining equilibrium between the solution and the topcoat. As in the uptake study, this volume of liquid was used to ensure the concentration of FSII in the solution did not decrease during the duration of exposure. This was verified by analyzing the concentration of DiEGME in a solution before and after exposure, which did not change significantly over the two days.

When the panels were removed, they were washed with a small amount of hexane to remove the remaining solution from the BMS 10-39 panel. One of the panels was immediately tested for its pencil hardness, while the other was allowed to dry in a fume hood for two hours prior to evaluation. The latter approach was performed to determine the ability of the topcoat to re-harden and/or re-adhere over time as the FSII evaporates from the topcoat material.

Fuel Tank Topcoat Pealing (FTTP) Simulation Study

This study was designed to simulate the conditions in aircraft fuel tanks which promote topcoat degradation, as well as to quantify the effects of FSII concentration and temperature on the resulting pencil hardness of exposed BMS 10-39 panels. The experiment was used to test the hypothesis that DiEGME concentrates in the ullage and condenses at high concentrations on the topcoat surface, which results in degradation. This simulation was also used to determine if the lower vapor pressure of TriEGME results in a decreased potential for creating a FSII rich ullage. The system (Figure 3) consisted of a 28.3L (1 ft³) aluminum box which contained the fuel along with a plate heat exchanger with an attached BMS 10-39 panel. The box containing the fuel was placed inside an environmental chamber, allowing control of the fuel and box surface temperatures. The heat exchanger/panel placed above the fuel level, allowed independent temperature control of the topcoat panel which was secured by clamps on the edges and top of the panel. A recirculating cooling water bath was used to control the heat exchanger temperature and the surface temperature of the topcoat panel. This heat exchanger was maintained at a lower temperature than the fuel to promote selective condensation onto the topcoat specimen.

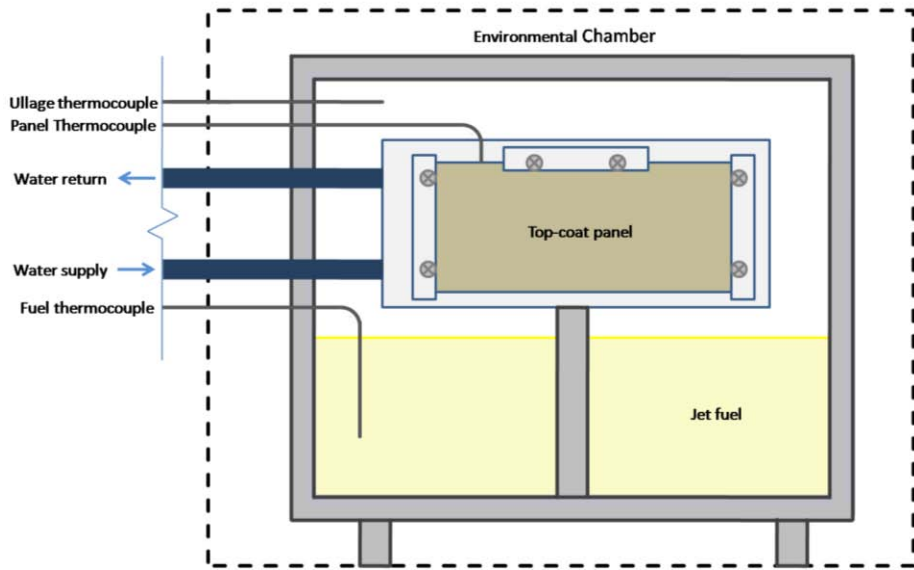


Figure 3. The FSII simulation box apparatus.

The BMS 10-39 panels used for the simulation were 3" x 6" in size to provide a large surface area for contact with the condensate, and for visible confirmation of topcoat peeling. The box was typically filled with 9 L (approximately 1/3 of the total volume) of jet fuel and agitated throughout the duration of the experiment with a magnetic stir bar. This volume was used to create a similar ratio of total mass of FSII to area of topcoat as shown in the Uptake and Pencil Hardness Study, such that any absorption of FSII in the topcoat panel would not reduce the FSII concentration in the bulk fuel. Thermocouples were placed in the vapor headspace of the box, submerged into the fuel, and placed between the topcoat panel and heat exchanger surface. During the experiment, the box was closed after the fuel was added, and then the environmental chamber was heated to a specified temperature. After the desired test duration (2 to 5 days) and cooling to near ambient temperatures, samples of the bulk fuel and condensate were collected. Condensate samples were obtained using a chromatographic syringe to collect droplets on the panel or the heat exchanger. The initial fuel samples, final fuel samples, and the condensate samples were analyzed by GC-MS to obtain FSII concentrations. Data was collected at varying initial FSII concentrations in the bulk fuel, temperature of the box and/or heat exchanger, and the exposure durations of FSII in contact with the topcoat panel. The topcoat panel was removed from the apparatus and immediately evaluated for its hardness at five locations: the center of the panel and each of the four corners.

Analytical Techniques Used for Quantification of FSII

Analytical techniques were developed for quantification of levels of FSII in water, acetone, and fuel. While there is an ASTM standard for determination of DiEGME in fuel (ASTM D5006), the technique requires a large volume of fuel (80 to 160 mL) which was not available for the current studies. In addition, the variability of this method is greater than required for these studies.

Verification of the FSII concentration in water before exposure to the topcoat material was performed by refractive index using a Reichert AR200 Digital Refractometer over a concentration range of 0 to 100% FSII. Individual calibration curves were determined for DiEGME and TriEGME at approximately 10 vol% increments. The reproducibility is approximately $\pm 10\%$ of the FSII concentration.

Quantifying the concentration of FSII in acetone solutions was required for the topcoat absorption study and was performed by gas chromatography with a flame ionization detection (GC-FID). An HP 5890 Series II GC-FID was used to quantify the dilute FSII component in acetone in ranges from 0 to 0.20 vol% to a reproducibility of $\pm 10\%$ of the FSII concentration.

For analysis of FSII in fuel, fuel surrogate, and fuel condensate, a method was developed which employed gas chromatography with a mass spectrometer detector (GC-MS) detector. The FSII component in fuel could not be separated chromatographically due to co-elution with the other fuel components. Thus the selective ion mode of the detector was used to monitor the 45, 59, and 89 ions. These ion peaks are selective for both DiEGME and TriEGME, which allows the FSII peak to be resolved from the other fuel components. The reproducibility is approximately $\pm 10\%$ of the FSII concentration.

RESULTS AND DISCUSSION

FSII Fuel Absorption Results

Studies were performed to investigate the absorption of DiEGME and TriEGME into BMS 10-39 topcoat panels as a function of concentration and time. The exposure studies were performed at ambient temperature and pressure as these were representative of ground conditions for aircraft fuel tanks. Unless specified, the panels were submerged in 20 mL FSII solutions for

five days. The uptake data obtained using new panels in Jet A-1 is shown in Figure 4, with each data point representing the average of two or three panel measurements. The line labeled “concentration level of failed topcoat flakes” at 0.66 mol FSII/L topcoat is from an uptake measurement obtained from failed topcoat flakes from the field. These failed topcoat flakes, which were obtained from B-52 aircraft, were analyzed by the same acetone extraction methodology as used to analyze the test panels during the absorption studies. Three separate flakes were analyzed in this fashion and the level of DiEGME was averaged with a reproducibility of $\pm 20\%$ of this concentration.

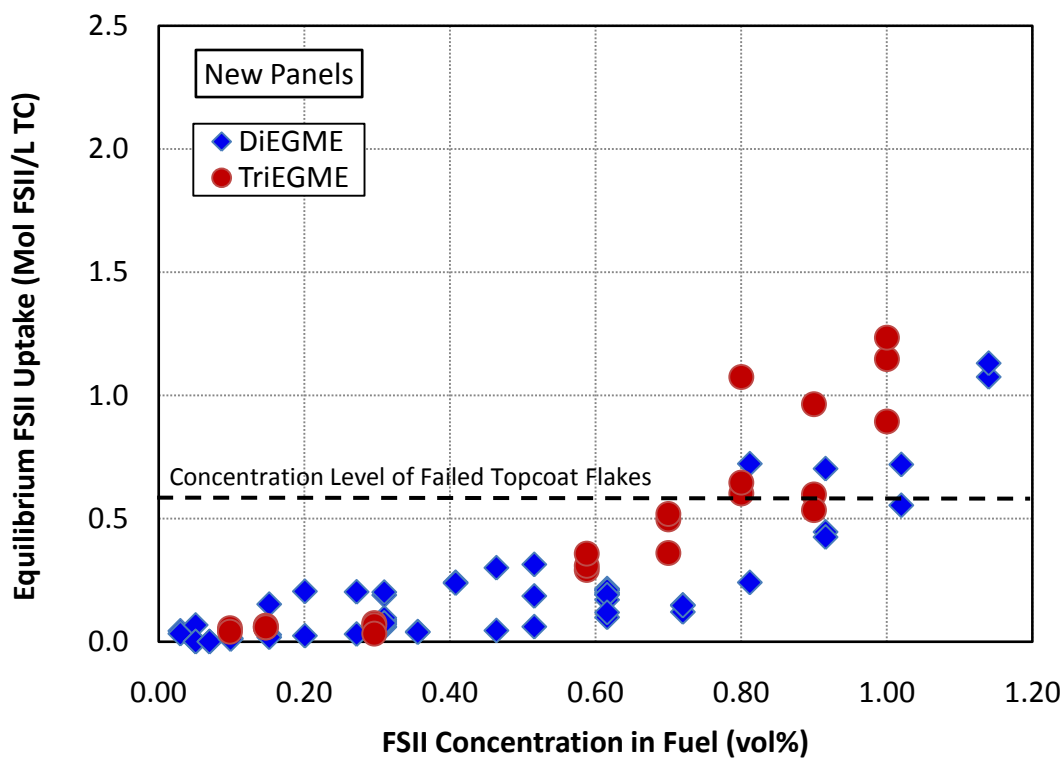


Figure 4. The equilibrium uptake of new panels exposed to DiEGME and TriEGME in Jet A-1.

The figure shows that increasing the initial concentration of FSII in the fuel increases the quantity of FSII absorbed into the topcoat layer. The uptake increases significantly at concentrations greater than 0.50 to 0.80 vol% FSII. The figure shows that DiEGME and TriEGME performed similarly and follow the same trend. The FSII uptake increases above the level of failed topcoat flakes at approximately 0.80 vol% FSII in the fuel. This suggests that the concentration in the fuel required for failure to occur is at least 0.80% FSII in cases of direct

contact, although additional analysis and correlation with topcoat integrity (e.g., pencil hardness measurements) is needed for verification. It is likely that the concentration of FSII in these flakes has decreased over time due to evaporation from the coating. The reproducibility of the absorption data can be fairly poor at some concentrations, with the data varying up to $\pm 100\%$ of an average concentration. There are a number of factors that may contribute to this, including variations in the GC analysis, slightly unequal topcoat thickness, and possible degradation of the topcoat after repeated use of some panels.

To provide an understanding of changes that can occur in the topcoat after 40 years of aging and contact with fuel, the absorption of FSII into BMS 10-39 was also determined using old panels. The absorption data for old panels in Jet A-1 fuel is shown in Figure 5 under ambient temperatures and an exposure time of five days.

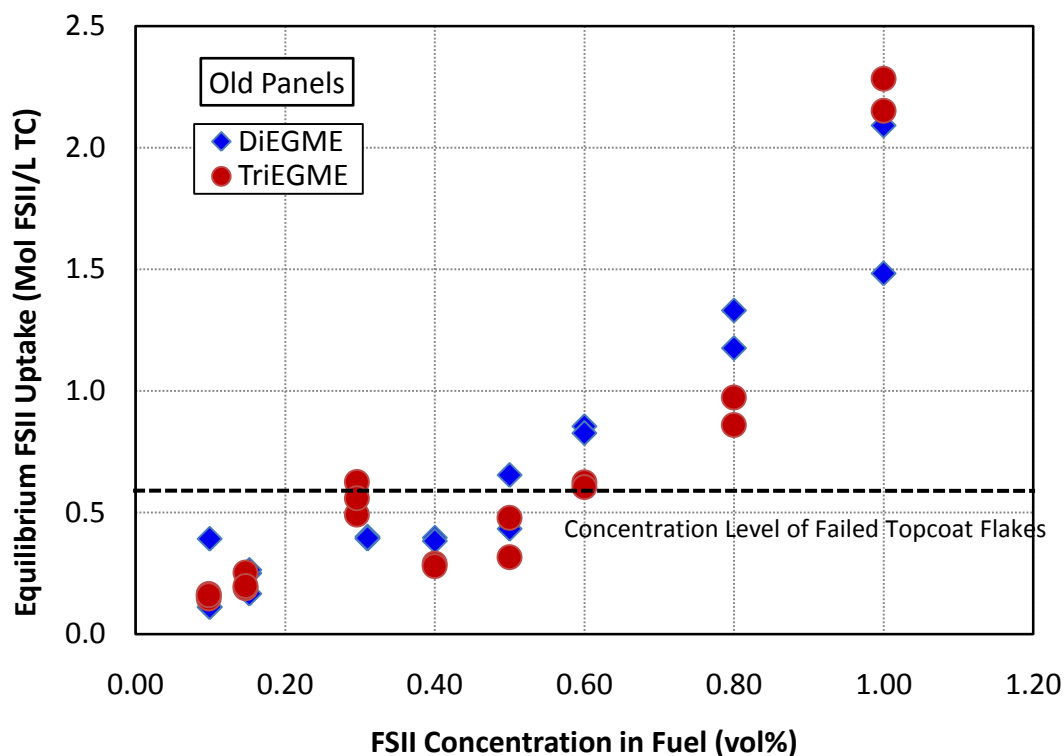


Figure 5. The uptake of DiEGME and TriEGME in Jet A-1 obtained for old panels that were in service for over 40 years.

The old panels show a significant increase in the topcoat uptake relative to the newer panels at equivalent FSII concentrations. This may be due to the old topcoat having a reduced resistance to absorption due to weakening of the polymer matrix which allows more molecules to absorb into the coating. The old panels reach an uptake value higher than the failed topcoat flakes at 0.50 vol% FSII, which is significantly lower than the 0.80 vol% level found for the new panels. If the ability of topcoat to absorb FSII correlates with the tendency to exhibit degradation, these data imply that old panels would be expected to exhibit much higher levels of degradation. This correlation is addressed in the pencil hardness studies report below.

When comparing DiEGME and TriEGME on a molar basis, the additives show similar extents of absorption in both the old and new topcoat panels, but on a mass basis TriEGME has a higher equilibrium uptake than DiEGME. This can be explained by the molecular weight of TriEGME (164 g/mol) being one-third higher than DiEGME (120 g/mol), while the absorption of FSII is likely a function of the number of molecules a given volume of topcoat can absorb, rather than the mass. This FSII absorption data agrees qualitatively with the equilibrium solvent uptake (ESU) measurements of topcoat flakes performed by Aliband et al.² which was performed via gravimetric differences following exposure. Their data show a relatively level 6% ESU uptake from 0 to 0.75 vol% DiEGME in the fuel, which then increases rapidly at higher DiEGME levels. The higher uptake observed by Aliband et al.² is likely caused by absorption of other fuel components into the topcoat, as their technique measures total uptake of all species into the topcoat flakes.

FSII Aqueous Absorption Results

To better understand the occurrence of FTTP from exposure to water bottoms of fuel tanks, measurements were performed to determine the absorption of FSII into the topcoat from FSII/water solutions. These measurements were performed at ambient temperature with the panels exposed to aqueous solutions for five days. Figure 6 shows the results for new and old panels with each data point representing the average of 2 or 3 uptake measurements.

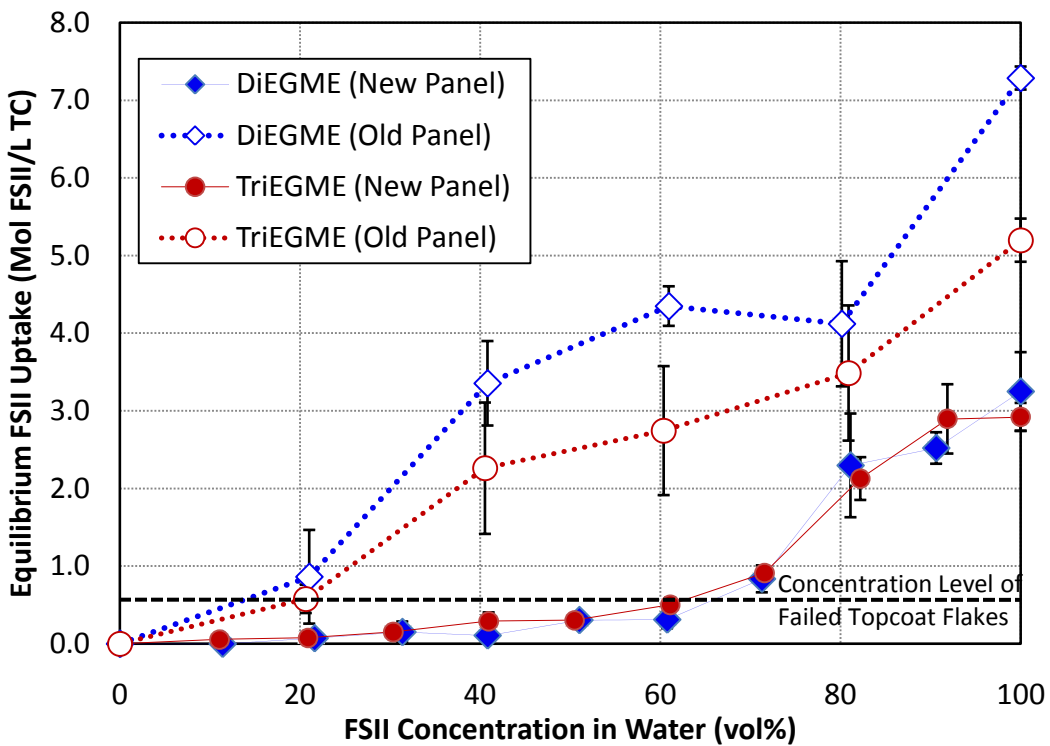


Figure 6. The uptake of DiEGME and TriEGME with new and old panels in aqueous solutions.

The new panels show little uptake until a concentration of approximately 70 vol% FSII is achieved, while the uptake for older panels increase relatively smoothly with increasing FSII concentration. At concentrations greater than approximately 80 vol% FSII, the new panel uptake appears to plateau, or at least not increase as rapidly. These trends are similar to the aqueous ESU data obtained by Aliband et al.² Their data shows a distinct “S” shaped curve with the ESU measurements reaching a plateau at levels above 75 vol% DiEGME.

The new panel uptake shown in Figure 6 are above the failed topcoat flakes concentration at 70 vol% FSII and greater, while the old panels achieve this level at a significantly lower concentration of approximately 20 vol% FSII. The older panels absorb more FSII from aqueous mixtures than the newer panels as also observed in the fuel absorption studies. Overall, the aqueous solutions show a much higher maximum uptake than the FSII in fuel solutions. The maximum uptake for aqueous solutions is ~7.2 mol FSII/L TC at 100 vol% FSII, while the maximum uptake for fuel exposures was ~2.3 mol FSII/L TC at 1.0 vol% FSII. This may be due to the significantly higher concentration of FSII in the aqueous solutions. While the topcoat was

still physically intact after exposure to 100% solutions of DiEGME and TriEGME, it was easily damaged upon contact.

FSII Desorption Results

While the results show that DiEGME and TriEGME have similar absorption rates, it is important to assess relative desorption rates as a slower desorption can contribute to increased topcoat degradation over time. To evaluate the relative desorption rate of FSII from the topcoat polymer matrix, the exposed panels were allowed to dry in a fume hood at ambient temperatures for various periods of time, rather than being immediately analyzed after exposure. The uptake for aqueous solutions of DiEGME was measured as a function of time and is shown in Figure 7.

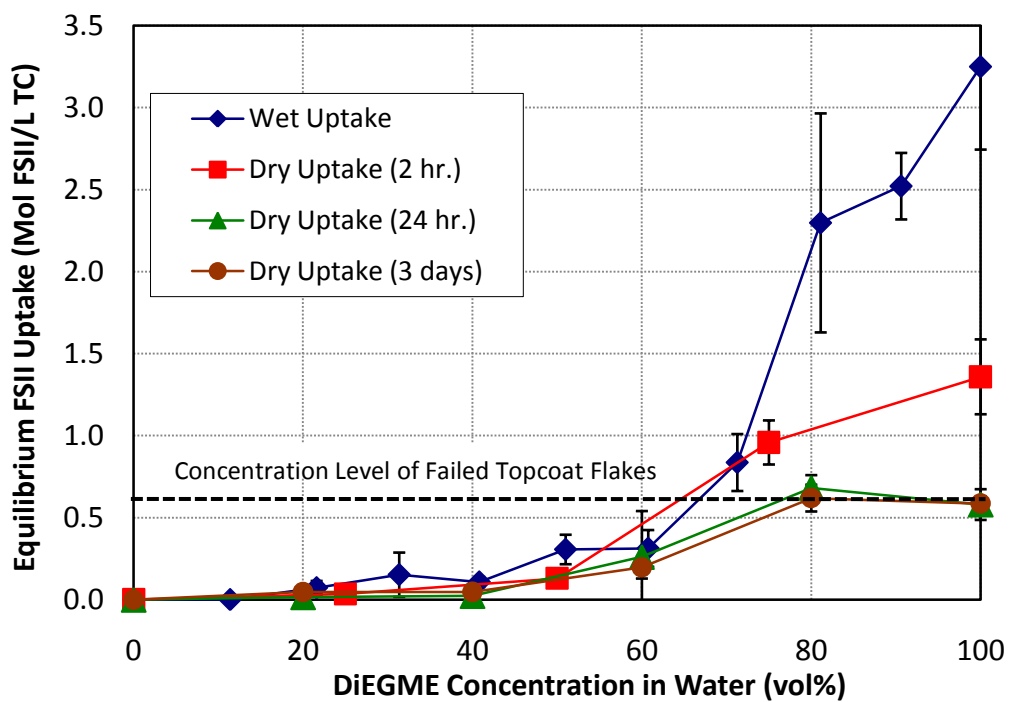


Figure 7. The uptake of DiEGME in aqueous solutions as a function of drying time with new panels.

The figure shows evidence for DiEGME desorption from the topcoat at the higher concentrations studied. At DiEGME concentrations less than 70 vol%, the equilibrium uptake is very similar for the four tested time periods. At concentrations greater than 70 vol%, there is a very large decrease in the DiEGME absorbed in the topcoat after only two hours, and at longer

times the desorption rate slows down significantly. The DiEGME concentration in the coating reaches its final equilibrium level in less than 24 hours. It is interesting to note that DiEGME does not completely desorb from the topcoat, and the resulting final concentration of DiEGME in the topcoat is the same as the uptake level from the failed topcoat flakes at ~ 0.7 mol FSII/L topcoat for concentrations greater than 80 vol% in the water. In order for the dried flakes to have such a high concentration of FSII, they must have been exposed to an even greater concentration of DiEGME. Once the topcoat is exposed to a sufficient concentration of FSII to cause a failure, it is possible that the FSII in the coating will tend to desorb to this level.

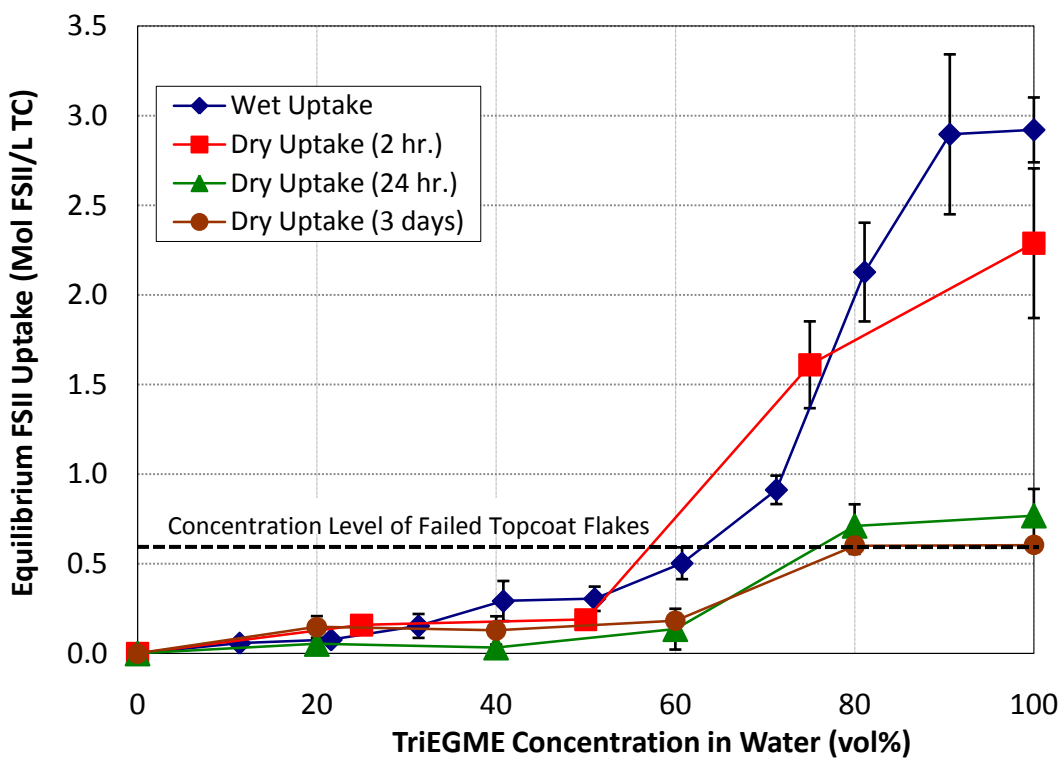


Figure 8. The uptake of TriEGME in aqueous solutions as a function of drying time with new panels.

As shown in Figure 8, the equilibrium uptake of TriEGME as a function of time is low up to a concentration of 50 vol% TriEGME. At higher concentrations the data shows evidence of desorption, but the TriEGME desorption is significantly slower at the two hour mark. At the 100% FSII level, TriEGME is only reduced to 78% of the original concentration after two hours, while the DiEGME concentration is reduced to 42%. This difference is likely due to the lower

vapor pressure of TriEGME, which will cause it to evaporate more slowly from the topcoat. The slower rate of TriEGME desorption may also result from its larger molecular size causing slower diffusion of the molecules through the polymer matrix. DiEGME and TriEGME desorb to a similar final concentration when given enough time to reach equilibrium.

The results show that TriEGME and DiEGME desorb to similar final equilibrium values, although their initial desorption rates vary. This difference in desorption rates at high concentrations of FSII indicates that it might be possible for high concentrations of TriEGME in the topcoat to be maintained for longer periods of time, with a resulting higher occurrence of topcoat degradation. However, it is expected that these high concentrations of TriEGME will not be achieved due to the lower vapor pressure of the additive resulting in a reduced concentration in the condensate. This absorption/desorption study does not fully evaluate the entire FTTP process; however, it provides insight into the required concentration of FSII in jet fuel or water which will promote high absorption levels and subsequent topcoat degradation.

Pencil Hardness Study Results

Further studies were performed to evaluate topcoat integrity after the absorption of FSII has occurred. These studies provide insight into what concentration ranges of FSII in fuel or water provide sufficient absorption to cause topcoat degradation and promote FTTP. Pencil hardness measurement after exposure was selected as a simple technique to indicate topcoat degradation. A two day exposure time was selected to complete measurements in a reasonable time, while still maintaining the minimum exposure duration for equilibrium to be reached between the solution and topcoat. Each pencil hardness data point represents a single panel that was tested at the given FSII concentration. The first study used the surrogate condensate, discussed in the experimental section, which simulates the condensable fuel components from the fuel ullage. As it is hypothesized that the condensed vapors are the fuel components in contact with the fuel ullage tank walls where FTTP occurs, it is reasonable to study this using the fuel condensate surrogate mixture. Figure 9 shows a plot of the equilibrium uptake and pencil hardness of new panels in the surrogate as a function of the FSII concentration.

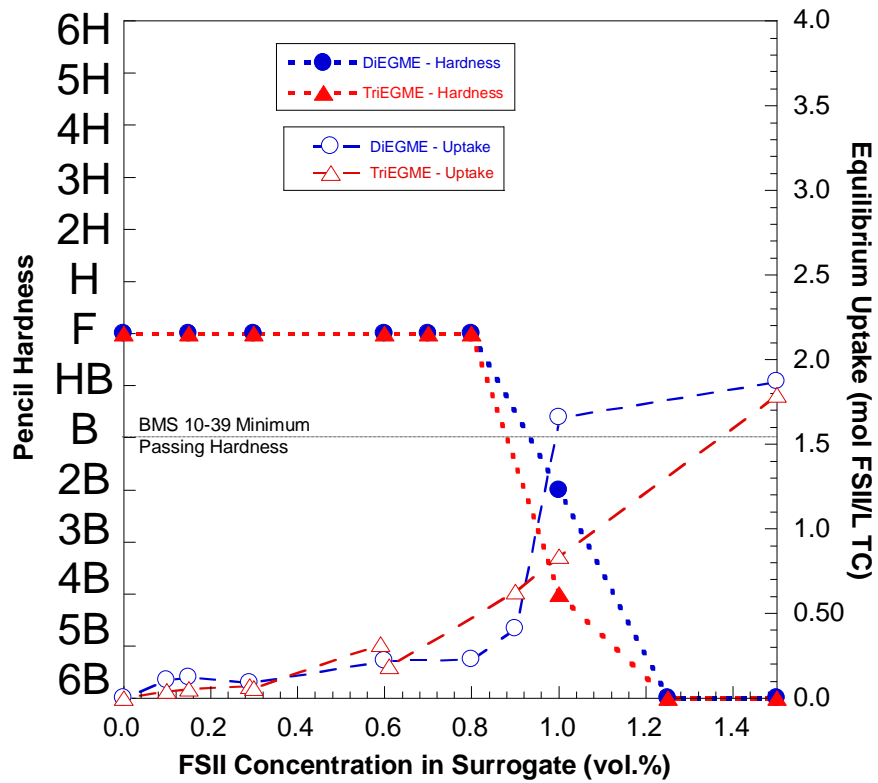


Figure 9. New panel uptake and wet pencil hardness in a fuel condensate surrogate.

The figure shows a strong correlation between the pencil hardness of BMS 10-39 and the equilibrium uptake. The pencil hardness of the panel is unaffected at low FSII concentrations, but as the uptake begins to increase (>0.80 vol%) a very sharp decrease is observed. DiEGME and TriEGME behave very similarly in this pencil hardness evaluation. The equilibrium uptake level corresponding to the degradation of BMS 10-39 occurs at uptake levels greater than approximately 1.0 mol FSII/L topcoat. The topcoat integrity continues to decrease and adhesion is lost as the concentration in the topcoat increases further. Exposure of BMS 10-39 topcoat panels to jet fuel (Jet A-1) containing FSII was compared to the surrogate mixture exposures, and in all cases it was found that the surrogate and jet fuel uptake and pencil hardness measurements were identical within experimental uncertainty. As both fuel and surrogate produce similar results, the surrogate was used for further pencil hardness studies to more closely simulate the conditions for FTTP.

Pencil hardness measurements were also performed with old panels to determine the effect of increased uptake on the hardness of the topcoat. If the older panels represent a worst-case scenario for the current BMS 10-39 coating in B-52 aircraft, then studying the pencil hardness of these panels after exposure to FSII is critical for investigating the requisite conditions for FTTP. The results are shown in Figure 10, along with FSII uptake measurements for old panels in the condensate surrogate.

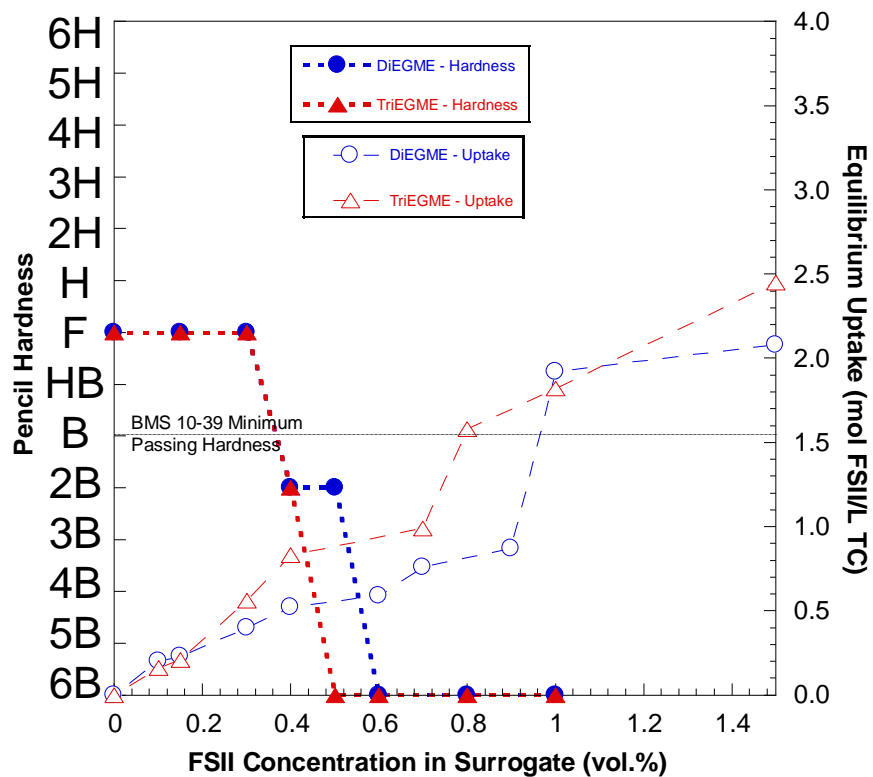


Figure 10. The uptake and pencil hardness of DiEGME and TriEGME in the condensate surrogate for old panels.

The pencil hardness begins to decline rapidly at approximately 0.30 vol% FSII, which corresponds to an increase in the uptake. This FSII concentration is only twice the maximum procurement concentration for JP-8. The pencil hardness falls below the minimum passing rating of „B“ at a FSII concentration of approximately 0.40 vol% FSII in the surrogate. This is a significant decrease from the concentration necessary to fail newer panels (approximately 1.0 vol% FSII). Overall, the older panels show a highly decreased ability to maintain coating

hardness, as is evident by the increased absorption of FSII. These data imply that older panels have increased void spaces and weakened polymer bonds resulting in a degradation of the topcoat matrix. These results indicate that older panels should be used for conservative analysis of aircraft fuel tank scenarios, due to the degraded properties of the topcoat after exposure to fuel and environmental conditions over many years.

Pencil hardness testing was adapted to investigate the effect of FSII desorption from the topcoat. Instead of evaluating the hardness immediately after removal from the solution, testing was performed after drying for two hours in a fume hood. This study was performed using the condensate surrogate and new panels under ambient conditions. The data is shown in Figure 11. It should be noted that the uptake data included in Figure 11 was obtained from extractions performed without adding a drying time before analysis.

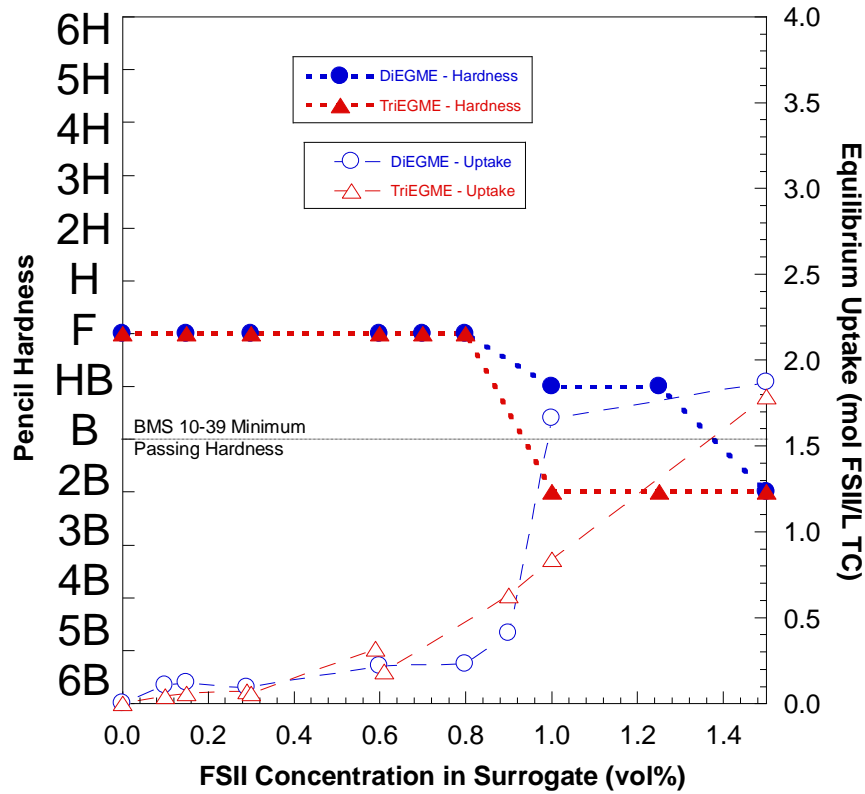


Figure 11. Pencil hardness for new panels in surrogate after two hours of drying.

The pencil hardness of BMS 10-39 topcoat decreases as the concentration of FSII in the surrogate increases, however the hardness does not decrease to nearly the same extent as the panels evaluated immediately after contact with FSII. Panels exposed to DiEGME remain above the minimum passing hardness for BMS 10-39, except for 1.5 vol% DiEGME in the surrogate. Panels exposed to TriEGME fall below the passing level at a concentration of 1.0 vol%. When the panels were evaluated “wet” (Figure 9), both DiEGME and TriEGME decreased the hardness at the same concentration of 1.0 vol% FSII. As discussed above, this difference could be due to the lower vapor pressure of TriEGME, which causes it to desorb and evaporate more slowly from the coating. It would be expected for the pencil hardness to reach the same level in both DiEGME and TriEGME if more time is given for desorption to occur, as the desorption data show that these additives reach the same final level in the topcoat. These data show that BMS 10-39 exposed to high concentrations of TriEGME will have a reduced hardness for a longer period of time compared to DiEGME. This could potentially increase the timeframe for FTTP to occur, although these high concentrations of TriEGME in the topcoat are not expected to occur on tank ullage walls, as discussed below.

To study FTTP occurring in fuel tank water bottom areas, the pencil hardness was evaluated for new BMS 10-39 panels after exposure to aqueous solutions. Similar to the fuel and surrogate pencil hardness testing, this provides insight into the requisite concentrations in water bottoms for degradation. Figure 12 shows the “wet” pencil hardness testing and uptake as a function of aqueous FSII concentration for new panels.

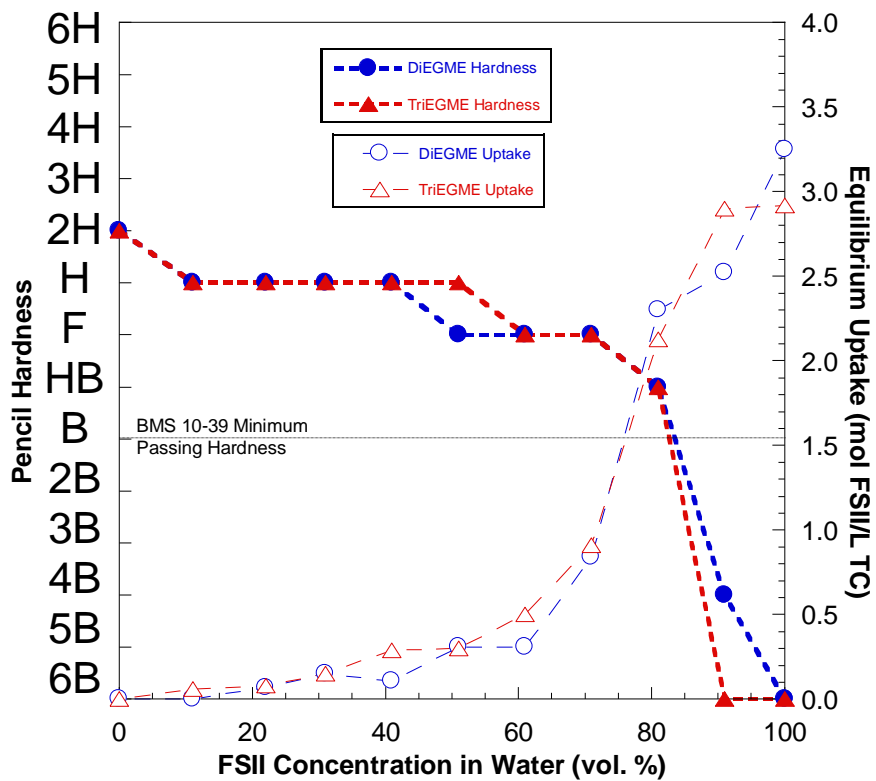


Figure 12. Pencil hardness and equilibrium FSII uptake of new panels in aqueous solutions with varying concentrations of FSII.

The uptake dramatically increases at approximately 70 vol% FSII, while the pencil hardness also begins to decrease rapidly. New topcoat exposed to surrogate or fuel has been shown to degrade at approximately 2.0 mol FSII/L topcoat and the aqueous solutions also show a very similar uptake concentration for failure. This degradation requires concentrations greater than 70 vol% DiEGME or TriEGME in water in contact with the topcoat. This is much higher than that expected concentrations (30 to 50 vol%) in tank bottoms at ambient conditions with specification FSII levels in fuel.⁸ The initial hardness of these panels exposed to aqueous solutions was slightly higher than those exposed to fuel surrogate solutions. While there was some variation with the initial hardness from both the new and old panels used, the surrogate alone seemed to have a very slight softening effect of one pencil lead on the topcoat. This could potentially be due to some slight swelling due to absorption of unknown fuel species into the BMS 10-39 coating.

The pencil hardness testing has been able to provide a comparison between DiEGME and TriEGME, which has shown statistically identical behavior for nearly all absorption measurements. It has also provided a greater understanding into what concentrations are necessary to initiate FTTP. Concentrations of FSII greater than 1.0 vol% are required to severely weaken the topcoat of new panels in a fuel or surrogate. Older panels only require concentrations of FSII greater than approximately 0.40 vol% FSII in the fuel or surrogate to degrade the topcoat below the minimum hardness. As discussed above, this difference in concentration is a result of the reduced capability of the older panels to resist FSII absorption. Aqueous solutions require concentrations greater than 80 vol% for new panels to fail.

The only differences between DiEGME and TriEGME were observed in the desorption studies. The more rapid recovery in the hardness of DiEGME exposed panels is most likely due to its higher vapor pressure. Because there is less FSII remaining in the topcoat, there is less swelling and the coating retains a higher hardness. While DiEGME and TriEGME performed similarly in the absorption study, different pencil hardness results are expected when the vaporization process of FSII in the bulk fuel is combined with the condensation process of the fuel/FSII vapor onto the topcoat. It is expected for TriEGME to have a much lower concentration in the vapor, and thus a much lower concentration in contact with the topcoat, because of its reduced vapor pressure. The next section demonstrates a simulation system which attempts to reproduce the overall behavior of the fuel/FSII/topcoat system.

Fuel Tank Topcoat Peeling (FTTP) Simulation Results

A fuel tank simulation system was developed to attempt to re-create the required conditions for FTTP, as well as to evaluate the ability of TriEGME to reduce FTTP. In previous work,⁶ the concentrations of DiEGME and TriEGME in the fuel condensate were compared. The results show that the concentration of DiEGME in the condensate increased with each distillate fraction and further vaporization, while the concentration of TriEGME in the condensate maintained a level below the initial concentration in the bulk fuel. While this previous work focused only on collecting and analyzing the fuel condensate, the FTTP simulation described here will promote fuel/FSII vaporization with subsequent selective condensation of the fuel vapor on an old topcoat panel. This simulation was designed to re-create all necessary steps for

FTTP in a controlled setting. It also serves to investigate the effects of specific conditions on FTTP, such as the initial concentration of FSII in the bulk fuel, the temperature of the fuel, and the temperature of the condensing topcoat surface. Selective condensation on the topcoat panel was achieved by attaching a heat exchanger with a recycling cooled water bath to the back of the panel. Old panels were employed to provide a conservative measure of the effect of the FSII additives. The concentration range of FSII in the fuel was from 0 to 0.15 vol%, while the temperatures investigated were 50 or 60⁰C in the environmental chamber, and a cooled panel surface of 10 to 30⁰C. These ranges of concentrations and temperatures were selected as they are believed to closely represent the worst-case ground conditions for FTTP in aircraft fuel tanks. Fuel and condensate samples were collected, their DiEGME and TriEGME concentration were quantified after three to five days. This was shown to be sufficient for equilibrium to be reached, as discussed below. The data obtained from this set of experiments, at a fuel temperature of 60⁰C and a cooling surface temperature of 20⁰C, along with the quantified FSII concentrations are summarized in Table 2. Figure 13 presents the pencil hardness data as a function of the initial concentration for the experimental conditions in Table 2.

At concentrations equal to or below approximately 0.05 vol% DiEGME in the fuel, there were no visible changes in the panel after exposure, and the hardness of the topcoat was unaffected. This is evident by Figure 14, which shows the BMS 10-39 panel exposed to condensate from 0.05 vol% DiEGME in the fuel for three days. At concentrations of 0.06 to 0.10 vol% DiEGME in the fuel, there were initial signs of swelling in the panels. The hardness began to degrade quickly with any further increase in the DiEGME concentration in the fuel, although the panels were still relatively intact and did not show any severe signs of swelling and blistering. Figure 15 shows BMS 10-39 panels after a three day exposure to condensate from ~0.08 vol% DiEGME in the bulk fuel. There were no visible changes in the topcoat panel after exposure to the DiEGME rich condensate in this range; however, the hardness of the panel did decrease significantly on some portions of the coating. The center of the panel did pass a hardness of “H,” which is above the minimum passing hardness for BMS 10-39, however the edges only yielded a hardness of “4B.”

Table 2. DiEGME and TriEGME Experiments with the Environmental Chamber at 60⁰C
and the Condensation Surface at 20⁰C

	Initial FSII Conc. (vol%)	Final FSII Conc. (vol%)	Condensate FSII Conc. (vol%)	Exposure Time (Days)	Pencil Hardness
DiEGME	0	0.006	0.033	3	2H
	0.030	0.026	0.031	3	2H
	0.047	0.049	0.062	3	H-2H
	0.055	0.047	0.077	3	H-2H
	0.067	0.067	0.12	3	F-H
	0.067	0.069	0.076	5	F-H
	0.078	0.076	0.14	3	4B-H
	0.100	0.094	0.67	3	<6B-4B
	0.101	0.100	0.25	4	<6B-4B
	0.140	0.135	0.72	2	<6B
	0.156	0.138	1.09	5	<6B
TriEGME	0.051	0.052	0.065	3	2H
	0.080	0.101	0.12	4	2H
	0.135	0.135	0.15	3	H-2H

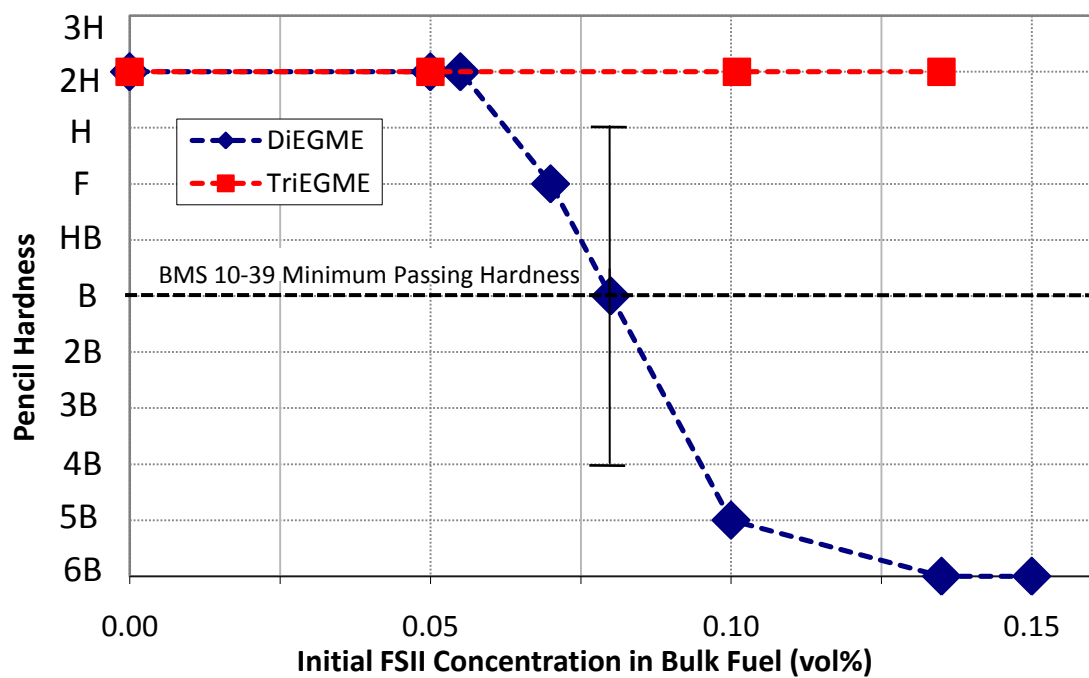


Figure 13. Pencil hardness of older panels after exposure to varying initial FSII concentrations in the bulk fuel.



Figure 14. Old panel exposed to condensed vapors from 0.05 vol% DiEGME in the bulk fuel.

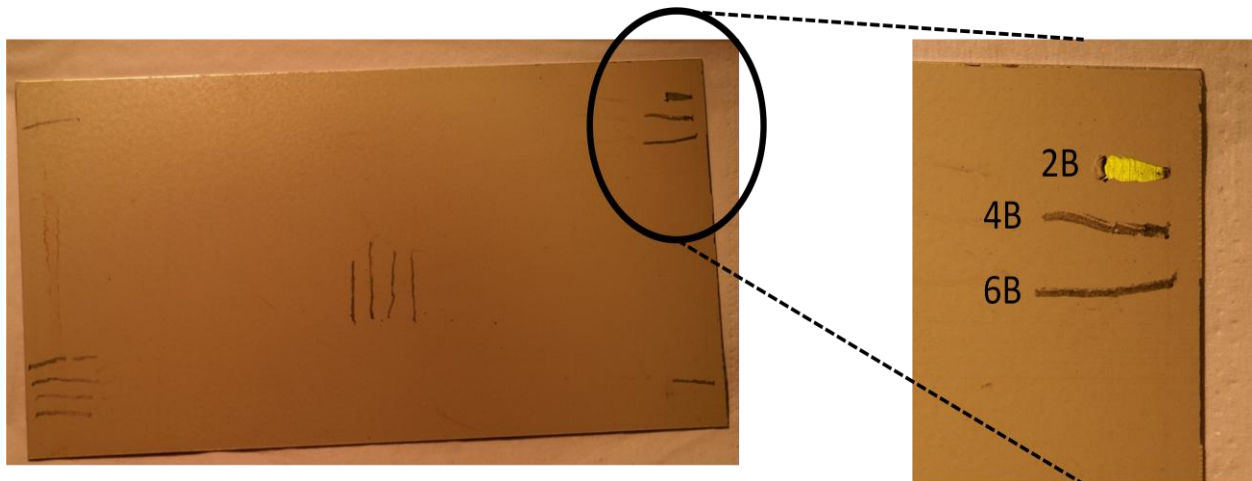


Figure 15. Old panel exposed to condensed vapors from 0.08 vol% DiEGME in the fuel with the pencil hardness measurements shown.

A complete failure of the topcoat panels was evident for initial concentrations of approximately 0.10 vol% DiEGME in the fuel or greater. Along with the hardness decreasing below the minimum specification, the coating itself exhibited signs of severe swelling and blistering as well as a loss of adhesion from the aluminum substrate. Figure 16 shows a topcoat panel after three days exposure to condensate from ~0.10 vol% DiEGME in the fuel. The center of the panel yielded a hardness of 4B, while the edges of the panel were not tested, as they were severely swollen and delaminated from the aluminum substrate. The largest failure regions on the panel typically occurred on the sides and edges of the panel, while the center showed slightly less degradation. This could be explained by a non-uniform condensation on the surface of the panel due to non-uniform surface temperatures created by inadequate contact with the heat exchanger. The panel was attached to the cooled steel heat exchanger plate by clamps on the edges and along the top of the panel. This may have provided better contact to the heat exchanger and a colder surface that selectively condensed the FSII rich vapor in these regions.



Figure 16. Old panel exposed to condensed vapors from 0.10 vol% DiEGME in the bulk fuel.

The use of TriEGME in this FTTP simulation study in place of DiEGME provided completely different results for all aspects of this experiment. BMS 10-39 panels showed no degradation after exposure to condensed vapors from TriEGME-containing fuels at all of the concentrations tested. Figure 17 shows a topcoat panel after exposure to condensate from ~0.10 vol% TriEGME in the bulk fuel. The figure shows a topcoat panel that was completely unaffected by contact with concentrations of approximately 0.12 vol% TriEGME in the condensate. There is no visible discoloration or swelling after exposure, and the pencil hardness of the coating did not decrease. At these concentration levels, TriEGME exhibits excellent anti-icing performance.⁶



Figure 17. Old panel exposed to condensed vapors from 0.10 vol% TriEGME in the bulk fuel.

As DiEGME and TriEGME performed almost identically in the uptake and pencil hardness testing shown above, the reason for the decreased degradation caused by TriEGME is due to the lower concentration in contact with the topcoat, which results from the lower vapor pressure of TriEGME. Gas chromatograms of fuels, DiEGME, and TriEGME (not shown) suggest that DiEGME is more volatile than most jet fuel components, while TriEGME is slightly less volatile than the average fuel components. Thus at temperatures below the initial fuel boiling point (<200⁰C), DiEGME will preferentially concentrate in the vapor relative to most fuel components, while TriEGME will vaporize along with the fuel components and not increase in concentration in the vapor. Thus, the topcoat will be exposed to concentrations of TriEGME which are far below that shown to cause degradation in the absorption studies reported above.

Table 2 shows a significant difference between the DiEGME and TriEGME concentrations in the sampled condensate. It should be noted that these FSII concentration determinations were difficult to perform, as only microliter volumes could be collected from the panel surface using a GC syringe. The concentrations of DiEGME in the condensate increased by a factor of up to seven compared to the initial bulk fuel concentration. Typically, higher concentrations of DiEGME in the fuel yielded much higher concentrations in the condensate. For example, a concentration of approximately 0.15 vol% DiEGME in the fuel resulted in a condensate of 1.09 vol% DiEGME. TriEGME does not show this large increase in the condensate concentration and only increases by a factor of 1.2 on average for the runs. A

maximum value of 0.15 vol% TriEGME in contact with the topcoat is not sufficient to cause degradation, as was also confirmed by the previous pencil hardness study experiments (Figure 10). In the pencil hardness study, the pencil hardness of old panels after exposure to concentrations of 1.0 vol% DiEGME in the surrogate resulted in a hardness of <6B, which is seen under these simulation conditions. The increase in DiEGME concentrations in the condensate is also supported by the ullage box data obtained from previous work.⁶ Table 2 shows that the concentration of DiEGME in the condensate clearly increased from the initial concentration in the fuel for each experimental condition. However, the TriEGME result differs from the previous work. The data from Table 2 shows an increase of TriEGME in the condensate, while the previous study showed a significant decrease in the TriEGME condensate. This difference could be explained by the relatively low distillation percentage collected in the previous work. Also, the glass collector used previously condensed the fuel condensate at a much lower temperature of -10⁰C. This lower temperature may not selectively condense TriEGME from the vapor, but rather, lighter fuel components may be more likely to condense, lowering the concentration of TriEGME.

The time needed to reach equilibrium between the vapor, the condensate, and the topcoat was also studied as shown in Table 2. Degradation could be seen as early as one day for concentrations of 0.07 vol% DiEGME or greater in the bulk fuel; however, more time was given to ensure the entire panel reached equilibrium. Figure 18 shows a BMS 10-39 panel clamped to the heat exchanger while exposed to approximately 0.10 vol% DiEGME after one day. It is evident there are droplets of the FSII rich condensate in contact with the topcoat surface, which has begun to swell and blister. Figure 18 also serves to show the increased condensation on the edges of the panel, where greater amounts of fluid are present. Three days of exposure was found to be sufficient in reaching an equilibrium state between the fuel and the topcoat, as well as to obtain a visual confirmation of the integrity of the topcoat. This was confirmed by running two experiments at 0.067 vol% DiEGME in the fuel, with one panel being exposed for three days and the other for five days. While there was a small difference in the DiEGME concentration in the condensate, the pencil hardness and visual appearance of the panels were identical.



Figure 18. Old BMS 10-39 panel in the FTTP simulation box showing severe swelling after one day of exposure to vapors from 0.10 vol% DiEGME in the fuel.

The effects of temperature on the degradation process were also studied to determine the conditions necessary for FTTP to occur. The temperature of the environmental chamber and the cooling surface were varied to determine how they affected the vaporization and condensation processes and topcoat degradation. These additional DiEGME experiments also served to evaluate the minimum concentration of DiEGME in the bulk fuel which would no longer produce FTTP. BMS 10-39 panels were evaluated based upon their pencil hardness as a function DiEGME concentration and temperature, as shown in Table 3. The bulk fuel and condensate DiEGME concentrations were also measured.

The environmental chamber was heated to 50 or 60°C, while the cooling surface temperature was varied between 10 and 30°C for this study. These temperatures were used to simulate the expected ground conditions in a fuel tank, as well as determine what temperatures will cause the most severe degradation. The initial runs at 60°C fuel, 20°C cooling (60/20°C) showed a significant amount of degradation, especially at concentrations greater than 0.10 vol% DiEGME in the fuel. To further investigate the other temperatures, an initial fuel concentration of approximately 0.07 vol% DiEGME was used as this was within the transition range for

topcoat failure at the 60/20⁰C conditions. This concentration could then be altered based upon the topcoat behavior to further evaluate the effect of temperature.

Increasing the cooling surface to 30⁰C increased the hardness of the panel compared to a cooling surface of 20⁰C, for the two tested concentrations of approximately 0.07 and 0.09 vol% DiEGME in the bulk fuel. This is most likely due to the surface temperature being high enough such that DiEGME no longer selectively condensed relative to fuel vapors on the panel. The condensate samples did contain lower concentrations of DiEGME than was measured in the 20⁰C cooling surface experiments. Lowering the cooling surface temperature to 10⁰C also did not promote FTTP as readily. While increasing the initial DiEGME concentration in the fuel to approximately 0.11 vol% did reduce the pencil hardness below the minimum passing hardness at this condition, it was still not as severe of a failure as the 60/20⁰C condition at a similar initial concentration. Lowering the cooling surface to 10⁰C appeared to promote condensation of two phases on the topcoat panel, an aqueous and a hydrocarbon phase. Two condensed liquid phases were observed visually on the topcoat surface. The identity of the phases was confirmed by refractive index as well as GC-MS analysis of the composition and DiEGME concentration. The addition of an aqueous phase on the topcoat surface may provide a benefit to the topcoat integrity, as DiEGME will partition readily into the aqueous phase reducing the concentration in the hydrocarbon phase. This benefit will only be realized as long as high concentrations (>70%) are not reached in the aqueous phase.

The other runs involved reducing the fuel temperature to 50⁰C to determine if lowering the temperature would significantly reduce the vaporization of DiEGME. The 50/20⁰C experiment at approximately 0.07 vol% DiEGME did not produce any detectable change in the pencil hardness, or any visual evidence of failure. It was unclear if sufficient exposure time was given to reach equilibrium at this lower temperature, as it would require more time to vaporize DiEGME and accumulate sufficient amounts in the topcoat to cause degradation. The second run at a higher concentration of approximately 0.09 vol% DiEGME was exposed for 14 days. The BMS 10-39 panel did decrease in pencil hardness slightly, although the coating was still two pencil leads above the minimum passing hardness. This decrease in hardness was most likely a function of the increased concentration of DiEGME in the fuel and subsequent condensate, and not the increased exposure time. An environmental chamber temperature of 50⁰C reduced the

vaporization of DiEGME in the system such that the condensate concentration did not cause a significant decrease in the topcoat hardness or initiate severe swelling. The final run of 50/10⁰C also did not degrade the topcoat panel. This condition created two phases on the panel surface, which seemed to indicate that a cooling surface of 10⁰C was sufficient to condense any water within the system.

Table 3. Experimental Simulations with DiEGME Performed at Various Temperatures and Concentrations

Fuel Temperature (°C)	Cooling Surface Temperature (°C)	Initial Conc. (vol%)	Final Conc. (vol%)	Condensate Conc. (vol%)	Test Period (days)	Pencil Hardness
60	20	0	0	0	3	H-2H
		0.047	0.049	0.062	3	H-2H
		0.055	0.047	0.077	3	H-2H
		0.067	0.067	0.12	3	F-H
		0.078	0.076	0.14	3	4B-H
		0.100	0.094	0.67	4	<4B
		0.101	0.100	0.25	4	<4B
		0.140	0.135	0.72	2	<6B
		0.156	0.138	1.09	5	<6B
	30	0.070	0.069	0.046	3	H-2H
	30	0.088	0.087	0.087	3	H-2H
	10	0.070	0.060	0.19(56.4%)*	3	HB-H
		0.109	0.086	0.28(62.5%)*	3	2B-F
50	20	0.072	0.070	0.10	3	H-2H
		0.093	0.091	0.20	14	F-H
	10	0.079	0.072	0.25(57.1%)*	3	H-2H

(* denotes 2nd aqueous phase concentration)

Overall, experimental simulation of FTTP in this system provided data for the determination of the concentrations and temperatures necessary to promote this phenomenon. The initial conditions of 60/20⁰C were ideal for creating an FTTP scenario. While other temperatures did produce some deterioration of the BMS 10-39 coating, the hardness of the panel was still above the minimum specification. The fuel temperature needs to be sufficiently warm such that high concentrations of DiEGME are vaporized, and the condensing surface temperature needs to be low enough to selectively condense DiEGME, but not so low as to

condense water. Based upon this study, continued use of DiEGME as the FSII additive will require a significant decrease in concentration, as FTTP will occur at current procurement concentrations if the correct temperature conditions are reached. The highest concentration that did not cause the hardness of the topcoat to fall below the minimum specification was approximately 0.07 vol% DiEGME. TriEGME did not cause topcoat degradation at any of the concentrations tested in this simulation (up to 0.135 vol%).

CONCLUSIONS

The compatibility of DiEGME and TriEGME with BMS 10-39 topcoat material was studied to provide a better understanding of the fuel tank topcoat peeling mechanisms, to determine the requisite conditions for degradation to occur, and to determine the conditions under which degradation can be prevented. Under liquid exposure conditions, both fuel system icing inhibitor additives were found to partition equally, on a molar basis, into the topcoat over a wide range of concentrations. This was demonstrated for aqueous, fuel, and fuel surrogate solution exposures for both old and new topcoat panels. The absorption of FSII was found to increase dramatically for old panels relative to new panels. The old panels are considered to be representative of topcoat surfaces of real fuel tank walls in the current USAF fleet. The new panels studied are likely more resistant to FSII absorption than what is currently present in B-52 aircraft.

The desorption rate of FSII out of the topcoat differed between DiEGME and TriEGME. Initially, TriEGME showed a slower desorption rate than DiEGME, which can be explained by its lower vapor pressure and greater molecular size. After two hours, the DiEGME and TriEGME concentrations in the panel began to reach similar levels, and eventually reached a final concentration of approximately 0.7 mol FSII/L topcoat after aqueous exposures of 80 vol% FSII or greater. This concentration was similar to that from failed topcoat flakes, which suggests that the FSII component in the topcoat will not completely desorb or evaporate after exposure to high concentrations. In the pencil hardness study, both DiEGME and TriEGME performed identically within experimental error. There was a large difference between the new and old panels, with the old panels falling below the passing hardness lead of “B” when exposed to FSII concentrations as low as 0.40 vol% in the fuel surrogate, while the new panels required concentrations of 1.0

vol% for failure. In pencil hardness measurements of FSII desorption, the hardness of the topcoat was found to increase as desorption occurs. This hardening effect is indicative of relamination of the topcoat after FSII exposure and topcoat softening.

The experimental simulation that was developed to re-create FTTP in a controlled setting was the first laboratory system able to reproduce the entire FTTP process and to determine the requisite conditions for topcoat failure. DiEGME was found to concentrate in the ullage vapor by a factor of two to seven times the initial concentration in the fuel. These high condensate concentrations resulted in severe degradation of the topcoat. The highest concentration in the bulk fuel that did not cause a failure, as rated by the pencil hardness of the coating, was at ~0.07 vol% DiEGME. However, TriEGME proved very effective as it did not lower the pencil hardness of the topcoat panel up to approximately 0.14 vol% TriEGME. The resulting TriEGME condensate concentration did increase on average by a factor of 1.2, although this small increase did not prove detrimental to the BMS 10-39 panel. The lower vapor pressure of TriEGME was determined to be the major reason in its improved topcoat compatibility for fuel tank ullage surfaces. Based upon these results, TriEGME has been shown to be an excellent FSII replacement in terms of BMS 10-39 topcoat material compatibility. During the scenarios analyzed in these studies, TriEGME would not cause degradation to the topcoat at the current concentrations employed for DiEGME in JP-8. If DiEGME continues to be used as the specification FSII additive, it is recommended that the maximum concentration in aircraft tanks be no more than 0.07 vol% to prevent topcoat degradation. This should prevent high concentrations of DiEGME vaporizing and condensing on topcoat surfaces. Adherence to required maintenance practices, such as sumping of fuel tanks, is essential to the prevention of FTTP in water bottoms when either FSII additive is used.

The occurrence of FTTP in the simulated fuel tank box was dependent on the temperatures of the fuel and condensing surfaces. Fuel temperatures of 60⁰C were able to selectively vaporize levels of DiEGME sufficient to cause swelling and blistering. Lower temperatures were unable to provide condensate concentrations that were sufficient to cause degradation of the coating during the test period. The optimum cooled surface temperature for selective condensation of DiEGME and topcoat degradation is near 20⁰C. At higher temperatures the surface condensate had reduced DiEGME concentrations, and below 20⁰C an aqueous phase

condensed on the topcoat surface, which decreased the concentration of DiEGME in contact with the polymer.

ACKNOWLEDGEMENTS

This material is based on research sponsored by Air Force Research Laboratory under agreement number F33615-03-2-2347. The U.S. Government is authorized to reproduce and distribute reprints for Governmental purposes notwithstanding any copyright notation thereon. The view and conclusions contained herein are those of the authors and should not be interpreted as necessarily representing the official policies or endorsements, either expressed or implied, of Air Force Research Laboratory or the U.S. Government.

The authors would like to acknowledge funding support from the U.S. Department of Defense Reduction of Total Ownership Cost program through Ed Wells of USAF ASC/ENFA.

REFERENCES

1. Martel, C.R., Air Force Wright Aeronautical Laboratories Technical Report, AFWAL-TR-2062, 1987.
2. Aliband, A.; Lenz, D.; Dupois, J.; Alliston, K.; Sorhaug, V.; Stevenson, L.; Whitmer, T.; Burns, D.; Stevenson, W. *Progress in Organic Coatings*, **2006**, *56*, 285-296.
3. Aliband, A.; Lenz, D.; Stevenson, L.; Whitmer, T.; Cash, R.; Burns, D.; Stevenson, W. *Progress in Organic Coatings* **2008**, *63*, 139-147.
4. Williams, T.F.; Vangsness, M.; Shardo, J.; Ervin, J., Air Force Research Laboratory Report, AFRL-PR-WP-TR-2005-2103, February 2005.
5. Hufnagle, D., University of Dayton Research Institute Report UDR-TR-2008-00032, 2008.
6. Zabarnick S.; West Z.; DeWitt M.; Shafer L.; Striebich R.; Adams R.; Delaney C.; Phelps D. *IASH 2007, the 10th International Conference on Stability, Handling and Use of Liquid Fuel*, October 2007.

7. DeWitt, M.J.; Zabarnick, S.; Shaeffer, S.; Williams, T.; West, Z.; Shafer, L.; Striebich, R.; Breitfield, S.; Adams, R.; Cook, R.; Delaney, C.L.; Phelps, D. *IASH 2009, the 11th International Conference on Stability, Handling and Use of Liquid Fuel*, October 2009.
8. West, Z.; Shafer, L.; Striebich, R.; Zabarnick, S.; Delaney, C.; Phelps, D.; DeWitt, M.J., manuscript in preparation, 2009.

Appendix C. Fuel Systems Materials Compatibility

INTENTIONALLY LEFT BLANK

**Material Compatibility of a Proposed Alternative Fuel System
Icing Inhibitor (FSII) Additive: TriEGME
(Materials Evaluation)**

7 December 2010

**Evaluation Report
(SA104002)**

Report No. AFRL/RXS 10-090

AUTHORS

**Alan J. Fletcher
And
Ryan P. Osysko (University of Dayton Research Institute)
Air Force Research Laboratory/Materials Integrity Branch (AFRL/RXSA)
Building 652, Room 122
2179 12th Street
Wright-Patterson Air Force Base, Ohio 45433-7718**

REQUESTER

**AFRL/RZPF
Tim Edwards**

DISTRIBUTION STATEMENT A: Approved for public release; distribution unlimited.

88ABW-2010-6140

EXECUTIVE SUMMARY

Testing and evaluation were performed by the University of Dayton Research Institute for the Air Force Research Laboratory/Adhesives, Composites, and Elastomers Section to determine the material compatibility of triethylene glycol monomethyl ether (TriEGME), a proposed substitute for the current fuel system icing inhibitor, diethylene glycol monomethyl ether (DiEGME), with fuel tank, airframe, and engine materials. Testing was performed on representative materials to determine if there would be any detrimental short-term effects. Based on results of testing performed after aging materials in four times the normal concentration of the additives, it was determined further testing was required for some materials. Therefore, Phase II testing was performed at 1.5 times the normal concentration of each additive. The results indicated TriEGME is no more aggressive toward materials than the current additive, DiEGME.

ACKNOWLEDGMENTS

This report would not have been possible without the expert help of many others. Special thanks go to Mr. Bill Fortener of the University of Dayton Research Institute whose engineering expertise was invaluable.

TABLE OF CONTENTS

	Page
PURPOSE.....	1
BACKGROUND.....	1
TEST PROCEDURE.....	2
TEST RESULTS.....	4
CONCLUSIONS.....	6
RECOMMENDATION	7
FIGURES.....	9
TABLES.....	13

Material Compatibility of a Proposed Alternative Fuel System Icing Inhibitor (FSII) Additive: TriEGME

PURPOSE

The purpose of this testing was to determine if a proposed fuel system icing inhibitor (FSII) substitute, triethylene glycol monomethyl ether (TriEGME), would have any detrimental effects on aircraft materials.

BACKGROUND

The Air Force Research Laboratory/Adhesives, Composites, and Elastomers Section (AFRL/RXSAC) was asked to perform expedited materials compatibility testing to determine the compatibility of fuel tank materials with TriEGME, a proposed substitute for the current FSII, diethylene glycol monomethyl ether (DiEGME). The possibility of substituting TriEGME for DiEGME is being explored, because DiEGME has caused detrimental effects to the coatings used in fuel tanks. Based on previous material compatibility tests with the JP-8+100 and other fuel additives, it was decided to utilize a short list of materials (metallic and nonmetallic) for screening purposes. These specific materials were chosen as representatives for each general type of material, with an emphasis on those particular compounds that were most affected during previous additive testing.

The test parameters for this evaluation were the same as have been used on other material compatibility programs, and the baseline (no soak) data were taken from other programs. A 28-day fuel exposure at elevated temperatures in Jet A-1 containing DiEGME and Jet A-1 containing TriEGME was followed by standard physical and mechanical properties testing to measure the effects of the fuels on the materials. For Phase I, to best simulate a worst-case fuel, additives were included in the fuel at four times the amount that would be used in normal service. The fuels tested in Phase I were POSF 5119 (DiEGME) and POSF 5120 (TriEGME). Exposure temperatures selected were based on the usage temperature of each specific material.

Based on the results of Phase I testing, it was determined further testing was required to ensure TriEGME was not more detrimental to materials than DiEGME. For the follow-up testing, it was determined the additive concentrations in the fuel would be 1.5 times their normal concentration as opposed to the 4 times normal used for Phase I. This testing, referred to as Phase II, was performed on the following materials that were selected based on significant degradation of properties during Phase I testing or recommendation by AFRL/RXSAC:

- Vinyl Phenolic Adhesive
- Epoxy Adhesive
- Nitrile Bladder Innerliner
- Polyurethane Bladder Innerliner
- AMS-S-4383 Nitrile Fuel Tank Coating
- AMS-C-27725 Polyurethane Fuel Tank Coating
- BMS 10-39 Epoxy Fuel Tank Coating
- AMS3283 Polysulfide Noncuring Groove Sealant

All of the nonmetallic material testing was conducted at the University of Dayton Research Institute (UDRI) in August through November 2007. For the metallic materials, exposures were performed at UDRI, the light optical and scanning electron microscopy were performed by the U.S. Air Force Academy Center for Aircraft Structural Life Extension (CAStLE), with final analysis and examination performed by AFRL/RXSAC.

TEST PROCEDURE

All testing was in accordance with established ASTM International and SAE International test procedures outlined below. The materials tested were comprised of five adhesives, three fuel bladder materials, five coatings, six sealants, two noncuring groove sealants, two composite materials, one foam material, four specific types of O-rings, two hose materials, four wire insulation materials, one potting compound, and thirty metallic alloys. Unless otherwise noted, all test results represent an average of a minimum of three replicate specimens. Required testing for the nonmetallic materials included the following:

Adhesives

Lap Shear	ASTM D 1002
Static Shear	ASTM D 4562

Fuel Bladders

Tensile Strength & Elongation	ASTM D 412
Volume Swell	ASTM D 471

Coatings

Pencil Hardness	ASTM D 3363
Tape Adhesion	ASTM D 3359, Method A

Sealants

Peel Strength	SAE AS5127/1
Hardness, Shore A	ASTM D 2240
Tensile Strength & Elongation	SAE AS5127/1
Volume Swell	ASTM D 412
	SAE AS5127/1
	ASTM D 471
	SAE AS5127/1

Composite Materials

Interlaminar Shear	ASTM D 790
--------------------	------------

Foam Material

Tensile Strength & Elongation	ASTM D 412
Resistivity	ASTM D 257

O-rings

Hardness, Shore M	ASTM D 2240
Tensile Strength & Elongation	ASTM D 1414
Compression Set	ASTM D 395
Volume Swell	ASTM D 471

Hose Material

Hardness, Shore A	ASTM D 2240
Tensile Strength & Elongation	ASTM D 412
Volume Swell	ASTM D 471

Wire Insulation

Tensile Strength & Elongation	ASTM D 412
-------------------------------	------------

Potting Compound

Hardness, Shore A	ASTM D 2240
Tensile Strength & Elongation	ASTM D 412
Peel Strength	SAE AS5127/1

The evaluation methods used to determine the microstructural degradation (mainly the presence and extent of corrosion) of the metallic materials were light optical and scanning electron microscopy. All metallic samples were optically examined up to 500x magnification for surface deposits, staining, and microstructural anomalies. When needed, scanning electron microscopy was used to characterize surface morphology, with energy dispersive x-ray spectroscopy (EDS) used to analyze for elemental constituents. Disposition of the +100 additive samples was determined by direct comparison to the JP-8 samples.

For Phase I testing, the additives were incorporated into the fuel at a concentration 4 times greater than would normally be used in service. This increased concentration was meant to exaggerate and help identify any potential compatibility problems that could occur. For Phase II testing, the additives were incorporated at a concentration 1.5 times greater than what will normally be used.

In analyzing the data, a logical evaluation criterion was to compare the results after aging in the baseline fuel containing DiEGME with results after aging in the fuel containing TriEGME to identify any significant differences. For each test, "allowable" variations were determined based on standard deviations in the test methods. Differences greater than these allowable variations indicate increased possibility variations in the data are significant and cannot be attributed to normal data scatter for this type of test. When this occurred, the data required closer examination to determine if additional testing was needed, or if the data clearly indicated a failure. For some materials there are specification limits, expressed as maximum or minimum values, that can help determine if the material still meets certain requirements after aging. Test requirements noted in the data tables were based on specification limits, when available. Otherwise, test requirements provided were based on experience and previous test programs. In the tables, a value outside the allowable variation from the baseline is marked in red, as is a failure to meet the test requirements. However, a red marking in the tables does not necessarily

mean the material tested is incompatible with the fuel. Final determination of compatibility considered the overall test results for a given material and the implications of these results for in-service aircraft.

TEST RESULTS

The completed nonmetallic Phase I test results are contained in Tables 1, 2, 3, 4, 5, 6, 7, 8, and 9. Results after fuel aging in Jet A-1 containing TriEGME and Jet A-1 containing DiEGME are compared to one another, with variations calculated and noted in the tables. Unaged values for each of the materials are included as additional references. Failures to meet the test requirements are listed in red, as are values outside of the allowable variation criteria. Items marked with a # sign represent retested values.

An evaluation letter containing the metallic test results is provided in the Appendix. Similar to the nonmetallic testing, the results obtained after aging in Jet A-1 containing TriEGME are compared against the Jet A-1 containing DiEGME baseline specimens. The overall metallic test results showed no signs of increased corrosion for any of the materials tested when exposed to the Jet A-1 containing TriEGME.

Phase I

- All adhesives evaluated by lap shear met the test requirements, and there were no results outside of the allowable variation. In the adhesives tested by static shear, the cyanoacrylate adhesive aged in DiEGME did not meet the test requirement, and the methacrylate adhesive results were outside of the allowable variation from the baseline (Table 1).
- All bladder innerliner materials evaluated met the test requirements except for volume swell of the polyurethane material after aging in DiEGME. The only result outside of the allowable variation for bladder testing was tensile strength of polyurethane (Table 2).
- The majority of the coating materials evaluated met the test requirements, however, there were several that did not: pencil hardness for the AMS-S-4383 nitrile coating (> unaged) after aging in both DiEGME and TriEGME, tape adhesion for the AMS-S-4383 nitrile and BMS 10-39 epoxy coatings after aging in TriEGME, and pencil hardness for the AMS-C-27725 polyurethane and BMS 10-39 epoxy coatings after aging in TriEGME. The only result outside of the allowable variation was pencil hardness of the BMS 10-39 epoxy (Table 3).
- All sealant materials evaluated met the test requirements except for the percent cohesive failure in the peel strength testing of the AMS3279 polythioether/polyurethane material after aging in TriEGME. There were also several results outside of the allowable variation from the baseline: elongation for the AMS-S-8802 dichromate-cured polysulfide material, Shore A hardness for the AMS-S-8802 manganese dioxide-cured polysulfide material, AMS3279 polythioether/polyurethane material, and AMS3277

polythioether material, and peel strength for the AMS3375 fluorosilicone material (Table 4).

- After evaluation of the two noncuring groove sealants, the only result that did not meet test requirements listed was volume swell of the AMS 3283 polysulfide material after aging in TriEGME. This result was also outside of the allowable variation (Table 5).
- All results for the two composite materials evaluated met the test requirement and were within the allowable variation (Table 6).
- All results for the foam material evaluated met the test requirements and were within the allowable variations (Table 7).
- All results for the O-ring materials evaluated met the test requirements except Shore M hardness of the AMS-P-5315 nitrile material after aging in DiEGME. Results outside of the allowable variation included Shore M hardness of the AMS-P-5315 nitrile material and compression set of the AMS-P-83485 fluorocarbon good-to-low-temperature (GLT) material (Table 8).
- The following results for the two hose materials tested did not meet the test requirements:
 1. Shore A hardness for the MIL-H-4495 acrylic/nitrile material after aging in both DiEGME and TriEGME.
 2. Tensile strength results for the MIL-DTL-26521 nitrile material after aging in both DiEGME and TriEGME.
 3. Volume swell for the MIL-DTL-26521 nitrile material after aging in both DiEGME and TriEGME.
 4. Shore A hardness for the MIL-DTL-26521 nitrile material after aging in both DiEGME and TriEGME.

There were, however, no results outside of the allowable variation between the DiEGME and TriEGME for either of the two materials tested (Table 9).

- All results for the four wire insulation materials evaluated met the test requirements, but there were two instances in which the results were outside of the allowable variation from the baseline: tensile strength of the Teflon® film and elongation of the nylon film material (Table 10).
- All results for the polysulfide potting compound (MIL-PRF-8516) met the test requirements and were within the allowable variations from the baseline (Table 11).

Phase II (Retests)

- All of the results for the two adhesive materials retested met the test requirements and were within the allowable variation from the baseline (Table 12).

- All of the results for the two bladder innerliner materials retested met the test requirements except for volume swell of the polyurethane material after aging in both DiEGME and TriEGME. There were no results outside of the allowable variation from the baseline for the retested bladder materials (Table 13).
- All of the coatings retested met the test requirements except for pencil hardness of the AMS-S-4383 nitrile material after aging in both DiEGME and TriEGME in both the vapor and liquid phases, as well as pencil hardness of the BMS 10-39 epoxy coating material after aging in DiEGME in both the vapor and liquid phases at both 200°F and 160°F. It is important to note one out of the three AMS-S-4383 nitrile coated panels retested failed tape adhesion after aging in TriEGME (Figure 1). The only result outside of the allowable variation from the baseline was pencil hardness of the AMS-S-4383 nitrile coating in the liquid phase (Table 14).
- In testing the AMS-C-27725 polyurethane coating, although all of the results met the test requirements, there was some discoloration of the coating itself, as well as discoloration of the fuel in which the panels were aged (Figures 2 and 3). Due to this discoloration, the 28-day aging in 1.5 times normal concentration of additive was repeated. As was the case for the previous results, the fuel and coating were both slightly discolored; however, the severity of the discolorations was much lower. The fuel in which the panels were aged was then analyzed, and this analysis showed no deterioration of the AMS-C-27725 coating. Additionally, the panels passed both pencil hardness and tape adhesion testing.
- Both results for the noncuring groove sealant retested did not meet the test requirements for volume swell. However, the results after aging in the fuel containing TriEGME were within the allowable variation from the results after aging in the fuel containing DiEGME (Table 15).

CONCLUSIONS

Based on both Phase I and Phase II testing, the following conclusions have been made:

TriEGME, similar to DiEGME, is aggressive toward coatings.

In general, when TriEGME and DiEGME degraded materials, they did so in a similar fashion.

TriEGME may be less aggressive in the vapor phase than DiEGME.

Reducing the concentration from 4 times normal to 1.5 times normal significantly reduced the effects DiEGME and TriEGME had on the materials.

RECOMMENDATION

Careful engineering review and risk analyses must be performed by weapon systems managers considering switching from DiEGME to TriEGME. Material compatibility data indicate TriEGME has a lower potential for coating failures in the vapor phase and similar potential in the liquid phase. Additionally, decreasing the concentration of the FSII will significantly reduce the effects of both glycols on nonmetallic materials.

PREPARED BY



ALAN J. FLETCHER
Adhesive, Composites, and Elastomers Section (RXSAC)
Materials Integrity Branch
Systems Support Division
Materials and Manufacturing Directorate

REVIEWED BY



JAMES J. MAZZA, Section Chief
Adhesive, Composites, and Elastomers Section (RXSAC)
Materials Integrity Branch
Systems Support Division
Materials and Manufacturing Directorate

PUBLICATION REVIEW: This report has been reviewed and approved.



MARY ANN PHILLIPS, Branch Chief
Materials Integrity Branch
Systems Support Division
Materials and Manufacturing Directorate

FIGURES

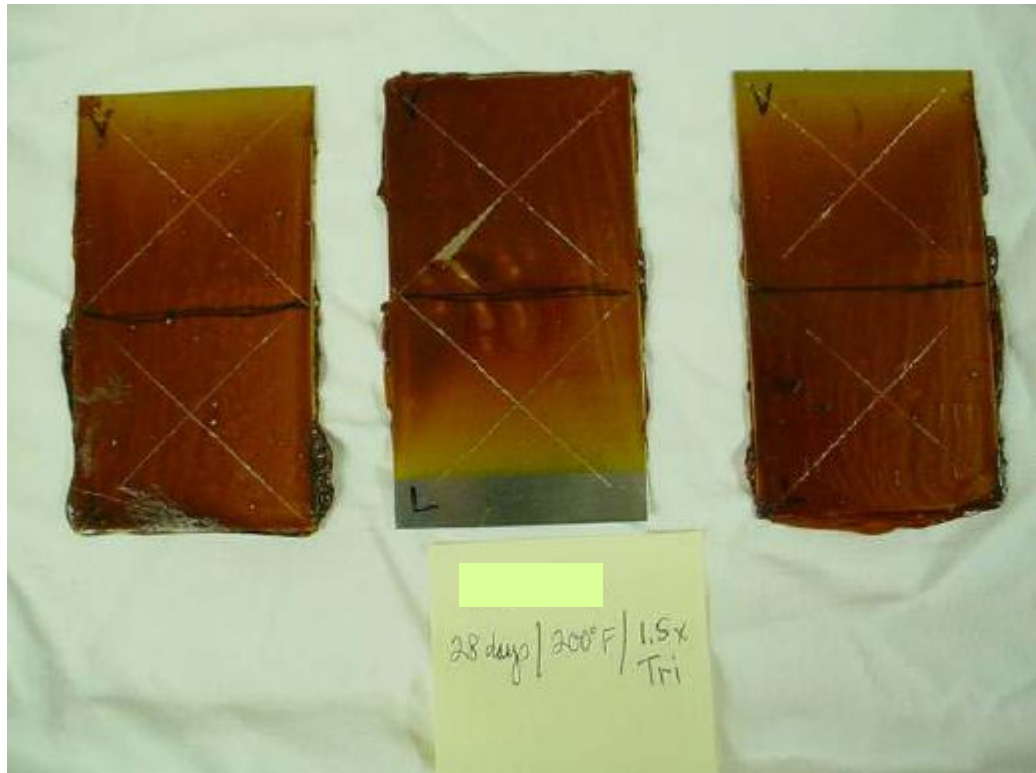


Figure 1. AMS-S-4383 Nitrile coating panels after testing at 1.5 times concentration in TriEGME.



Figure 2. AMS-C-27725 Polyurethane coating panels after aging in 1.5 times concentration TriEGME.



Figure 3. Fuel Discoloration of 1.5 times TriEGME after aging AMS-C-27725 polyurethane coating specimens.

TABLES

Table 1. Adhesives

Material Description	Test	Conditioning	Evaluation Criteria		Test Results	Variation from DiEGME
			Test Requirement	Allowable Variation from DiEGME Baseline		
Vinyl Phenolic	Lap Shear	Unaged 28d/200°F/DiEGME (4x) 28d/200°F/TriEGME (4x)	>1500 psi >1500 psi >1500 psi	N/A N/A 250 psi decrease	3755 psi 3910 psi # 3895 psi #	N/A N/A -15
Epoxy	Lap Shear	Unaged 28d/200°F/DiEGME (4x) 28d/200°F/TriEGME (4x)	>1500 psi >1500 psi >1500 psi	N/A N/A 250 psi decrease	4294 psi 3582 psi 3422 psi	N/A N/A -160
Nitrile Phenolic	Lap Shear	Unaged 28d/200°F/DiEGME (4x) 28d/200°F/TriEGME (4x)	>1500 psi >1500 psi >1500 psi	N/A N/A 250 psi decrease	3132 psi 2900 psi 2816 psi	N/A N/A -84
Methacrylate	Static Shear	Unaged 28d/200°F/DiEGME (4x) 28d/200°F/TriEGME (4x)	>1200 psi >1200 psi >1200 psi	N/A N/A 250 psi decrease	2474 psi 2716 psi 2312 psi	N/A N/A -404
Cyanoacrylate	Static Shear	Unaged 28d/200°F/DiEGME (4x) 28d/200°F/TriEGME (4x)	>1200 psi >1200 psi >1200 psi	N/A N/A 250 psi decrease	2199 psi 1194 psi 1391 psi	N/A N/A +197

= retested results

Table 2. Bladder Innerliners

Material Description	Test	Conditioning	Evaluation Criteria		Test Results	Variation from DiEGME
			Test Requirement	Allowable Variation from DiEGME Baseline		
Nitrile	Tensile Strength	Unaged	>1500 psi	N/A	2441 psi	N/A
		28d/160°F/DiEGME (4x)	>1500 psi	N/A	1962 psi	N/A
		28d/160°F/TriEGME (4x)	>1500 psi	200 psi decrease	2003 psi	+41
	Elongation	Unaged	>300%	N/A	568%	N/A
		28d/160°F/DiEGME (4x)	>300%	N/A	326%	N/A
		28d/160°F/TriEGME (4x)	>300%	40% decrease	352%	+26%
	Volume Swell	Unaged	N/A	N/A	N/A	N/A
		28d/160°F/DiEGME (4x)	<25%	N/A	2.4%	N/A
		28d/160°F/TriEGME (4x)	<25%	5% increase	-12.1%	-14.5%
Polyurethane	Tensile Strength	Unaged	>1500 psi	N/A	3292 psi	N/A
		28d/200°F/DiEGME (4x)	>1500 psi	N/A	2800 psi	N/A
		28d/200°F/TriEGME (4x)	>1500 psi	200 psi decrease	2168 psi	-632
	Elongation	Unaged	>300%	N/A	449%	N/A
		28d/200°F/DiEGME (4x)	>300%	N/A	632%	N/A
		28d/200°F/TriEGME (4x)	>300%	40% decrease	633%	+1%
	Volume Swell	Unaged	N/A	N/A	N/A	N/A
		28d/200°F/DiEGME (4x)	<25%	N/A	34.0%	N/A
		28d/200°F/TriEGME (4x)	<25%	5% increase	5.0%	-29.0%
Bladder, Self-Sealing Layer) (MIL-DTL-5578)	Volume Swell	Unaged	N/A	N/A	N/A	N/A
		30m/RT/DiEGME (4x)	TBD	N/A	57.0%	N/A
		30m/RT/TriEGME (4x)	TBD	TBD	60.1%	+3.1%

Table 3. Coatings

Material Description	Test	Conditioning	Evaluation Criteria		Test Results	Variation from DiEGME
			Test Requirement	Allowable Variation from DiEGME Baseline		
AMS-S-4383 (Nitrile)	Pencil Hardness	Unaged	N/A	N/A	2H*	N/A
		28d/200°F/DiEGME (4x)	≥ unaged	N/A	2B*	N/A
	Tape Adhesion	28d/200°F/TriEGME (4x)	≥ unaged	± 1 pt	2B*	0
		Unaged	Pass	N/A	Passed*	N/A
AMS-C-27725 (Polyurethane)	Pencil Hardness	28d/200°F/DiEGME (4x)	Pass	N/A	Passed*	N/A
		28d/200°F/TriEGME (4x)	Pass	N/A	Passed*	N/A
	Tape Adhesion	Unaged	Pass	N/A	Failed*	N/A
		28d/200°F/DiEGME (4x)	Pass	N/A	Passed*	N/A
BMS 10-20 (Epoxy)	Pencil Hardness	28d/200°F/TriEGME (4x)	Pass	N/A	Passed*	N/A
		Unaged	Pass	N/A	Passed*	N/A
	Tape Adhesion	28d/200°F/DiEGME (4x)	Pass	N/A	Passed*	N/A
		28d/200°F/TriEGME (4x)	Pass	N/A	Passed*	N/A
BMS 10-39 (Epoxy)	Pencil Hardness	Unaged	N/A	N/A	≥ 6H*	N/A
		28d/200°F/DiEGME (4x)	≥ unaged	N/A	≥ 6H*	N/A
	Tape Adhesion	28d/200°F/TriEGME (4x)	≥ unaged	± 1 pt	≥ 6H*	0
		Unaged	Pass	N/A	Passed*	N/A
	Tape Adhesion	28d/200°F/DiEGME (4x)	Pass	N/A	Passed*	N/A
		28d/200°F/TriEGME (4x)	Pass	N/A	Passed*	N/A

6B – 5B – 4B – 3B – 2B – B – HB – F – H – 2H – 3H – 4H – 5H – 6H
Softer Harder

* = results obtained from one 2.75" x 6" coated substrate

Table 3 Cont. Coatings

Material Description	Test	Conditioning	Evaluation Criteria		Test Results	Variation from DiEGME
			Test Requirement	Allowable Variation from DiEGME Baseline		
MIL-DTL-24441 (Epoxy Polyamide)	Pencil Hardness	Unaged	N/A	N/A	>6H*	N/A
		28d/120°F/DiEGME (4x)	≥ unaged	N/A	>6H*	N/A
		28d/120°F/TriEGME (4x)	≥ unaged	± 1 pt	>6H*	0
	Tape Adhesion	Unaged	Pass	N/A	Passed*	N/A
		28d/120°F/DiEGME (4x)	Pass	N/A	Passed*	N/A
		28d/120°F/TriEGME (4x)	Pass	N/A	Passed*	N/A

* = results obtained from one 2.75" x 6" coated substrate

Table 4. Sealants

Material Description	Test	Conditioning	Evaluation Criteria		Test Results	Variation from DiEGME
			Test Requirement	Allowable Variation from DiEGME Baseline		
AMS-S-8802, B-2 (Polysulfide) (Dichromate-cured)	Tensile Strength	Unaged	>200 psi	N/A	518 psi	N/A
		28d/200°F/DiEGME (4x)	>200 psi	N/A	300 psi	N/A
		28d/200°F/TriEGME (4x)	>200 psi	35 psi decrease	277 psi	-23
	Elongation	Unaged	>150%	N/A	507%	N/A
		28d/200°F/DiEGME (4x)	>150%	N/A	198%	N/A
		28d/200°F/TriEGME (4x)	>150%	25% decrease	153%	-45%
	Volume Swell	Unaged	<20%	N/A	N/A	N/A
		28d/200°F/DiEGME (4x)	<20%	N/A	4.7%	N/A
		28d/200°F/TriEGME (4x)	<20%	5% increase	-3.2%	-7.9%
	Shore A Hardness	Unaged	>35	N/A	62	N/A
		28d/200°F/DiEGME (4x)	>35	N/A	59	N/A
		28d/200°F/TriEGME (4x)	>35	± 5 pts	61	+2
	Peel Strength (AMS-C-27725)	Unaged	>20 lbs / 100%	N/A	36 lbs / 100% ¹	N/A
		28d/200°F/DiEGME (4x)	>20 lbs / 100%	N/A	39 lbs / 100%	N/A
		28d/200°F/TriEGME (4x)	>20 lbs / 100%	8 lbs decrease	45 lbs / 100%	+6
AMS-S-8802, B-2 (Polysulfide) (Manganese Dioxide Cured)	Tensile Strength	Unaged	>200 psi	N/A	395 psi	N/A
		28d/200°F/DiEGME (4x)	>200 psi	N/A	379 psi	N/A
		28d/200°F/TriEGME (4x)	>200 psi	35 psi decrease	351 psi	-28
	Elongation	Unaged	>150%	N/A	271%	N/A
		28d/200°F/DiEGME (4x)	>150%	N/A	239%	N/A
		28d/200°F/TriEGME (4x)	>150%	25% decrease	250%	+11%
	Volume Swell	Unaged	<20%	N/A	N/A	N/A
		28d/200°F/DiEGME (4x)	<20%	N/A	-1.4%	N/A
		28d/200°F/TriEGME (4x)	<20%	5% increase	-0.7%	+0.7%
	Shore A Hardness	Unaged	>35	N/A	62	N/A
		28d/200°F/DiEGME (4x)	>35	N/A	56	N/A
		28d/200°F/TriEGME (4x)	>35	± 5 pts	48	-8
	Peel Strength (AMS-C-27725)	Unaged	>20 lbs / 100%	N/A	52 lbs / 100% ¹	N/A
		28d/200°F/DiEGME (4x)	>20 lbs / 100%	N/A	45 lbs / 100%	N/A
		28d/200°F/TriEGME (4x)	>20 lbs / 100%	8 lbs decrease	39 lbs / 100%	-6

1 = Data taken from *Small Particulate Emission Control Fuel Additives Materials Compatibility Study*, UDR-TR-2005-00181 (Sept, 2005)

Table 4 Cont. Sealants

Material Description	Test	Conditioning	Evaluation Criteria		Test Results	Variation from DiEGME
			Test Requirement	Allowable Variation from DiEGME Baseline		
AMS3375 (Fluorosilicone)	Tensile Strength	Unaged	>200 psi	N/A	643 psi	N/A
		28d/200°F/DiEGME (4x)	>200 psi	N/A	218 psi	N/A
		28d/200°F/TriEGME (4x)	>200 psi	35 psi decrease	308 psi	+90
	Elongation	Unaged	>150%	N/A	355%	N/A
		28d/200°F/DiEGME (4x)	>150%	N/A	124%	N/A
		28d/200°F/TriEGME (4x)	>150%	25% decrease	200%	+76%
	Volume Swell	Unaged	<20%	N/A	N/A	N/A
		28d/200°F/DiEGME (4x)	<20%	N/A	1.6%	N/A
		28d/200°F/TriEGME (4x)	<20%	5% increase	1.4%	-0.2%
	Shore A Hardness	Unaged	>35	N/A	45	N/A
		28d/200°F/DiEGME (4x)	>35	N/A	39	N/A
		28d/200°F/TriEGME (4x)	>35	± 5 pts	44	+5
	Peel Strength (AMS-C-27725)	Unaged	>10 lbs / 100%	N/A	14 lbs / 100% ¹	N/A
		28d/200°F/DiEGME (4x)	>10 lbs / 100%	N/A	25 lbs / 100%	N/A
		28d/200°F/TriEGME (4x)	>10 lbs / 100%	8 lbs decrease	14 lbs / 100%	-11
AMS3279 (Polythioether / Polyurethane)	Tensile Strength	Unaged	>200 psi	N/A	2496 psi	N/A
		28d/200°F/DiEGME (4x)	>200 psi	N/A	500 psi	N/A
		28d/200°F/TriEGME (4x)	>200 psi	35 psi decrease	712 psi	+212
	Elongation	Unaged	>150%	N/A	562%	N/A
		28d/200°F/DiEGME (4x)	>150%	N/A	804%	N/A
		28d/200°F/TriEGME (4x)	>150%	25% decrease	864%	+60%
	Volume Swell	Unaged	<30%	N/A	N/A	N/A
		28d/200°F/DiEGME (4x)	<30%	N/A	14.0%	N/A
		28d/200°F/TriEGME (4x)	<30%	5% increase	12.7%	-1.3%
	Shore A Hardness	Unaged	>35	N/A	67	N/A
		28d/200°F/DiEGME (4x)	>35	N/A	60	N/A
		28d/200°F/TriEGME (4x)	>35	± 5 pts	66	+6
	Peel Strength (AMS-C-27725)	Unaged	>20 lbs / 100%	N/A	27 lbs / 100% ¹	N/A
		28d/200°F/DiEGME (4x)	>20 lbs / 100%	N/A	24 lbs / 100%	N/A
		28d/200°F/TriEGME (4x)	>20 lbs / 100%	8 lbs decrease	23 lbs / 93%#	-1

1 = Data taken from *Small Particulate Emission Control Fuel Additives Materials Compatibility Study*, UDR-TR-2005-00181 (Sept, 2005)

= retested results

Table 4 Cont. Sealants

Material Description	Test	Conditioning	Evaluation Criteria		Test Results	Variation from DiEGME
			Test Requirement	Allowable Variation from DiEGME Baseline		
AMS3277 (Polythioether)	Tensile Strength	Unaged	>200 psi	N/A	338 psi	N/A
		28d/200°F/DiEGME (4x)	>200 psi	N/A	211 psi	N/A
		28d/200°F/TriEGME (4x)	>200 psi	35 psi decrease	234 psi	+23
	Elongation	Unaged	>150%	N/A	323%	N/A
		28d/200°F/DiEGME (4x)	>150%	N/A	199%	N/A
		28d/200°F/TriEGME (4x)	>150%	25% decrease	203%	+4%
	Volume Swell	Unaged	< 25%	N/A	N/A	N/A
		28d/200°F/DiEGME (4x)	< 25%	N/A	7.8%	N/A
		28d/200°F/TriEGME (4x)	< 25%	5% increase	8.2%	+0.4%
	Shore A Hardness	Unaged	>35	N/A	48	N/A
		28d/200°F/DiEGME (4x)	>35	N/A	31	N/A
		28d/200°F/TriEGME (4x)	>35	± 5 pts	39	+8
	Peel Strength (AMS-C-27725)	Unaged	>20 lbs / 100%	N/A	58 lbs / 100% ¹	N/A
		28d/200°F/DiEGME (4x)	>20 lbs / 100%	N/A	40 lbs / 100%	N/A
		28d/200°F/TriEGME (4x)	>20 lbs / 100%	8 lbs decrease	46 lbs / 100%	0
AMS3281 (Polysulfide)	Tensile Strength	Unaged	>200 psi	N/A	266 psi	N/A
		28d/200°F/DiEGME (4x)	>200 psi	N/A	224 psi	N/A
		28d/200°F/TriEGME (4x)	>200 psi	35 psi decrease	220 psi	-4
	Elongation	Unaged	>150%	N/A	596%	N/A
		28d/200°F/DiEGME (4x)	>150%	N/A	280%	N/A
		28d/200°F/TriEGME (4x)	>150%	25% decrease	298%	+18%
	Volume Swell	Unaged	<20%	N/A	N/A	N/A
		28d/200°F/DiEGME (4x)	<20%	N/A	-2.9%	N/A
		28d/200°F/TriEGME (4x)	<20%	5% increase	-3.5%	-0.6%
	Shore A Hardness	Unaged	>35	N/A	38	N/A
		28d/200°F/DiEGME (4x)	>35	N/A	44	N/A
		28d/200°F/TriEGME (4x)	>35	± 5 pts	40	-4
	Peel Strength (AMS-C-27725)	Unaged	>20 lbs / 100%	N/A	36 lbs / 100% ¹	N/A
		28d/200°F/DiEGME (4x)	>20 lbs / 100%	N/A	34 lbs / 100%	N/A
		28d/200°F/TriEGME (4x)	>20 lbs / 100%	8 lbs decrease	29 lbs / 100%	-5

1 = Data taken from *Small Particulate Emission Control Fuel Additives Materials Compatibility Study*, UDR-TR-2005-00181 (Sept, 2005)

Table 5. Non-curing Groove Sealants

Material Description	Test	Conditioning	Evaluation Criteria		Test Results	Variation from DiEGME
			Test Requirement	Allowable Variation from DiEGME Baseline		
AMS3283 (Polysulfide)	Volume Swell	Unaged	N/A	N/A	N/A	N/A
		28d/160°F/DiEGME (4x)	5% to 35%	N/A	6.3%	N/A
		28d/160°F/TriEGME (4x)	5% to 35%	5% increase / decrease	-2.4%	-8.7%
Mil-S-85334 (Fluorosilicone)	Volume Swell	Unaged	N/A	N/A	N/A	N/A
		28d/160°F/DiEGME (4x)	5% to 35%	N/A	18.2%	N/A
		28d/160°F/TriEGME (4x)	5% to 35%	5% increase / decrease	19.0%	0.8%

Table 6. Composites

Material Description	Test	Conditioning	Evaluation Criteria		Test Results	Variation from DiEGME
			Test Requirement	Allowable Variation from DiEGME Baseline		
Epoxy Graphite	Interlaminar Shear	Unaged	>5000 psi	N/A	11,141 psi	N/A
		28d/200°F/DiEGME (4x)	>5000 psi	N/A	8061 psi	N/A
		28d/200°F/TriEGME (4x)	>5000 psi	500 psi decrease	8056 psi	-5
Graphite Bismaleimide	Interlaminar Shear	Unaged	>5000 psi	N/A	12,330 psi	N/A
		28d/200°F/DiEGME (4x)	>5000 psi	N/A	10,810 psi	N/A
		28d/200°F/TriEGME (4x)	>5000 psi	500 psi decrease	10,950 psi	+140

Table 7. Foam

Material Description	Test	Conditioning	Evaluation Criteria		Test Results	Variation from DiEGME
			Test Requirement	Allowable Variation from DiEGME Baseline		
MIL-PRF-87260 (conductive) Foamex Type VI (Polyurethane)	Tensile Strength	Unaged	>10 psi	N/A	15 psi	N/A
		28d/200°F/DiEGME (4x)	>10 psi	N/A	11 psi	N/A
		28d/200°F/TriEGME (4x)	>10 psi	5 psi decrease	11 psi	0
	Elongation	Unaged	>100%	N/A	118%	N/A
		28d/200°F/DiEGME (4x)	>100%	N/A	148%	N/A
		28d/200°F/TriEGME (4x)	>100%	15% decrease	162%	+14%
	Resistivity	Unaged	<1.0E+12	N/A	1.3E+11	N/A
		28d/200°F/DiEGME (4x)	<1.0E+12	N/A	1.5E+10	N/A
		28d/200°F/TriEMGE (4x)	<1.0E+12	N/A	5.5E+9	N/A

Table 8. O-rings

Material Description	Test	Conditioning	Evaluation Criteria		Test Results	Variation from DiEGME
			Test Requirement	Allowable Variation from DiEGME Baseline		
AMS-P-5315 (Nitrile)	Tensile Strength	Unaged	>1000 psi	N/A	1783 psi	N/A
		28d/160°F/DiEGME (4x)	>1000 psi	N/A	1260 psi	N/A
		28d/160°F/TriEGME (4x)	>1000 psi	125 psi decrease	1202 psi	-58
	Elongation	Unaged	>200%	N/A	309%	N/A
		28d/160°F/DiEGME (4x)	>200%	N/A	240%	N/A
		28d/160°F/TriEGME (4x)	>200%	35% decrease	230%	-10%
	Volume Swell	Unaged	N/A	N/A	N/A	N/A
		28d/160°F/DiEGME (4x)	0 to 25%	N/A	15.6%	N/A
		28d/160°F/TriEGME (4x)	0 to 25%	10% increase	16.1%	+0.5%
	Shore M Hardness	Unaged	N/A	N/A	68	N/A
		28d/160°F/DiEGME (4x)	±5 pts from unaged	N/A	76	N/A
		28d/160°F/TriEGME (4x)	±5 pts from unaged	±5 pts	69	-7
	Compression Set	Unaged	N/A	N/A	N/A	N/A
		28d/160°F/DiEGME (4x)	<50%	N/A	22.8%	N/A
		28d/160°F/TriEGME (4x)	<50%	5% increase	20.3%	-2.5%
AMS-R-25988 (Fluorosilicone)	Tensile Strength	Unaged	>500 psi	N/A	984 psi	N/A
		28d/225°F/DiEGME (4x)	>500 psi	N/A	612 psi	N/A
		28d/225°F/TriEGME (4x)	>500 psi	125 psi decrease	577 psi	-35
	Elongation	Unaged	>125%	N/A	195%	N/A
		28d/225°F/DiEGME (4x)	>125%	N/A	155%	N/A
		28d/225°F/TriEGME (4x)	>125%	35% decrease	140%	-15%
	Volume Swell	Unaged	N/A	N/A	N/A	N/A
		28d/225°F/DiEGME (4x)	0 to 25%	N/A	12.1%	N/A
		28d/225°F/TriEGME (4x)	0 to 25%	10% increase	12.3%	+0.2%
	Shore M Hardness	Unaged	N/A	N/A	69	N/A
		28d/225°F/DiEGME (4x)	- 20 pts from unaged	N/A	71	N/A
		28d/225°F/TriEGME (4x)	- 20 pts from unaged	±5 pts	72	+1
	Compression Set	Unaged	N/A	N/A	N/A	N/A
		28d/225°F/DiEGME (4x)	<65%	N/A	36.1%	N/A
		28d/225°F/TriEGME (4x)	<65%	5% increase	43.4%	7.3%

Table 8 Cont. O-rings

Material Description	Test	Conditioning	Evaluation Criteria		Test Results	Variation from DiEGME
			Test Requirement	Allowable Variation from DiEGME Baseline		
AMS-P-83485 (Fluorocarbon) (Viton GLT)	Tensile Strength	Unaged	>1000 psi	N/A	1644 psi	N/A
		28d/325°F/DiEGME (4x)	>1000 psi	N/A	1133 psi	N/A
		28d/325°F/TriEGME (4x)	>1000 psi	125 psi decrease	1099 psi	-34
	Elongation	Unaged	>150%	N/A	166%	N/A
		28d/325°F/DiEGME (4x)	>150%	N/A	208%	N/A
		28d/325°F/TriEGME (4x)	>150%	35% decrease	198%	-10%
	Volume Swell	Unaged	N/A	N/A	N/A	N/A
		28d/325°F/DiEGME (4x)	0 to 10%	N/A	9.7%	N/A
		28d/325°F/TriEGME (4x)	0 to 10%	10% increase	8.3%	-1.4%
	Shore M Hardness	Unaged	N/A	N/A	76	N/A
		28d/325°F/DiEGME (4x)	±5 pts from unaged	N/A	75	N/A
		28d/325°F/TriEGME (4x)	±5 pts from unaged	±5 pts	76	+1
	Compression Set	Unaged	N/A	N/A	N/A	N/A
		28d/325°F/DiEGME (4x)	<60%	N/A	26.1%	N/A
		28d/325°F/TriEGME (4x)	<60%	5% increase	32.3%	+6.2%
AMS 7276 (Fluorocarbon)	Tensile Strength	Unaged	>1000 psi	N/A	1799 psi ¹	N/A
		28d/325°F/DiEGME (4x)	>1000 psi	N/A	1348 psi	N/A
		28d/325°F/TriEGME (4x)	>1000 psi	125 psi decrease	1318 psi	-30
	Elongation	Unaged	>150%	N/A	229% ¹	N/A
		28d/325°F/DiEGME (4x)	>150%	N/A	242%	N/A
		28d/325°F/TriEGME (4x)	>150%	35% decrease	225%	-17%
	Volume Swell	Unaged	N/A	N/A	N/A	N/A
		28d/325°F/DiEGME (4x)	0 to 10%	N/A	7.5%	N/A
		28d/325°F/TriEGME (4x)	0 to 10%	10% increase	7.4%	-0.1%
	Shore M Hardness	Unaged	N/A	N/A	76 ¹	N/A
		28d/325°F/DiEGME (4x)	±5 pts from unaged	N/A	77	N/A
		28d/325°F/TriEGME (4x)	±5 pts from unaged	±5 pts	77	+3
	Compression Set	Unaged	N/A	N/A	N/A	N/A
		28d/325°F/DiEGME (4x)	<60%	N/A	29.9%	N/A
		28d/325°F/TriEGME (4x)	<60%	5% increase	34.2%	+4.3%

1 = Data taken from *Small Particulate Emission Control Fuel Additives Materials Compatibility Study*, UDR-TR-2005-00181 (Sept, 2005)

Table 9. Hoses

Material Description	Test	Conditioning	Evaluation Criteria		Test Results	Variation from DiEGME
			Test Requirement	Allowable Variation from DiEGME Baseline		
MIL-H-4495 (Acrylic/Nitrile)	Tensile Strength	Unaged	>1200 psi	N/A	1684 psi	N/A
		28d/160°F/DiEGME (4x)	>1200 psi	N/A	1224 psi	N/A
		28d/160°F/TriEGME (4x)	>1200 psi	125 psi decrease	1266 psi	+42
	Elongation	Unaged	>150%	N/A	250%	N/A
		28d/160°F/DiEGME (4x)	>150%	N/A	223%	N/A
		28d/160°F/TriEGME (4x)	>150%	25% decrease	229%	+6%
	Volume Swell	Unaged	N/A	N/A	N/A	N/A
		28d/160°F/DiEGME (4x)	<8%	N/A	1.7%	N/A
		28d/160°F/TriEGME (4x)	<8%	5% increase	2.1%	+0.4%
	Shore A Hardness	Unaged	N/A	N/A	66	N/A
		28d/160°F/DiEGME (4x)	±5 pts from unaged	N/A	58	N/A
		28d/160°F/TriEGME (4x)	±5 pts from unaged	±5	56	-2
MIL-DTL-26521 (Nitrile)	Tensile Strength	Unaged	>1500 psi	N/A	1806 psi	N/A
		28d/160°F/DiEGME (4x)	>1500 psi	N/A	1203 psi	N/A
		28d/160°F/TriEGME (4x)	>1500 psi	125 psi decrease	1321 psi	+118
	Elongation	Unaged	>300%	N/A	538%	N/A
		28d/160°F/DiEGME (4x)	>300%	N/A	456%	N/A
		28d/160°F/TriEGME (4x)	>300%	25% decrease	486%	+30%
	Volume Swell	Unaged	N/A	N/A	N/A	N/A
		28d/160°F/DiEGME (4x)	<8%	N/A	9.5%	N/A
		28d/160°F/TriEGME (4x)	<8%	5% increase	10.7%	+1.2%
	Shore A Hardness	Unaged	N/A	N/A	62	N/A
		28d/160°F/DiEGME (4x)	±5 pts from unaged	N/A	56	N/A
		28d/160°F/TriEGME (4x)	±5 pts from unaged	±5	52	-4

Table 10. Wire Insulation Films

Material Description	Test	Conditioning	Evaluation Criteria		Test Results	Variation from DiEGME
			Test Requirement	Allowable Variation from DiEGME Baseline		
TFE Teflon Film	Tensile Strength	Unaged (new)	>500 psi	N/A	4153 psi	N/A
		28d/160°F/DiEGME (4x)	>500 psi	N/A	4341 psi	N/A
		28d/160°F/TriEGME (4x)	>500 psi	150 psi decrease	3812 psi	-529
	Elongation	Unaged (new)	>25%	N/A	308%	N/A
		28d/160°F/DiEGME (4x)	>25%	N/A	278%	N/A
		28d/160°F/TriEGME (4x)	>25%	15% decrease	270%	-8%
Polyethylene Film	Tensile Strength	Unaged (new)	>500 psi	N/A	3818 psi	N/A
		28d/160°F/DiEGME (4x)	>500 psi	N/A	3870 psi	N/A
		28d/160°F/TriEGME (4x)	>500 psi	250 psi decrease	3773 psi	-97
	Elongation	Unaged (new)	>25%	N/A	343%	N/A
		28d/160°F/DiEGME (4x)	>25%	N/A	80%	N/A
		28d/160°F/TriEGME (4x)	>25%	50% decrease	88%	+8%
Nylon 101	Tensile Strength	Unaged (new)	>500 psi	N/A	10,431 psi	N/A
		28d/160°F/DiEGME (4x)	>500 psi	N/A	12,899 psi	N/A
		28d/160°F/TriEGME (4x)	>500 psi	850 psi decrease	12,418 psi	-481
	Elongation	Unaged (new)	>25%	N/A	360%	N/A
		28d/160°F/DiEGME (4x)	>25%	N/A	218%	N/A
		28d/160°F/TriEGME (4x)	>25%	5% decrease	207%	-11%
Kapton	Tensile Strength	Unaged	>500 psi	N/A	19,400 psi	N/A
		28d/200°F/DiEGME (4x)	>500 psi	N/A	20,704 psi	N/A
		28d/200°F/TriEGME (4x)	>500 psi	1800 psi decrease	20,342 psi	-362
	Elongation	Unaged	>25%	N/A	42%	N/A
		28d/200°F/DiEGME (4x)	>25%	N/A	51%	N/A
		28d/200°F/TriEGME (4x)	>25%	5% decrease	52%	+1%

Table 11. Potting Compound

Material Description	Test	Conditioning	Evaluation Criteria		Test Results	Variation from DiEGME
			Test Requirement	Allowable Variation from DiEGME Baseline		
Mil-PRF-8516 (Type II, Class 1) (Polysulfide)	Tensile Strength	Unaged	100 psi	N/A	215 psi	N/A
		28d/160°F/DiEGME (4x)	100 psi	N/A	136 psi	N/A
		28d/160°F/TriEGME (4x)	100 psi	35 psi decrease	151 psi	+15
	Elongation	Unaged	150%	N/A	192%	N/A
		28d/160°F/DiEGME (4x)	150%	N/A	324%	N/A
		28d/160°F/TriEGME (4x)	150%	25% decrease	394%	+70%
	Shore A Hardness	Unaged	>20 points	N/A	45	N/A
		28d/160°F/DiEGME (4x)	>20 points	N/A	33	N/A
		28d/160°F/TriEGME (4x)	>20 points	± 5 points	32	-1
	Peel Strength (AMS-C-27725)	Unaged	>10 lbs / 100%	N/A	14 lbs/100%	N/A
		28d/160°F/DiEGME (4x)	>10 lbs / 100%	N/A	17 lbs/100%	N/A
		28d/160°F/TriEGME (4x)	>10 lbs / 100%	8 lbs decrease	21 lbs/100%	+4

Table 12. Adhesives Retest

Material Description	Test	Conditioning	Evaluation Criteria		Test Results	Variation from DiEGME
			Test Requirement	Allowable Variation from DiEGME Baseline		
Vinyl Phenolic	Lap Shear	Unaged	>1500 psi	N/A	3755 psi	N/A
		28d/200°F/DiEGME (1.5x)	>1500 psi	N/A	3777 psi	N/A
		28d/200°F/TriEGME (1.5x)	>1500 psi	250 psi decrease	3702 psi	-75
Epoxy	Lap Shear	Unaged	>1500 psi	N/A	4032 psi	N/A
		28d/200°F/DiEGME (1.5x)	>1500 psi	N/A	3973 psi	N/A
		28d/200°F/TriEGME (1.5x)	>1500 psi	250 psi decrease	4002 psi	+29

Table 13. Bladder Innerliners Retest

Material Description	Test	Conditioning	Evaluation Criteria		Test Results	Variation from DiEGME
			Test Requirement	Allowable Variation from DiEGME Baseline		
Nitrile	Tensile Strength	Unaged	>1500 psi	N/A	2501 psi	N/A
		28d/160°F/DiEGME (1.5x)	>1500 psi	N/A	1982 psi	N/A
		28d/160°F/TriEGME (1.5x)	>1500 psi	200 psi decrease	1978 psi	+4
	Elongation	Unaged	>300%	N/A	348%	N/A
		28d/160°F/DiEGME (1.5x)	>300%	N/A	324%	N/A
		28d/160°F/TriEGME (1.5x)	>300%	40% decrease	345%	+21%
	Volume Swell	Unaged	N/A	N/A	N/A	N/A
		28d/160°F/DiEGME (1.5x)	<25%	N/A	1.5%	N/A
		28d/160°F/TriEGME (1.5x)	<25%	5% increase	1.6%	+0.1%
Polyurethane	Tensile Strength	Unaged	>1500 psi	N/A	3292 psi	N/A
		28d/160°F/DiEGME (1.5x)	>1500 psi	N/A	2996 psi	N/A
		28d/160°F/TriEGME (1.5x)	>1500 psi	200 psi decrease	2924 psi	-72
	Elongation	Unaged	>300%	N/A	449%	N/A
		28d/160°F/DiEGME (1.5x)	>300%	N/A	542%	N/A
		28d/160°F/TriEGME (1.5x)	>300%	40% decrease	562%	+20%
	Volume Swell	Unaged	N/A	N/A	N/A	N/A
		28d/160°F/DiEGME (1.5x)	<25%	N/A	28.7%	N/A
		28d/160°F/TriEGME (1.5x)	<25%	5% increase	26.1%	-2.6%

Table 14. Coatings Retest

Material Description	Test	Conditioning	Evaluation Criteria		Test Results Vapor / Liquid	Variation from DiEGME
			Test Requirement	Allowable Variation from DiEGME Baseline		
AMS-S-4383 (Nitrile)	Pencil Hardness	Unaged	~	~	2H / 2H	~
		28d/200°F/DiEGME (1.5x)	≥ unaged	~	2B / 2B	~
		28d/200°F/TriEGME (1.5x)	≥ unaged	± 1 pt	2B / 4B	0 / -2
	Tape Adhesion	Unaged	Pass	~	Passed / Passed	~
		28d/200°F/DiEGME (1.5x)	Pass	~	Passed / Passed	~
		28d/200°F/TriEGME (1.5x)	Pass	~	Passed* / Passed	~
AMS-C-27725 (Polyurethane)	Pencil Hardness	Unaged	~	~	>6H / >6H	~
		28d/200°F/DiEGME (1.5x)	≥ unaged	~	>6H / >6H	~
		28d/200°F/TriEGME (1.5x)	≥ unaged	± 1 pt	>6H / >6H	0
	Tape Adhesion	Unaged	Pass	~	Passed / Passed	~
		28d/200°F/DiEGME (1.5x)	Pass	~	Passed / Passed	~
		28d/200°F/TriEGME (1.5x)	Pass	~	Passed / Passed	~
BMS 10-39 (Epoxy)	Pencil Hardness	Unaged	~	~	>6H / >6H	~
		28d/200°F/DiEGME (1.5x)	≥ unaged	~	4H / 5H	~
		28d/200°F/TriEGME (1.5x)	≥ unaged	± 1 pt	>6H / >6H	+2 / +1
		28d/160°F/DiEGME (1.5x)	≥ unaged	~	5H / 4H	~
		28d/160°F/TriEGME (1.5x)	≥ unaged	± 1 pt	>6H / >6H	+1 / +2
	Tape Adhesion	Unaged	Pass	~	Passed / Passed	~
		28d/200°F/DiEGME (1.5x)	Pass	~	Passed / Passed	~
		28d/200°F/TriEGME (1.5x)	Pass	~	Passed / Passed	~
		28d/160°F/DiEGME (1.5x)	Pass	~	Passed / Passed	~
		28d/160°F/TriEGME (1.5x)	Pass	~	Passed / Passed	~

6B – 5B – 4B – 3B – 2B – B – HB – F- H – 2H – 3H – 4H – 5H – 6H

Softer

Harder

* = 2 out of 3 replicates met the test requirement.

Table 15. Non-curing Groove Sealant Retest

Material Description	Test	Conditioning	Evaluation Criteria		Test Results	Variation from DiEGME
			Test Requirement	Allowable Variation from DiEGME Baseline		
AMS3283 (Polysulfide)	Volume Swell	Unaged 28d/160°F/DiEGME (1.5x) 28d/160°F/TriEGME (1.5x)	~ 5% to 35% 5% to 35%	~ ~ ± 5%	~ 1.7% -0.7%	~ ~ -2.4%

APPENDIX

DiEGME and TriEGME Metallic Material Evaluation Letter



DEPARTMENT OF THE AIR FORCE
AIR FORCE RESEARCH LABORATORY
WRIGHT-PATTERSON AIR FORCE BASE OHIO 45433

21 MAY 2008

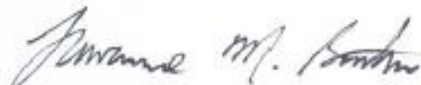
MEMORANDUM FOR AFRL/RZTG (ROBERT MORRIS)

FROM: AFRL/RXSA

SUBJECT: DiEGME and TriEGME Metallic Material Evaluation - Revised

1. This letter is issued as a second revision to the original letter dated 11 February 2008 and the first revision dated 17 April 2008. This letter contains results from all materials, including 7075-T6 Chromate Conversion Coated Class 1A, evaluated following exposure to JP8 fuel and to the DiEGME and TriEGME fuel system icing inhibitors.
2. Background - The objective of these evaluations was to compare the effects of exposure to the TriEGME fuel system icing inhibitor at 200°F to exposure to the DiEGME fuel system icing inhibitor at 200°F or 325°F (depending upon the material). Exposure periods were 28 days with fluid change at 7-day intervals. Exposed metallic samples were representative of engine and airframe materials. Additional testing (performed by The University of Dayton Research Institute) was conducted to determine sample weight loss gain, fluid conductivity, and fluid color.
2. Discussion - The metallic samples were examined utilizing light optical microscopy and scanning electron microscopy. Optical microscopic surface evaluations at a magnification up to 500X checked for surface deposits, staining, and microstructural anomalies. Some samples exhibited staining, which is considered primarily a benign surface phenomenon. Staining results in no appreciable weight loss or gain and indicates the formation of a passive layer that inhibits corrosion. Scanning electron microscopic (SEM) evaluations of a cross-section of each sample characterized surface morphology and analyzed elemental constituents using energy dispersive X-ray spectroscopy. The SEM evaluations revealed no surface or microstructural attack on any of the samples. Disposition of the TriEGME samples was determined using direct comparison to the control DiEGME samples.
3. Conclusion - All evaluated TriEGME samples performed equivalent to or exceeded the control DiEGME samples.

Material	Surface, Light Optical Stereo-Microscopic Evaluation			Cross-Section, Scanning Electron Microscopic (SEM) Evaluation		
	JP8	DiEGME	TriEGME	JP8	DiEGME	TriEGME
304SS	Non-uniform staining	Clean	Light staining	Clean	Clean	Clean
17-4 PH	Same as reference	Clean	Light staining	Clean	Clean	Clean
440 SS	Light deposit	Black deposit	Dark brown/black deposits	Clean	Clean	Clean
Ti - 8Al - 1V - 1Mo	Light staining	Clean	Clean	Clean	Clean	Clean
Ti - CP - 70	Light staining	Light Staining	Clean	Clean	Clean	Clean
Ti - 3Al - 2.5V	Light staining	Clean	Clean	Clean	Clean	Clean
4130 IVD Coating	Light Staining	Clean	Clean	Clean	Clean	Clean
Alloy Steel Fastener MS24694 HL21PN20-16	Clean	Clean	Clean	Clean	Clean	Clean
A286 Fastener MS24694 HL49GU20-16	Light Staining	Clean	Clean	Clean	Clean	Clean
CPM 10V	Black deposit	Black deposit	Black deposit	Clean	Clean	Clean
INCO 625	Clean	Clean	Light staining	Clean	Clean	Clean
INCO 718	Light discoloration	Clean	Light staining	Clean	Clean	Clean
Nitralloy 135	Light discoloration	Clean	Light discoloration	Clean	Clean	Clean
IN 200 Ni	Black deposit	Light black deposit	Light staining	Clean	Clean	Clean
Monel 400	Same as reference	Clean	Light staining	Clean	Clean	Clean
WASP Alloy	Light staining	Minor brown stain	Light staining	Clean	Clean	Clean
Lead	White powdery deposits	Black deposit	Black deposit	Clean	Clean	Clean
268 Brass Sheet	Black dense deposit	Clean	Light and dark staining	Clean	Clean	Clean
TAP MS 285	Black dense deposit	Black deposit	Black deposit	Clean	Clean	Clean
Mag Wire Type 1	Dark Staining	Clean	Clean	Clean	Clean	Clean
Sn/Pb 60/40 Solder	Non-uniform staining	Brown staining	Clean	Clean	Clean	Clean
Cu/Ni 90/10	Same as reference	Light staining	Light staining	Clean	Clean	Clean
7075-T6 CAA Type I	Light deposit	Clean	Light brown staining	Clean	Clean	Clean
7075-T6-CCC Class IA	Light staining	Light brown staining	Light staining	Clean	Clean	Clean
7075-T6-SAA Type IIB	Light staining	Clean	Clean	Clean	Clean	Clean
7050-T74	Light staining	Clean	Clean	Clean	Clean	Clean
6061-T6-Bare	Light Staining	Clean	Clean	Clean	Clean	Clean
5052-H34-Bare	Clean	Clean	Clean	Clean	Clean	Clean
2024-T3-Bare	Light Staining	Clean	Clean	Clean	Clean	Clean
A356-T6	Back deposit	Clean	Clean	Clean	Clean	Clean



LAWRENCE M. BUTKUS, Team Lead
 Structural Materials Evaluation
 Materials Integrity Branch
 Systems Support Division
 Materials and Manufacturing Directorate

cc:

Richard Streibich (AFRL/RXTG)

Appendix D. Biostat Evaluation

INTENTIONALLY LEFT BLANK

**EFFECTS OF DIETHYLENE GLYCOL MONOMETHYL
ETHER (DiEGME) AND TRIETHYLENE GLYCOL
MONOMETHYL ETHER (TriEGME) ON MICROBIAL
CONTAMINATION OF JET FUEL**

**Lori M.T. Balster, Marlin D. Vangsness, Loryn L. Bowen, Susan S. Mueller,
and Lisa M. Brown**

University of Dayton Research Institute (UDRI)

Ellen M. Strobel and Daniel L. Pike

**Fuels and Energy Branch
Power Division
Air Force Research Laboratory
Wright-Patterson Air Force Base, OH 45433-7251**

ABSTRACT

Triethylene glycol monomethyl ether (TriEGME) is under consideration as a replacement for diethylene glycol monomethyl ether (DiEGME), an additive widely used in military aircraft as a fuel system icing inhibitor (FSII) and as an inhibitor of microbial growth. Currently, DiEGME's high dosage rate results in significant expense for the Air Force and Navy, and DiEGME has also been implicated in a number of aircraft system problems, including fuel tank topcoat peeling in the B-52. As a result, an investigation is underway to determine if it is possible to replace DiEGME with TriEGME. TriEGME is a similar molecule, but its lower vapor pressure would eliminate the topcoat issue, and its higher partition coefficient may allow more of it to enter the water phase at a given temperature, making it more dose effective than DiEGME (that is, given the same concentration of DiEGME and TriEGME, more TriEGME will partition into the water—where it is needed to prevent freezing and/or microbial growth—making it more effective than the same level of DiEGME). This study addresses the microbiological component of the overall investigation; i.e., whether the biocidal/biostatic effectiveness of TriEGME is similar to that of DiEGME. Basic questions addressed in this study include: whether the same microorganisms currently affected by DiEGME are also affected by TriEGME, whether the concentration of TriEGME required to stop their growth is equivalent to that of DiEGME, and whether microorganisms recently gathered from the field may have greater tolerance for TriEGME than lab cultured microorganisms. Methodologies utilized here are primarily based on traditional culture methods. Fuel/water mixtures in French square bottles are used to simulate tank conditions. Microorganisms obtained from the American Type Culture Collection (ATCC) and from the field were introduced into these test setups, where they were challenged by DiEGME and TriEGME concentrations from 0-30% by volume in the water phase. Results suggest that the ability of DiEGME and TriEGME to halt microbial growth is both concentration and microbe dependent. Concentrations greater than 10% DiEGME and 15% TriEGME by volume in the aqueous phase were shown to retain biocidal/biostatic effectiveness in all test cases. However, due to TriEGME's higher partition coefficient, the effective additive concentration in the fuel phase would be similar to that of DiEGME. Due to the persistence of two of the field microbe strains even at 30%, additional tests were conducted at 30-60% in the aqueous phase for both FSII. These microbes were still viable even at 60% DiEGME. However, at 40% TriEGME and above they were eventually eradicated. The results suggest that DiEGME and TriEGME at reduced concentrations would still be effective at controlling microbial growth. DiEGME and TriEGME's ability to inhibit biofilm growth is also demonstrated. TriEGME is shown to be a suitable replacement for DiEGME, offering equivalent protection against microbial contaminants in aviation fuel.

PREFACE

The results presented in this report are part of a larger Reduction of Total Ownership Cost (RTOC) program funded by the RTOC DoD office through ASC/EN. The authors especially thank Ed Wells of ASC/EN for his support of the RTOC efforts. The RTOC study is a FSII replacement study being conducted jointly by AFRL (RZPF and MLSA), AFPET, ASC/EN, UDRI, UTC, Encore Logistics Support Systems, B-52 SPO, and the KC-135 SPO. The authors thank Steven Zabarnick and Matthew DeWitt of the University of Dayton Research Institute and Chuck Delaney of Encore Logistics Support Systems for their technical support and guidance. The authors also thank Charles Bleckmann of the Air Force Institute of Technology (AFIT/ENV) for his technical advice.

1. Summary

The goal of this study was to find whether the replacement of DiEGME with TriEGME in aviation fuel would result in a change in any anti-microbial properties currently attributed to DiEGME. This study evaluated TriEGME's microbial activity at aqueous phase concentrations from 0-30% levels at ambient temperature (~0.0-0.04% in the fuel phase), compared to the ~30-60% levels at ambient temperature (~0.04%-0.10% in the fuel phase) typically expected of a FSII present in aircraft fuel tanks. The lower concentrations of TriEGME were chosen for this study due to the prevailing desire to reduce the current FSII concentration significantly, for the purposes of lower cost, topcoat peeling prevention, and lower toxicity. The lower concentrations of TriEGME were also chosen in order to observe the fall-off of TriEGME's effectiveness level. The current study is similar to one recently conducted by this laboratory on DiEGME at reduced concentrations. Two different groups of microbes were challenged in this study: lab cultured microbes acquired from ATCC, and microorganisms recently collected from aircraft fuel tanks in Roswell, NM and Victorville, CA commercial air bases. These two types of microorganisms were chosen for the current study due to their possible differences in behavior to FSII exposure. The current study suggests a minimum of 10% DiEGME in the aqueous phase at ambient temperature (~0.01% by volume in the fuel phase) or, in the case of the possible replacement FSII, TriEGME, 15% minimum by volume in the aqueous phase at ambient temperature (~0.01-0.02% by volume in the fuel phase) will be necessary to adequately control microbial growth. Additional tests on the field consortia at levels currently expected for FSII in the field of 30-60% by volume in the aqueous phase of DiEGME (~0.05-0.15% by volume in the fuel phase) and TriEGME (~0.04-0.10% by volume in the fuel phase) suggest that two field consortia microbe strains persist at 30-60% in the aqueous phase for the DiEGME, but that TriEGME at 40-60% in the aqueous phase (~0.06-0.10% by volume in the fuel phase) was able to eradicate all field consortia growth. However, eradication did not occur until after 30 days of exposure to TriEGME. These results suggest that both DiEGME and TriEGME are beneficial for controlling microbial growth, and that no negative effects will occur due to the substitution of TriEGME for DiEGME.

2. Introduction

Microbial contamination has been blamed for a multitude of problems in aviation fuel systems, including blockage of fuel filters, surface pitting, degradation of fuel and/or fuel additives, aircraft down time, and aircraft failure (1, 2, 3, 4, 5). Enabling problems associated with microbial growth is the presence of residual water in tanks, which can easily accumulate in the absence of proper fuel maintenance. While fuel provides hydrocarbons, which microbes can utilize as an energy source, water provides nutrients which encourage microbial proliferation. Water can also directly cause clogging in fuel systems if icing occurs (6). As a result of several icing instances, the U. S. Air Force (USAF) added ethylene glycol monomethyl ether (EGME) to the specification for military jet fuel as a precautionary fuel system icing inhibitor. Several microbially related operational delays were also reported prior to the introduction of EGME (2, 3, 4, 7, 8), but it was found that EGME also deterred microbial growth in aviation fuel, an unintended benefit (9, 10). In 1984, the U. S. Navy substituted another FSII to the JP-5 specification, diethylene glycol monomethyl ether (DiEGME). DiEGME also proved to be an effective deterrent to microbial growth in aviation fuel. In the early 1980s, the USAF replaced EGME with DiEGME due to toxicity concerns, whereas the Navy replaced it due to flashpoint concerns surrounding EGME (2, 4, 11, 12). Several studies have explored the effectiveness of DiEGME and other FSII additives in curbing or eliminating microbial growth (13, 14, 15, 16, 17, 18, 19). These studies generally recommended that FSII levels of 15% or greater in the aqueous phase must be maintained for the control and/or elimination of microbial growth.

Years after the introduction of DiEGME into USAF fuel systems, the Air Force has seen a gradual increase in operational problems due to the effects of DiEGME. DiEGME has been implicated in topcoat peeling in the B-52 and in the disarming of filter coalescers (20). As a result, studies have been conducted to determine whether the FSII concentration can be lowered to ameliorate these problems, while at the same time retaining FSII's desirable traits, such as the prevention of ice crystal formation in fuel and control of microbial growth (21). In addition, studies have been conducted to assess whether it is possible to replace DiEGME with another additive with lower volatility, such as TriEGME. Such a replacement would solve the problem of topcoat peeling.

In recent years, the USAF has also seen an increase in incidents related to microbial contamination. It has been hypothesized that the number of microbes tolerant of DiEGME has been gradually increasing, resulting in more maintenance issues in fuel systems (22). There is also some contention as to whether DiEGME is still an effective biocide/biostat, and if so, what minimum concentration is required for it to be effective (17, 19, 22, 23). The USAF has similar concerns about TriEGME, the proposed replacement for DiEGME.

The current study was undertaken to consider issues concerning microbial activity of TriEGME at low concentrations, similar to those tested in the reduced FSII (DiEGME) program. The minimum FSII microbial growth data appears in a previous U.S. Air Force technical report (24). No study to date has addressed the biostatic/biocidal activity of DiEGME and TriEGME at low levels on standard lab consortia tested in the past, and also on recently collected field microbes. Due to many variables such as: regional temperature changes, free water differences, humidity, and aircraft tank geometry, it becomes very difficult to duplicate the variety and numbers of microbial contaminants found in the field. Nevertheless, a wing tank sampling study conducted by this lab in 2004-2006, ranging over 93 aircraft, 15 airframes, and 14 airbases made it possible for a fairly representative microbial sampling consortia to be available for the current study (22, 25). Five bacteria and one fungus isolated from Roswell and Victorville air bases were chosen to represent wild consortia for this study, based on their genera's high frequency of occurrence in the overall sampling study across all airbases and airframes, and the fact that viable cultures were obtainable (22).

The methodology of the current study is modeled after a study performed by Phillips in 1964 (26), which used 100 mL French square bottles with 35 mL fuel and 50 mL Bushnell Haas (BH) solution to simulate tank conditions, and traditional plate colony counts to enumerate viable microbes. Additive levels tested in the current study were at or below the lowest levels expected in aircraft fuel systems, which corresponds to 0-30% FSII in the aqueous phase.

Figure 1 expresses the relationship between the amount of TriEGME added to the fuel phase and the volume of TriEGME expected in the aqueous phase (20), and compares the values for TriEGME with the values for the current FSII additive, DiEGME.

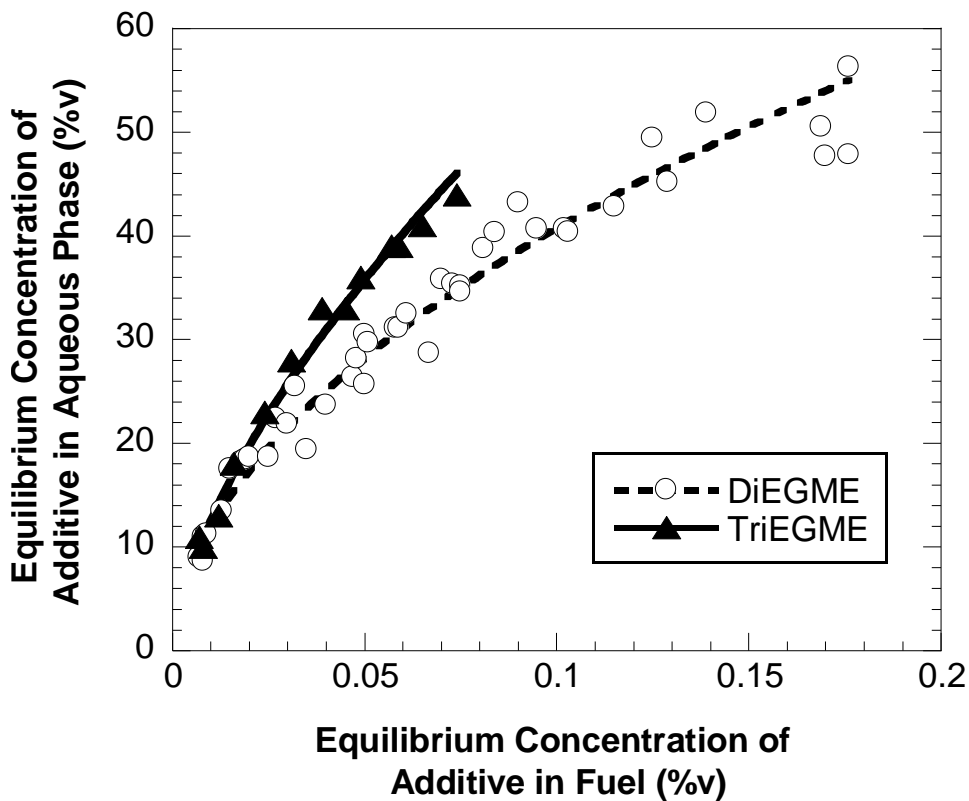


Figure 1. Equilibrium concentration of DiEGME and TriEGME in fuel vs. aqueous phase

Both DiEGME and TriEGME have non-polar and polar features to their molecules, allowing them to partition into either the fuel or aqueous phase. They partition preferentially into the aqueous phase, however, with more DiEGME or TriEGME entering the aqueous phase as the temperature drops, or as the amount added to the fuel increases. DiEGME and TriEGME are similar molecules, but TriEGME has a higher partition coefficient. At equilibrium, the partition coefficient is expressed as:

$$PC = \frac{\text{Volume \% concentration of additive in water}}{\text{Volume \% concentration of additive in fuel}}$$

The higher partition coefficient of TriEGME means that when the same amount of DiEGME or TriEGME is added to fuel, the result will be more TriEGME in the aqueous phase, as Figure 1 suggests. For example, under the same experimental conditions at equilibrium, the partition coefficient for DiEGME has been expressed as 538, compared to 1120 for TriEGME (17). The actual amount of DiEGME or TriEGME in the fuel or aqueous phase, however, is dependent on a variety of factors, such as the amount of water, temperature, and multiple mixing events (changes in a fuel's icing inhibitor content due to the additive's accumulation in the water phase, plus the addition of new additized fuel plus its water content in multiple occurrences). In this study, these variations were minimized by the use of single temperature, static French square liquid setups with water bottoms large enough that it can be assumed that back diffusion (the return of the FSII additive to the fuel phase) does not significantly change the FSII level in the water phase, and that all of the additive remains in the aqueous phase. All DiEGME and TriEGME used in these experiments was added directly to the aqueous phase at known percentage volumes.

The current study explored TriEGME levels of 0-30% in the aqueous phase, which corresponded to additized fuel levels of 0-0.04% by volume in the fuel, according to the chart above. This chart was obtained at 20° C. The DiEGME data for figure 1 was obtained with 130-560 ppm of water, and the TriEGME data was obtained with 300 ppm of water. Due to the manner in which the information is plotted, however, the water content differences have no impact. The results of several

studies (13, 17, 19) suggested that DiEGME and TriEGME levels of 15% by volume and above in the water phase would be adequate for control of microbial growth, which would correspond to a 0.01-0.02% dosage in the fuel phase using the chart above. This dosage level would equal one-seventh or less of the current typical dosage.

3. Methods, Assumptions, and Procedures

3.1 Materials

Clear French square 100 mL bottles from Fisher Scientific were sterilized by autoclave. The test setup for each French square consisted of 35 mL of Jet A aviation fuel POSF 4877 for the fuel phase and 50 mL of aqueous phase made from Bushnell-Haas broth nutrient solution (Sigma-Aldrich, Inc. St. Louis, MO) with DiEGME or TriEGME added as appropriate. Fuel was filtered with a 0.45 μ m hydrophobic cellulose nitrate filter (Nalge Nunc, Rochester, NY) prior to use in the test setup. The Bushnell-Haas solution was sterilized by autoclave. Microbes were cultured on Luria-Bertani (LB) agar plates. LB broth and Difco granulated agar were obtained from Sigma-Aldrich and Becton-Dickinson (Sparks, MD), respectively. All plating was performed in a laminar flow hood. A Reichert Quebec Darkfield colony counter (Depew, NY) was used to quantify microbial growth.

3.2 ATCC Lab Cultured Microorganisms

Lab culture microorganisms were obtained from ATCC. They included: *Pseudomonas aeruginosa* (ATCC catalog # 33988), *Hormoconis (Cladosporium) resinae* (ATCC # 20495), and *Yarrowia (Candida) tropicalis* (ATCC # 20336). *P. aeruginosa* is a type of bacteria, *C. resinae* is a fungus, and *C. tropicalis* is a yeast. The *P. aeruginosa* originated from a fuel storage tank in Ponca City, OK, and was deposited into the ATCC collection by R. Allred in 1982. The *C. resinae* originated from an aircraft fuel tank and was deposited by J. J. Marshall from the NLABS collection in 1977. The *C. tropicalis* was deposited in 1971. The ATCC microorganisms were chosen based on their prevalence in the fuels literature; for example, they are used in the ASTM method E 1259-01 for evaluating antimicrobials in liquid fuel (27), and they were used by Neihof, Westbrook, and Hill (13, 16, 19).

3.3 Wild Type Microbe Collection

The wing tanks of several civilian aircraft in long term storage were sampled from 2004 to 2005. Military aircraft were also sampled throughout 2005. Preliminary results were compiled in a previously published technical report (22). The Victorville and Roswell microbes were obtained from wing tanks on commercial DC-9 aircraft that had been idle for at least a year. All Victorville and Roswell aircraft fuel tank samples contained fuel with water bottoms. Microorganisms obtained from Roswell and Victorville aircraft fuel tanks in 2004-2005 included: a *Methylobacterium* species, a *Pseudomonas* species, *Bacillus licheniformis*, *Clostridium intestinalis*, *Rhodococcus equi*, and *Hormoconis (Cladosporium) resinae*. All are bacteria except for *C. resinae*. These field microorganisms were the most common found overall in the most recent study of microbial contaminants in aircraft fuel, and were chosen to roughly approximate a realistic test set (22). Due to the fact that microbial consortia are typically not dispersed in fuel systems in a homogenous manner, it may not be possible to truly capture a representative picture of microbial growth over an entire fleet of aircraft (27). The extensive sampling efforts undertaken by this lab in 2004-2005 were, however, the best recent attempt at representing the likely widespread classes of consortia encountered in the field today (22). DiEGME levels were not recorded for the commercial aircraft during the 2004-2005 sampling study. The military aircraft in the 2004-2005 study, however, were known to be exposed to DiEGME in many cases, and in many instances data on DiEGME levels was recorded (24). The frequency of different types of microbial contaminants from 2004 to 2005 in both commercial and military aircraft was noted in the 2004-2005 sampling study, with the six most common being chosen to represent the field consortia in the current study.

The microorganisms cultured from the field were identified by 16S ribosomal RNA sequencing as: *Pseudomonas* sp. (obtained from Roswell, NM air base), *Bacillus licheniformis* (Roswell), *Clostridium intestinalis* (Roswell), *Rhodococcus equi* (Victorville, CA air base), and *Methylobacterium* sp. (Victorville). Sequencing was performed by MWG Biotech of High Point, NC. Fuel sampling procedures, DNA extraction, purification, and sequencing procedures are detailed elsewhere (11, 22, 24). Procedures used for bacterial sequence identification are also listed elsewhere

(11). *Cladosporium resinae* (Roswell) was identified by light microscopy, performed by Forensic Analytical of Rancho Dominguez, CA.

3.4 Test Procedure

All microorganisms were revived from frozen cultures stored at -80° C. They were incubated in unsealed, autoclaved steel-capped glass test tubes containing 5 mL of LB broth, POSF 4877 fuel + BH broth, and BH broth alone. LB and BH full-strength broth were autoclaved to sterilize, while the fuel was not autoclaved but was filtered before use. After inoculation, when visible inspection showed significant microbial growth (indicated by cloudiness or an increase of solid or fluffy material at test tube bottom) of the LB, the fuel + BH, and/or the BH test tubes, the cultures were deemed viable. Two hundred microliter aliquots of each microorganism grown in BH broth were then pipetted separately in the case of the single organism tests, or they were pipetted and combined to make a mixed culture in the case of the mixed culture tests. One hundred microliters of the single or mixed culture was then used to inoculate each French square bottle at each DiEGME test level. French square bottles were incubated at 28° C. At the time of initial plating, referred to as Day 0, the microbes were exposed to DiEGME for at least 4, but no more than 24 hours. Colony counts were not taken prior to the Day 0 plating. For all test points, the fuel/water French square setups were manually shaken for 30 seconds, the phases were allowed to re-separate, and a 100 μ L aliquot was drawn from the aqueous phase. The aliquot was spread on an LB plate. A second aliquot was used to make dilutions as needed with the BH, typically 1:100, 1:1000, and/or 1:10,000. Growth rates were microorganism dependent, with colonies typically appearing 24 to 72 hours after plating. Following incubation, the colony forming units (CFU) on each plate were enumerated using a counter probe. The countable range for a raw plate is between 30 and 300 CFU (28). In practice, however, colonies were sometimes above or below the countable range, despite the dilutions performed. Due to the dilution method used, the maximum corrected raw colony count in the present experiments was 30,000,000 per mL, values above this were considered to be too numerous to count (TNTC). This corresponded to a raw count above 300 on a plate with a 1/10,000 dilution. Colony counting uncertainty is expected to be plus or minus an order of magnitude. This uncertainty is based on colony counting results obtained from random, multiple platings. Most of the colony counts reported here were the results of single platings. Although there is not always a direct relationship between colony count and level of microbial contamination of aviation fuel—due to the fact that over 90% of microbes in the environment may not be culturable on agar plates (29)—it is safe to assume that relationship in the current study, as all of the microbes utilized have been previously cultured on agar plates. In addition, it is often the case that a large colony count is directly suggestive of a significant potential for microbially-induced problems such as biofilm formation. However, no numerical standards have been universally accepted which define a particular colony count level as problematic (27). This fact is explicitly stated in the standard guide for microbial contamination in fuels and fuel systems, ASTM D 6469-99 (12).

The current study employs a direct comparison between DiEGME and TriEGME to ascertain the relative effectiveness of these two additives in inhibiting microbiological growth. The rest of the test procedure used in this study is based on a Phillips report from 1964 (26). Essentially, the Phillips method requires plating of the liquid test setups approximately every three days during a 46 day test duration. Blank fuel/water mixtures were also maintained throughout the test cycle for each DiEGME and TriEGME concentration level. DiEGME and TriEGME concentration levels tested in this study were: 0, 5, 10, 15, 20, 30, 40, 50, and 60% by volume in the water phase. Blanks (fuel/water mixtures with no inoculants added) at each level were also plated randomly throughout the test period. Blanks did not show any growth throughout the test period.

4. Results and Discussion

4.1 ATCC Microorganism Tests

In these tests, *Pseudomonas aeruginosa*, *Cladosporium resinae*, and *Candida tropicalis* were revived from separate frozen cultures. They were tested singly and collectively for their resistance to DiEGME and TriEGME at low additive concentration levels. These three microorganisms were grown in the test setups, plated on LB plates, and their colonies were counted after 72 hours of incubation for each test point, as *C. resinae* colonies were not clearly visible prior to 72 hours. Three types of information are shown below: 1) Figures 2-9 show French square test setups following the 46 day test duration, which present visual comparisons of the liquid ATCC inoculated samples at different DiEGME and TriEGME concentrations. Test setups which show particulate matter and/or cloudiness in the bottom (aqueous) layer have significant microbial contamination; 2) Figures 10-15 show agar plate growth of the ATCC consortia, Figures 16-33 show plate growth for ATCC *Pseudomonas* alone, ATCC *Cladosporium* alone, and ATCC *Candida* alone, at several different points during the experiment. The agar plates shown were used for visual inspection and/or enumeration of colony growth; 3) Figures 34-41 below summarize ATCC microbial growth for the 46 day test period for the mixed ATCC consortia, as well as the ATCC microorganisms tested singly.

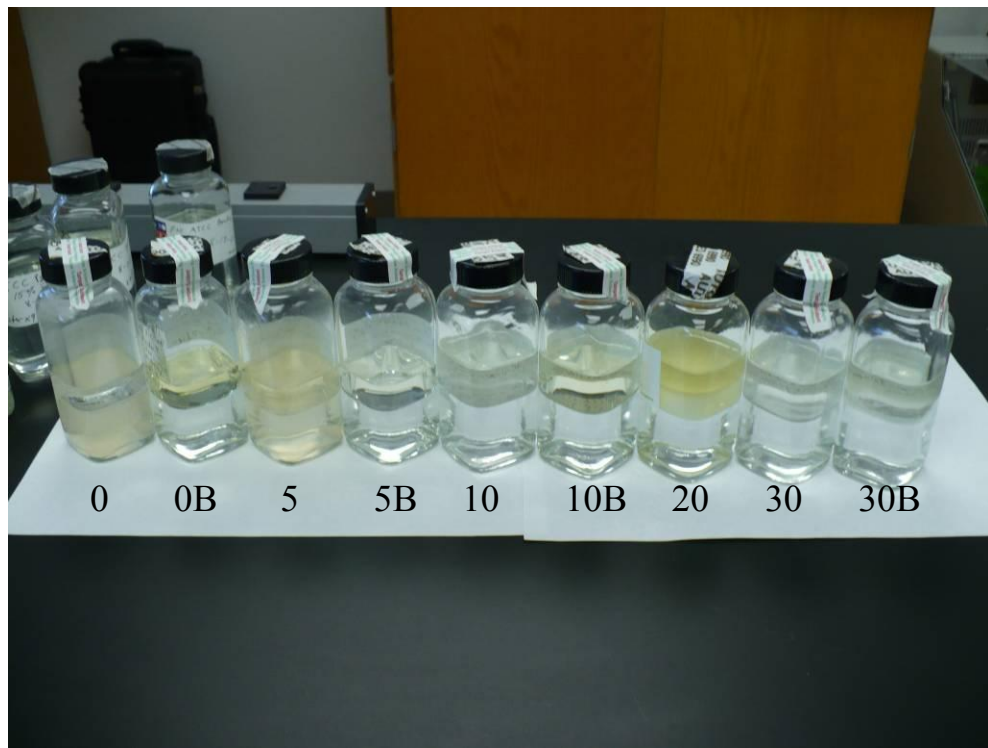


Figure 2. ATCC consortia following 46 day test, side by side with respective blank, except for 20%. DiEGME concentrations are, from left to right: 0, 5, 10, 20, and 30% by volume in aqueous phase

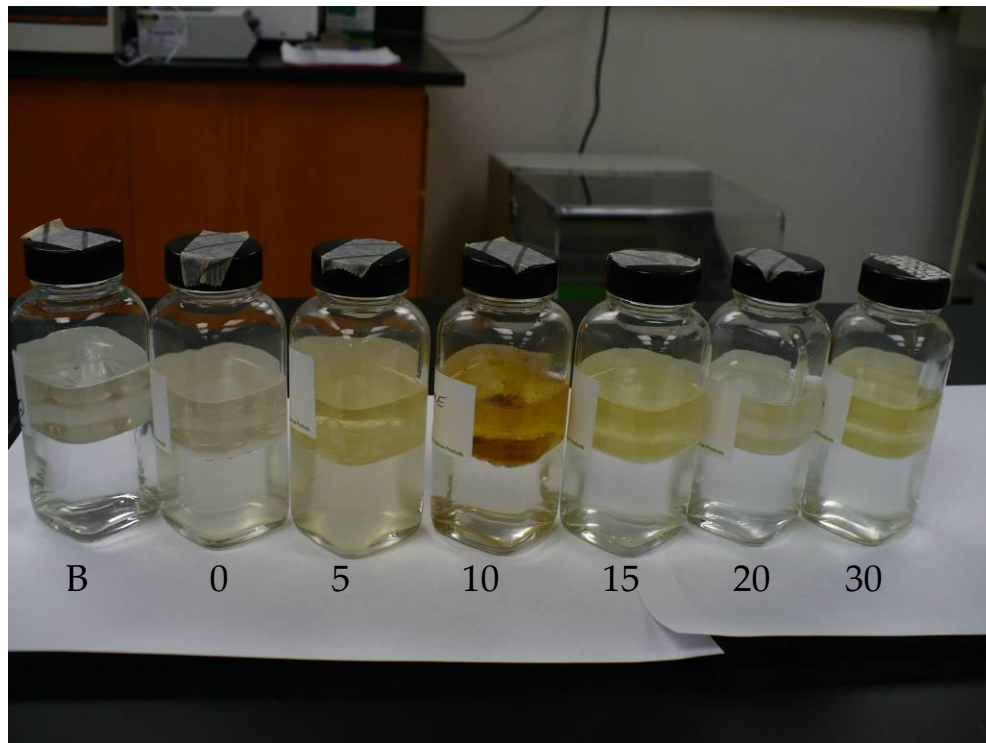


Figure 3. ATCC consortia following 46 day test. A blank (POSF 4877 Jet A fuel/Bushnell-Haas water solution) is shown, followed by TriEGME concentrations of: 0, 5, 10, 15, 20, and 30% by volume in water phase.

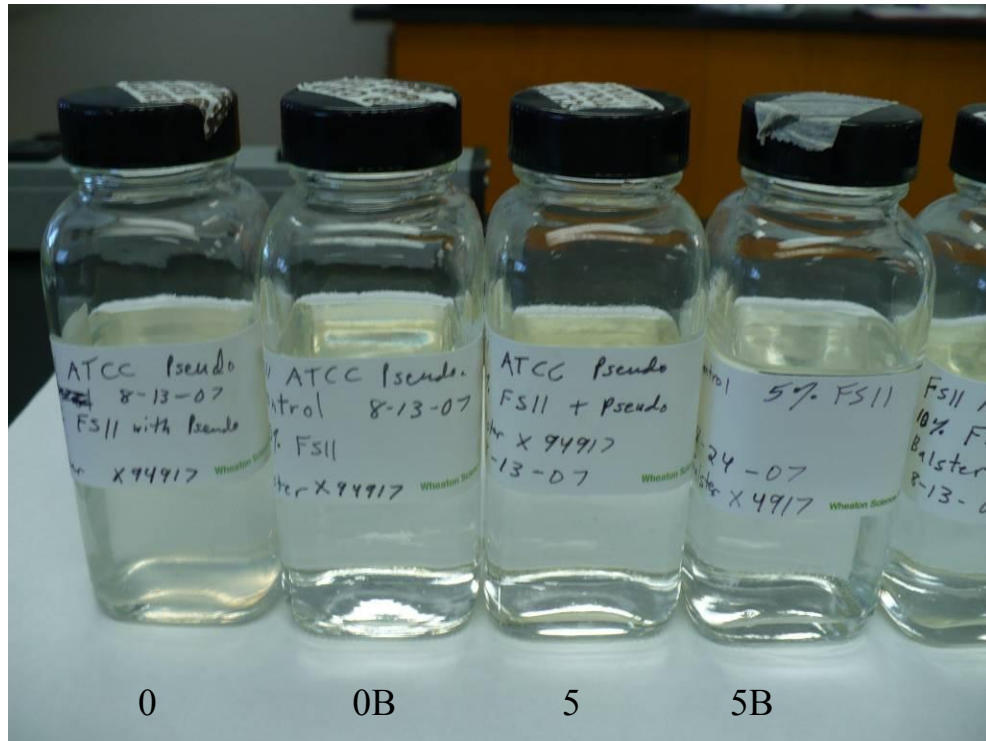


Figure 4. ATCC *Pseudomonas* following 46 day test. DiEGME concentrations are: 0 and 5% by volume in aqueous phase, paired with respective blanks.

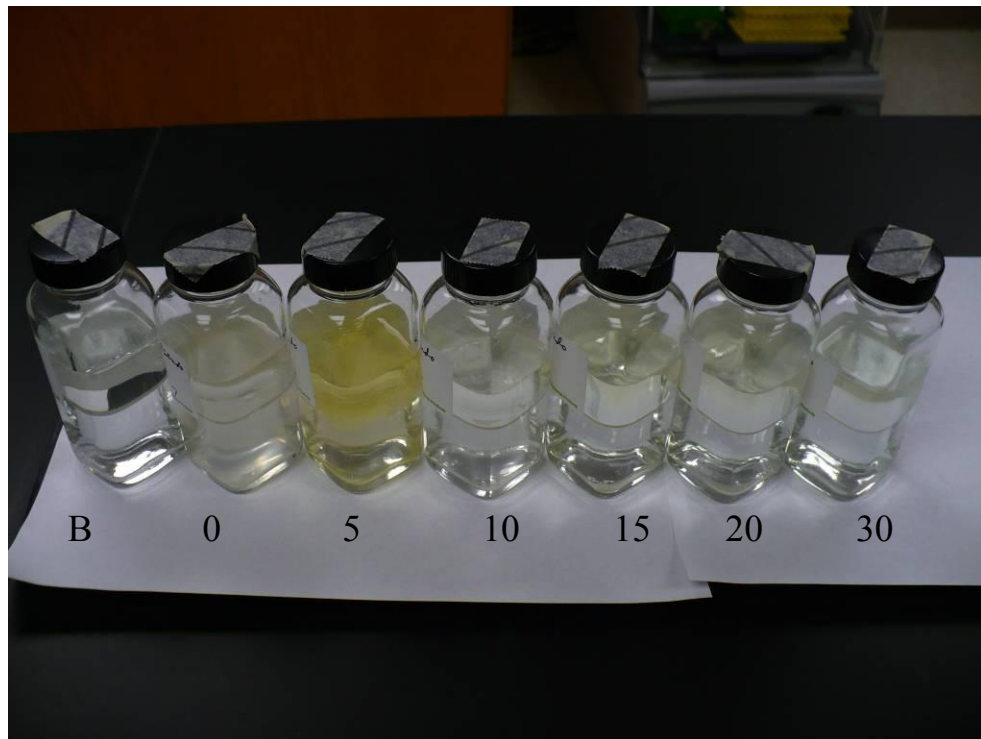


Figure 5. ATCC *Pseudomonas* following 46 day test. A blank is shown followed by TriEGME concentrations of: 0, 5, 10, 15, 20, and 30% by volume in the water phase.

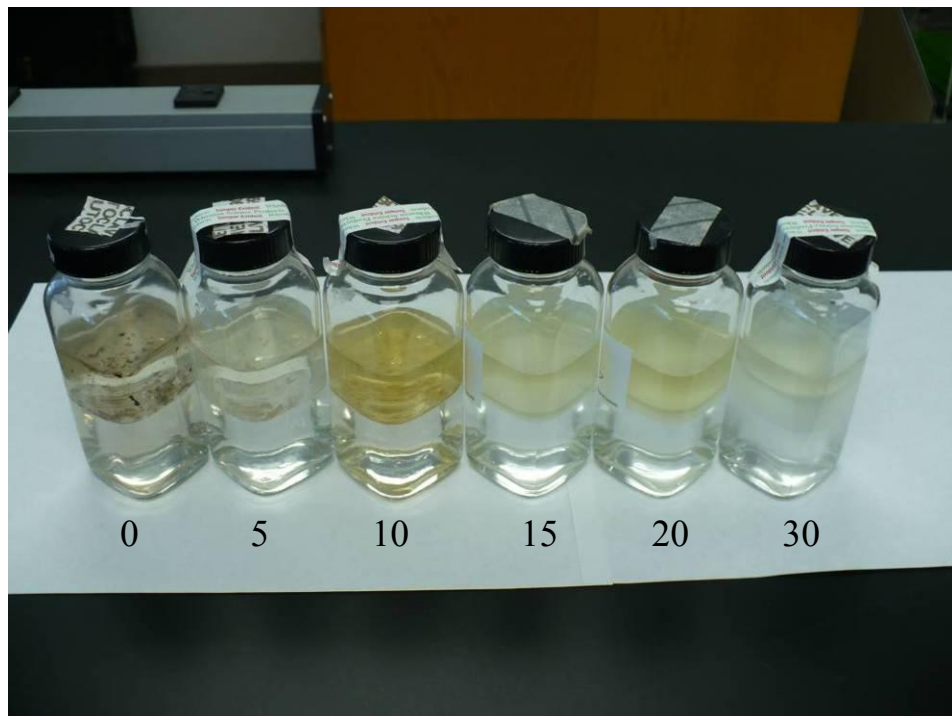


Figure 6. ATCC *Cladosporium* following 46 day test. DiEGME concentrations are: 0, 5, 10, 15, 20, and 30% by volume in aqueous phase.

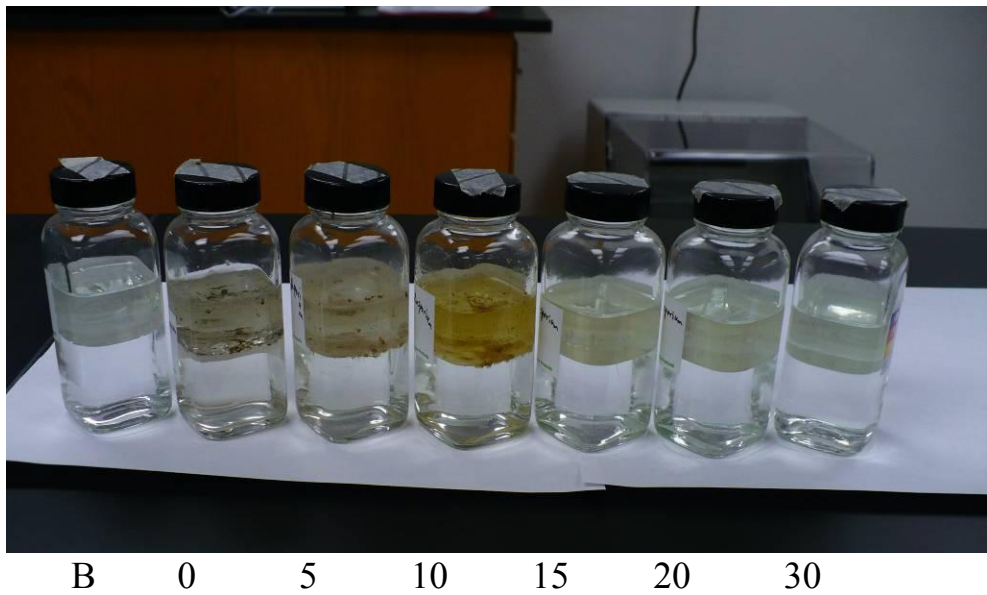


Figure 7. ATCC *Cladosporium* following 46 day test. A blank is shown, followed by TriEGME concentrations of: 0, 5, 10, 15, 20, and 30% by volume in water phase.

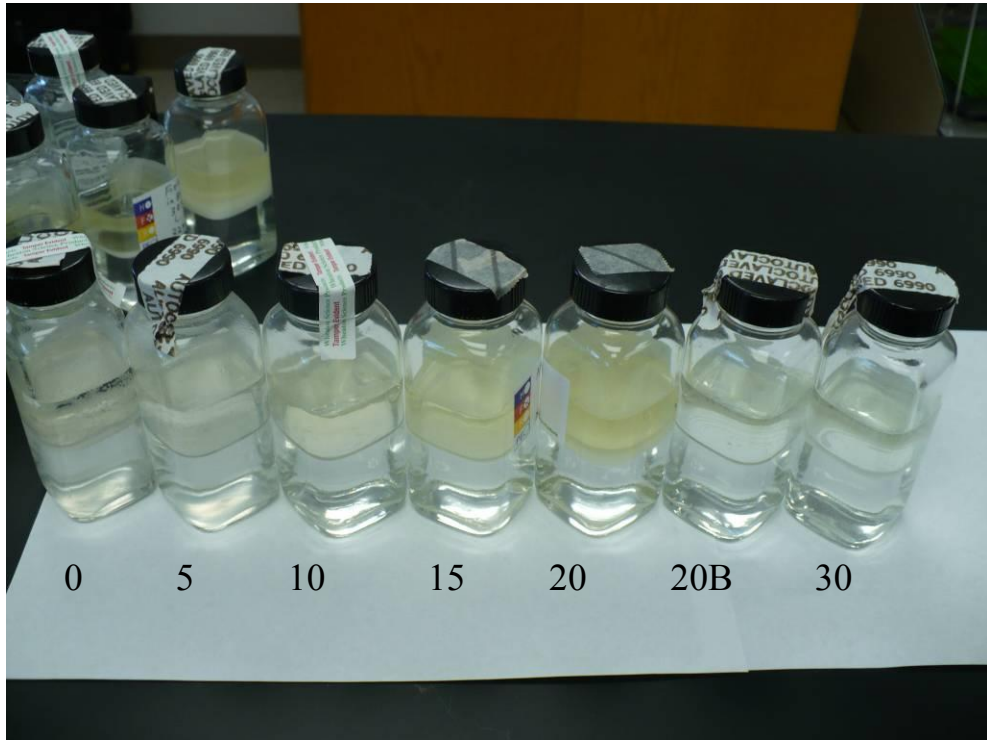


Figure 8. ATCC *Candida* following day 46 of test. DiEGME concentrations are: 0, 5, 10, 15, 20, and 30% by volume in aqueous phase, with 20% next to 20% blank.

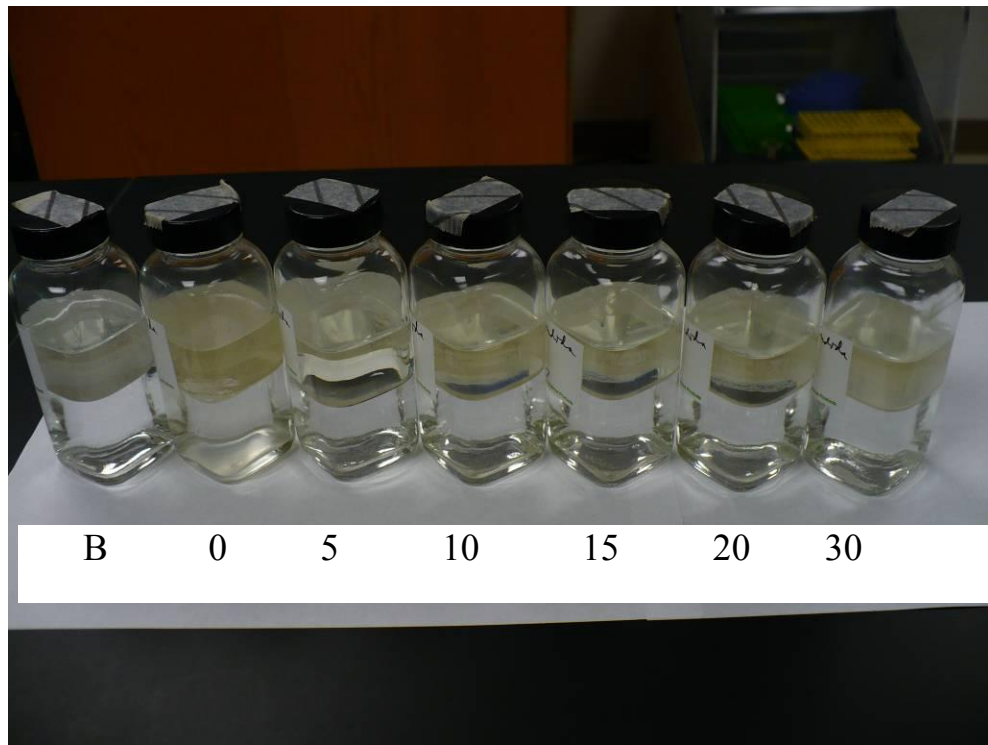


Figure 9. ATCC *Candida* following day 46 of test. A blank is shown, followed by TriEGME concentrations of: 0, 5, 10, 15, 20, and 30% by volume in water phase.

Several observations become apparent from visual inspection of the ATCC consortia test setups, as well as those from the separate ATCC microorganisms. All the DiEGME 0% test setups, shown in Figures 2,4,6, and 8, and all of the 0% TriEGME test setups, shown in Figures 3,5,7, and 9, have cloudiness and/or brown particulates in the water phase. Cloudiness that doesn't dissipate is considered to be a very good indicator of microbial activity, as is the generation of large, brown particulates--hallmarks of biofilm formation. In fuel systems, a biofilm is a microbial growth formation that typically appears as a sheen, pellicle, or mat that forms between the fuel and water layers or on the interior sides of a tank. Biofilms consist of microbes, inert detritus, water, and extracellular polymeric substances (EPS)—also known as the glycocalyx, which is a polysaccharide or peptide slime. The formation of a biofilm in a fuel system can have important consequences. Biofilms protect bacteria, fungus, and/or yeast and encourage their growth, which in turn promotes the deleterious effects of microbial contamination, such as microbially induced corrosion (MIC) and fuel degradation. The presence of biofilms can also lead directly to the plugging of fuel lines and filters (27).

For the liquid samples, it was always the case that the unadditized control had significantly more growth, which could be discerned visually as a biofilm at the fuel/water interface and by cloudiness in the aqueous phase. The contrast between the unadditized sample and those containing DiEGME or TriEGME was quite clear. In the 5% DiEGME and TriEGME setups, cloudiness and/or particulates are evident in the ATCC consortia, the *Pseudomonas*, and the *Cladosporium*, shown in Figures 2-5. The *Candida*, however, is clear at 5%. For the 10% TriEGME, only the ATCC consortia and the *Cladosporium* by itself show obvious brown particulates, suggesting that the *Cladosporium* is responsible for the persistence of growth at this TriEGME level. All the other 10% setups are clear. At TriEGME levels of 15% and higher, there is no cloudiness or particulate formation for any of the ATCC microbes tested.

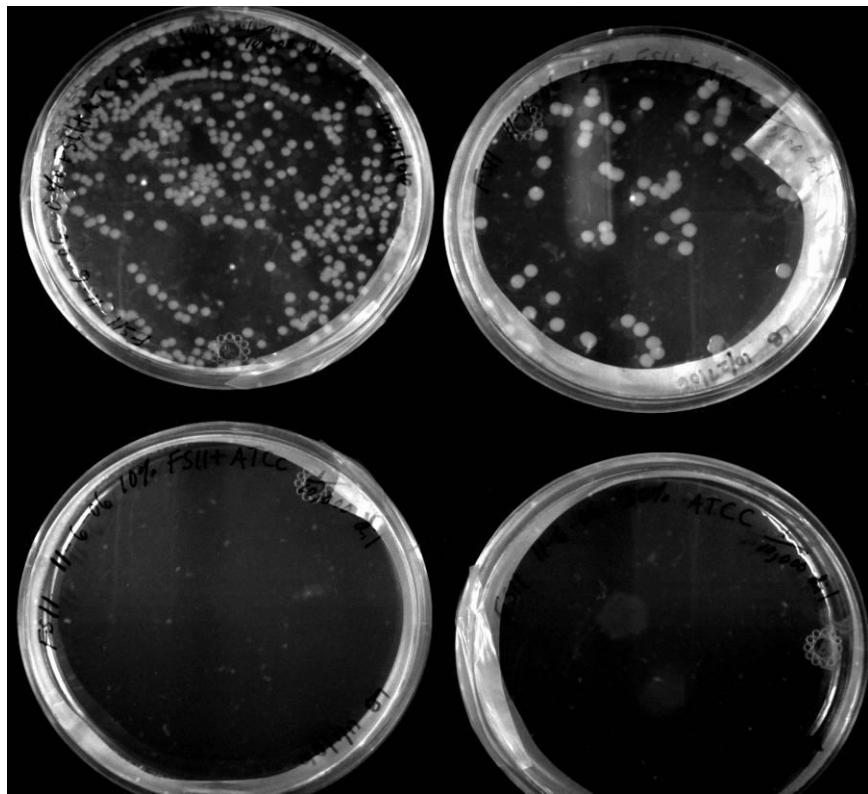


Figure 10. ATCC consortia at day 6 of incubation. DiEGME concentrations, 1/10,000 dilution, are: 0% (upper left), 5% (upper right), 10% (lower left), and 30% (lower right) by volume in water phase. Colonies are only growing at the 0 and 5% levels.

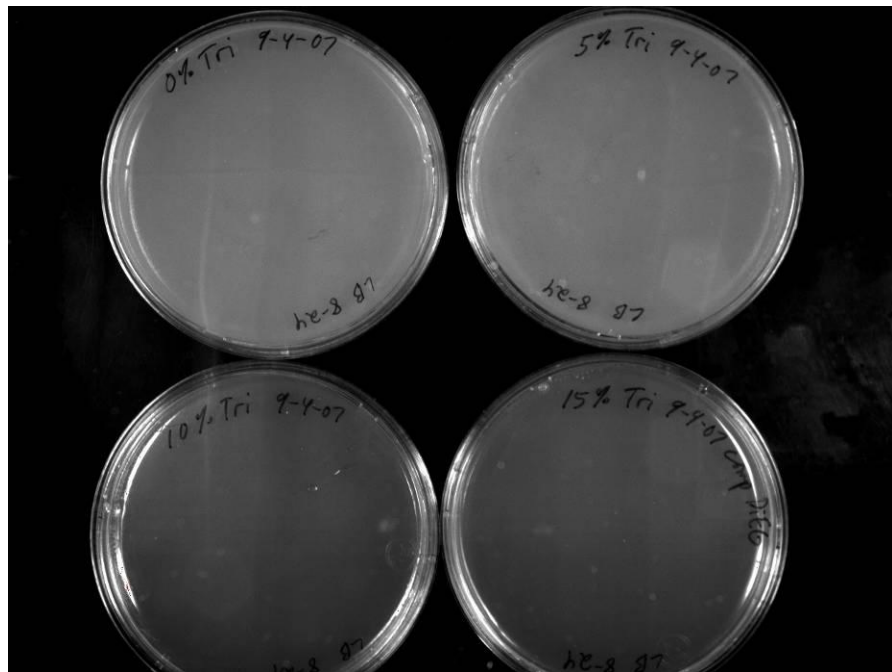


Figure 11. ATCC consortia at day 8 of incubation. TriEGME concentrations are: 0% (upper left), 5% (upper right), 10% (lower left), and 15% (lower right) by volume in water phase. Colonies are swarming the plates at the 0 and 5% levels. The other two plates have no growth.

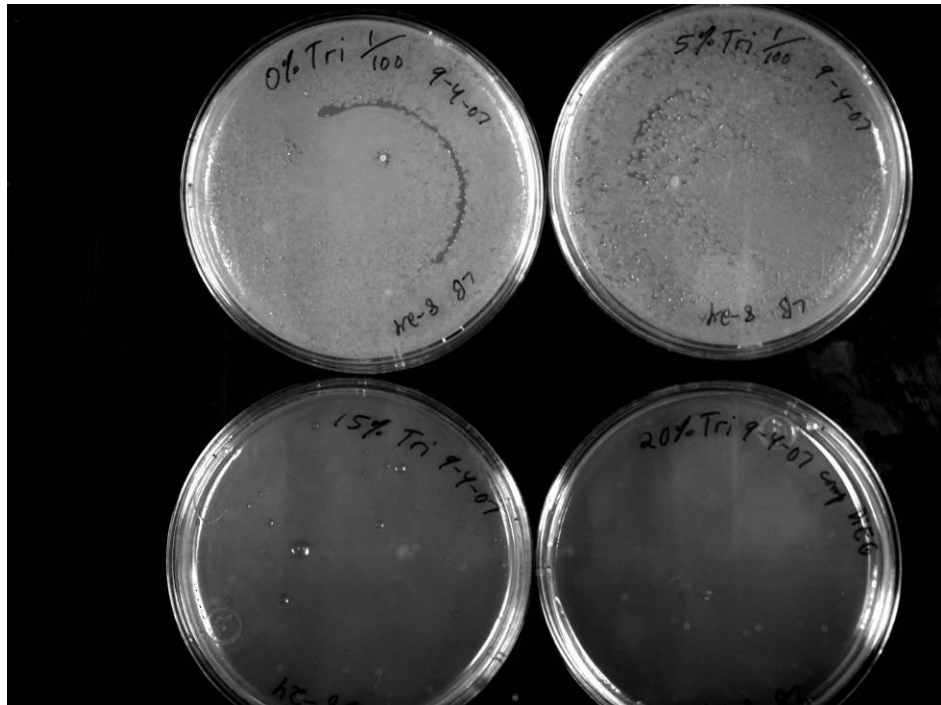


Figure 12. ATCC consortia at day 8 of incubation. TriEGME concentrations, 1/100 dilution, are: 0% (upper left), 5% (upper right), 15% (lower left), and 20% (lower right) by volume in water phase. Colonies are only growing at the 0 and 5% levels.

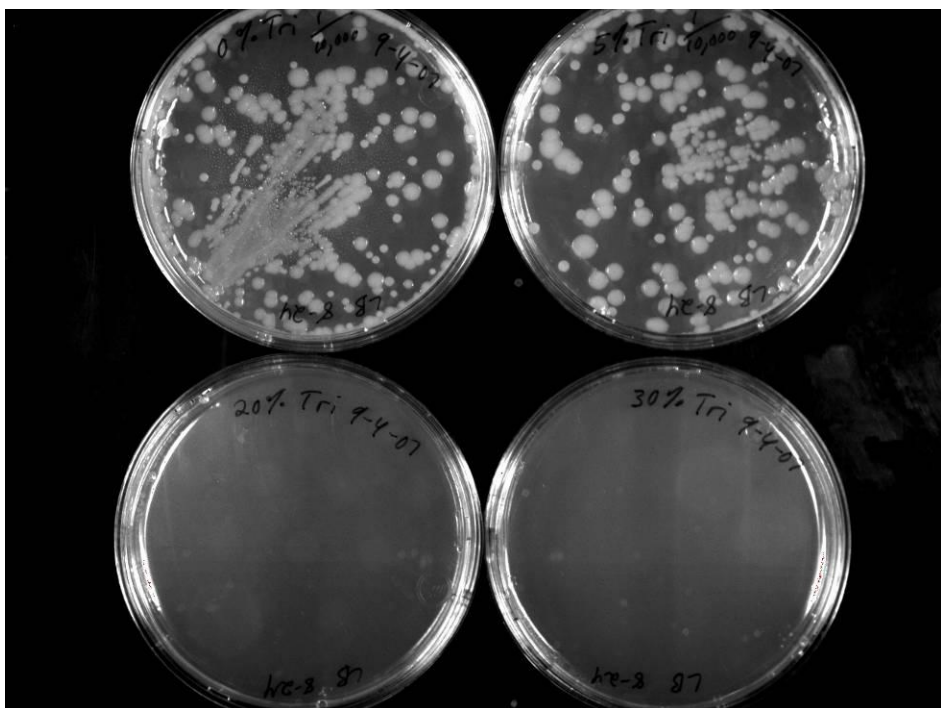


Figure 13. ATCC consortia at day 8 of incubation. TriEGME concentrations, 1/10,000 dilution, are: 0% (upper left), 5% (upper right), and with no dilution, 20% (lower left), and 30% (lower right) by volume in water phase. Colonies are only growing at the 0 and 5% levels.

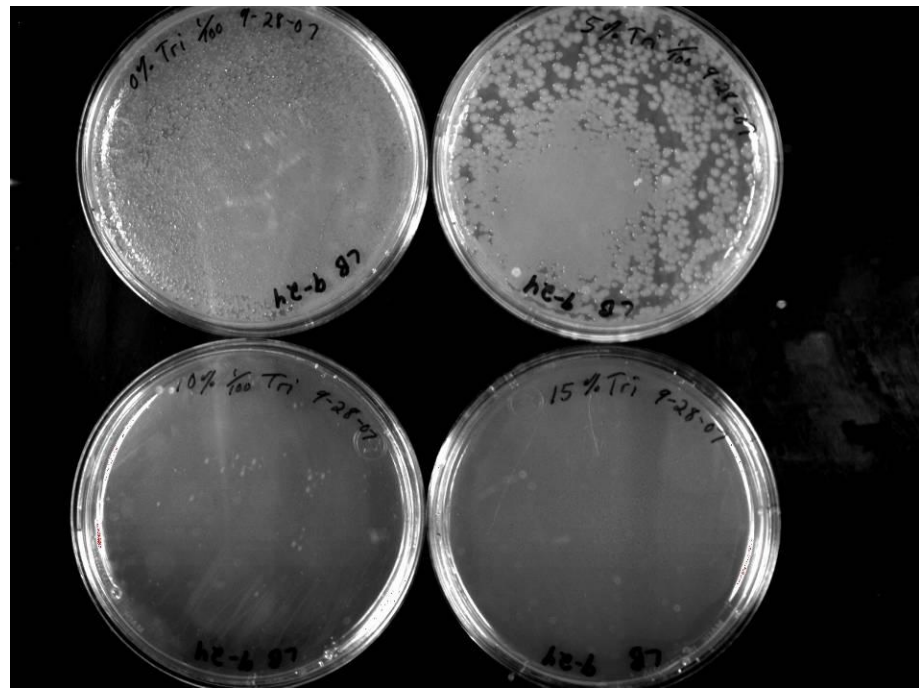


Figure 14. ATCC consortia at day 32 of incubation. TriEGME concentrations, 1/100 dilution, are: 0% (upper left), 5% (upper right), 10% (lower left), and 15% (lower right) by volume in water phase. Bacterial or yeast colonies are growing at the 0 and 5% levels, and fungal colonies from *Cladosporium* are growing at the 10% level.

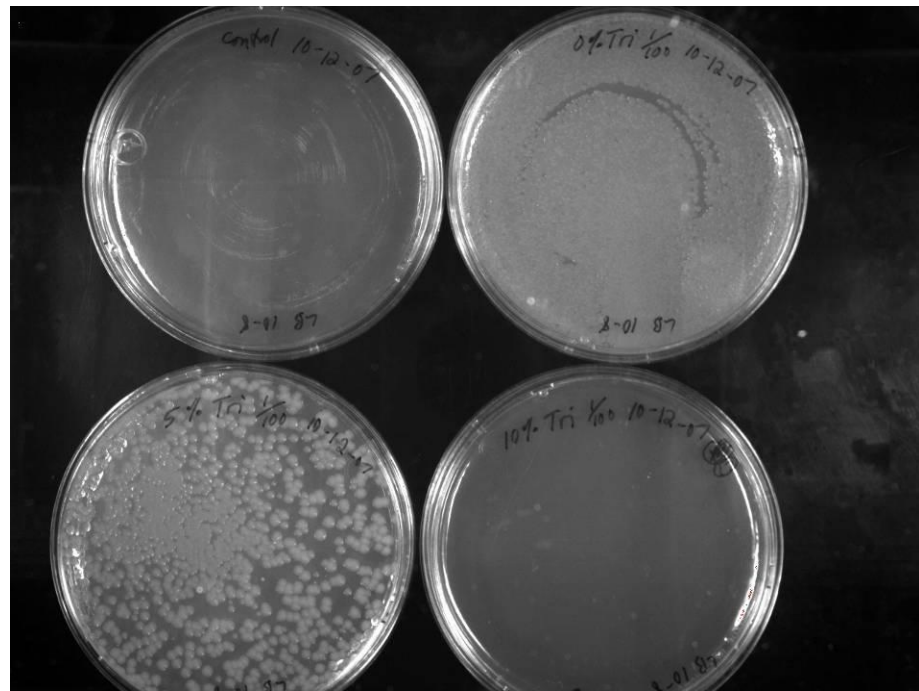


Figure 15. ATCC consortia at day 46 of incubation. The uninoculated control blank (upper left), with no colony growth, is shown with TriEGME concentrations, 1/100 dilution, of: 0% (upper left), 5% (lower left), and 10% (lower right). Bacterial colonies are growing at the 0 and 5% levels, and fungal colonies from *Cladosporium* are growing at the 10% level.

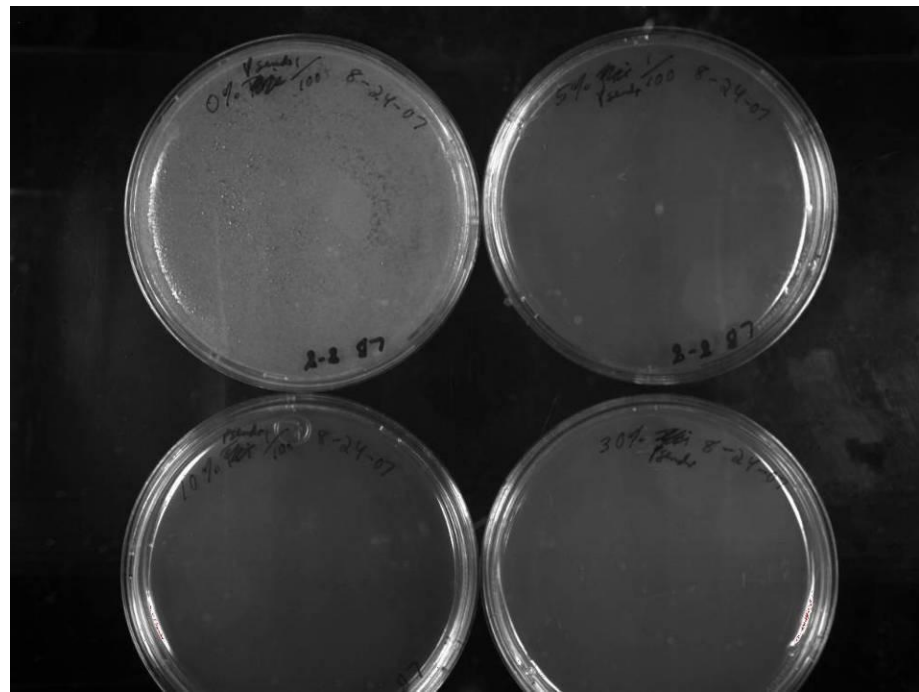


Figure 16. ATCC *Pseudomonas* at day 11. DiEGME concentrations, 1/100 dilution, are: 0,5,10, and 30%. The 0% plate (upper left) is swarming with growth; the other plates have no colonies.

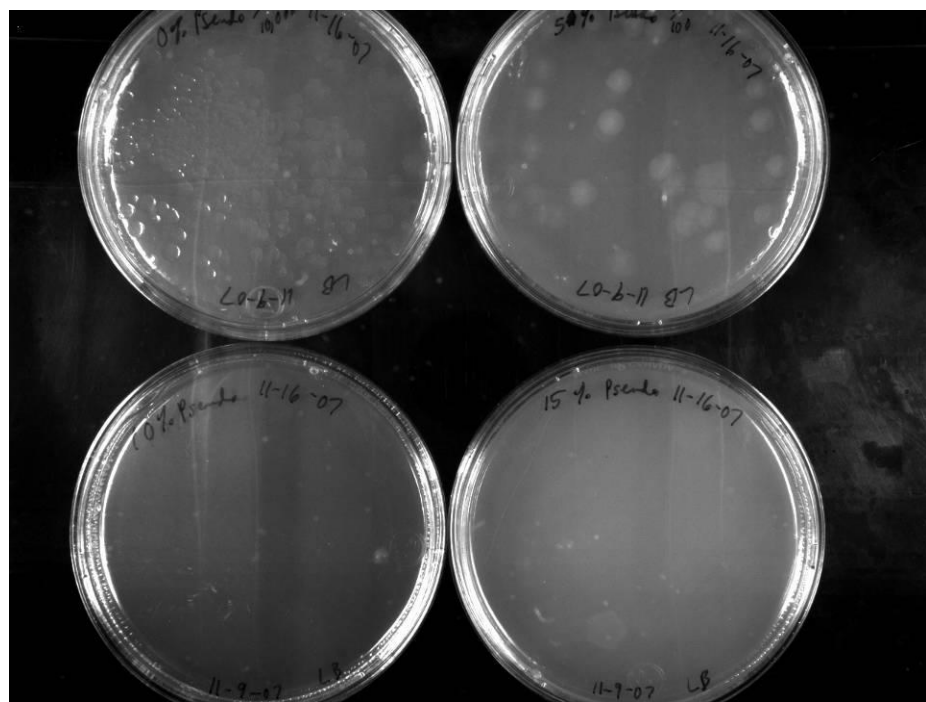


Figure 17. ATCC *Pseudomonas* at day 3. TriEGME concentrations, 1/100 dilution, are: 0,5,10, and 30%. The 0% plate (upper left) is swarming with growth, the 5% plate (upper right) has less growth; the other plates have no colonies.

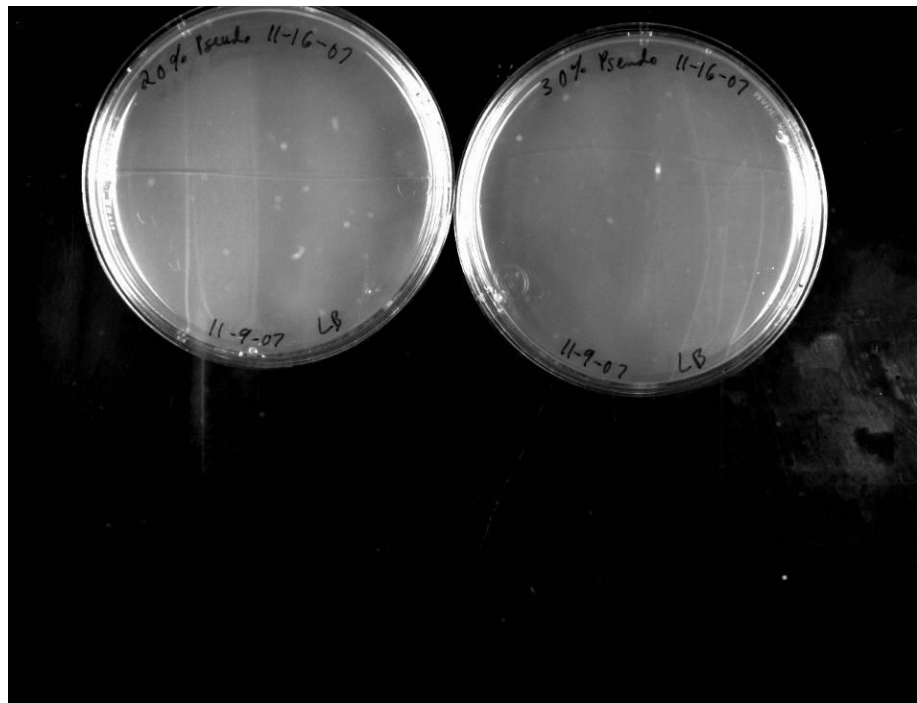


Figure 18. ATCC *Pseudomonas* at day 3. TriEGME concentrations are: 20 and 30%. These plates have no growth.

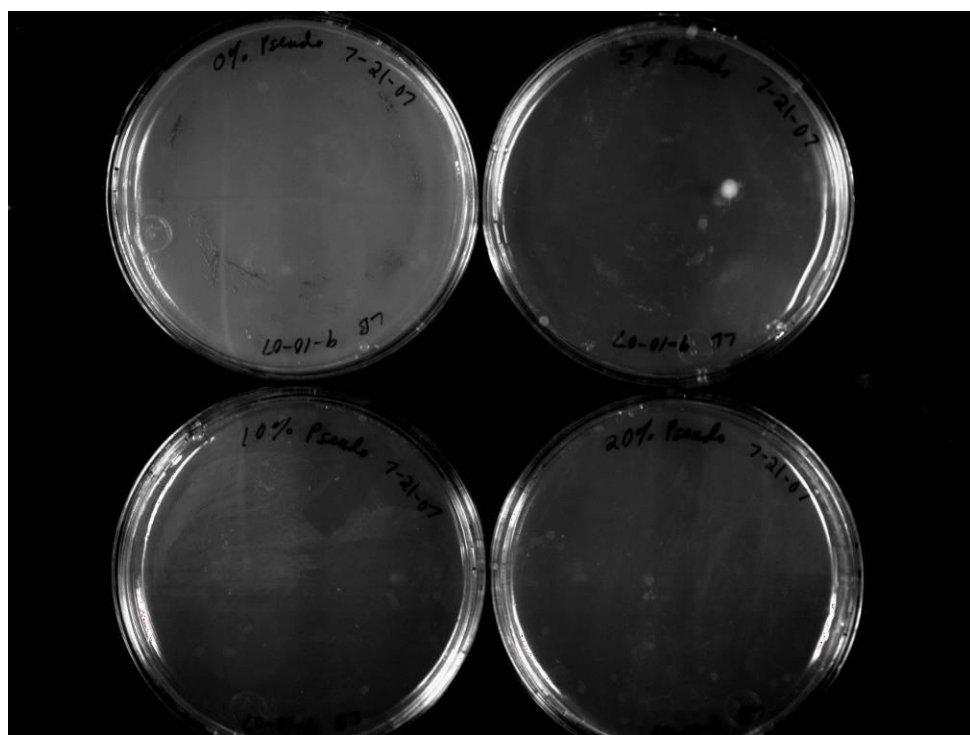


Figure 19. ATCC *Pseudomonas* at day 38. DiEGME concentrations are: 0,5,10, and 20%. The 0% plate (upper left) is swarming with growth; the 5% plate (upper right) has one colony. The 10 and 20% plates (lower left and right) have none.

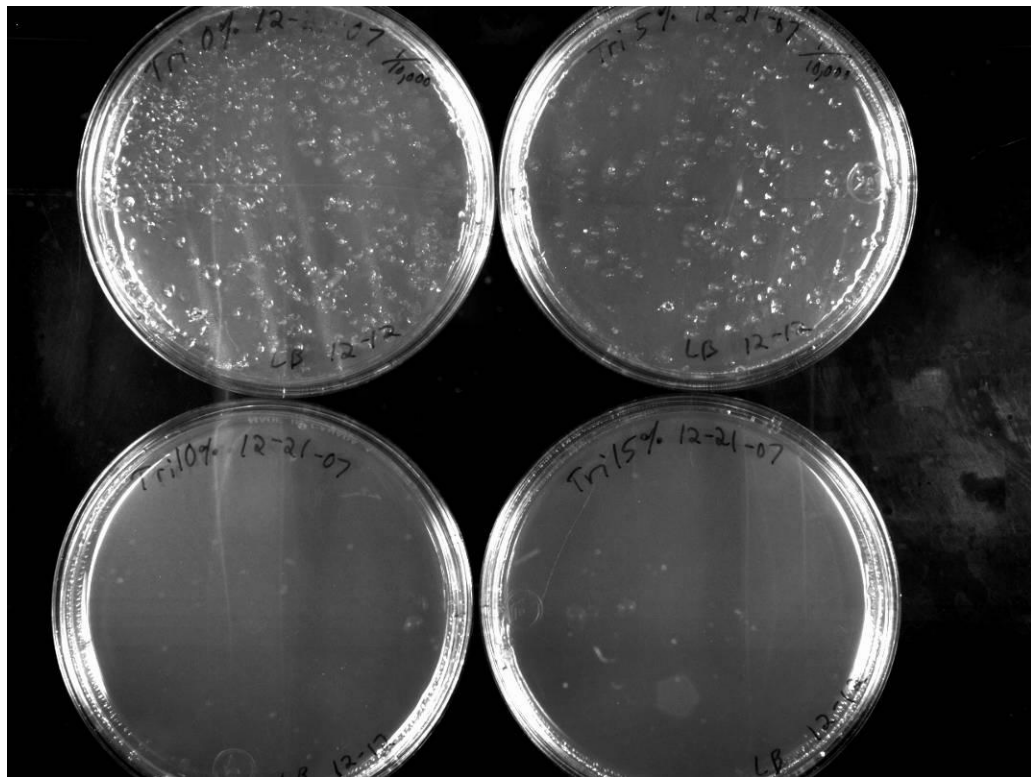


Figure 20. ATCC *Pseudomonas* at day 38. TriEGME concentrations are: 0,5,10, and 15%. The 0% plate (upper left) and 5% plates (upper right) are swarming with growth. The 10 and 15% plates (lower left and right) have none.

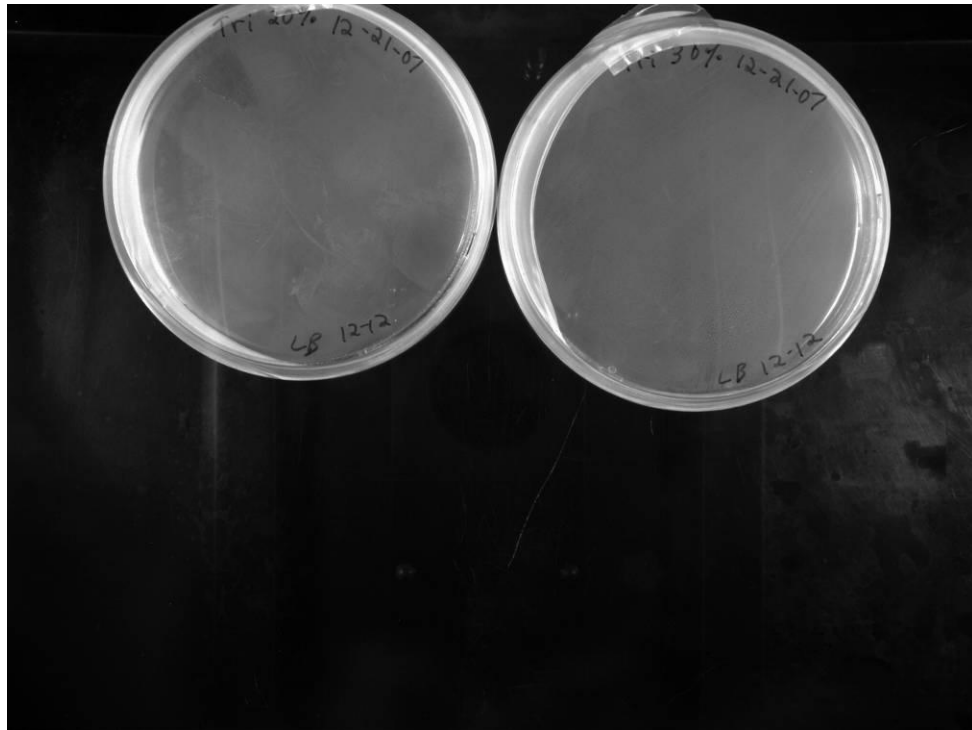


Figure 21. ATCC *Pseudomonas* at day 38. TriEGME concentrations are: 20 and 30%. The plates have no growth.

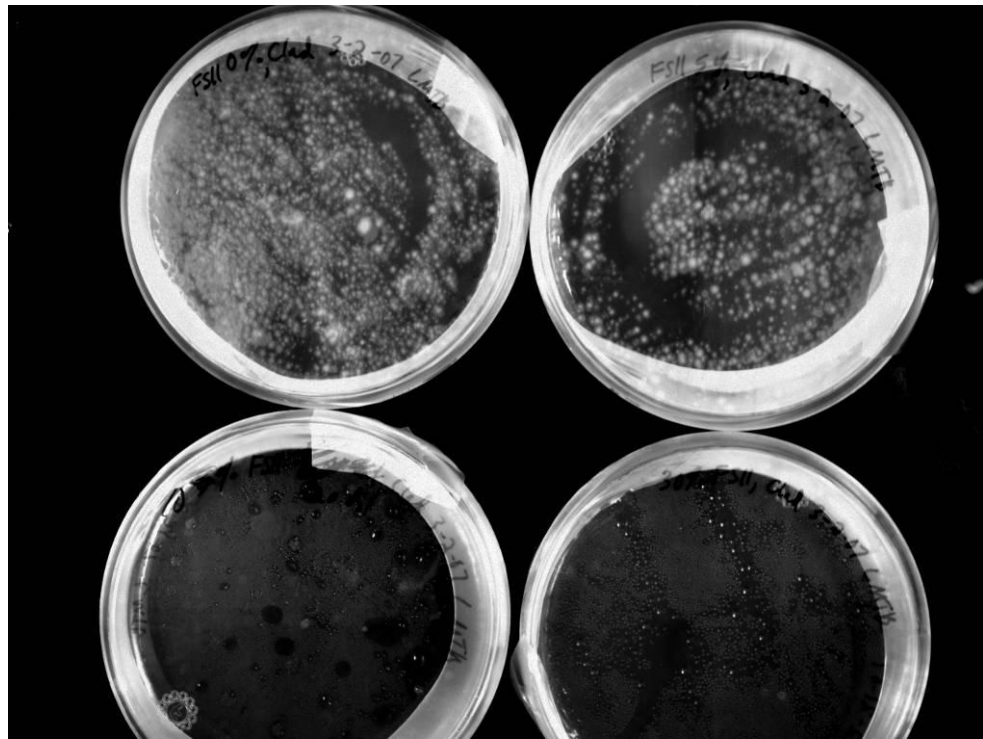


Figure 22. ATCC *Cladosporium* at day 30 of incubation. DiEGME concentrations are: 0 (upper left), 5 (upper right), 20 (lower left) and 30% (lower right). Lower plates have condensation, not colonies.

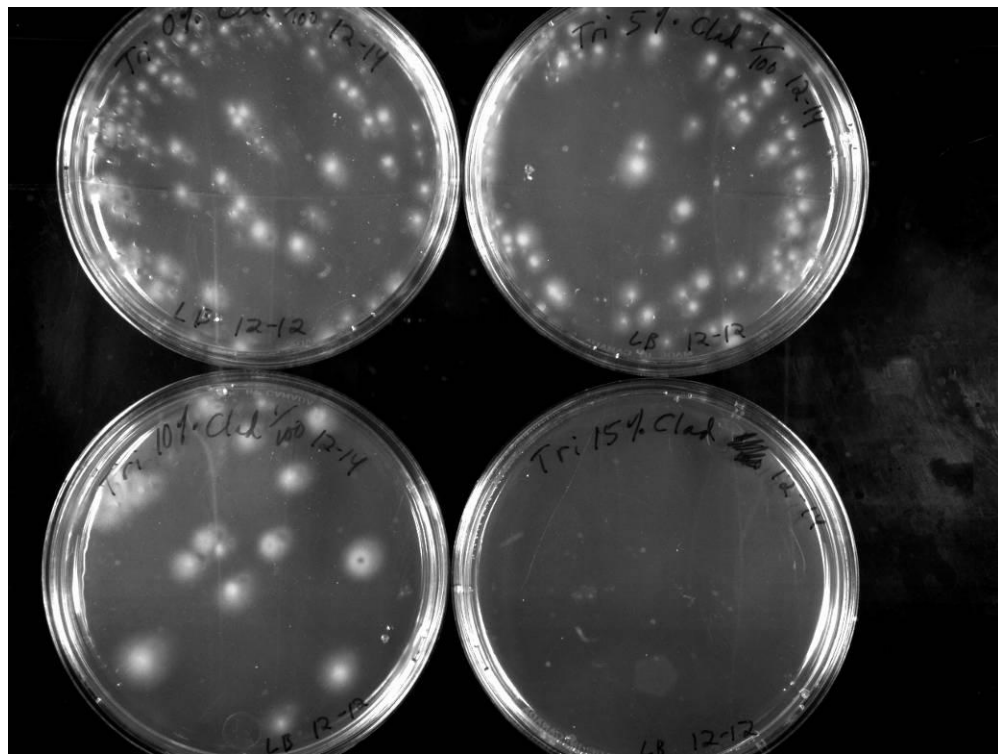


Figure 23. ATCC *Cladosporium* at day 31 of incubation. TriEGME concentrations are: 0 (upper left), 5 (upper right), 10 (lower left) and 15% (lower right).

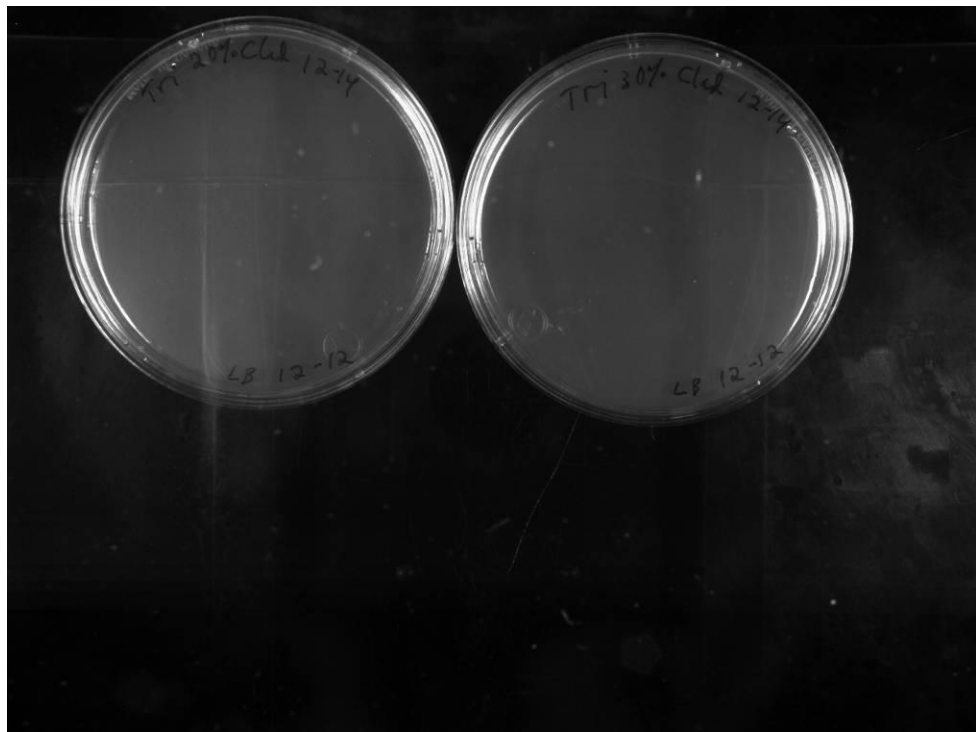


Figure 24. ATCC *Cladosporium* at day 31. TriEGME concentrations are: 20 and 30%. These plates have no colonies.

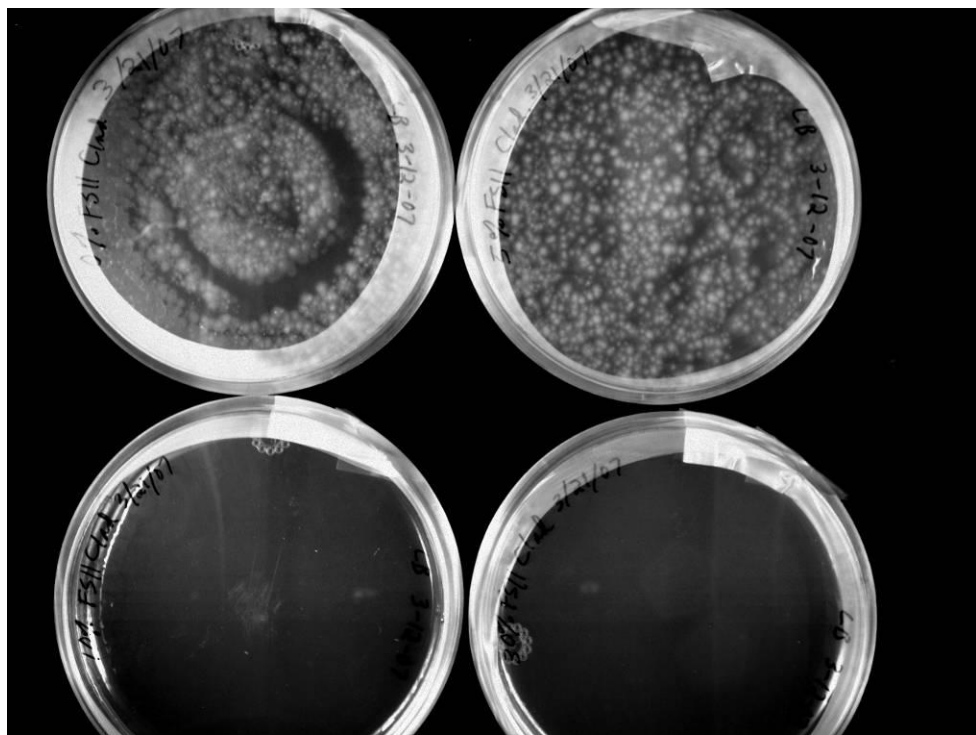


Figure 25. ATCC *Cladosporium* at day 47. DiEGME concentrations are: 0 (upper left), 5 (upper right), 10 (lower left), 30% (lower right). The 10 and 30% plates have no colonies.

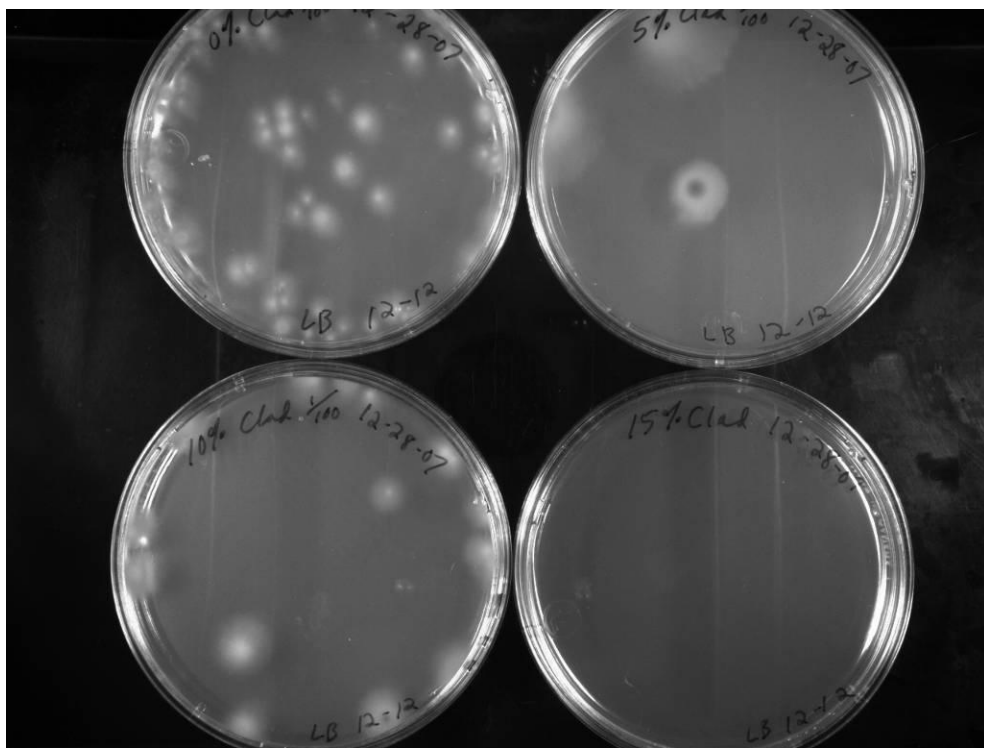


Figure 26. ATCC *Cladosporium* at day 48. TriEGME concentrations are: 0 (upper left), 5 (upper right), 10 (lower left), 15% (lower right). The 15% plate has no colonies.

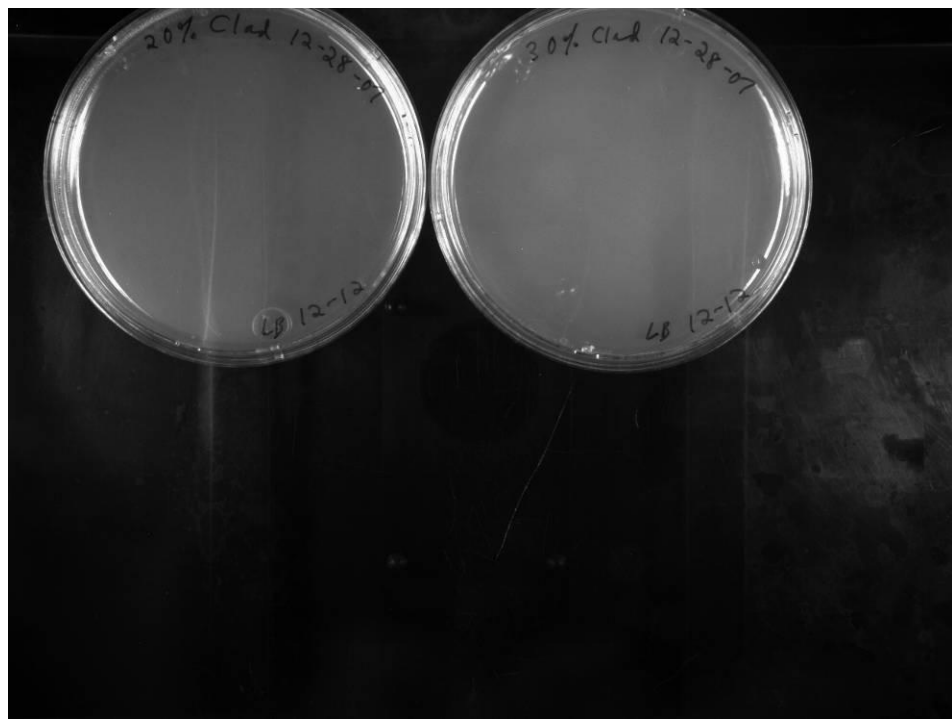


Figure 27. ATCC *Cladosporium* at day 48. TriEGME concentrations are: 20 and 30%. These plates have no colonies.

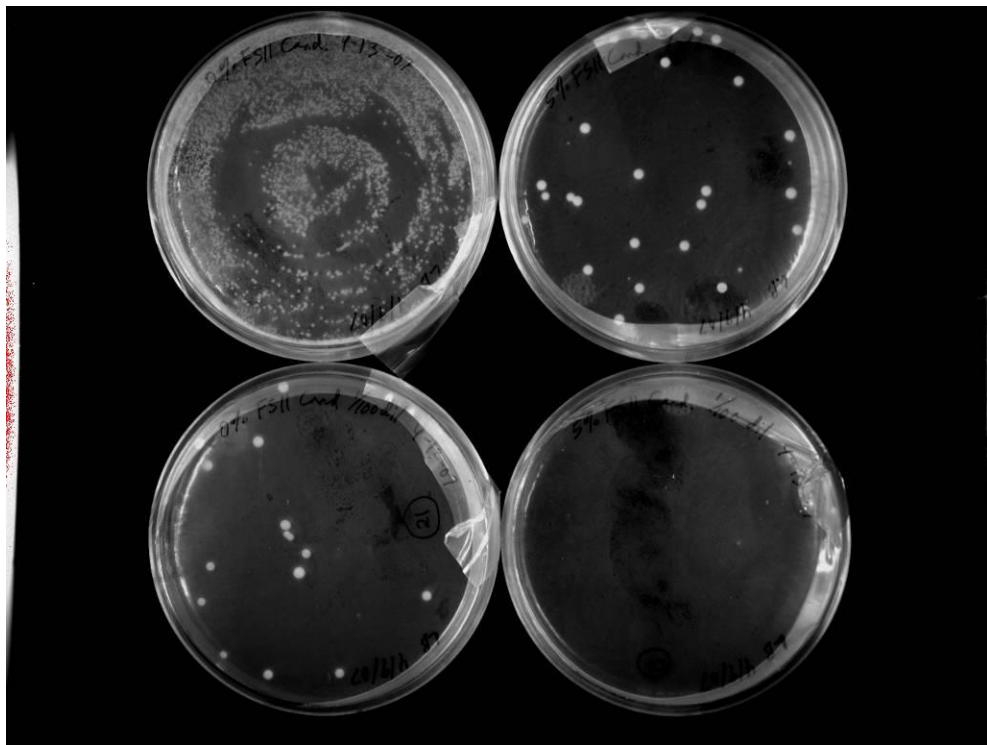


Figure 28. ATCC *Candida* at day 8. DiEGME concentrations are: 0 (no dilution, upper left), 5 (no dilution, upper right), 0 (1/100 dilution, lower left), and 5 (1/100 dilution, lower right). The 5% 1/100 dilution plate has no colonies.

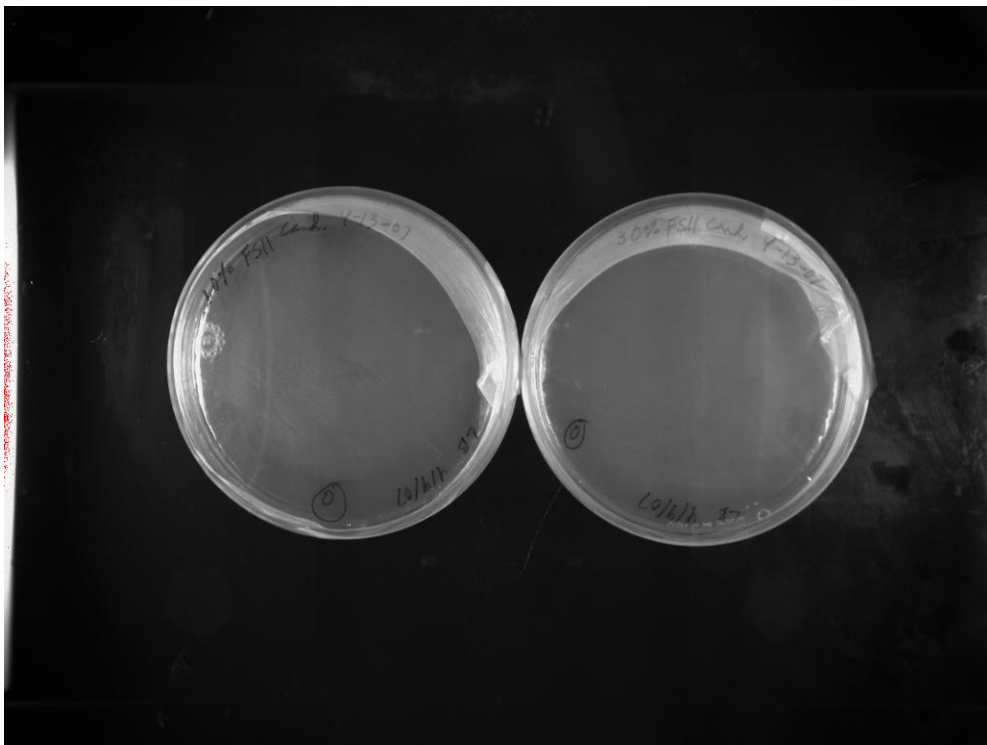


Figure 29. ATCC *Candida* at day 8. DiEGME concentrations are: 10 (left) and 30% (right). Neither plate has colonies.

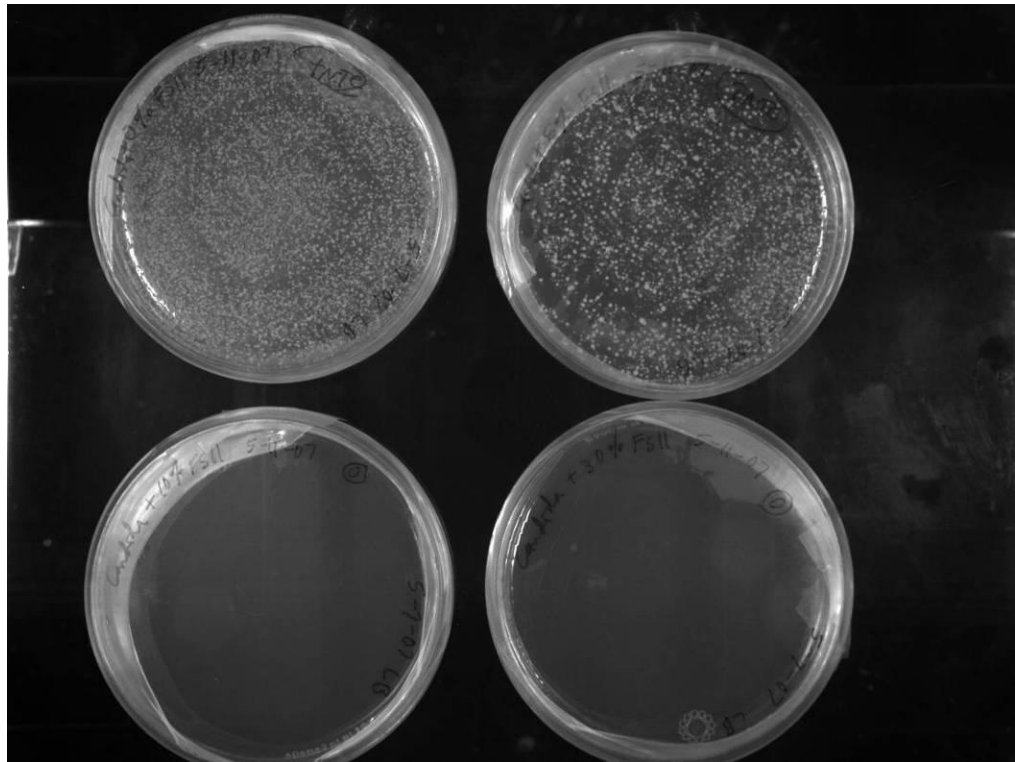


Figure 30. ATCC *Candida* at day 35. DiEGME concentrations are: 0% (upper left), 5% (upper right), 10% (lower left), and 30%. Neither lower plate has colonies.

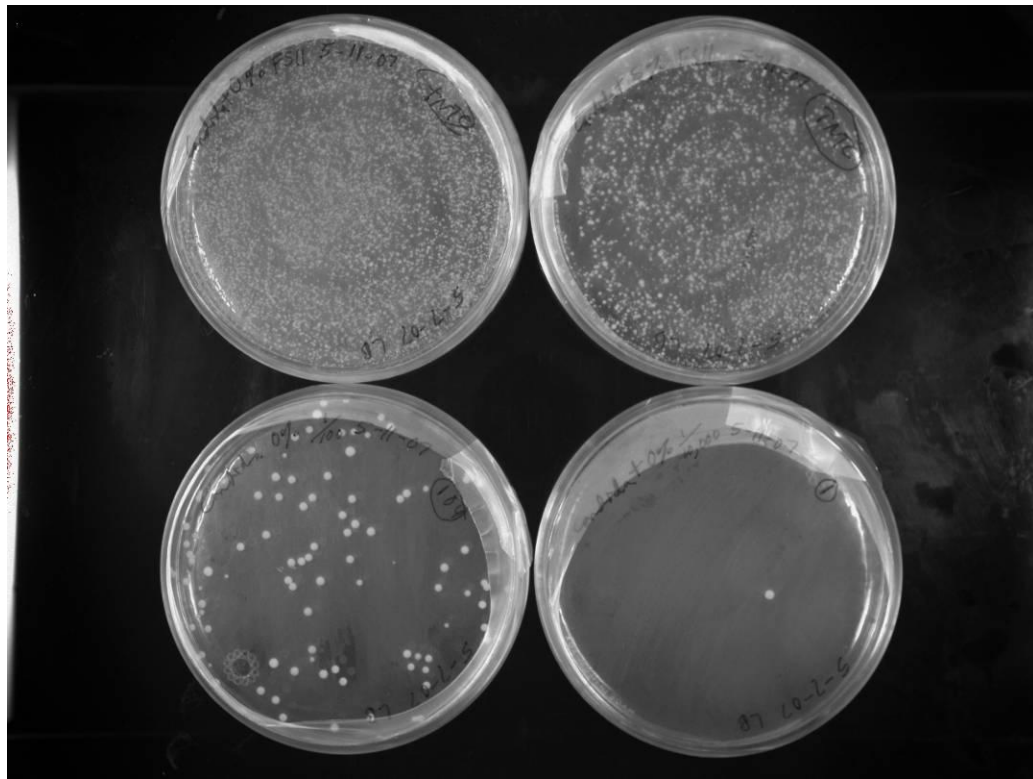


Figure 31. ATCC *Candida* at day 35. DiEGME concentrations are: 0% (upper left), 5% (upper right) at 1/10,000 dilution, 0% at 1/100 dilution (lower left), and 0% at 1/10,000 dilution (lower right). Neither lower plate has colonies.

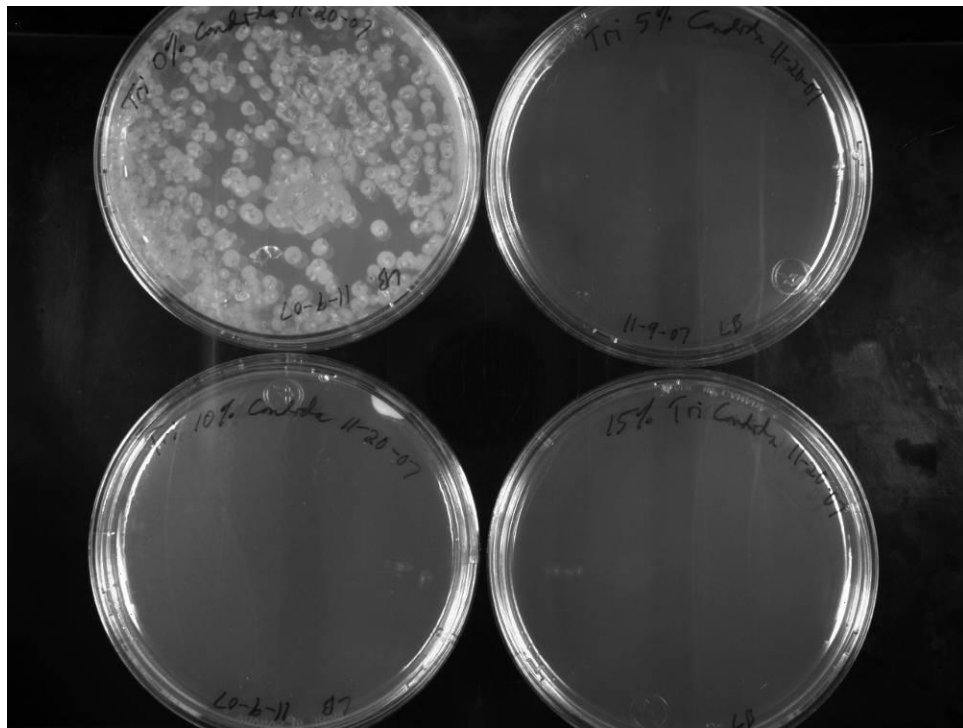


Figure 32. ATCC *Candida* at day 7. TriEGME concentrations are: 0 (no dilution, upper left), 5 (no dilution, upper right), 10 (no dilution, lower left), and 15 (1/100 dilution, lower right). Only the 0% plate has colonies.

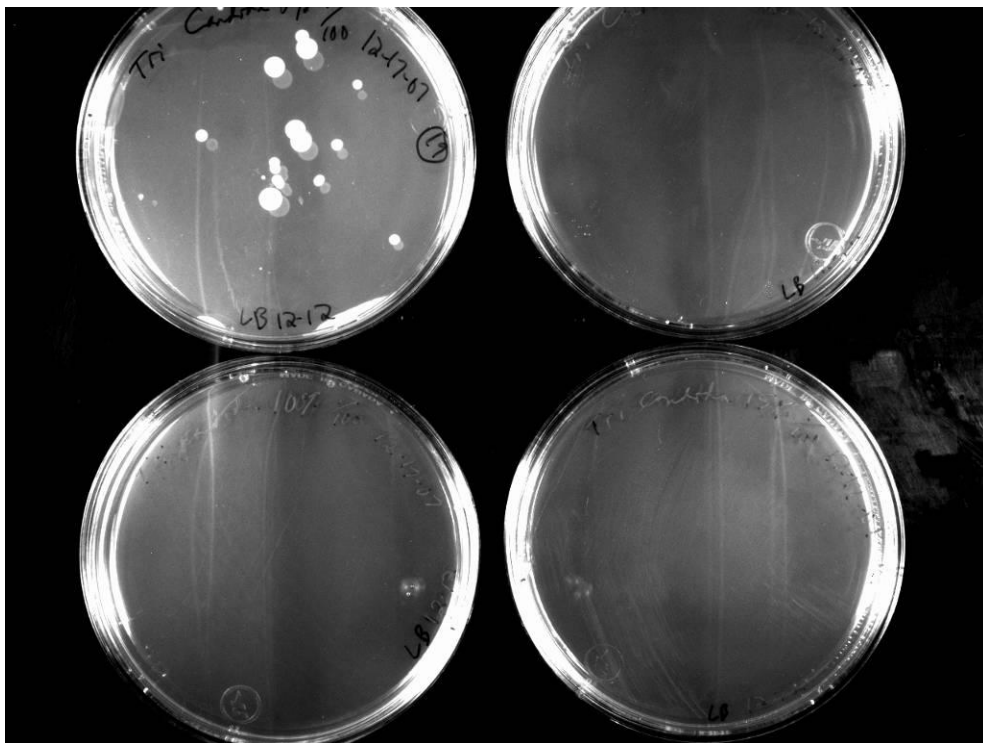


Figure 33. ATCC *Candida* at day 35. TriEGME concentrations are: 0, 5, 10, and 15%. Only the 0% plate has colonies.

Similar observations can be made concerning the colony growth on the LB agar plates over the 46 day test period. The ATCC consortia plates shown in Figures 10-33 clearly indicate that 0 and 5% FSII levels permit microbial growth, although 5% has less growth than 0% FSII. The ATCC single species plates show the same trend, with the exception of *Candida*, which was unable to grow at concentrations of 5% or greater. The FSII levels of 10% and above seem to have the capacity to completely eliminate growth for *Pseudomonas* and *Candida*, but the ATCC consortia and *Cladosporium* alone required TriEGME concentrations of 15% or greater by volume in the aqueous phase to be subdued. Compared to DiEGME, TriEGME seemed to have a greater effect on the *Candida*, and a lesser effect on the *Pseudomonas* and *Cladosporium*. Concentrations of TriEGME at or above 15% seem adequate for control of microbial growth. However, because TriEGME has a greater partition coefficient, the effective dosage rate for TriEGME would be similar to that expected for DiEGME.

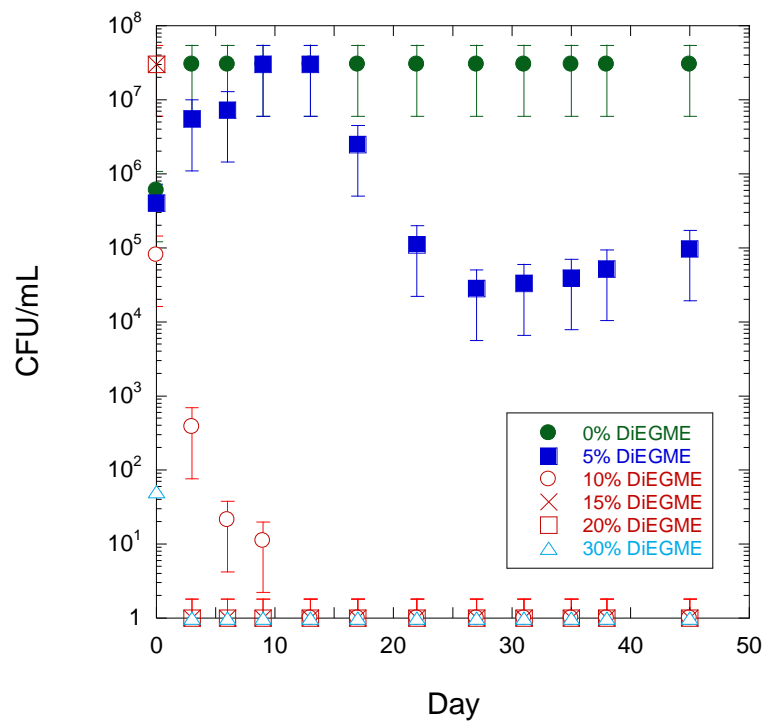


Figure 34. Semi-log plot of ATCC consortia colony forming units (CFU) per mL of liquid sample over the 46 day test period for several DiEGME levels. DiEGME level is indicated as % volume in water phase.

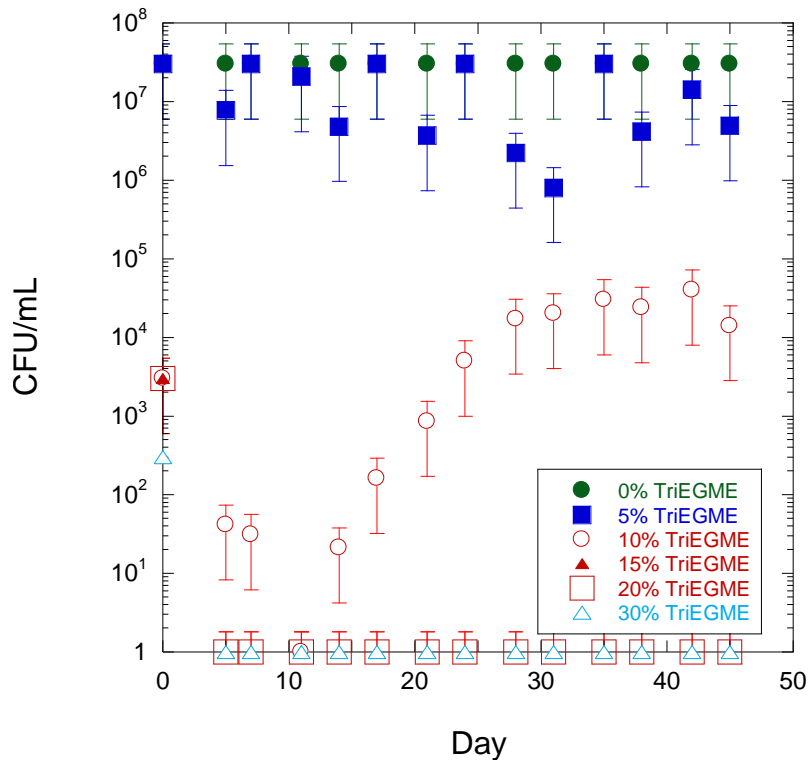


Figure 35. Semi-log plot of ATCC consortia colony forming units (CFU) per mL of liquid sample over the 46 day test period for several TriEGME levels. TriEGME level is indicated as % volume in water phase.

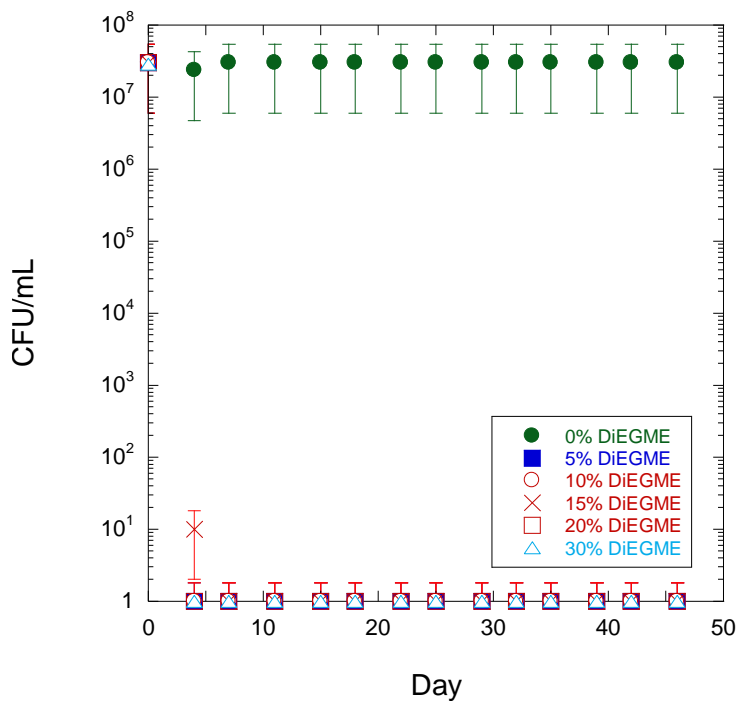


Figure 36. Semi-log plot of ATCC *Pseudomonas* colony counts over a 46 day test period for several DiEGME levels. DiEGME level is indicated as % volume in water phase.

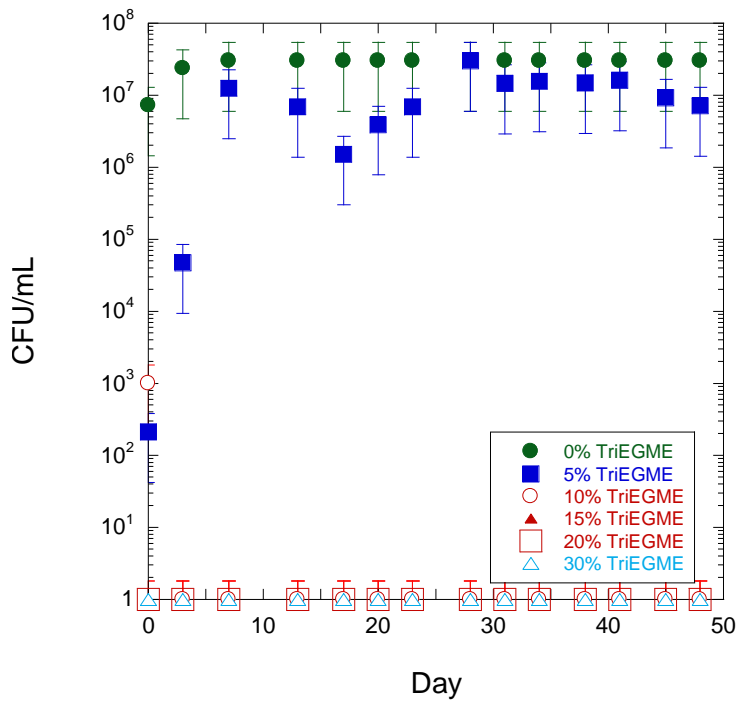


Figure 37. Semi-log plot of ATCC *Pseudomonas* colony counts over a 46 day test period for several TriEGME levels. TriEGME level is indicated as % volume in aqueous phase.

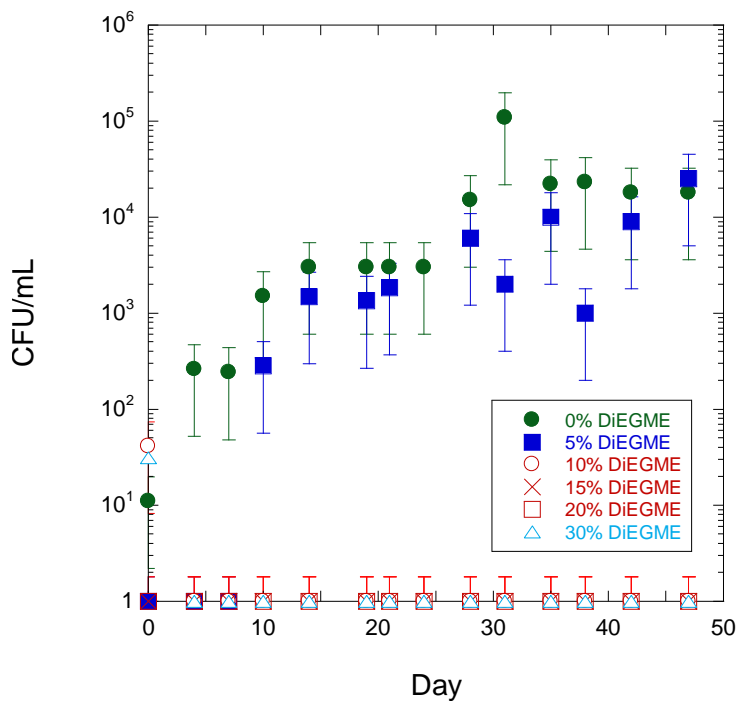


Figure 38. Semi-log plot of ATCC *Cladosporium* colony counts over a 46 day test period for several DiEGME levels. DiEGME level is indicated as % volume in water phase.

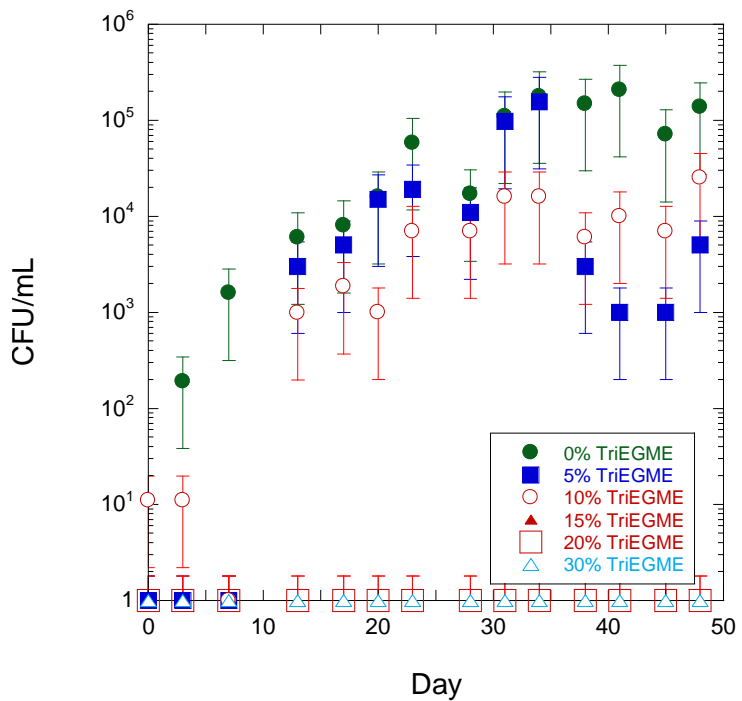


Figure 39. Semi-log plot of ATCC *Cladosporium* colony counts over a 46 day test period for several TriEGME levels. TriEGME level is indicated as % volume in aqueous phase.

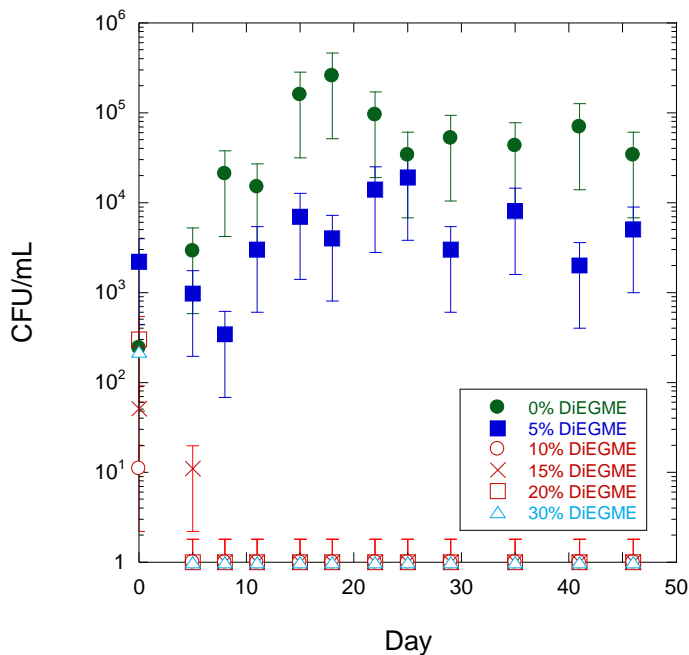


Figure 40. Semi-log plot of ATCC *Candida* colony counts over a 46 day test period for several DiEGME levels. DiEGME level is indicated as % volume in water phase.

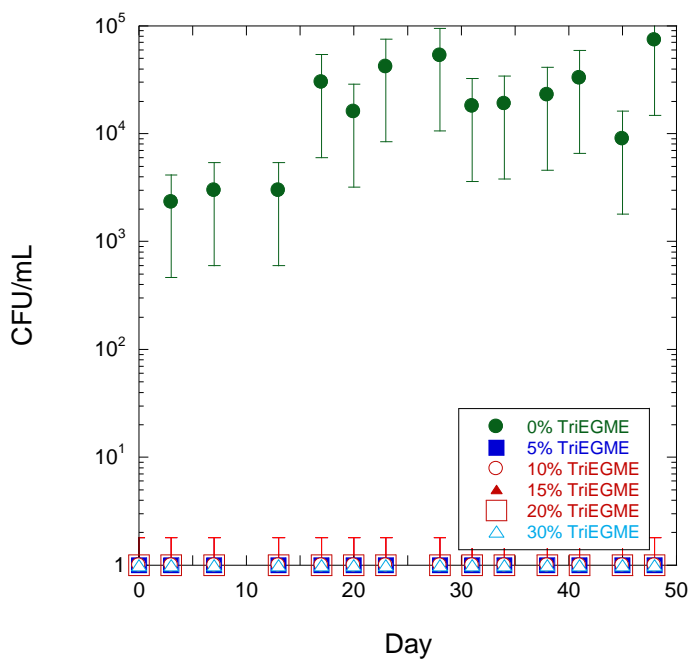


Figure 41. Semi-log plot of ATCC *Candida* colony counts over a 46 day test period for several TriEGME levels. TriEGME level is indicated as % volume in aqueous phase.

It is clear from the Figures 34-41 shown that *Pseudomonas* produces the greatest number of colonies compared to the other ATCC microorganisms, but it also experiences the greatest inhibition due to DiEGME, with only 5% DiEGME completely eliminating its population after 4 days. Although the *Candida* and *Cladosporium* produce fewer colonies, their growth continues unabated at the 5% DiEGME level, though it is also halted at 10% DiEGME in nine days or fewer. The ATCC consortia test with DiEGME containing all three microorganisms shows similar results, though the growth patterns of the consortia are somewhat different, most likely due to interaction among the three types of microorganisms and their metabolites. The microorganisms at all levels of DiEGME treatment still showed growth after four hours exposure to the icing inhibitor. However, as early as Day 1, there were significant declines in colony count for all DiEGME levels above 5% by volume in the water phase. Results suggest that a DiEGME level of 10% by volume in the water phase is adequate for elimination of microbial growth for these microorganisms. This level is slightly lower than that suggested by previous studies.

With regards to the TriEGME tests, it is clear from the plots shown that neither 0 nor 5% TriEGME reduces ATCC consortia or single microorganism colony counts to a significant degree, with the exception of *Candida*, whose colonies are significantly reduced with only 5% TriEGME. Ten percent TriEGME and above reduced colony count significantly, with the exceptions of the ATCC consortia and *Cladosporium* alone, due to the persistence of *Cladosporium*, even at 10% levels of TriEGME. These results suggest that 15% TriEGME and above in the aqueous phase is adequate for suppression or elimination of microbial growth. Using the Figure 1 partitioning data, this would correspond to a TriEGME in fuel concentration of ~0.015 volume % at 23° C.

4.2 Field Microorganisms Consortia Test

Six microorganisms were obtained from the field, cultured, isolated, then frozen at -80°C. These microorganisms included: *Pseudomonas* sp., *Rhodococcus equi*, *Bacillus licheniformis*, *Clostridium intestinal*, *Methylobacterium* sp., and *Cladosporium resinae*. They were revived from the frozen state separately by incubation at 28°C on an LB agar plate, then utilized in the same procedure listed above. The field microorganisms were tested as a consortia only. The same DiEGME and TriEGME levels were used as previously mentioned. Figures 42-44 below shows the French square test setups following the 46 day test. Figures 45-50 below show agar plate growth at several different points during the experiment. Figures 51 and 52 show colony counts at all DiEGME and TriEGME levels over the 46 day test period.

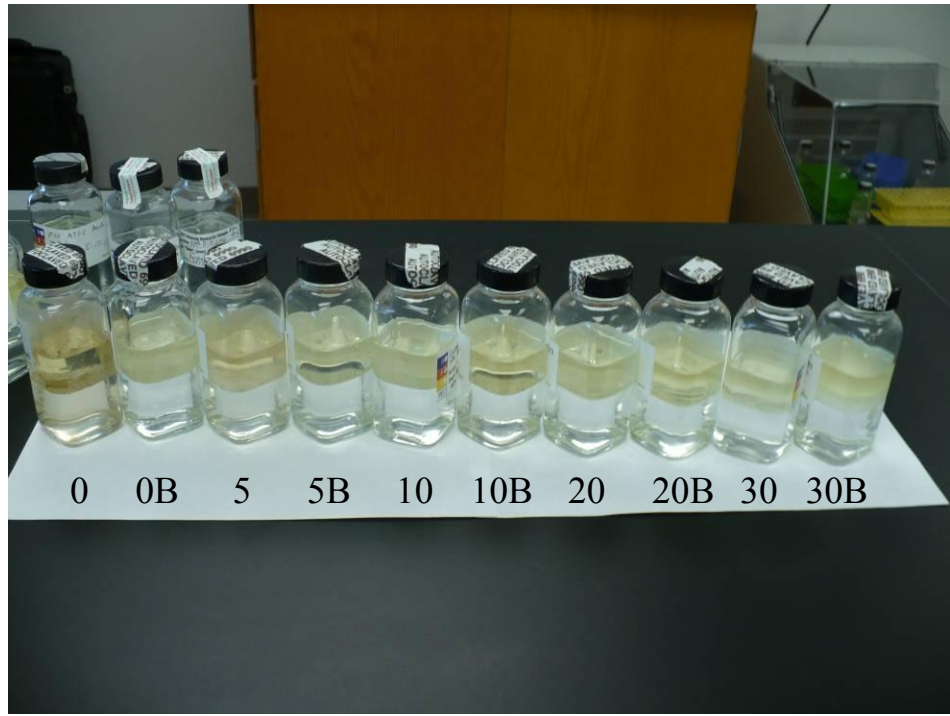


Figure 42. Field consortia following day 46 of test. DiEGME concentrations are: 0, 5, 10, 20, and 30% by volume in water phase, with each next to its respective blank.

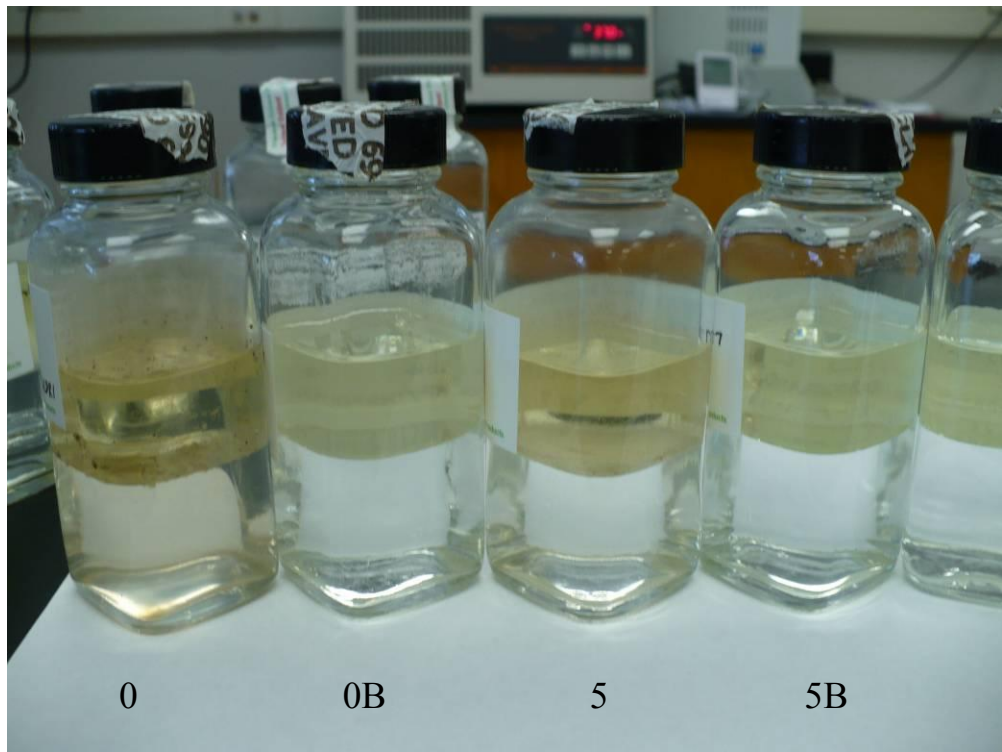


Figure 43. Field consortia following day 46 of test. DiEGME concentrations are: 0 and 5% by volume in water phase, with each next to its respective blank.

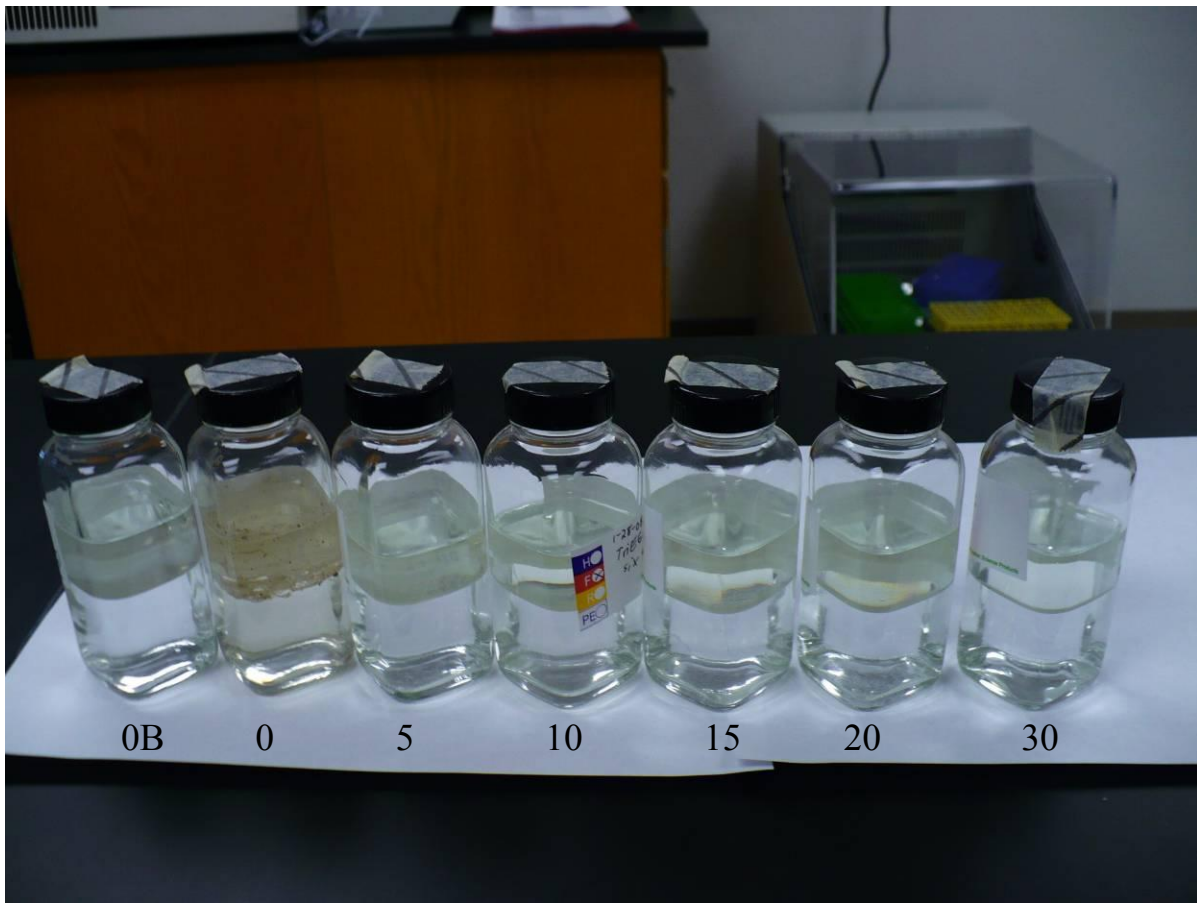


Figure 44. Six field consortia following day 46 of test. The blank fuel/water setup is on the left, followed by TriEGME concentrations of: 0, 5, 10, 15, 20, and 30% by volume in the aqueous phase.

Figures 42-44 show that the field consortia test setups are visually similar to the ATCC consortia setups. Like the ATCC setups, the field consortia setups show some cloudiness in the water layer, as well as particulates and cloudiness in the fuel layer for the 0% TriEGME levels. However, no visual differences were apparent for the 5% level and above test setups.

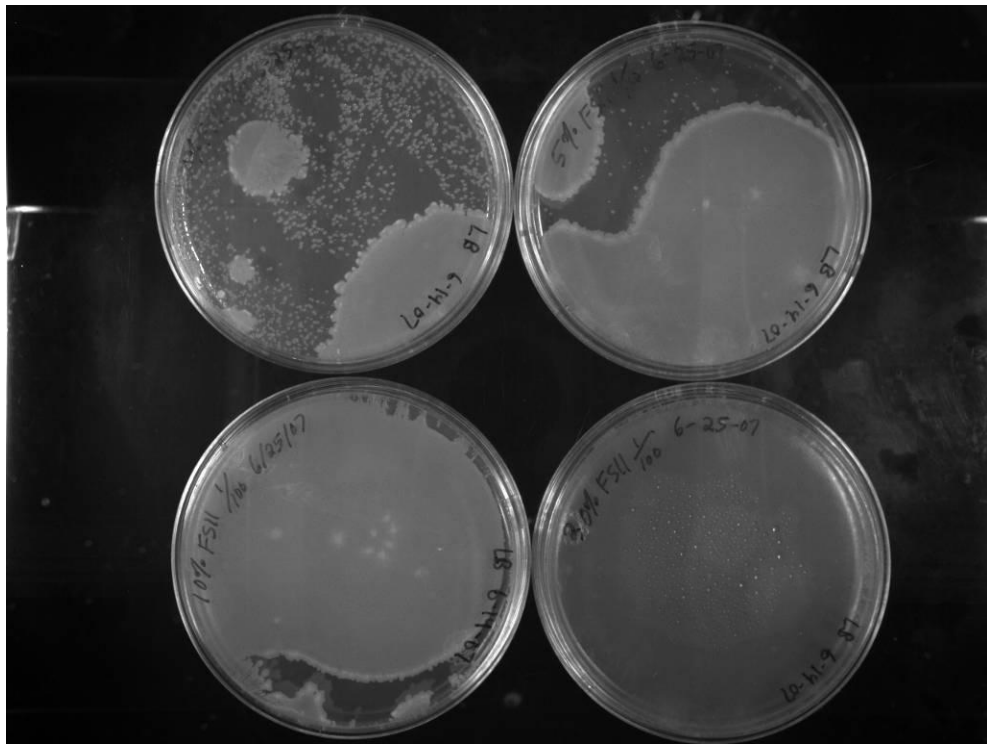


Figure 45. Six field consortia at day 11. DiEGME concentrations are: 0 (upper left), 5 (upper right), 10 (lower left), 20% DiEGME (lower right), 1:100 dilution. All plates are swarming with growth.

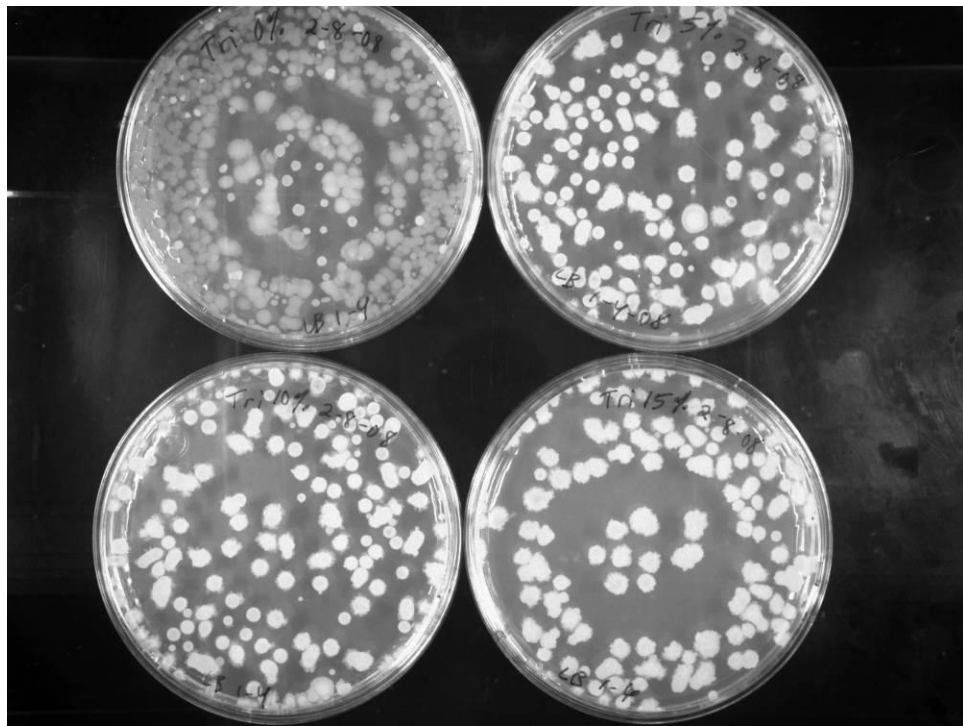


Figure 46. Six field consortia at day 11. TriEGME concentrations are: 0 (upper left), 5 (upper right), 10 (lower left), and 15% (lower right). All plates show growth.

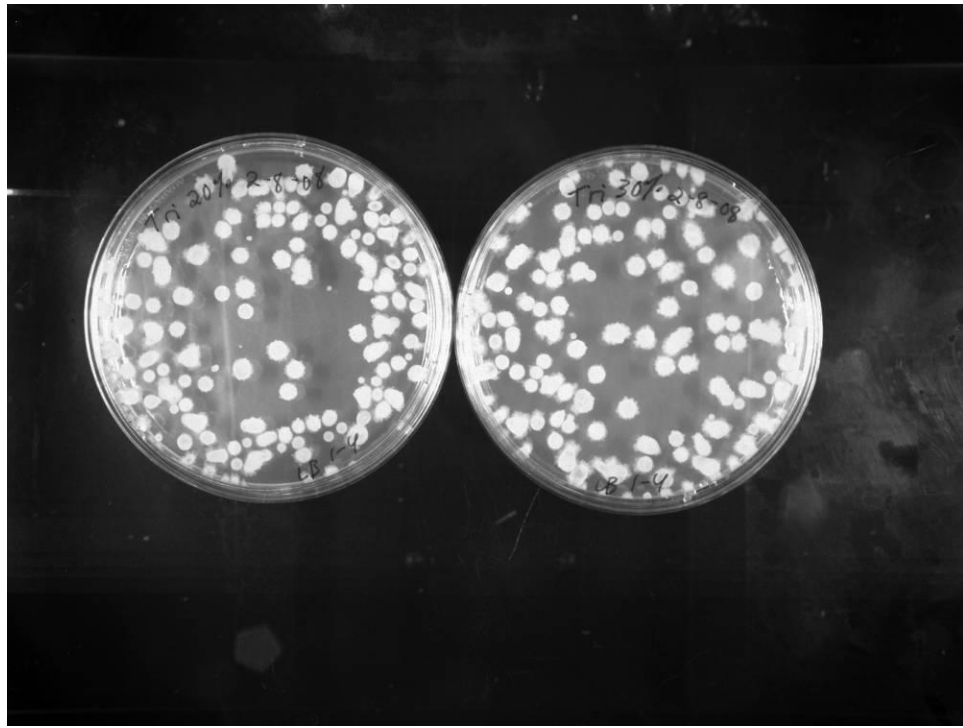


Figure 47. Six field consortia at day 11. TriEGME concentrations are: 20% (left) and 30% (right). Growth shown on both plates.

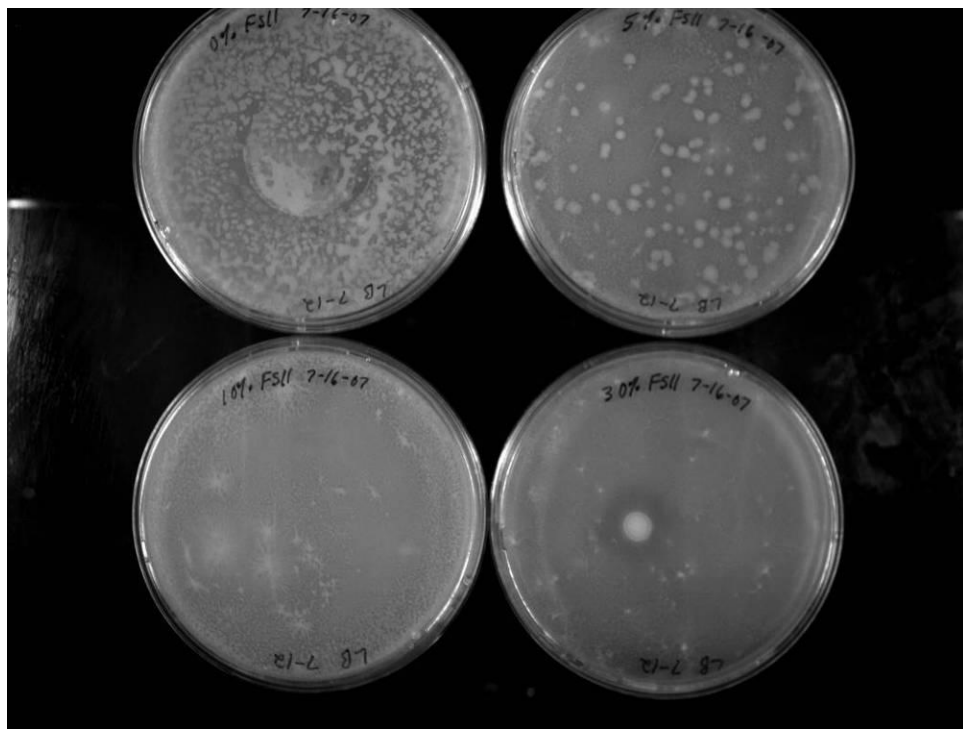


Figure 48. Six field consortia at day 32. DiEGME concentrations are: 0 (upper left), 5 (upper right), 10 (lower left), and 30% DiEGME (lower right).

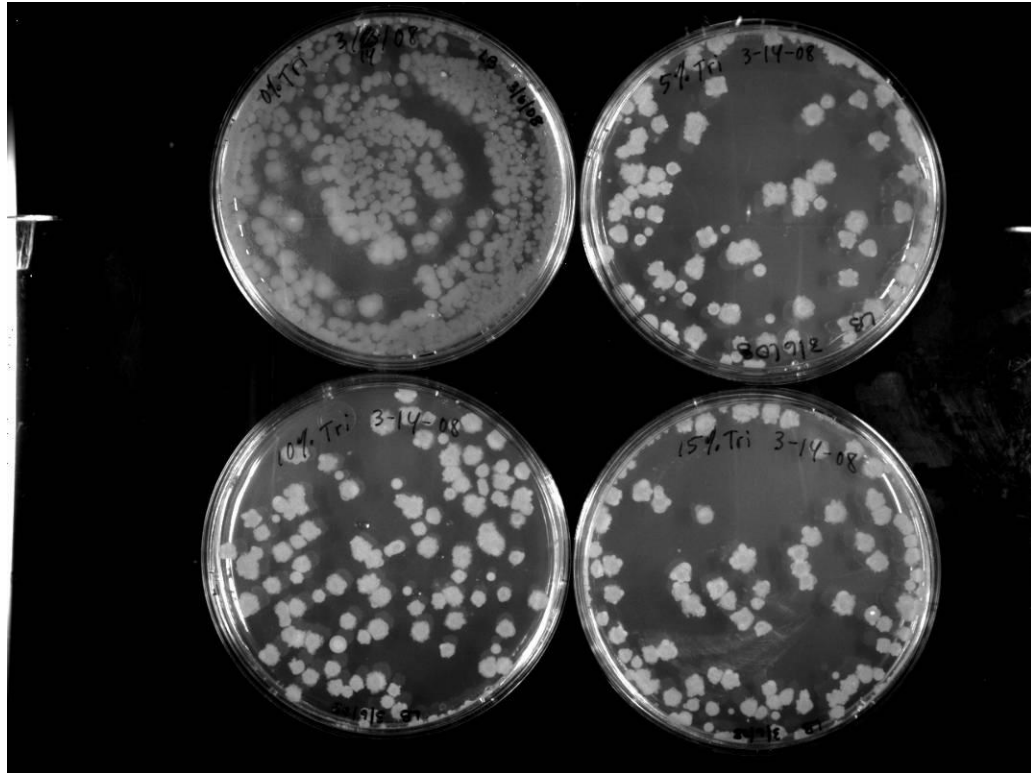


Figure 49. Six field consortia at day 46. TriEGME concentrations are: 0 (upper left), 5 (upper right), 10 (lower left), and 15% DiEGME (lower right). Growth on all plates.

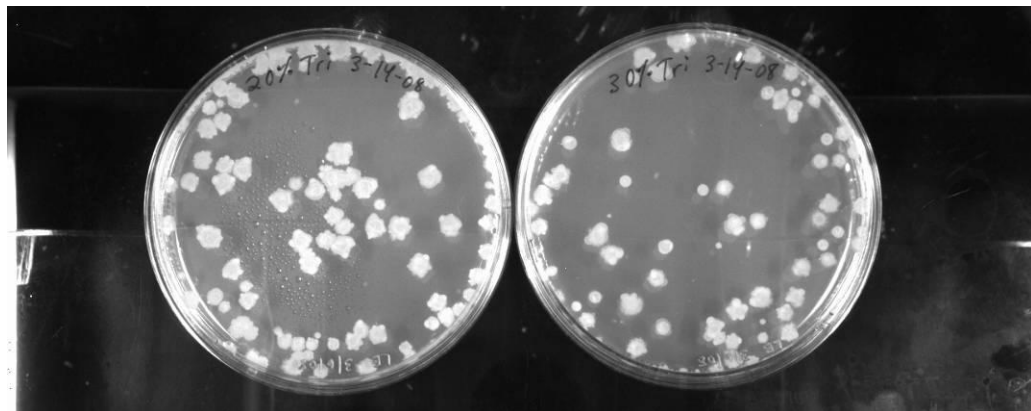


Figure 50. Six field consortia at day 46. TriEGME concentrations are: 20% (left) and 30% (right). Growth shown on both plates.

Figures 45-50 show agar plates at several points during the 46 day test period. Differences can be seen between the ATCC microorganisms' colony growth and that of the field consortia. It is apparent that, although the 5% and higher FSII levels are reducing levels of microbial growth, they are not halting the growth completely for the field microorganisms. However, the addition of higher levels of TriEGME, greater than 5%, did not result in further antimicrobial benefits. Once the "biostatic" concentration for the field microorganisms was reached, higher additive concentrations did not significantly reduce microbial growth.

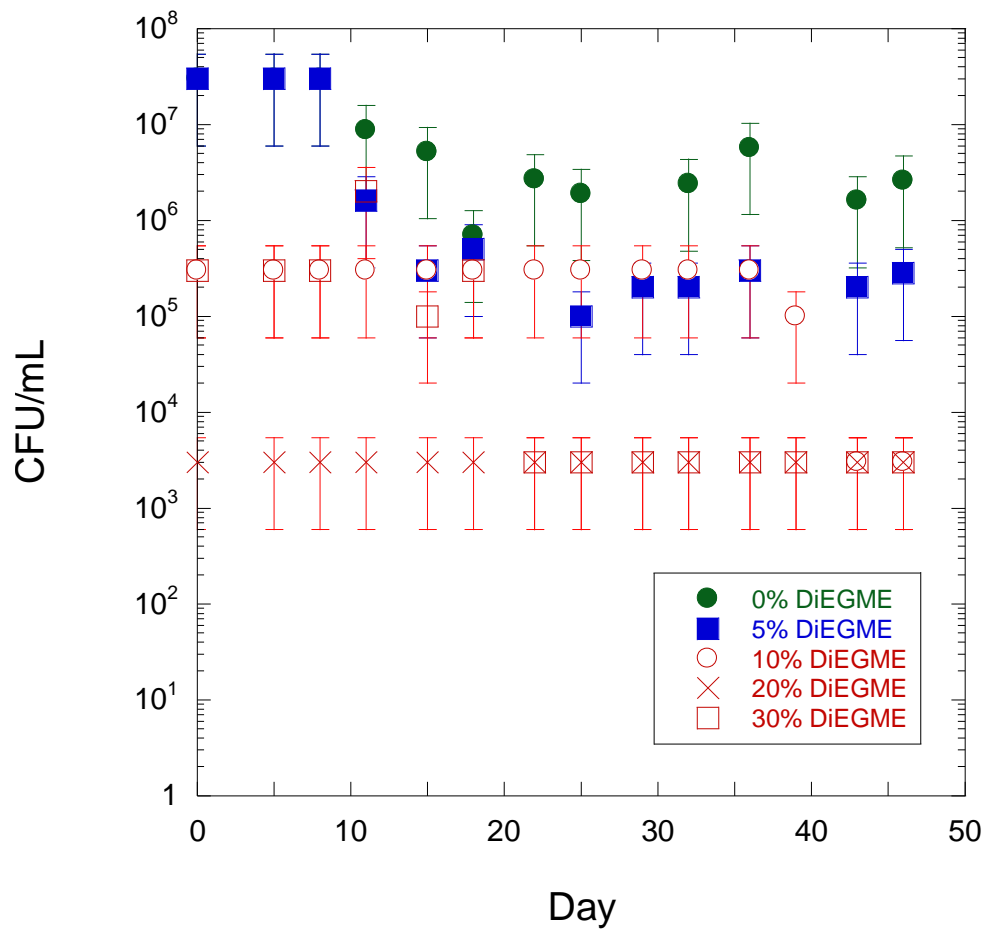


Figure 51. Semi-log plot of six field consortia colony counts over a 46 day test period for several DiEGME levels. DiEGME level is indicated as % volume in water phase.

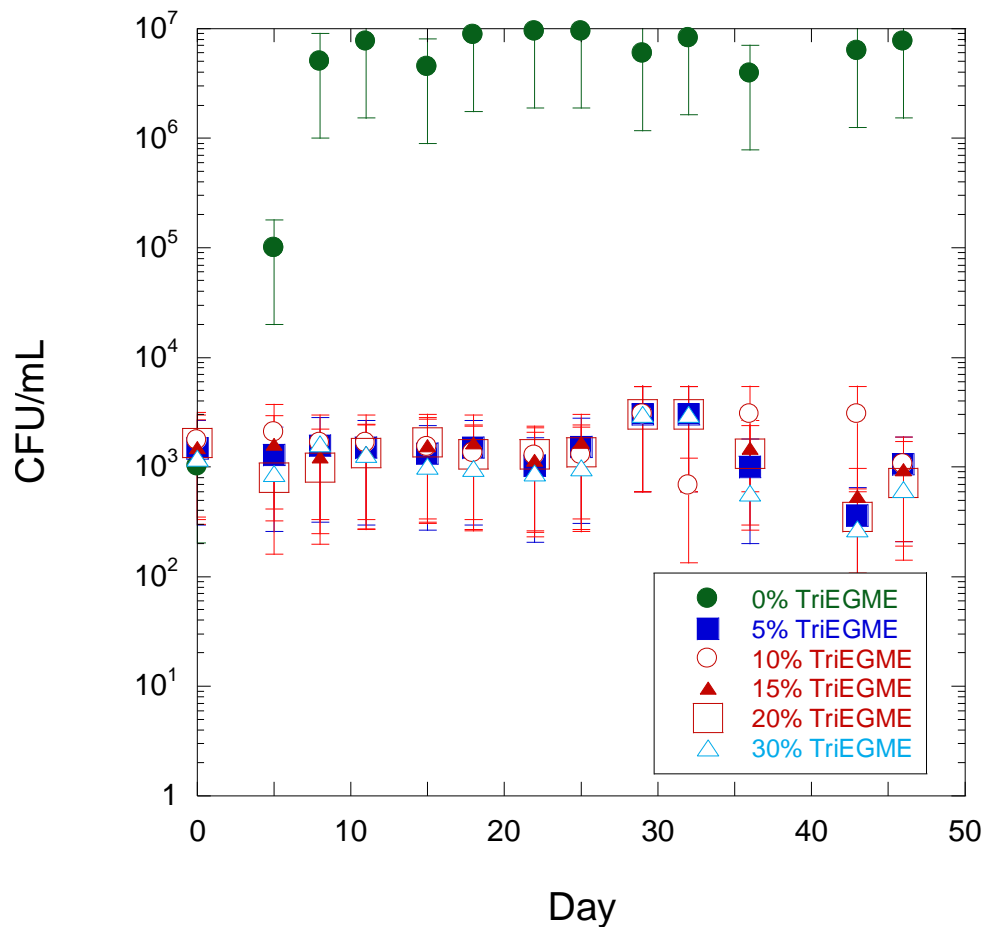


Figure 52. Semi-log plot of six field consortia colony counts over a 46 day test period for several TriEGME levels. TriEGME level is indicated as % volume in water phase.

Figures 51 and 52 show that, unlike the ATCC consortia, the mixed field consortia grew throughout the test period at each tested DiEGME and TriEGME concentration. However, the presence of DiEGME or TriEGME reduced the amount of growth at each test period. It seems possible that differences in response to FSII are the result of genetic mutations within the field microbes. These mutations can occur gradually, due to low exposure to a similar substance in the environment over time, or it can occur quickly, after a single exposure to the additive. Another possibility is that resistance was transferred to the field microbes tested here by other microbes in the environment that became resistant following their own exposure to a similar substance, via plasmid swapping. Still another possibility is hypermutation, wherein microorganisms under stress (due to a toxic agent or environmental change) mutate at increased rates, leading to a higher probability of survival by at least some mutated microorganisms (30). Also, it is possible that some of the microbes are naturally resistant, requiring no exposure to the additive at all.

Until the field consortia are tested singly, or colony morphology is studied further, it will not be clear which members have developed tolerance or if, perhaps, all of them have. Although it is clear that the low levels of DiEGME and TriEGME in this study did not kill the six field microorganisms, the difference between the 0% DiEGME and TriEGME samples and the other low level samples was dramatic, indicating the continuing positive effect of a biocidal/biostatic fuel additive. Generally, it can be said that, regardless of whether the microorganisms are lab cultured or from the field, DiEGME and TriEGME still have a beneficial biocidal/biostatic effect. The current study suggests that a DiEGME level of 10% in the aqueous phase (~0.01-0.02% by volume added to the fuel), or a TriEGME level of 15% by volume in the aqueous phase at minimum (~0.01-0.02% by volume added to the fuel) is required to control microbial growth and prevention of harmful biofilms.

4.3 Additional Field Microorganisms Consortia Test at Higher DiEGME/TriEGME Concentrations

Because two of the six field microbes persisted in the original microbiological study using 0-30% DiEGME and TriEGME by volume in aqueous phase, an additional study was conducted to determine whether DiEGME and TriEGME were more effective on these microbes at typical DiEGME concentrations seen in the field, which can be ~30-60% in the aqueous phase. A similar study was also conducted for corresponding levels of TriEGME. Morphological features suggested that the two surviving microbes were *Bacillus* and *Clostridium*. The additional study was conducted with the same methodology utilized in section 3.4, except the concentrations tested were: 30, 40, 50, and 60% DiEGME or TriEGME by volume in the aqueous phase, which corresponds to ~0.05-0.15% in the fuel phase for DiEGME, and ~0.04-0.1% for TriEGME. Figures 53-56 show liquid test setups following the 46 day test. Figures 57-62 show colony plating results at several points during the test. Figures 63 and 64 illustrate colony counts throughout the 46 day test period.



Figure 53. Additional field consortia liquid setups after 46 days. Concentrations are 0, 30, 40, 50, and 60% DiEGME in the aqueous phase. Each is shown with its respective blank.



Figure 54. Additional field consortia liquid setups after 46 days. Concentrations are 0, 30, 40, 50, and 60% TriEGME in the aqueous phase. Each is shown with its respective blank.

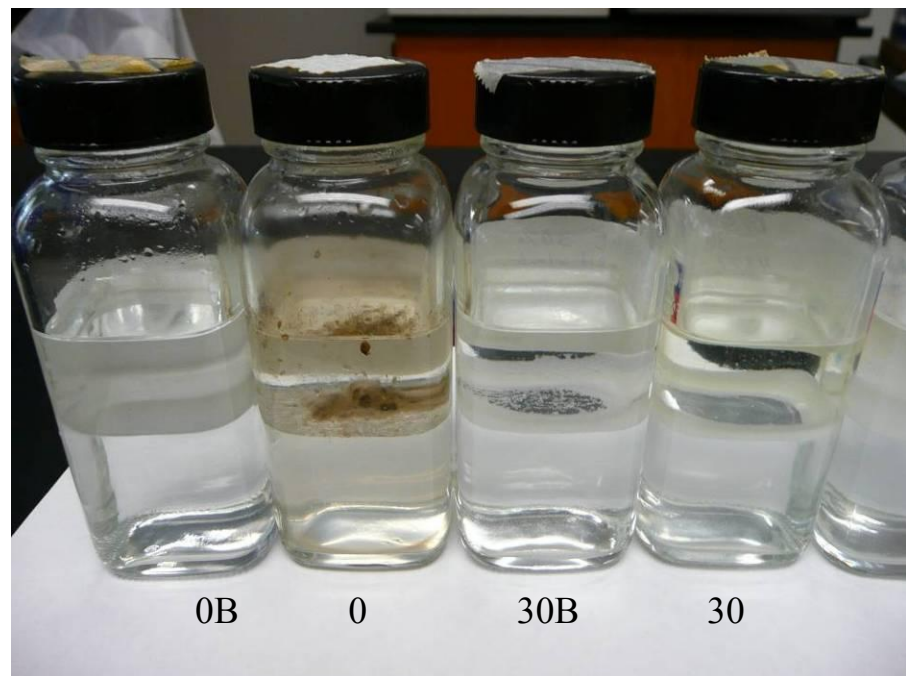


Figure 55. Additional field consortia on day 46. Closeup of 0 and 30% DiEGME with their blanks.

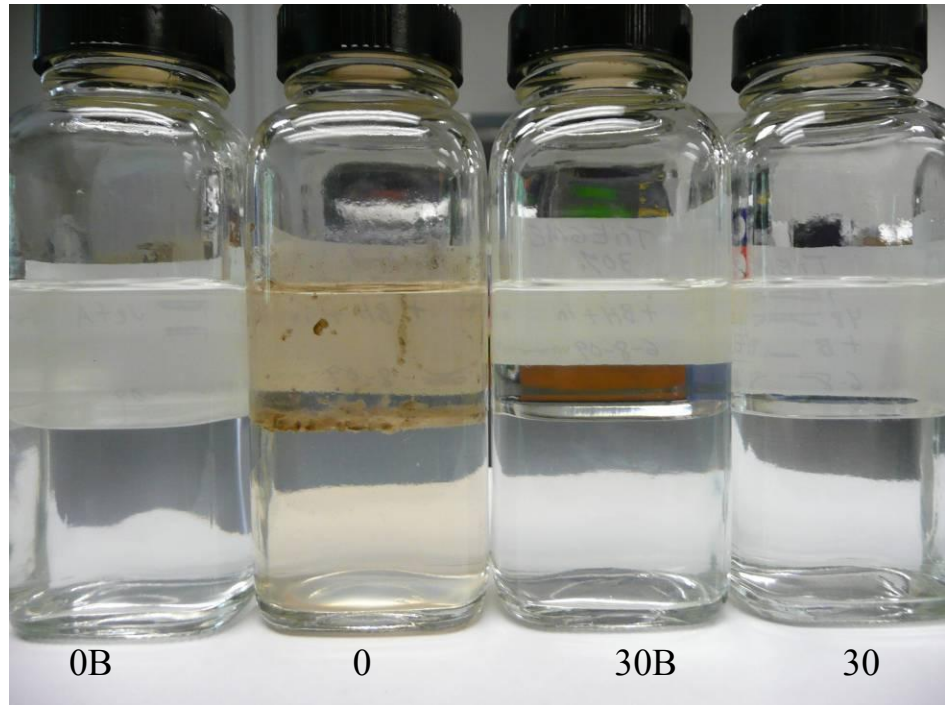


Figure 56. Closeup of additional field consortia liquid setups after 46 days. Concentrations are 0 and 30% TriEGME in the aqueous phase. Each is shown with its respective blank.

Figures 53-56 indicate that substantial growth is only present in the 0% DiEGME or TriEGME liquid setup. A brown biofilm in the hydrocarbon phase is readily apparent, as is significant cloudiness in the aqueous phase. Both suggest significant microbial contamination. The corresponding blank has no growth nor obvious cloudiness. The 30-60% DiEGME and TriEGME liquid setups appear very similar to their blanks, although the blanks appear to be slightly less cloudy in the aqueous phase. At these concentrations of DiEGME and TriEGME, emulsions are persistent and occur for both inoculated and blank liquid setups.

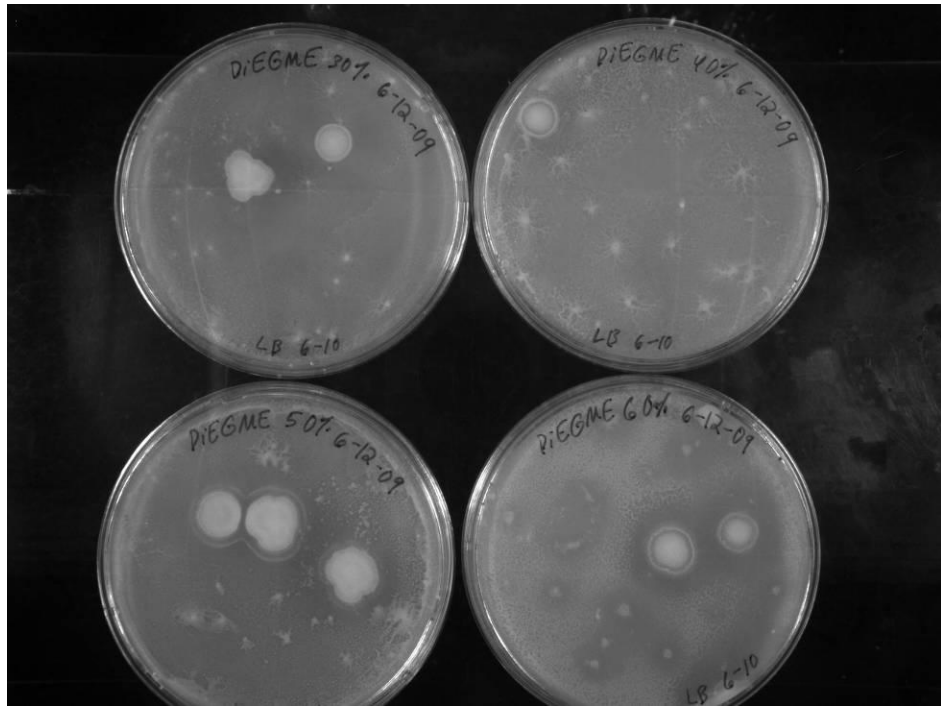


Figure 57. Additional field consortia study on day 4. DiEGME concentrations of 30, 40, 50, and 60% in the aqueous phase are shown.

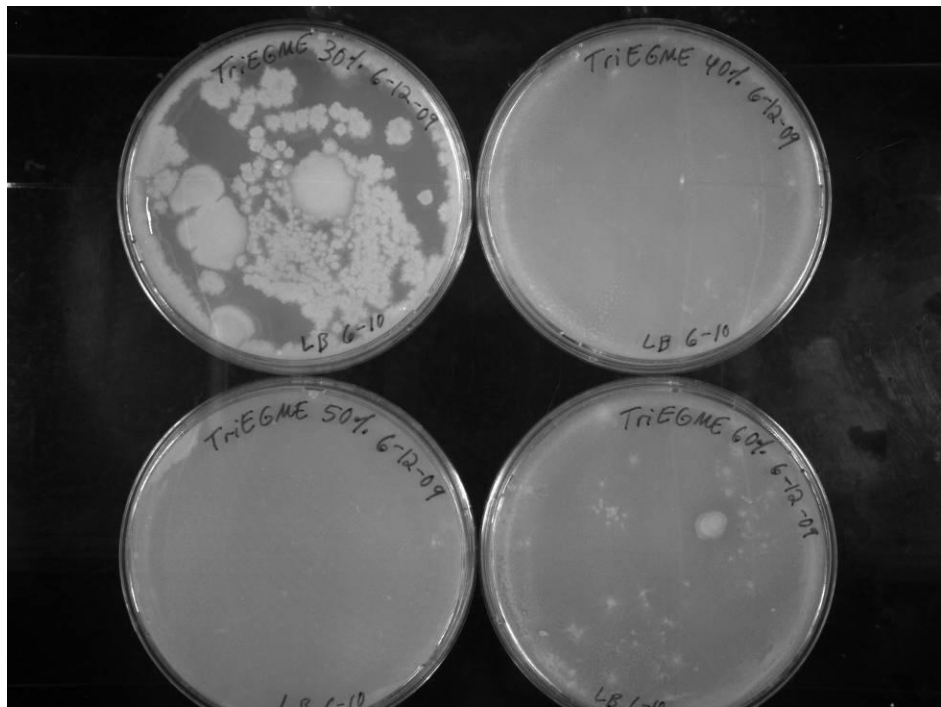


Figure 58. Additional field consortia study on day 4. TriEGME concentrations of 30, 40, 50, and 60% in the aqueous phase are shown.

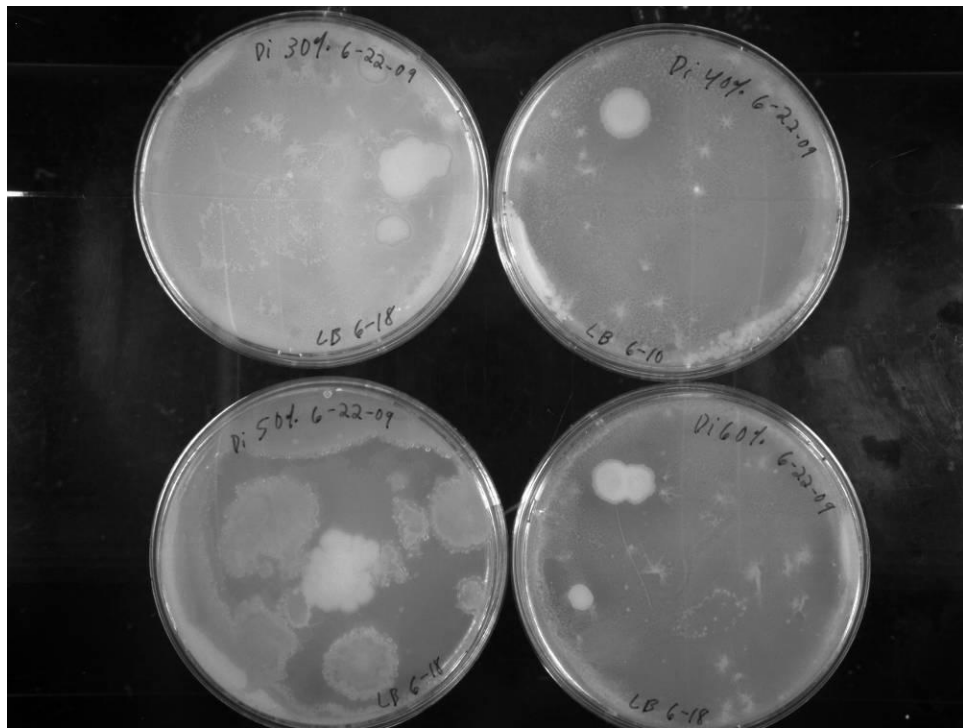


Figure 59. Additional field consortia study on day 14. DiEGME concentrations of 30, 40, 50, and 60% in the aqueous phase are shown.

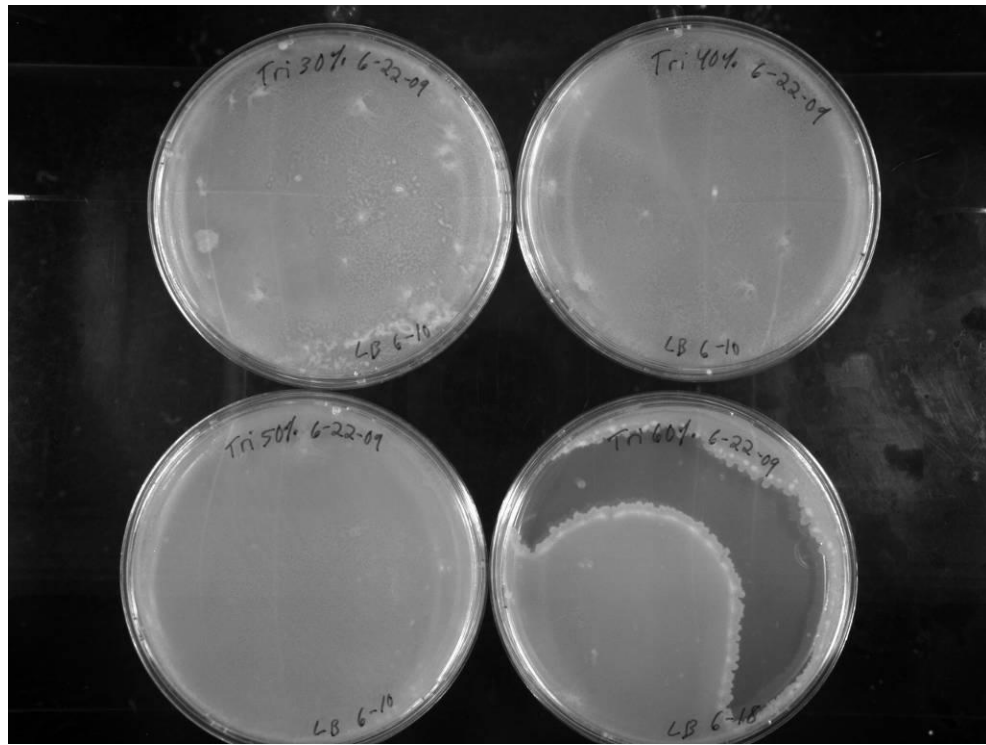


Figure 60. Additional field consortia study on day 14. TriEGME concentrations of 30, 40, 50, and 60% in the aqueous phase are shown.

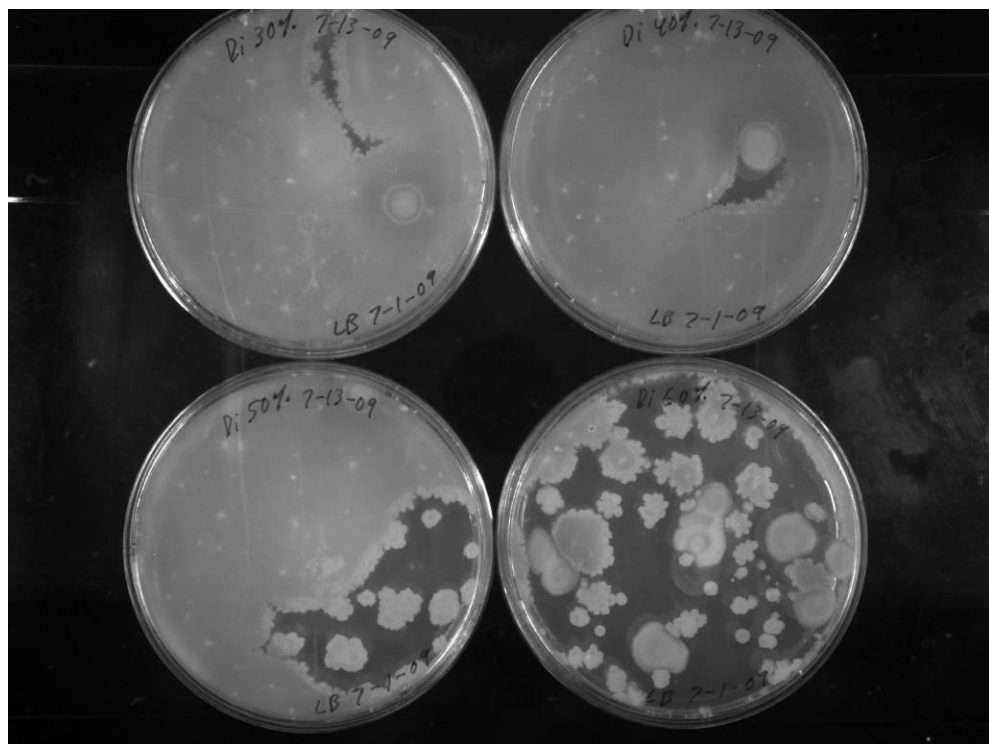


Figure 61. Additional field consortia study on day 35. DiEGME concentrations of 30, 40, 50, and 60% in the aqueous phase are shown.

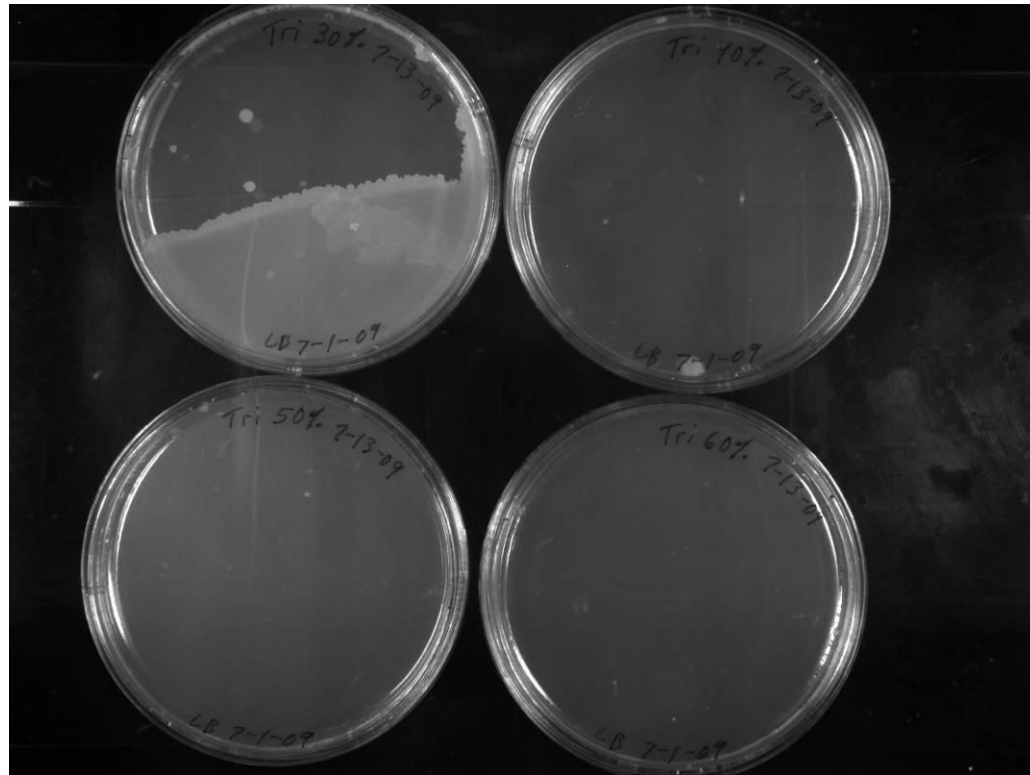


Figure 62. Additional field consortia study on day 35. TriEGME concentrations of 30, 40, 50, and 60% in the aqueous phase are shown.

The colony plate results shown in Figures 57, 59, and 61 indicate healthy microbial growth at all test points shown for DiEGME, although it does appear that the amount of colonies is somewhat decreased in the second half of the test duration. Morphological evaluation of these colonies suggests that the *Bacillus* and *Clostridium* obtained from the field are able to survive in the presence of DiEGME, even at concentrations of 30-60% DiEGME in the aqueous phase.

For TriEGME, shown in Figures 58, 60, and 62, clearly at 40% and above growth is eventually eradicated. The 30% growth is lower than reported in the previous TriEGME chart, but still present.

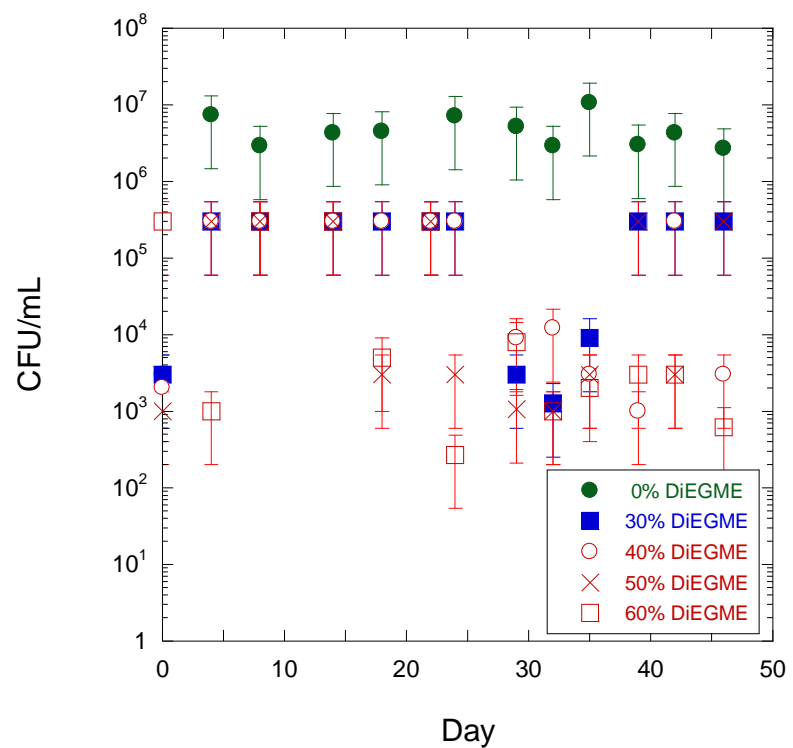


Figure 63. Semi-log plot of additional field consortia test colony counts over a 46 day test period for several DiEGME levels. DiEGME level is indicated as % volume in water phase.

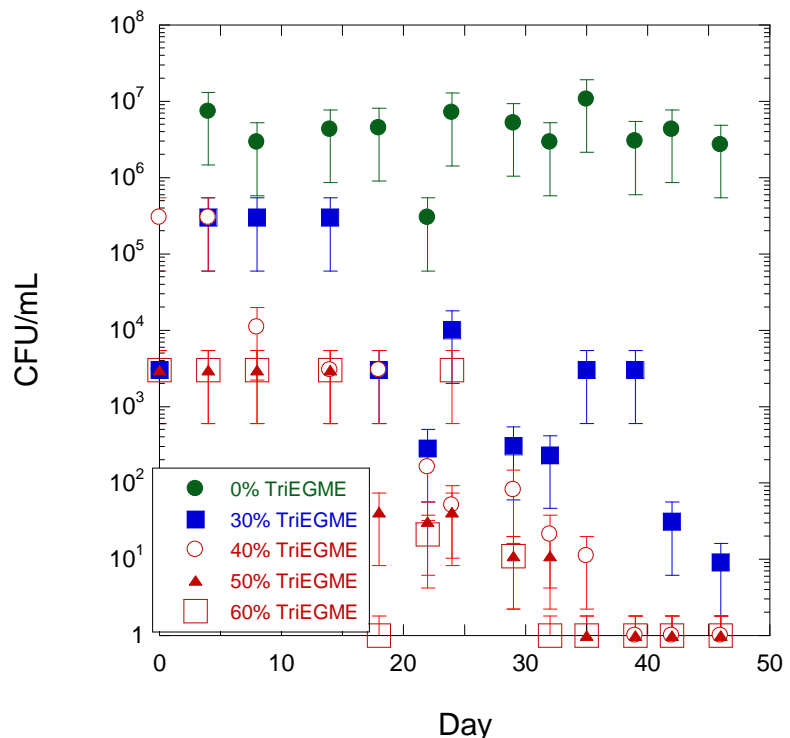


Figure 64. Semi-log plot of additional field consortia test colony counts over a 46 day test period for several TriEGME levels. TriEGME level is indicated as % volume in water phase.

Figure 63 illustrates that, over the 46 day test period, the presence of DiEGME at 30-60% decreases the amount of field consortia colonies present, but does not eliminate growth completely. Furthermore, decreases in numbers are not necessarily obtained with an increase in DiEGME concentration. Rather, the threshold seen for the original study—DiEGME present at 10% or greater in the aqueous phase—seems to provide approximately the same protection as the higher DiEGME concentrations currently present in the field (24). As Figure 64 suggests, over the 46 day test period for TriEGME the results are different at higher concentrations than they are for DiEGME. At levels of 40% and above of TriEGME, even *Bacillus* and *Clostridium* growth was eventually eliminated. This is an interesting result, as TriEGME is generally thought to be less toxic than DiEGME (31). It is possible that, since the growth at 30% was lower than before, that this result reflects experimental variation in colony growth measurements, and should be performed again to determine if the elimination of the field microbes at higher concentrations is repeatable. On the other hand, it is possible that the two microbes' resistance of DiEGME over the entire test period is a reflection of their natural or acquired resistance, one that they do not have to quite the same extent for TriEGME, though they might develop it over time.

5. Conclusions

The current study provides valuable information regarding potential effects of adding DiEGME or TriEGME to fuel systems, and it also provides a better understanding of the current role of DiEGME and TriEGME with respect to microbial contamination. This study of the biocidal/biostatic effects of TriEGME at reduced levels, similar to the levels targeted for the reduced FSII (DiEGME) program, was conducted in support of an RTOC program aimed at replacing DiEGME with TriEGME. TriEGME has preferential vapor properties that would prevent topcoat peeling problems in the B-52 and also has a partition coefficient which would make possible similar additive dosage rates compared to DiEGME. This study explored the biological impact of replacing DiEGME with TriEGME at the reduced levels expected to be implemented for DiEGME, i.e. from ~30-60% by volume in the aqueous phase to 0-30%. In this study, where field microorganisms were included, in addition to lab cultured ATCC microbes, it was found that TriEGME levels of 15% by volume in the water phase or greater were sufficient to eliminate microbial growth of all three lab cultured, ATCC microorganisms tested and were sufficient to significantly limit the growth of the field microorganisms. The results of this study suggest that DiEGME levels of 10% and above and TriEGME levels of 15% and above in the aqueous phase at ambient temperature (~0.01-0.02% in the fuel phase) are beneficial for controlling microbial growth in aircraft fuel systems. Additional tests at higher DiEGME levels suggest that even 30%-60% DiEGME in the aqueous phase did not completely eliminate field consortia growth. The field *Bacillus* and *Clostridium* strains tested were shown to be viable, even at these high concentrations. However, TriEGME levels of 40% and above were sufficient to eliminate all field microbes tested here, but only after 30-40 days of exposure. Examination of post-test liquid setups suggests that the presence of DiEGME or TriEGME can dramatically curtail active microbial growth and/or biofilm formation in fuel/water liquid samples. Overall, it appears that DiEGME or TriEGME would still act beneficially, even at reduced levels, to control microbial growth in current fuel systems. It is expected that a reduction in dosage to the minimum levels indicated would result in the same performance as is currently seen at the higher additive levels used in the field today.

6. References

1. Zobell, Claude E. Action of Microorganisms on Hydrocarbons. 1946. Scripps Institution of Oceanography. New series no. 295. vol. 10 pp. 1-49.
2. Martel, C. R. 1987. Military Jet Fuels, 1944 -1987. Summary Report AFWAL-TR-87-2062. Aero Propulsion Laboratory, Air Force Wright Aeronautical Laboratories.
3. Blanchard, G. C., and C. R. Goucher. 1965. Metabolic Products Formed By Hydrocarbon Oxidizing Microorganisms. Technical Report. Melpar Inc.
4. Finefrock, V. H., and S. A. London. 1968. Microbial Contamination of USAF JP-4 Fuels. Technical Report AFAPL-TR-68-01. Air Force Aero Propulsion Laboratory.
5. Van Hamme, Jonathan D., Singh A, Ward OP. Recent advances in petroleum microbiology. *Microbiology and molecular biology reviews* 2003, 67, 503-49.
6. Langer, G. JP-4 Fuel System Icing. Armour Research Foundation of IIT, ARF 3165-3, 1960.
7. Bakanauskas, S. 1958. Bacterial Activity in JP-4 Fuel. Technical Report WADC Technical Report 58-32. Wright Air Development Center.
8. Elderfield, R. C. Proceedings on Jet Fuel Microbiology and Corrosion Conference. Prevention of Deterioration Center, Division of Chemistry and Chemical Technology, National Academy of Sciences-National Research Council. Washington, D. C. April 6-10, 1962.
9. Finefrock, V. H., and S. A. London. 1966. Microbial Contamination of USAF JP-4 Fuels. Technical Report AFAPL-TR-66-91.
10. Gandee, G., and T. Reed. 1964. Fuel contamination and fuel system corrosion technical report SEG TDR 64-47. Systems Engineering Group, Research and Technology Division, Air Force Systems Command.
11. Rauch M. E., Graef H. W., Rozenzhak S. M., Jones S. E., Bleckmann C. A., Kruger R. L., Naik R. R., Stone M. O. 2006. Characterization of Microbial Contamination in United States Air Force Aviation Fuel Tanks. *J. of Indust. Microb. & Biotech.* (33) 1, 29-36.
12. ASTM Method D 6469. 1999. Standard Guide for Microbial Contamination in Fuels and Fuel Systems, Annual Book of ASTM Standards, vol. 05.04. ASTM, West Conshohocken, PA.
13. Neihof, R. A.; Bailey, C. A. Biocidal Properties of Anti-Icing Additives for Aircraft Fuels. *Applied and Environmental Microbiology* (1978) vol.35, no. 4, pg. 698-703.
14. Neihof, R. A., "Microbes in fuel: An Overview with a Naval Perspective," *Distillate Fuel: Contamination, Storage, and Handling*, ASTM STP 1005, H. L. Chesneau and M. M. Dorris, Eds., American Society for Testing and Materials, Philadelphia, 1988, pp. 6-14.
15. Meshako, C. E., C. A. Bleckmann, and M. N. Goltz. 1999. Biodegradability and Microbial Toxicity of Aircraft Fuel System Icing Inhibitors. *Environ. Toxicol.* **14**:383-390.
16. Westbrook, S. R. Compatability and efficacy of selected diesel fuel biocides. Proceedings of the International Conference on Stability and Handling of Liquid Fuels. Graz, Austria, September 24-29, 2000.
17. Krizovensky, J. Fuel System Icing Inhibitor: US Navy Experience. Fuel System Icing Inhibitor Workshop. 29-30 November 2000.

18. McNamara, C. J.; Perry IV, T. D.; Leard, R.; Bearce, K.; Dante, J.; Mitchell, R. Corrosion of aluminum alloy 2024 by microorganisms isolated from aircraft fuel tanks. *Biofouling*, 2005; 21 (5/6): 257-265.
19. Hill, G.; Hill, E. C.; Collins, D. J.; Anderson, S. Antimicrobial Characteristics of DiEGME in Relation to its Use Intermittently and at Sub-lethal Concentrations. Proceedings of the 9th Conference of the International Association for Stability, Handling, and Use of Liquid Fuels. September 18-22, 2005.
20. Zabarnick, S.; West, Z. J.; DeWitt, M. J.; Shafer, L. M.; Striebich, R. C.; Adams, R.; Delaney, C. L.; Phelps, D. K. Development of Alternative Fuel System Icing Inhibitor Additives that are Compatible with Aircraft Tank Topcoat Material. Proceedings of the 10th International Conference on Stability, Handling, and Use of Liquid Fuels. October 7-11, 2007.
21. DeWitt, M. J.; Zabarnick, S.; Williams, T. F.; West, Z. J.; Shafer, L. M.; Striebich, R. C.; Breitfield, S.; Delaney, C. L.; Phelps, D. K. Determination of Minimum Required FSII Dosage for Use on USAF Aircraft. Proceedings of the 10th Conference of the International Association for Stability, Handling, and Use of Liquid Fuels. October 7-11, 2007.
22. Denaro, T. R., Chelgren, S. K., Lang, J. N., Strobel, E.M., Balster, L. M. T., Vangsness, M. D. 2006. DNA Isolation of Microbial Contaminants in Aviation Turbine Fuel via Traditional Polymerase Chain Reaction (PCR) and Direct PCR—Preliminary Results. Technical Report AFRL-PR-WR-TR-2006-2049. U. S. Air Force Research Laboratory. Dayton, Ohio.
23. Westbrook, S. R.; Alexander, M. L. (1993) Compatibility and Efficacy of Biocides Qualified Under Military Specification. Fort Belvoir, VA. U.S. Army Belvoir Research, Development and Engineering Center, Interim Report BFLRF no. 282.
24. Balster, L. M., Vangsness, M. D., Bowen, L. L., Mueller, S. S., Brown, L. M., Strobel, E. M. 2010. "The Effect of DiEGME on Microbial Contamination of Jet Fuel: A Minimum Concentration Study," Technical Report AFRL-R2-WP-TR-2010-2002. U.S. Air Force Research Laboratory. Dayton, Ohio.
25. Vangsness, M.; Chelgren, S.; Strobel, E.; Balster, L.; Bowen, L.; Mueller, S. Microbial Contamination Studies in JP-8 Fueled Aircraft. Proceedings of the 10th International Conference on Stability, Handling, and Use of Liquid Fuels. October 7-11, 2007.
26. Phillips Petroleum Company. The Control of Bacterial and Fungal Growth in Jet Fuels By Use of a Fuel Additive. Research Division Report 3815-64R. Bartlesville, OK. 1964.
27. Passman, F. J. Fuel and Fuel System Microbiology: fundamentals, diagnosis, and contamination control. ASTM Manual Series: Mnl 47. ASTM International, West Conshohocken, PA. 2003.
28. Prescott, L. M.; Harley, J. P.; Klein, D. A. Microbiology. Fifth edition. McGraw Hill: New York, 2002. p. 118.
29. Amman, R. I., Ludwig, W., Schleifer, K. H. Phylogenetic Identification and In Situ Detection of Individual Microbial Cells without Cultivation. *Microbiol. Rev.* 1995;59:143-169.
30. Prescott, L. M.; Harley, J. P.; Klein, D. A. Microbiology. Fifth edition. McGraw Hill: New York, 2002. p. 246.
31. Registry of Toxic Effects of Chemical Substances, National Institute for Occupational Safety and Health, <http://www.cdc.gov/niosh/rtecs>

Appendix E. SwRI Filter-Coalescer Compatibility

INTENTIONALLY LEFT BLANK

S O U T H W E S T R E S E A R C H I N S T I T U T E ®

6220 CULEBRA RD. 78238-5166 • P.O. DRAWER 28510 78228-0510 • SAN ANTONIO, TEXAS, USA • (210) 684-5111 • WWW.SWRI.ORG

April 16, 2008

Mr. Lyle Lockwood
Universal Technology Corporation
1270 N. Fairfield Road
Dayton, OH 45432-2600

SUBJECT: Final Report for Southwest Research Institute® (SwRI®) Project No. 08.13389,
"RTOC FSII Filtration Test Plan" (S530—Task Order 008)

Dear Mr. Lockwood:

The letter report determining the impact of the replacement FSII additive (Tri-EGME) on the water separation and filterability of JP-8 and JP-8+100 with coalescer/separators and water absorbent monitors is provided below.

Background

Since the Air Force replaced JP-4 fuel with JP-8 as the standard jet fuel some aircraft, particularly the B-52, have experienced severe degradation of the tank topcoat. Extensive analysis and testing has determined the cause of the attack and subsequent peeling of the topcoat to be due to the vaporization of the Fuel System Icing Inhibitor (FSII) additive, Di-EGME, in the JP-8 when the aircraft is exposed to high ambient ground temperatures. The Di-EGME is then condensed on the exposed topcoat as the ambient ground temperature drops during the nighttime or when the aircraft is launched exposing the tank surface to cold outside air temperatures. The condensed Di-EGME absorbs in the topcoat causing it to be softened and lose its adhesion to the aluminum tank surface. This condition has resulted in fuel filter plugging and extremely high aircraft maintenance costs for the effected aircraft. So much so that the Department of Defense, through it's Reduced Total Operating Costs (RTOC) program, has allocated funds to the Air Force Research Laboratory (AFRL) to develop a replacement FSII additive which will not attack the topcoat in tanks of the B-52 and other aircraft.

In developing a replacement FSII that will not attack the topcoat in the ullage of the aircraft tank, AFRL has taken the approach of investigating additive candidates that have a lower vapor pressure than Di-EGME. Additive candidates investigated to date include Tri-EGME, Tri-EGEE, and Di-EGEE all of which have vapor pressures less than Di-EGME. However, because of its attractive partitioning coefficient, a measurement of its ability to solubilize in water and inhibit freezing of water, Tri-EGME appears to be the most attractive of the candidates to replace Di-EGME in JP-8. Also simple experiments conducted to date show that the concentration of Tri-EGME in the vapor produced upon heating fuel to the temperatures expected in the fuel tanks of



HOUSTON, TEX

215

; (301) 881-0226

Approved for public release; distribution unlimited

aircraft such as the B-52 is much less than that of Di-EGME measured under similar conditions. AFRL needs to conduct additional realistic experiments duplicating the conditions in aircraft fuel tanks to demonstrate that Tri-EGME will not attack the fuel tank topcoat, as does Di-EGME. However, the results of various icing and vaporization experiments conducted on Tri-EGME thus far are extremely encouraging. For this reason, draft test plans are being prepared to determine the impact of fuel containing Tri-EGME on the fuel's properties, aircraft components, materials performance and durability as well as on fuel filtration and water removal. While it appears at the present time that Tri-EGME is the likely candidate to replace Di-EGME, should this be proven in further experiments not to be the case, the tests plans for demonstrating fit for purpose for the replacement FSII additive will also apply to any other candidate.

Test Objective

The objective of this test program was to determine the impact of the replacement FSII additive on the water separation and filterability of JP-8 and JP-8+100. This was accomplished by making comparisons of the performance of the replacement additive with that of the same base fuel containing Di-EGME.

The following series of tests was utilized for this comparison:

- Water Reaction Interface in accordance with IP 289
- Microseparometer (MSEP) without other additive in accordance with ASTM D3948
- Single element tests in accordance with API/IP 1581, Edition 5, M+100 elements.
- Water absorbent monitors were tested using IP 1583 4th Edition monitors using only the 50-ppm water challenge and water slug test.
- Materials compatibility of JP-8 and JP-8+100 was accomplished utilizing API/IP 1581 5th Edition or IP 1583 5th Edition to compare and contrast the impacts of Di-EGME and Tri-EGME on coalescer and water monitor materials.

Test Matrix Summary

The summary of evaluations and material compatibility study performed during this research is provided below.

Filtration Testing

- Additized JP-8 w/Di-EGME - Baseline thru coalescer
- Additized JP-8+100 w/Di-EGME - Baseline thru coalescer
- Additized JP-8 w/Tri-EGME - thru coalescer
- Additized JP-8+100 w/Tri-EGME - thru coalescer
- Additized JP-8 w/Di-EGME - Baseline thru monitor
- Additized JP-8+100 w/Di-EGME - Baseline thru monitor
- Additized JP-8 w/Tri-EGME - thru monitor
- Additized JP-8+100 w/Tri-EGME - thru monitor

Materials Compatibility Testing

- Coalescer with additized JP-8 (4X Di-EGME)
- Coalescer with additized JP-8 (4X Tri-EGME)
- Coalescer with additized JP-8+100 (4X Di-EGME)
- Coalescer with additized JP-8+100 (4X Tri-EGME)
- Monitor with additized JP-8 (4X Di-EGME)
- Monitor with additized JP-8 (4X Tri-EGME)
- Monitor with additized JP-8+100 (4X Di-EGME)
- Monitor with additized JP-8+100 (4X Tri-EGME)

Test Results

Filtration Results

Velcon API/IP 1581 5th Edition M100 coalescer/separators were evaluated using API/IP 1581 5th Edition protocol for determining differences in performance between the Di- and Tri-EGME fuel system icing inhibitors. In addition to the required quantitative analysis (gravimetric and Aquaglo), on-line particle counting and turbidity analysis were included to provide additional data to support the results of this research.

Particle Counting

Gravimetric analysis determines the weight of the solids in the effluent. This method is widely used across the industry and is the standard method used in API/IP 1581. Gravimetric analysis only determines the weight of the debris – not the size and number of particles. Therefore, several large particle or several thousand smaller particles all having the same weight could be determined gravimetrically and have the same results. However, the different particle size distributions would cause different wear profiles on the hardware.

Particle counting has been used since the 1960's, mostly by the hydraulic fluid industry to determine fluid cleanliness. For the past few years, the aviation industry has begun to investigate the use of particle counting technologies to determine aviation fuel cleanliness levels. The current particle counter technology uses laser diodes to determine the contamination sizes. DEF STAN 91-91 is incorporating particle counting to determine the aviation fuel cleanliness level in conjunction with ISO 4406 - Hydraulic fluid power – Fluids – Method for coding the level of contamination by solid particles. No ISO 4406 cleanliness levels have been determined to this date, but the industry is working towards this goal.

A Parker ACM20 was used to measure the particle size distribution of the contaminant (dirt and water) passing through the test filter. The sample is obtained over a 2 minute period determining the counts per milliliter at 4-, 6-, 14-, 21-, 25-, and 30- μ m (c). The (c) associated with the particle size indicates the particle counters are calibrated to ISO 11171.

The particle count data allows the users to better understand the size and distribution of the contaminant. In this research, it provides an excellent tool for comparing the operational effects of the various additives to determine if they perform the same or if there are any adverse effects.

Turbidity

A Sigrist DualScat in-line turbidimeter with a dual-angle measurement sensor head was utilized to measure the turbidity of the effluent test fuel. Turbidity is the cloudiness or haziness of a fluid caused by individual particles that are generally invisible to the human eye. This technology is typically used in the water purification and beverage industry to measure the clarity of the fluids. The sensor measured the turbidity at 25° and 90°.

A property of the dirt and water contamination—that they will scatter a light beam focused on them—is considered a meaningful measurement of turbidity in a fluid. Turbidity measured this way uses an instrument called a nephelometer with the detector setup to the side of the light beam. More light reaches the detector if there are lots of small particles scattering the source beam than if there are few. The units of turbidity from a calibrated nephelometer are referred to as Nephelometric Turbidity Units (NTU). How much light reflects for a given quantity of contamination is dependent upon the properties of the contamination like their shape, color, size, and reflectivity. For this reason, a correlation between turbidity and total suspended solids or total water content is unique for each location and situation. This lack of correlation is shown in the turbidity data once the turbidity values approached approximately 1 NTU. For this application, the 25° reading is thought to represent water contamination, while the 90° reading is thought to represent solid or dirt contamination. However, this is not always the case.

Coalescer/Separators

Four API/IP 1581 5th Edition evaluations were performed to determine if the Tri-EGME fuel system icing inhibitor (FSII) performed the same or better than the currently used Di-EGME FSII. Both types of FSII were used in JP-8 and JP-8+100 types of aviation fuel. The data sheets for each evaluation are shown in the Appendix.

The differential pressure for all four evaluations is shown in Figure 1. The two fuel evaluations containing Tri-EGME FSII are bracketed by the two fuel evaluations containing Di-EGME FSII.

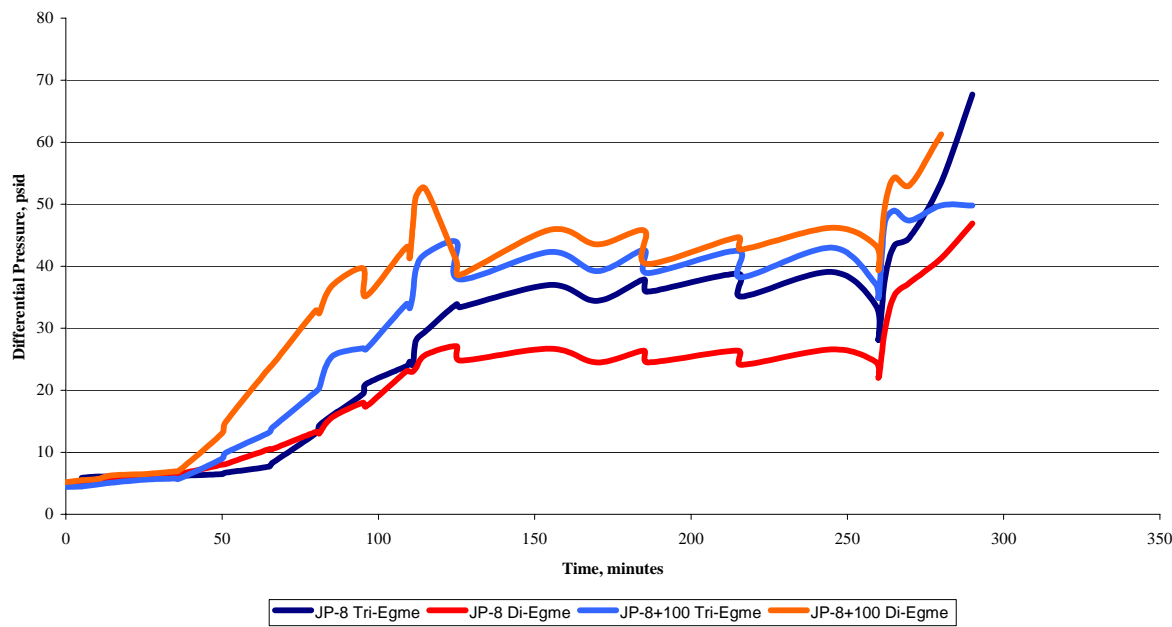


Figure 1. API/IP 1581 5th Edition – Differential Pressure

Figures 2 and 3 presents the effluent water content by Aqua-glo for JP-8 and JP-8+100 respectively. The JP-8 with Tri-EGME water contents is higher than those with Di-EGME during the 100-ppm water challenge (approximately 125 to 250 minutes). However, the effluent water content with the JP-8 with Tri-EGME for the first 20 minutes of the 3% water challenge is significantly better than the JP-8 with Di-EGME.

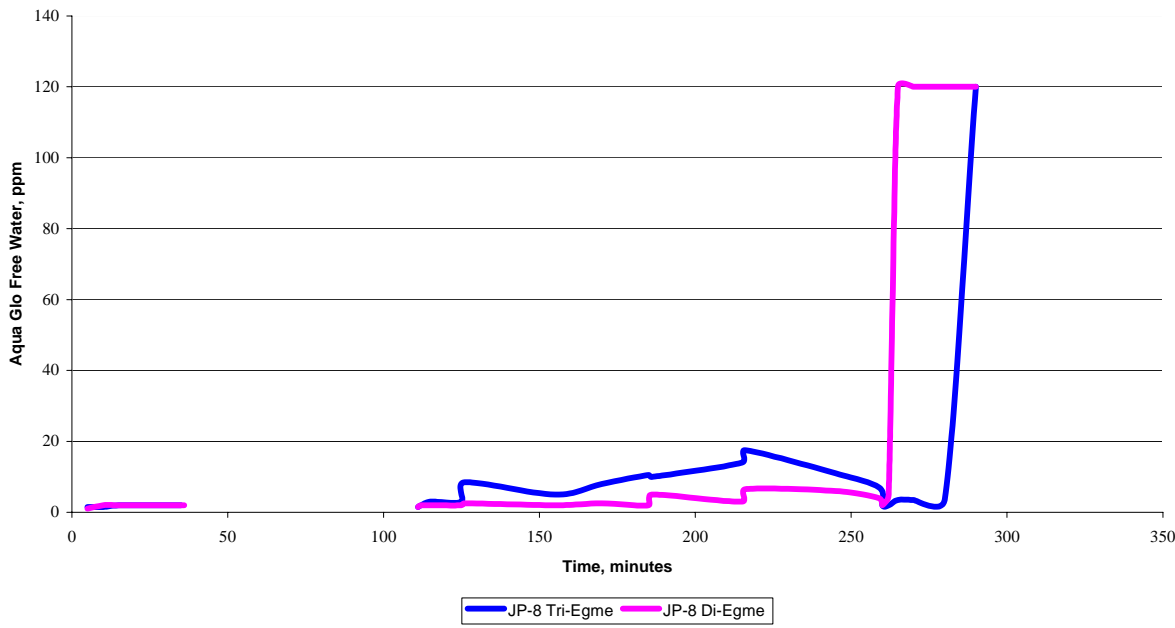


Figure 2. API/IP 581 5th Edition – JP-8 – Aqua glo Water Content

The effluent water contents for the JP-8+100 with Tri-EGME are below the 15 ppm limit set in API/IP 1581 5th Edition, whereas the water content with JP-8+100 with Di-EGME are significantly exceed this specification.

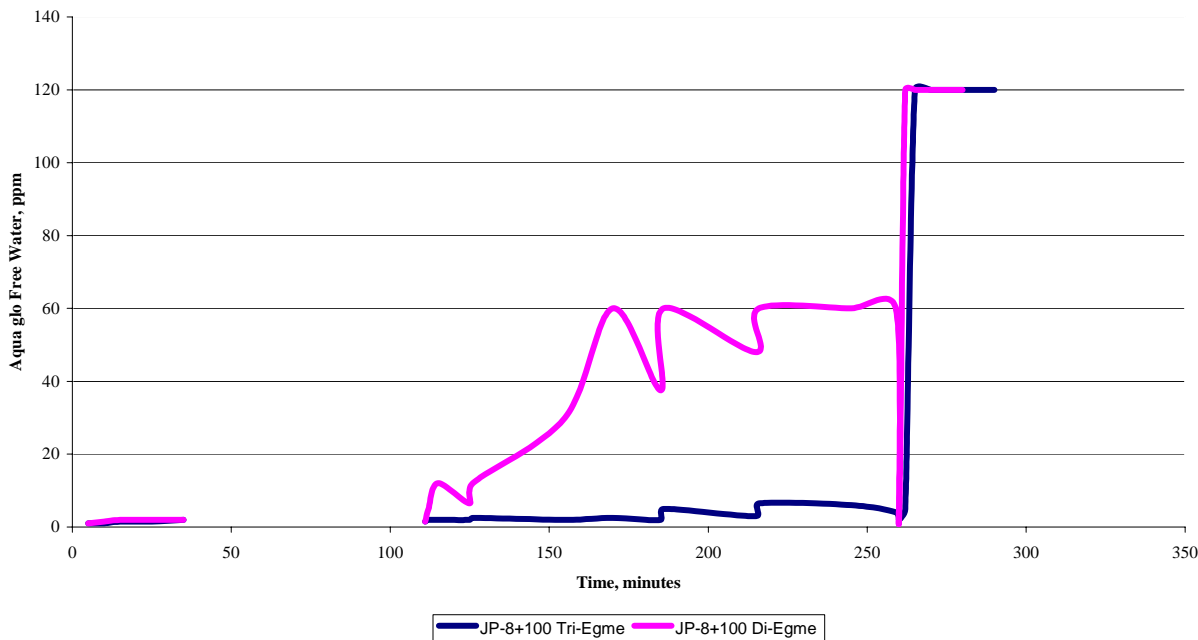


Figure 3. API/IP 581 5th Edition – JP-8+100 – Aqua glo Water Content

The solid content for most of the gravimetric readings was less than 0.26 mg/L – the maximum gravimetric solids content per API/IP 1581 5th Edition. Readings exceeding this value were measured with both the JP-8+100 with Di-EGME and Tri-EGME – 0.525 and 0.5 mg/L – respectively.

These results do not indicate any significant difference in performance based upon the aqua-glo or gravimetric solids results.

The particle count data in Figures 4-7 further illustrates the similarity in performance between the two fuels system icing inhibitors. The particle data for the JP-8 Di-EGME evaluation shows lower counts at the beginning of the evaluation when compared to the JP-8 Tri-EGME evaluation. However, towards the end of the test, the particle counts are very similar for both fuels. Comparing the particle count data for both JP-8+100 fuels, the particle count data is almost identical.

The turbidity data, Figures 8-11, further substantiate that there is little or no difference in performance between JP-8 and JP-8+100 fuels containing Di-EGME or Tri-EGME fuel system icing inhibitor.

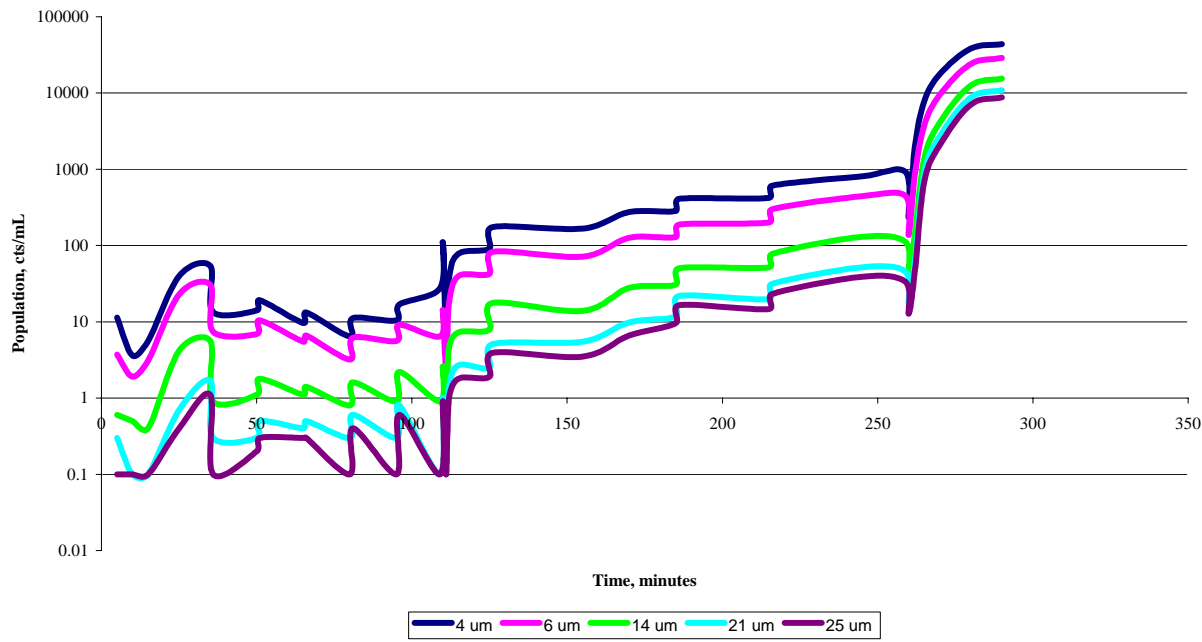


Figure 4. JP-8 – Di-EGME – Particle Counts

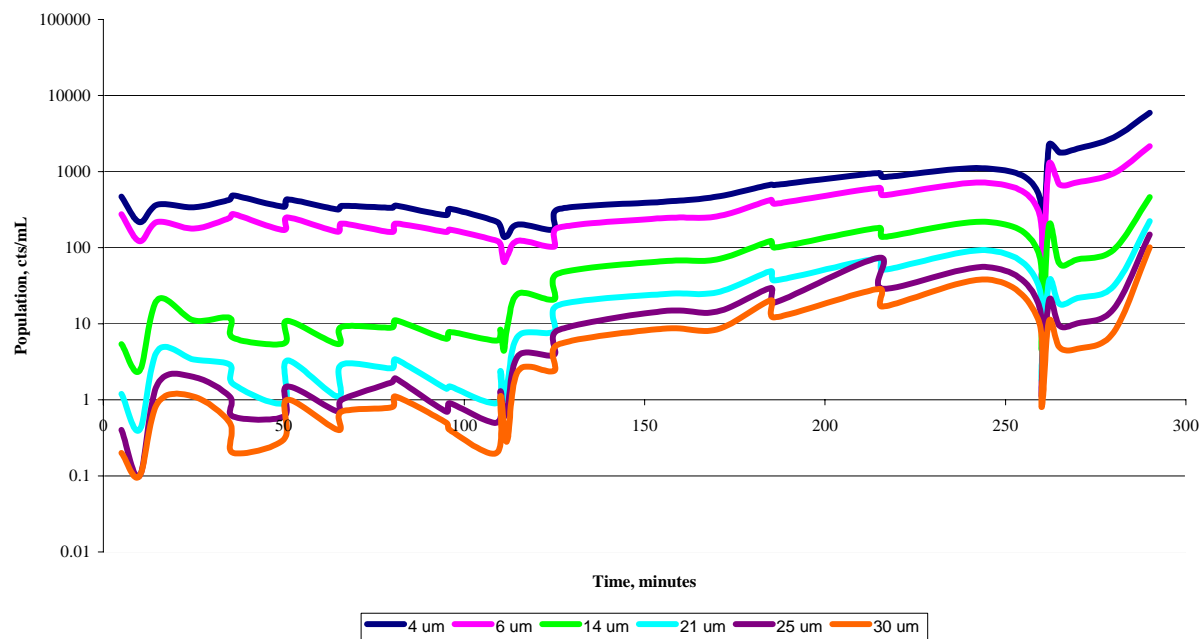


Figure 5. JP-8 – Tri-EGME – Particle Counts

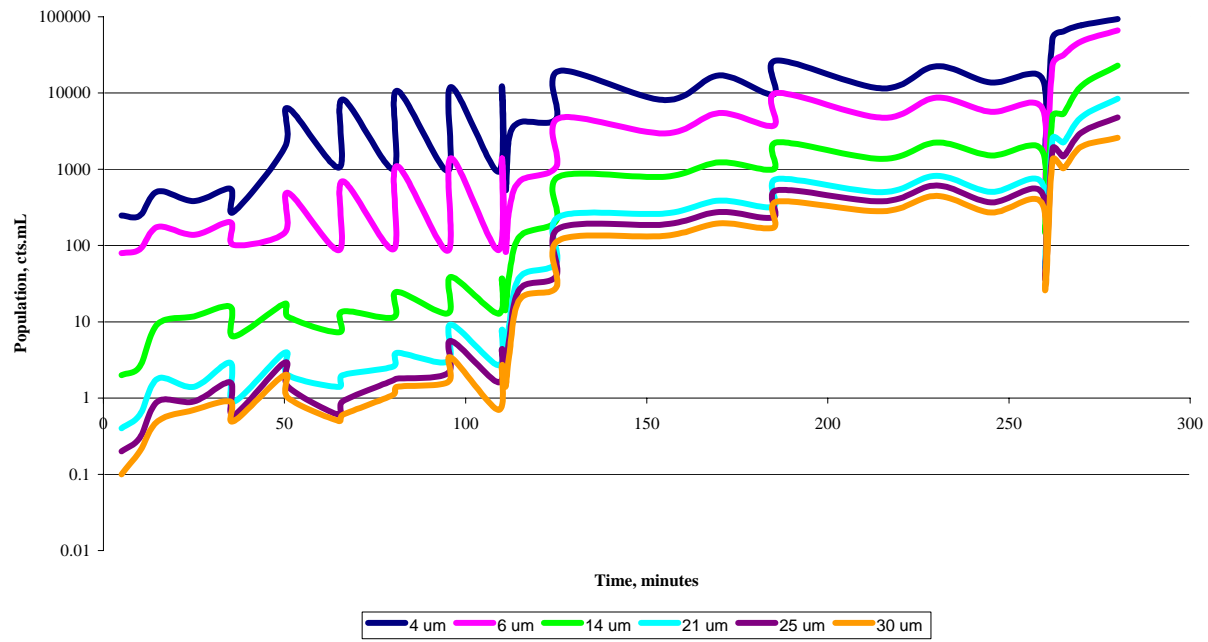


Figure 6. JP-8+100 – Di-EGME – Particle Counts

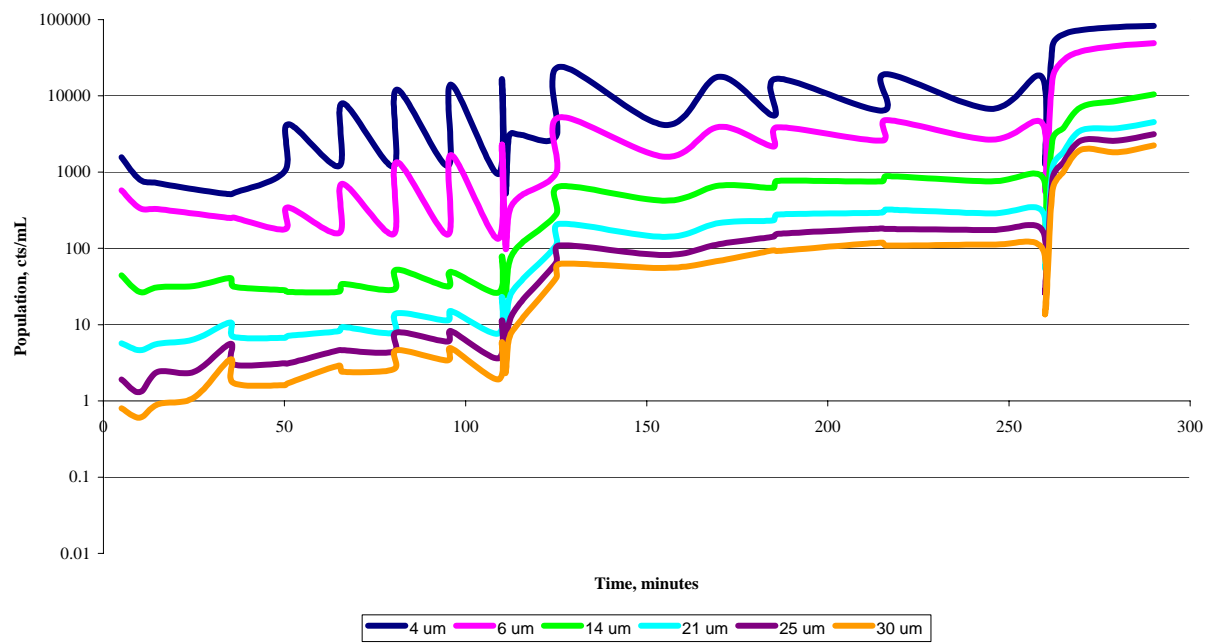


Figure 7. JP-8+100 – Tri-EGME – Particle Counts

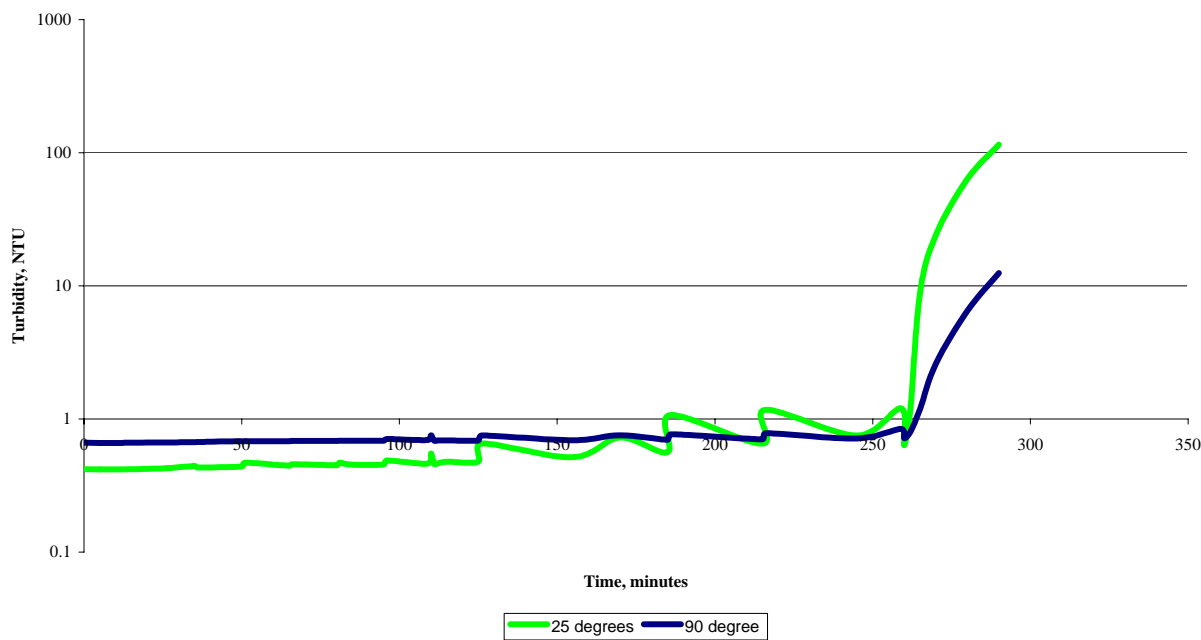


Figure 8. JP-8 – Di-EGME – Turbidity

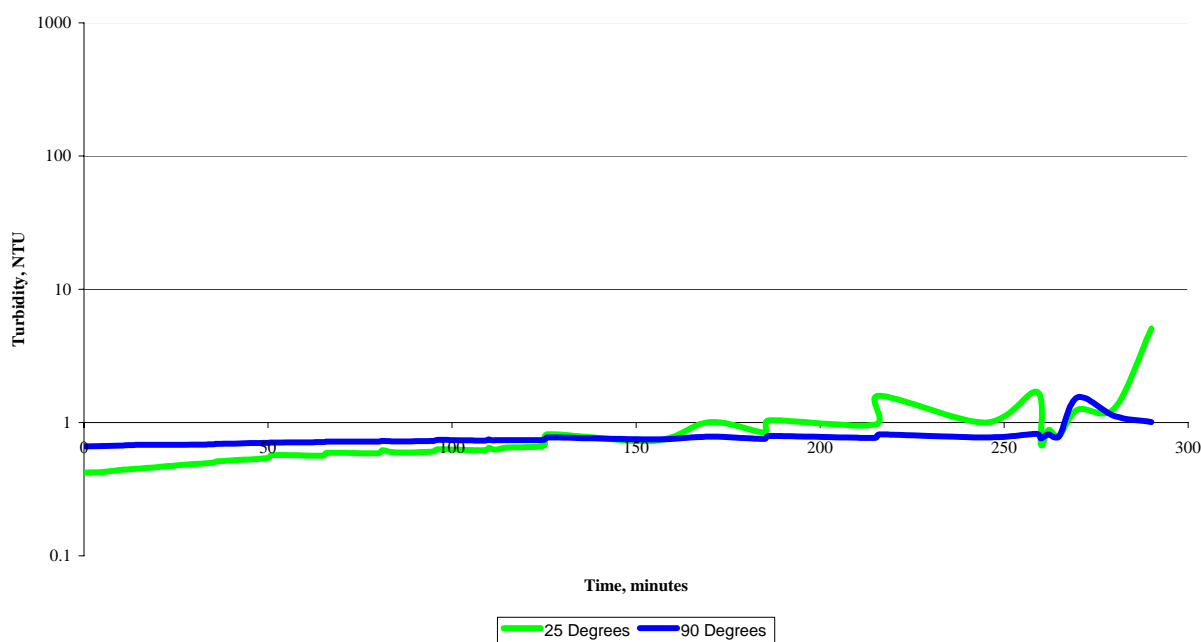


Figure 9. JP-8 – Tri-EGME – Turbidity

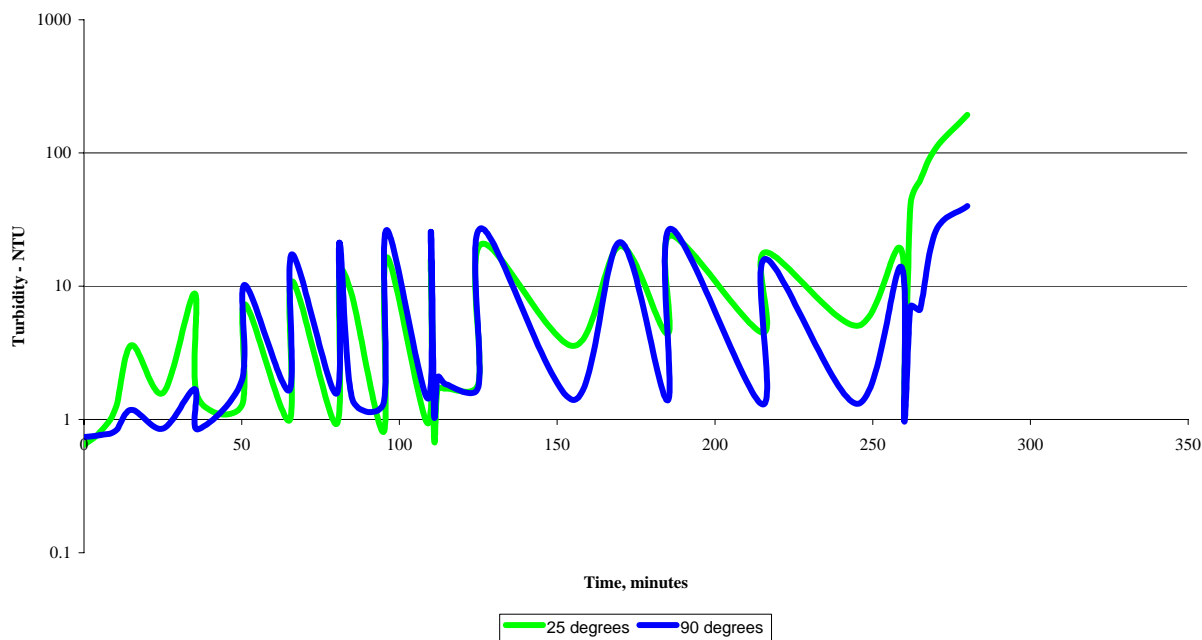


Figure 10. JP-8+100 – Di-EGME – Turbidity

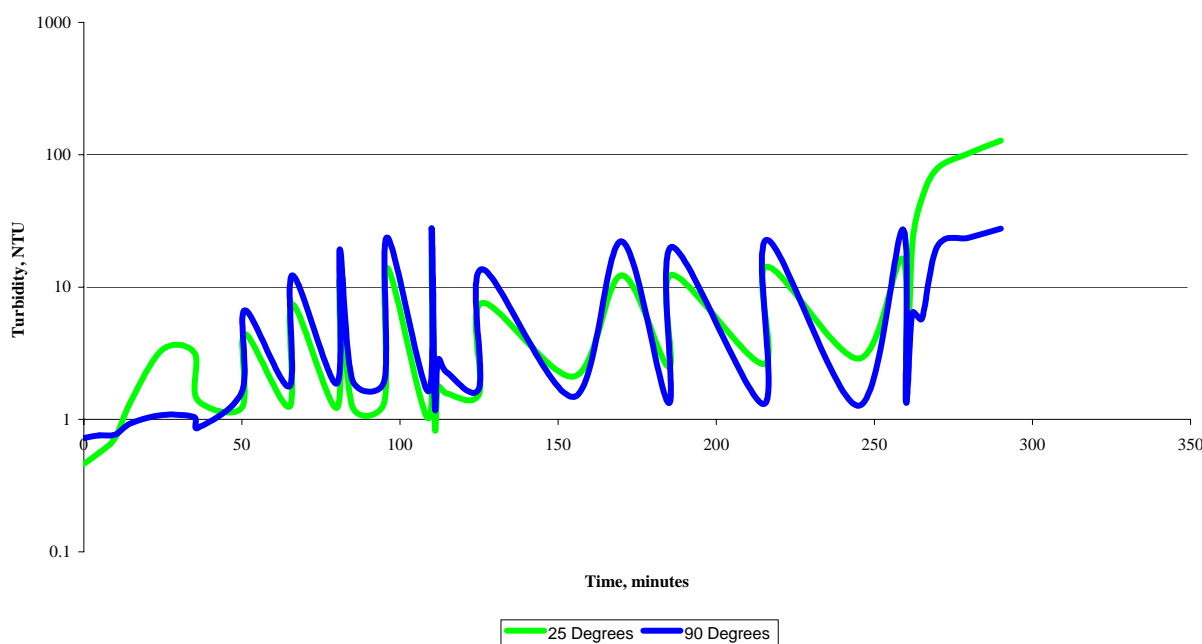


Figure 11. JP-8+100 – Tri-EGME – Turbidity

Based on the API/IP 1581 5th Edition results, in conjunction with the support data from the particle counting and turbidity measurements, there is no apparent difference in performance between fuels containing Di-EGME and Tri-EGME fuel system icing inhibitors.

Water Absorbent Monitors

While the Air Force no longer uses water monitors, monitors continue to be used in commercial sector, including use by many DESC Into-Plane contractors supporting military aircraft. Therefore, evaluations were performed using the same fuel chemistries as above with water absorbent monitors per API/IP 1583. Only the 50-ppm water challenge and the water slug evaluation were performed with each test fuel. Velcon API/IP 1583 4th Edition monitors were utilized for this analysis.

Figures 12 and 13 illustrate the poor performance of monitors when exposed to fuel containing FSII. Jet A was performed as a baseline to illustrate how the monitor should perform as designed. Although none of the evaluated fuels containing FSII had acceptable water removal performance, in this case, the Tri-EGME appears to have more detrimental effect on monitor performance than the fuels containing Di-EGME.

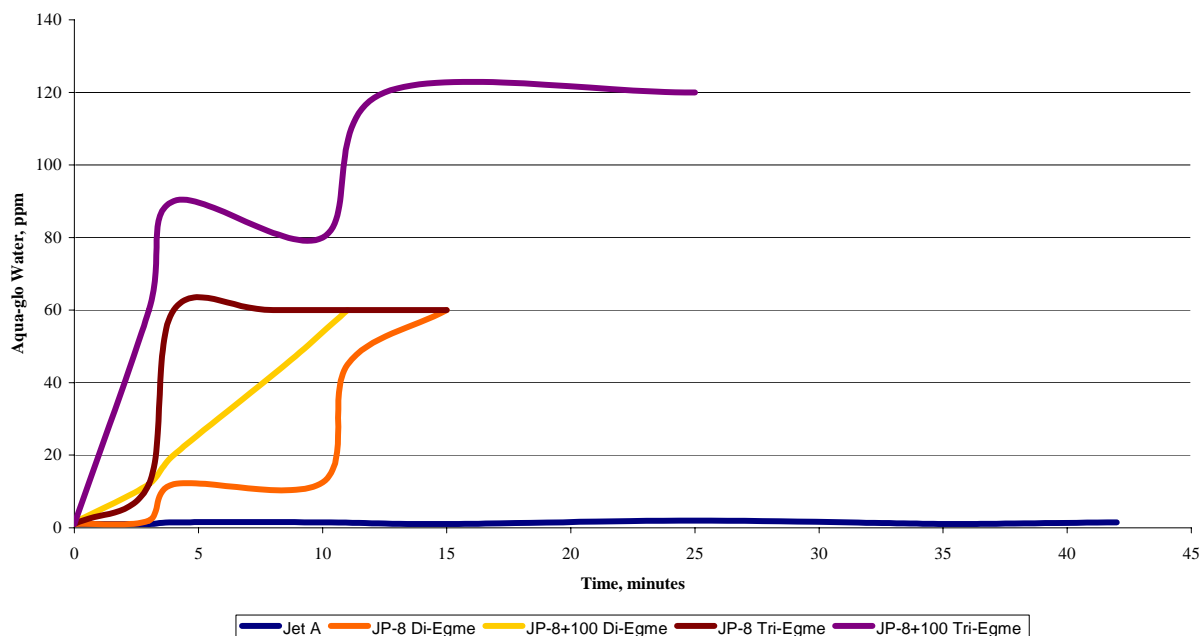


Figure 12. API/IP 1583 50-ppm Water Challenge

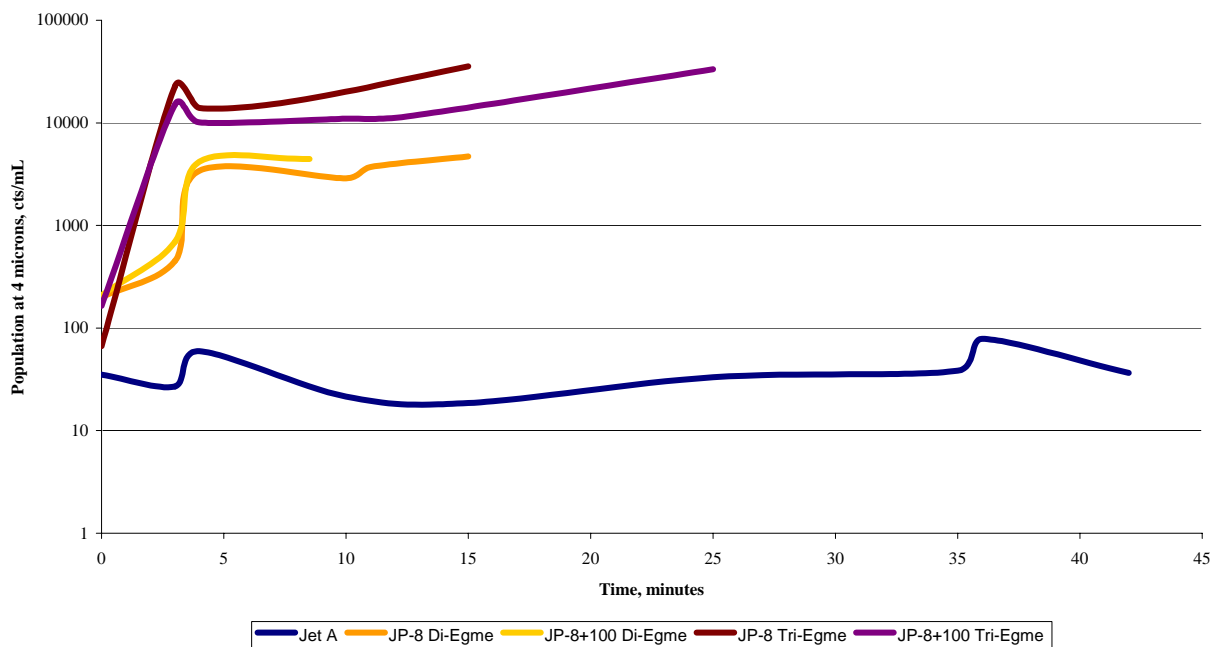


Figure 13. API/IP 1583 50 ppm Water Challenge – Particle Counts at 4- μ m (c)

The API/IP water slug results are shown in Tables 1-5. All of the results pass the requirements of less than 1% of the rated flow (30 gpm).

Table 1. API/IP 1583 Water Slug – Jet A

Time, minutes	Water Slug Leakage, mL
1	0
2	0
3	0
4	0
5	0

Table 2. API/IP 1583 Water Slug – JP-8 Di-EGME

Time, minutes	Water Slug Leakage, mL
1	38
2	2
3	1
4	1
5	34

Table 3. API/IP 1583 Water Slug – JP-8 +100 Di-EGME

Time, minutes	Water Slug Leakage, mL
1	1
2	10.5
3	3.5
4	28
5	13

Table 4. API/IP 1583 Water Slug – JP-8 Tri-EGME

Time, minutes	Water Slug Leakage, mL
1	3
2	20
3	28
4	25
5	32

Table 5. API/IP 1583 Water Slug – JP-8+100 Tri-EGME

Time, minutes	Water Slug Leakage, mL
1	8
2	3
3	11
4	46
5	11

Material Compatibility Results

The material compatibility analysis was performed using Velcon API/IP 1581 5th Edition M100 coalescer/separators and API/IP 1583 water absorbent monitors. Both sets of filters were exposed to the fuel matrix shown in Table 6.

Table 6. Material Compatibility Fuel Matrix

Filter Type	Fuel	Fuel System Icing Inhibitor (FSII)
Coalescer	JP-8	4X Di-EGME
Coalescer	JP-8	4X Tri-EGME
Coalescer	JP-8+100	4X Di-EGME
Coalescer	JP-8+100	4X Tri-EGME
Water Absorbent Monitor	JP-8	4X Di-EGME
Water Absorbent Monitor	JP-8	4X Tri-EGME
Water Absorbent Monitor	JP-8+100	4X Di-EGME
Water Absorbent Monitor	JP-8+100	4X Tri-EGME

The JP-8 and JP-8+100 fuel chemistry was composed of 2 mg/L of static dissipater (SDA), 15 mg/L of corrosion inhibitor (DCI4A), 0.15 vol% fuel system icing inhibitor (FSII), and 256 mg/L of the +100 Spec Aid 8Q462 (for JP-8+100 fuels only).

All elements were visually evaluated prior to storage in the test fuels containing 4 times the normal concentration of only the FSII. The test elements were stored for 336 hours at ambient conditions, visually inspected, stored for an additional 336 hours in fresh test fuel, and final visual inspection upon completion of the storage time. None of the elements exhibited deformation, swelling, or attack of the adhesive materials. The examples presented below, Figures 14–15, illustrate how all of the test elements appeared after completion of the material compatibility test.



Figure 14. Coalescer/Separator Material Compatibility – End of Test

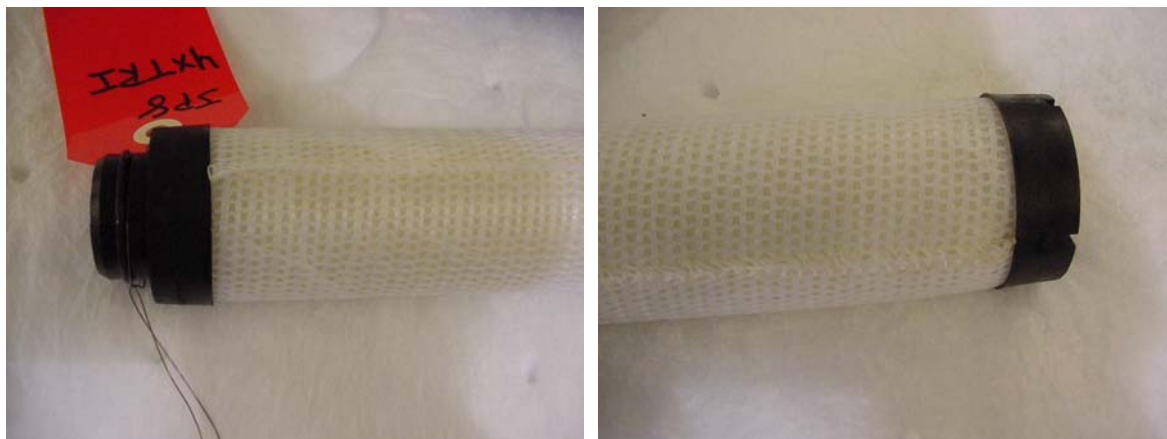


Figure 15. Water Absorbent Monitor Material Compatibility – End of Test

The existent gum content of the fuel before and after the storage is shown in Table 7. These results are fairly scattered but typically illustrate lower values with fuels containing Tri-EGME versus Di-EGME.

Table 7. Material Compatibility – Existence Gum

Sample	Existence Gum – Before, mg/100 mL	Existence Gum – 336 hrs, mg/100 mL	Existence Gum – End of Test, mg/100 mL
Jet A	5.6	6.0	5.8
JP-8 Di-EGME	12.2	22.0	17.6
JP-8 Tri-EGME	9.8	19.6	16.7
JP-8 Di-EGME F/W	12.6	42.8	41.2
JP-8 Tri-EGME F/W	9.8	10.4	10.0
JP-8 Di-EGME Monitor	12.4	31.6	31.4
JP-8 Tri-EGME Monitor	9.9	29.2	28.6
JP-8+100 Di-EGME	8.2	16.6	17.6
JP-8+100 Tri-EGME	7.8	14.6	15.7
JP-8+100 Di-EGME F/W	8.6	32.4	31.2
JP-8+100 Tri-EGME F/W	7.7	12.4	13.7
JP-8+100 Di-EGME Monitor	8.8	21.6	29.8
JP-8+100 Tri-EGME Monitor	7.9	16.5	28.6

The MSEP, interfacial tension (IFT), Saybolt color, and water reaction results are shown in Table 8. As with the previous data, the fuels containing Tri-EGME have similar or better values when compared to the fuels containing Di-EGME.

Table 8. Test Fuel Properties

Sample	MSEP	IFT, mN/m	Color	Appearance	Interface
Jet A	97	44.04	-12	1	1
JP-8 Di-EGME	0	35.95	-8	2	2
JP-8 Tri-EGME	40	32.90	-12	3	2
JP-8 Di-EGME F/W	0	23.28	-9	2	2
JP-8 Tri-EGME F/W	51	23.20	-12	2	3
JP-8 Di-EGME Monitor	0	21.44	-13	2	1b
JP-8 Tri-EGME Monitor	0	23.65	-12	3	4
JP-8+100 Di-EGME	0	36.45	-10	2	2
JP-8+100 Tri-EGME	0	34.56	-12	2	2
JP-8+100 Di-EGME F/W	0	21.68	-11	2	2
JP-8+100 Tri-EGME F/W	0	24.20	-13	2	2
JP-8+100 Di-EGME Monitor	0	23.04	-12	2	2
JP-8+100 Tri-EGME Monitor	0	24.56	-12	2	2

Conclusions

A variety of filtration and fuel property evaluations were performed on JP-8 and JP-8+100 fuels containing Di-EGME and Tri-EGME fuel system icing inhibitors. Both the gravimetric and water results for the API/IP 1581 5th Edition evaluations suggest there is no difference in performance between the two fuel system icing inhibitors. Additional particle counting and turbidity measurements agree with the gravimetric and standard water measurements.

The API/IP 1583 evaluations substantiated the poor performance of water absorbent monitors in fuels containing FSII. All fuels containing FSII performed poorly with the fuels containing Tri-EGME performing worse than the fuels containing Di-EGME. For the water slug evaluations, all fuels (even those containing FSII) passed with less than 1% of the rated flow passing through the monitor.

The material compatibility evaluations show no indications of compatibility issues up to 4X the concentration of the FSII. The resultant fuel properties were similar between the di- and Tri-EGME fuels.

As a result of the accumulated data comparing Di-EGME and Tri-EGME performance and physical properties, there is no indication there is any difference in performance.

If you have any questions, please contact me at 210-522-6941 or gbessee@swri.org.

Sincerely,



Gary B. Bessee, Manager
Fluids Filtration and Handling Research

Approved by:



Steven D. Marty, P.E., Director
Fuels & Lubricants Technology Department

GBB/rae
r:\working\13389\Final
Attachment [Appendix]
cc (via e-mail): M. Puterbaugh (UTC)
J. Klein (UTC)
S. Marty (SwRI)

This report must be reproduced in full, unless SwRI approves a summary or abridgement.

5th Edition Single Element Data Sheet

JP-8 Tri-EGME

Test Specification: API/IP 1581 5th Edition		SET: <input checked="" type="checkbox"/>							Date: 11/1/07					
Test No. 87		Full-Scale: <input type="checkbox"/>												
Vessel:		Filter/Coalescer: Velcon			Separator: Velcon			Type: <input checked="" type="checkbox"/> -S - <input type="checkbox"/> D						
Additive Addition		Model: I-614A4TB			Model: SO-606C			Manufacturing Date:						
Category:		M-100 <input type="checkbox"/>		M <input checked="" type="checkbox"/>		C <input type="checkbox"/>								
Tank Volume	Gallons	Additive	Conc. (Mg/L)	Amount Added	k (pS/m)	Additive	Conc. (Mg/L)	Amount Added	k (pS/m)	Additive	Conc. (Mg/L)	Amount Added	k (pS/m)	
Beginning		A	256			D	2,0	111.9 g		I	1,0			
Ending		B	0,15%			B	0,15%	22.17 gal		II	15			
Used		C	15			C	15	839.13 g						
Mixing Time: 40 minutes							MSEP	IFT						
Element Conditioning:		<input checked="" type="checkbox"/> in-Situ		<input type="checkbox"/> External				0	37.28					
Phase	Cum. Test Time (minutes)	Time (minutes)	Fuel Flow Rate (gpm)	ΔP (psid)	k (pS/m)	Water Flow Rate mL/min	Water Concent. (ppm)	Solids Rate <input checked="" type="checkbox"/> mg/L <input type="checkbox"/> mg/gal	Filter Sample ID	Solids Concent. Affluent (mg/L)	Turbidity, 25 Degrees	Turbidity, 90 Degrees	Temp <input type="checkbox"/> °C <input checked="" type="checkbox"/> °F	
Start-up	0	0	0	0	760/586	0	0			0.421	0.663	71		
Water 0,01%	5	0	33.9	5.9	769/625	13	1.5			0.425	0.666			
	10	5	34.2	6.1		13	1.5			0.442	0.672			
	15	10 s/s	34.2	6.1		13	2			0.452	0.68			
	25	20 s/s	34.2	6.3		13	2			0.476	0.681	71		
	35	30 s/s	34.2	6.3	793/721	13	2			0.5	0.686	71		
Notes/Comments:														

Phase	Cum. Test Time (minutes)	Time (minutes)	Fuel Flow Rate (gpm)	ΔP (psid)	k (pS/m)	Water Flow Rate mL/min	Water gpm	Concent. (ppm)	Solids	Filter Sample ID	Solids Concent. Affluent (mg/L)	Turbidity, 25 Degrees	Turbidity, 90 Degrees	Temp
						<input checked="" type="checkbox"/>	<input type="checkbox"/>		<input type="checkbox"/> Rate <input type="checkbox"/> mg/L <input type="checkbox"/> mg/gal					<input type="checkbox"/> °C <input checked="" type="checkbox"/> °F
Solids Holding Test (Continued until reaching 115 kPa (22.5 psid))	35	0	33.9	6.2	799/739				19	1	0	0.511	0.691	71
	50	15	33.9	6.5					19	2	0.275	0.542	0.704	
		15 s/s	34	6.7					19	3	0.025	0.571	0.708	
	65	30	33.9	7.7	806/745				19	4	0	0.564	0.712	71
		30 s/s	33.9	8.3					19	5	0	0.594	0.718	
	80	45	34	13.1					19	6	0.05	0.587	0.719	
		45 s/s	33.9	14.3					19	7	0	0.62	0.729	
	85	50	34.2	15.9								0.596	0.723	
	95	60	34.2	19.4	804/760				19	8	0	0.606	0.727	71
		60 s/s	34.1	21					19	9	0.05	0.631	0.742	
	110	75	34.1	23.9					19	10	0.075	0.618	0.732	
		75 s/s	34	24.6					19	11	0	0.645	0.749	
Notes/Comments:														

Phase	Cum. Test Time (minutes)	Time (minutes)	Fuel Flow Rate (gpm)	ΔP (psid)	k (pS/m)	Water Flow Rate mL/min □	Water Concent. (ppm)	Solids Rate mg/L □ mg/gal	Filter Sample ID	Solids Concent. Affluent (mg/L)	Turbidity, 25 Degrees	Turbidity, 90 Degrees	Temp □ °C ■ °F
Water Coalescence Test - 0.01%	110	0	33.9	24.1	813/785	0	1.5				0.629	0.736	72
	112	2	33.7	28		13	2				0.627	0.738	
	115	5	33.8	29.5		13	3				0.648	0.739	
	125	15	34.1	33.9	820/778	13	3				0.673	0.741	72
		30 s/s	34.2	33.4		13	8.5				0.817	0.775	
	155	45	33.9	37		13	5				0.729	0.747	
	170	60 s/s	34.2	34.4	820/795	13	8				1.01	0.785	
	185	75	33.9	37.9		13	10.5				0.841	0.755	73
		90 s/s	34.2	35.9		13	10				1.04	0.793	
	215	105	33.8	38.8	814/806	13	14				0.967	0.767	
		120 s/s	33.9	35.1		13	17.5				1.59	0.815	
	245	135	33.9	39.1		13	11				1	0.772	
		150 s/s	34.2	33.8		13	7				1.7	0.823	
	260	0	34.1	28.2	813/790	0	2				0.686	0.76	74
Water Coalescence Test - 3%	262	2	33.8	37.9		3.9 lpm	2				0.879	0.816	
	265	5	33.9	43.3		3.9 lpm	3.5				0.796	0.789	
		10 s/s	34.6	44.7	815/796	3.9 lpm	3.5				1.25	1.55	
		20 s/s	35	53.5		3.9 lpm	3.5				1.28	1.12	
	290	30	34	67.7		3.9 lpm	>120				5.06	1.01	75

Notes/Comments:

5th Edition Single Element Data Sheet

JP-8 Di-EGME

Test Specification: API/IP 1581 5th Edition			SET: <input checked="" type="checkbox"/>							Date: 11/7/07			
Test No. 88			Full-Scale: <input type="checkbox"/>										
Vessel:			Filter/Coalescer: Velcon			Separator: Velcon			Type: <input checked="" type="checkbox"/> -S - <input type="checkbox"/> D				
Additive Addition			Model: I-614A4TB			Model: SO-606C			Manufacturing Date:				
Category:		M-100 <input type="checkbox"/>				M <input checked="" type="checkbox"/>				C <input type="checkbox"/>			
Tank Volume	Gallons	Additive	Conc. (Mg/L)	Amount Added	k (pS/m)	Additive	Conc. (Mg/L)	Amount Added	k (pS/m)	Additive	Conc. (Mg/L)	Amount Added	k (pS/m)
Beginning		A	256			D	2,0	116.9 g		I	1,0		
Ending		B	0,15%			B	0,15%	23.2 gal		II	15		
Used		C	15			C	15	876.6 g					
Mixing Time: 35 minutes							MSEP	IFT					
Element Conditioning:		<input checked="" type="checkbox"/> in-Situ	<input type="checkbox"/> External				0	35.93					
Phase	Cum. Test Time (minutes)	Time (minutes)	Fuel Flow Rate (gpm)	ΔP (psid)	k (pS/m)	Water Flow Rate mL/min	Water Concent. (ppm)	Solids Rate <input type="checkbox"/> mg/L <input checked="" type="checkbox"/> mg/gal	Filter Sample ID	Solids Concent. Affluent (mg/L)	Turbidity, 25 Degrees	Turbidity, 90 Degrees	Temp <input type="checkbox"/> °C <input checked="" type="checkbox"/> °F
Start-up	0	0	34.2	4.9	878/577	0	0			0.419	0.662	72	
Water 0,01%	5	0	34	5.1	857/696	13	1			0.418	0.661		
	10	5	34.1	5.4		13	1			0.417	0.661		
	15	10 s/s	34	5.7		13	1.5			0.42	0.663		
	25	20 s/s	33.9	6.3		13	1.5			0.425	0.665	71	
	35	30 s/s	33.8	6.5	886/789	13	2			0.443	0.67	71	
Notes/Comments:													

Phase	Cum. Test Time (minutes)	Time (minutes)	Fuel Flow Rate (gpm)	ΔP (psid)	k (pS/m)	Water Flow Rate mL/min █ □	Water Concent. (ppm)	Solids Rate █ mg/L □ mg/gal	Filter Sample ID	Solids Concent. Affluent (mg/L)	Turbidity, 25 Degrees	Turbidity, 90 Degrees	Temp □ °C █ °F
Solids Holding Test (Continued until reaching 115 kPa (22.5 psid))	35	0	34.1	6.5	893/806				1	0.075	0.432	0.672	71
	50	15	34	8				19	2	0	0.44	0.68	
		15 s/s	33.9	8.1				19	3	0	0.468	0.681	
	65	30	33.9	10.5	858/827			19	4	0	0.445	0.681	71
		30 s/s	33.9	10.5				19	5	0.025	0.457	0.682	
	80	45	33.9	13.3				19	6	0.025	0.449	0.683	
		45 s/s	34.2	13				19	7	0.025	0.468	0.685	
	85	50	34.2	15.6							0.453	0.686	
	95	60	34.1	18	898/848			19	8	0	0.455	0.686	71
		60 s/s	34.2	17.4				19	9	0.025	0.488	0.706	
	110	75	33.9	23.1				19	10	0	0.463	0.695	
		75 s/s	34	23				19	11	0.05	0.55	0.753	
Notes/Comments:													

Phase	Cum. Test Time (minutes)	Time (minutes)	Fuel Flow Rate (gpm)	ΔP (psid)	k (pS/m)	Water Flow Rate mL/min ■ □	Water Concent. (ppm)	Solids Rate □ mg/L □ mg/gal	Filter Sample ID	Solids Concent. Affluent (mg/L)	Turbidity, 25 Degrees	Turbidity, 90 Degrees	Temp □ °C ■ °F
Water Coalescence Test - 0.01%	110	0	34.2	23	901/863	0 ■	1.5			0.459	0.686	71	
	112	2	34	23.6		13 □	2			0.462	0.688		
	115	5	34.1	25.7		13 □	2			0.477	0.688		
	125	15	34	27.1	907/856	13 □	2			0.479	0.688	71	
		30 s/s	34.3	24.8		13 □	2.5			0.656	0.752		
	155	45	34.2	26.7		13 □	2			0.515	0.692		
	170	60 s/s	34	24.5	905/856	13 □	2.5			0.725	0.755		
	185	75	34	26.4		13 □	2			0.564	0.698	71	
		90 s/s	34.2	24.5		13 □	5			1.07	0.767		
	215	105	34	26.4	913/873	13 □	3			0.653	0.704		
		120 s/s	34.2	24.1		13 □	6.5			1.17	0.781		
	245	135	34.1	26.6		13 □	6			0.752	0.712		
		150 s/s	34	24.6		13 □	4			1.2	0.841		
	260	0	33.8	22.1	905/865	0 ■	2			0.634	0.715	69	
Water Coalescence Test - 3%	262	2	32.9	29.6		3.9 lpm □	5			1.22	0.804		
	265	5	33.9	35.2		3.9 lpm □	>120			8.72	1.18		
		10 s/s	34.5	37.4	907/838	3.9 lpm □	>120			24	2.6		
		20 s/s	33.6	41.3		3.9 lpm □	>120			63.5	6.5		
	290	30	33.8	46.9		3.9 lpm □	>120			115	12.5	69	

Notes/Comments:

5th Edition Single Element Data Sheet

JP-8+100 Tri-EGME

Test Specification: API/IP 1581 5th Edition		SET: <input checked="" type="checkbox"/>							Date: 11/14/07				
Test No. 89		Full-Scale: <input type="checkbox"/>											
Vessel:		Filter/Coalescer: Velcon				Separator: Velcon				Type: <input checked="" type="checkbox"/> -S - <input type="checkbox"/> D			
Additive Addition		Model: I-614A4TB				Model: SO-606C				Manufacturing Date:			
Category:		M-100 <input type="checkbox"/>				M <input checked="" type="checkbox"/>				C <input type="checkbox"/>			
Tank Volume	Gallons	Additive	Conc. (Mg/L)	Amount Added	k (pS/m)	Additive	Conc. (Mg/L)	Amount Added	k (pS/m)	Additive	Conc. (Mg/L)	Amount Added	k (pS/m)
Beginning		A	256	13,759 g		D	2,0			I	1,0		
Ending		B	0,15%	21.3 gal		B	0,15%			II	15		
Used		C	15	806.2 g		C	15						
Mixing Time: 35 minutes								MSEP	IFT				
Element Conditioning:		<input checked="" type="checkbox"/> in-Situ		<input type="checkbox"/> External				0	37.7				
Phase	Cum. Test Time (minutes)	Time (minutes)	Fuel Flow Rate (gpm)	ΔP (psid)	k (pS/m)	Water Flow Rate mL/min	Water Concent. (ppm)	Solids Rate <input type="checkbox"/> mg/L <input checked="" type="checkbox"/> mg/gal	Filter Sample ID	Solids Concent. Affluent (mg/L)	Turbidity, 25 Degrees	Turbidity, 90 Degrees	Temp <input type="checkbox"/> °C <input checked="" type="checkbox"/> °F
Start-up	0	0	34.2	4.4	847/803	0	1			0.463	0.724	74	
Water 0,01%	5	0	33.8	4.5	764/799	13	2			0.564	0.758		
	10	5	34.1	4.8		13	2			0.73	0.768		
	15	10 s/s	34.5	5.1		13	2			1.39	0.939		
	25	20 s/s	34.3	5.6		13	2			3.4	1.08	74	
	35	30 s/s	34.2	5.8	846/823	13	2			3.18	1.04	74	
Notes/Comments:													

Phase	Cum. Test Time (minutes)	Time (minutes)	Fuel Flow Rate (gpm)	ΔP (psid)	k (pS/m)	Water Flow Rate mL/min ■ □	Water Concent. (ppm)	Solids Rate ■ mg/L □ mg/gal	Filter Sample ID	Solids Concent. Affluent (mg/L)	Turbidity, 25 Degrees	Turbidity, 90 Degrees	Temp □ °C ■ °F
Solids Holding Test (Continued until reaching 115 kPa (22.5 psid)	35	0	34	5.7	845/835				1	0.225	1.4	0.86	75
	50	15	33.9	9				19	2	0.525	1.23	1.62	
		15 s/s	34.3	9.9				19	3	0	4.41	6.68	
	65	30	34.1	13.2	853/839			19	4	0.1	1.25	1.78	75
		30 s/s	34.3	14				19	5	0	7.4	12.3	
	80	45	34	19.8				19	6	0.125	1.22	1.86	
		45 s/s	33.9	20.3				19	7	0	11.4	19.3	
	85	50	34.1	25.4							1.24	1.98	
	95	60	34.2	26.8	861/840			19	8	0	1.35	1.95	76
		60 s/s	34.2	26.6				19	9	0	14	23.8	
	110	75	33.8	33.9				19	10	0	1.02	1.63	
		75 s/s	34.2	33.2				19	11	0	16.8	27.9	
Notes/Comments:													

Phase	Cum. Test Time (minutes)	Time (minutes)	Fuel Flow Rate (gpm)	ΔP (psid)	k (pS/m)	Water Flow Rate mL/min █ □	Water Concent. (ppm)	Solids Rate █ mg/L □ mg/gal	Filter Sample ID	Solids Concent. Affluent (mg/L)	Turbidity, 25 Degrees	Turbidity, 90 Degrees	Temp □ °C █ °F
Water Coalescence Test - 0.01%	110	0	33.8	35.4	862/848	0	2.5			0.885	1.27	76	
	112	2	33.9	39.5		13	6			1.74	2.81		
	115	5	34.1	42		13	>12			1.57	2.25		
	125	15	34	43.9	861/849	13	12			1.57	1.74	77	
		30 s/s	34.2	37.9		13	>24			7.61	13.7		
	155	45	33.9	42.3		13	22			2.11	1.48		
	170	60 s/s	34.3	39.2	865/865	13	15			12.3	22.2		
	185	75	33.8	42.6		13	30			2.5	1.33	78	
		90 s/s	34	38.9		13	10			12.4	20.1		
	215	105	33.9	42.5	868/861	13	>30			2.62	1.31		
		120 s/s	34.2	38.2		13	12.5			14.3	22.7		
	245	135	34	43		13	20			2.88	1.27		
		150 s/s	33.8	37.2		13	12.5			16.4	27.1		
	260	0	34.3	35.1	868/879	0	4			1.37	1.37	78	
Water Coalescence Test - 3%	262	2	34.3	47.1		3.9 lpm	>120			20.6	6.34		
	265	5	34.2	49		3.9 lpm	>120			46.5	5.77		
		10 s/s	34.3	47.4	985/861	3.9 lpm	>120			79	20.4		
		20 s/s	34.2	49.8		3.9 lpm	>120			103	23.6		
	290	30	34.4	49.8		3.9 lpm	>120			128	27.6	78	

Notes/Comments:

5th Edition Single Element Data Sheet

JP-8+100 Di-EGME

Test Specification: API/IP 1581 5th Edition		SET: <input checked="" type="checkbox"/>							Date: 11/29/07				
Test No. 90		Full-Scale: <input type="checkbox"/>											
Vessel:		Filter/Coalescer: Velcon			Separator: Velcon			Type: <input checked="" type="checkbox"/> -S - <input type="checkbox"/> D					
Additive Addition		Model: I-614A4TB			Model: SO-606C			Manufacturing Date:					
Category:		M-100 <input type="checkbox"/>		M <input checked="" type="checkbox"/>		C <input type="checkbox"/>							
Tank Volume	Gallons	Additive	Conc. (Mg/L)	Amount Added	k (pS/m)	Additive	Conc. (Mg/L)	Amount Added	k (pS/m)	Additive	Conc. (Mg/L)	Amount Added	k (pS/m)
Beginning		A	256	14,118		D	2,0			I	1,0		
Ending		B	0,15%	21.8 gal		B	0,15%			II	15		
Used		C	15	827.2 g		C	15						
Mixing Time: 30 minutes								MSEP	IFT				
Element Conditioning:		<input checked="" type="checkbox"/> in-Situ		<input type="checkbox"/> External				89	36.28				
Phase	Cum. Test Time (minutes)	Time (minutes)	Fuel Flow Rate (gpm)	ΔP (psid)	k (pS/m)	Water Flow Rate mL/min	Water Concent. (ppm)	Solids Rate <input type="checkbox"/> mg/L <input checked="" type="checkbox"/> mg/gal	Filter Sample ID	Solids Concent. Affluent (mg/L)	Turbidity, 25 Degrees	Turbidity, 90 Degrees	Temp <input type="checkbox"/> °C <input checked="" type="checkbox"/> °F
Start-up	0	0	34.2	5.2	740/718	0				0.644	0.737	61	
Water 0,01%	5	0	34.2	5.5	744/715	13	1			0.803	0.765		
	10	5	34	5.7		13	1.5			1.21	0.821		
	15	10 s/s	34.2	6.3		13	2			3.61	1.18		
	25	20 s/s	33.9	6.5		13	2			1.58	0.855	61	
	35	30 s/s	34.1	6.9	762/743	13	2			8.83	1.69	61	
Notes/Comments:													

Phase	Cum. Test Time (minutes)	Time (minutes)	Fuel Flow Rate (gpm)	ΔP (psid)	k (pS/m)	Water Flow Rate mL/min ■ □	Water gpm Concent. (ppm)	Solids Rate ■ mg/L □ mg/gal	Filter Sample ID	Solids Concent. Affluent (mg/L)	Turbidity, 25 Degrees	Turbidity, 90 Degrees	Temp □ °C ■ °F
Solids Holding Test (Continued until reaching 115 kPa (22.5 psid)	35	0	34.2	7	762/755				1	0.325	1.48	0.842	61
	50	15	33.7	13.1				19	2	0	1.27	1.96	
		15 s/s	33.9	14.8				19	3	0.25	7.32	10.2	
	65	30	33.9	23.6	763/763			19	4	0.2	0.977	1.65	61
		30 s/s	34.7	24.1				19	5	0.5	10.9	17.4	
	80	45	34	32.9				19	6	0.125	0.92	1.56	
		45 s/s	34.2	32.4				19	7	0	12.9	21.2	
	85	50	33.7	36.8							8.34	1.42	
	95	60	34	39.7	776/775			19	8	0.125	0.807	1.35	61
		60 s/s	34.3	35.2				19	9	0	16.5	26.4	
	110	75	34.1	43.1				19	10	0.125	0.933	1.43	
		75 s/s	34.2	41.3				19	11		15.8	25.6	
Notes/Comments:													

Phase	Cum. Test Time (minutes)	Time (minutes)	Fuel Flow Rate (gpm)	ΔP (psid)	k (pS/m)	Water Flow Rate mL/min gpm	Water Concent. (ppm)	Solids Rate	Filter Sample ID	Solids Concent. Affluent (mg/L)	Turbidity, 25 Degrees	Turbidity, 90 Degrees	Temp
						■ mL/min	□ gpm	□ mg/L □ mg/gal					□ °C ■ °F
Water Coalescence Test - 0.01%	110	0	33.9	46.4	785/784	0	1.5				0.728	1.1	62
	112	2	33.9	51.2		13	5				1.66	2.07	
	115	5	33.9	52.5		13	>12				1.71	1.83	
	125	15	34.2	40.7	805/794	13	6.5				1.86	1.76	64
		30 s/s	33.8	38.6		13	>12				20.8	27.2	
	155	45	34.8	45.9		13	30				3.57	1.4	
	170	60 s/s	33.9	43.5	811/800	13	60				20	21.4	
	185	75	33.9	45.8		13	37.5				4.4	1.39	64
		90 s/s	34.2	40.4		13	>60				24	27	
	215	105	34	44.7	814/815	13	48				4.5	1.3	
		120 s/s	34	42.7		13	>60				18	16	
	245	135	34.1	46.2		13	>60				5.05	1.31	
		150 s/s	34.3	43.4		13	>60				19	14	
Water Coalescence Test - 3%	260	0	34.2	39.5	830/837	0	2				1.12	0.967	66
	262	2	34.5	49.6		3.9 lpm	>120				41	7	
	265	5	33.8	54.3		3.9 lpm	>120				62	6.7	
		10 s/s	34	53.1	836/850	3.9 lpm	>120				109	26	
		20 s/s	34.1	61.3		3.9 lpm	>120				193	40	
	290	30											

Notes/Comments:

INTENTIONALLY LEFT BLANK

Appendix F. Toxicity Evaluation

INTENTIONALLY LEFT BLANK



DEPARTMENT OF THE AIR FORCE
AIR FORCE RESEARCH LABORATORY
WRIGHT-PATTERSON AIR FORCE BASE OHIO 45433

8 January 2008

MEMORANDUM FOR AFRL/RZTG
1790 Loop Road N, Bldg 490
Wright-Patterson AFB, OH 45433-7251
ATTN: Donald K. Phelps

FROM: David R. Mattie, Ph.D.
Teresa R. Sterner
AFRL/RHPB
2729 R St, Bldg 837
Wright-Patterson AFB, OH 45433-5707

SUBJECT: Consultative Letter, AFRL-RHPB-WP-CL-2007-0001, Comparison of triethylene glycol monomethyl ether toxicity research results with other related fuel system icing inhibitors.

1. The Fuels Branch (AFRL/RZTG) requested a review of existing toxicity information on a proposed fuel system icing inhibitor (FSII), triethylene glycol monomethyl ether (TriEGME), as a potential additive for comparison with the existing FSII (diethylene glycol monomethyl ether, DiEGME). Our objective was to determine if TriEGME toxicity is equal to or lower than DiEGME. In order to aid in the comparison, the former FSII, ethylene glycol monomethyl ether (EGME), was added to the review. EGME is no longer used as an FSII, in part due to its reproductive toxicity.
2. The attachment to this consultative letter is a table of toxicity metrics comparing the three glycol ethers presented above. The general relative toxicities are discussed below. Specific research study references for individual tests are indicated within the table and the list of citations follows the table.
 - a. Inhalation studies have not been performed with TriEGME. Its vapor pressure is extremely low (<0.001 mm Hg at 25°C standard temperature/atmospheric pressures (STP)) and it is not possible to generate sufficient vapor exposure concentrations for inhalation studies. Therefore, there is no inhalation LC₅₀ (concentration that is lethal to 50% of the test population) to compare with those of DiEGME and EGME. It does not seem necessary at this time to perform low pressure (relative to high altitude) or high temperature (heating to engine or exhaust temperature) toxicity studies based on the acute studies described below.
 - b. The oral LD₅₀ value (dose that is lethal to 50% of the test population) for TriEGME indicates that this glycol ether is considered "slightly" toxic by acute standards. TriEGME has a higher oral LD₅₀ than DiEGME. The dermal LD₅₀ for TriEGME is not as high as that of DiEGME but is similar (7441 and 9400 mg/kg, respectively). Therefore, TriEGME is expected to be of similar toxicity as DiEGME, the current FSII, and much less toxic than the former FSII, EGME.

c. All of the glycol ethers produce slight to mild skin and eye irritation. DiEGME may be the least irritating to the skin; however this is uncertain as the studies were not conducted under identical conditions. Slight to mild dermal and eye irritation responses are not of great concern as the FSII compounds are mixed at low concentrations (% weight) into jet fuel which is a known irritant in the occupational setting.

d. Diffusion across human skin is much slower for TriEGME than for EGME, as seen in an *in vitro* study. The diffusion rate is similar to that of DiEGME across rat skin. Slower diffusion results in less internal exposure to the compound.

e. Comparable short term assays (2- to 3-week exposures) were not found between TriEGME and the current FSII, DiEGME. TriEGME was more than an order of magnitude less toxic than EGME in a 14-day drinking water study.

f. Comparable sub-chronic (13-week) studies were not found between TriEGME and DiEGME. TriEGME dosed in drinking water did result in similar responses (decreased bodyweight) as EGME, but at a higher dose (lowest observed adverse effect level (LOAEL) was 1.2 g/kg-dy, as compared to 0.2 g/kg-dy for EGME). TriEGME was not found to be toxic to the nervous system.

g. Reproductive and developmental effects are the main concern from EGME exposures. TriEGME was found to have no observed adverse effect levels (NOAELs) in the different studies that were 6-25 times higher than the LOAELs for EGME. The most comparable studies between DiEGME and TriEGME show that TriEGME has higher or similar NOAELs than the LOAELs for DiEGME. Overall, TriEGME appears to have the same type of reproductive toxicity as the other glycol ethers, but at higher concentrations.

h. TriEGME was not found to be mutagenic in three different assays. DiEGME was not mutagenic in the single assay in which it was tested. EGME may be mutagenic; these results were seen at very high concentrations, as compared to the test concentrations for TriEGME.

3. A review of the toxicity of the past, current and potential FSIIIs indicates that TriEGME has less or equal toxicity to the current FSII. Use of TriEGME should not pose any additional hazard than the current FSII, DiEGME, and may pose less of a reproductive hazard. Based on this toxicological review, TriEGME should be an acceptable replacement for DiEGME as a FSII. An exposure assessment of JP-8 with TriEGME should be conducted to ensure that there are no conditions under which TriEGME as an additive to the JP-8 fuel mixture might pose a greater exposure or hazard.

4. For further information please contact Teresa R. Sterner or David R. Mattie, PhD, DABT, at AFRL/RHPB. David Mattie may be reached by phone (937-904-9569, DSN 674-9569), fax (937-255-1474, DSN 785-1474) or e-mail (david.mattie@wpafb.af.mil). Teri Sterner may be reached by phone (937-904-9512, DSN 674-9512), fax (937-904-9610, DSN 674-9610) or e-mail (teri.sterner@wpafb.af.mil).



DAVID R. MATTIE, PhD, DABT
AFRL/RHPB



TERESA R. STERNER
HJF
Contracted to AFRL/RHPB

1st Ind, AFRL/RHPB

8 January 2008

MEMORANDUM FOR AFRL/RZTG
ATTN: Donald K. Phelps

This memorandum has been coordinated at the branch level and is approved for release.



JOHN J. SCHLAYER, PhD
Chief, Applied Biotechnology Branch
Biosciences and Protection Division
Human Effectiveness Directorate

Attachment: Toxicity Comparison Table for Three Glycol Ethers

Attachment: Toxicity Comparison Table for Three Glycol Ethers

Attachment: Toxicity Comparison Table for Three Glycol Ethers

Study Type	TriEGME Dose	TriEGME Effects	DiEGME Dose	DiEGME Effects	EGME Dose	EGME Effects
CAS #	112-35-6		111-77-3		109-86-4	
Acute Exposure Lethality Levels						
Inhalation LC ₅₀ (rat)	Vapor pressure too low (<0.01 mm Hg at 25°C) for inhalation study (1)		>40,690 ppm, aerosol, 1 hr (11)	LC ₅₀	1500 ppm, 7 hr (21)	LC ₅₀
Oral LD ₅₀ (rat)	11842 mg/kg (2, 3)	LD ₅₀	5500 mg/kg (F rat) (12)	LD ₅₀	2300 mg/kg, fasted (22)	LD ₅₀
Dermal LD ₅₀ (rabbit)	7441 mg/kg (2, 3)	LD ₅₀	9400 mg/kg (13)	LD ₅₀	1280 mg/kg (23)	LD ₅₀
Irritation Studies						
Skin Irritation (rabbit)	500 mg, 24 hr, occluded (2, 4)	Mild skin irritation			483 mg, 24 hr (24)	Mild skin irritation
	10 mg, 24 hr, open (3)	Mild skin irritation	6540 µl/kg (~13-26 mg, assuming 2-4 kg rabbit) (13)	Slight skin irritation		
Eye Irritation (rabbit)	500 mg, 24 hr (2, 4)	Mild eye irritation	500 mg (14)	Mild to moderate eye irritation	500 mg, 24 hr (25)	Mild eye irritation
In Vitro Human Skin (Epidermis) Penetration Study	Diffusion, 12 hr Skin damage ratio, 12 hr (5)	Diffusion Rate = 34 µg/cm ² ·hr Permeability post-exposure:pre-exposure = 3.36	(Rat Skin Penetration: Diffusion, 4 hr) (15)	(Rat value for comparison: 51.5 µg/cm ² ·hr)	Diffusion, 12 hr Skin damage ratio, 12 hr (5)	Diffusion Rate = 2200 µg/cm ² ·hr Permeability post-exposure:pre-exposure = 3.07

Study Type	TriEGME Dose	TriEGME Effects	DiEGME Dose	DiEGME Effects	EGME Dose	EGME Effects
Short Term (Two- to Three-Week Exposures)						
14-Day Short Term Functional Observation Battery (FOB) (Drinking Water – rat)	General NOAEL 1600 mg/kg-dy [time weighted average (TWA)] FOB NOAEL 3900 mg/kg-dy [TWA] (6.7)	General LOAEL 3900 mg/kg-dy [TWA] – Decreased food consumption & body weight FOB LOAEL 8000 mg/kg-dy [TWA] – Decreased mean hind limb grip strength & mean rearing events			General LOAEL 200 mg/kg-dy No FOB performed (26)	Decreased thymus weight (significant) due to decreased bodyweight (significant at ~360 mg/kg-dy) & water consumption
20-Day Short Term Repeated Oral Gavage (rat)			NOAEL 500 mg/kg-dy, 20 dy (16)	LOAEL 1000 mg/kg-dy- Decreased thymus weight (2000 mg/kg-dy - Decreased body, thymus, testes, liver & spleen weight)	LOAEL 100 mg/kg-dy (16)	Decreased body weight gain (300 mg/kg-dy - Decreased body, liver, spleen, thymus, heart & testis weight)
3-Week (15-Exposure) Dermal Toxicity Study (rabbit)	LOAEL 1000 mg/kg-dy, 6 hr/dy, 5 dy/wk, 3 wk (one-dose level) (5)	Erythema from day 6 or 7 to end; No effect on hematology, organ weights, testicular lesions				

Study Type	TriEGME Dose	TriEGME Effects	DiEGME Dose	DiEGME Effects	EGME Dose	EGME Effects
Sub-Chronic Studies						
13-Week Sub-Chronic Motor Activity & Neuropathology (Drinking Water – rat)	General NOAEL 400 mg/kg-dy Neurotoxicity & Motor Activity NOAEL 4000 mg/kg-dy (highest exposure) ⁽⁶⁾	General LOAEL 1200 mg/kg-dy – Decreased food consumption, body weight & weight gain			General NOAEL ~100 mg/kg-dy No Neurotoxicity & Motor Activity Testing ⁽²⁶⁾	LOAEL ~200 mg/kg-dy, Decreased bodyweight, thymus weight & sperm concentration
13-Week Sub-Chronic Dermal Toxicity (rat)	Systemic NOAEL 4000 mg/kg-dy (highest exposure) semi-occluded 6 hr/dy, 5 dy/wk ⁽⁶⁾	Small focal areas of abrasion irritation, all treatment levels except 0 mg/kg, no dermal pathology; No systemic toxicity				
13-Week Sub-Chronic Inhalation Toxicity (rat)	Vapor pressure too low (<0.01 mm Hg at 25°C) for inhalation study ⁽¹⁾	NOAEL 216 ppm, 6 hr/dy, 5 dy/wk ⁽¹⁷⁾	No adverse effect (216 ppm was maximum concentration practically attainable)	NOAEL 30 ppm, 6 hr/dy, 5 dy/wk ⁽²⁷⁾	NOAEL 100 ppm - Decreased body weight (females), Some mortality	

Study Type	TriEGME Dose	TriEGME Effects	DiEGME Dose	DiEGME Effects	EGME Dose	EGME Effects
Reproductive/Developmental Studies						
Reproduction (Oral Gavage – rat) GD 7-16	NOAEL 1000 mg/kg-dy, GD 7-16 (5)	No effect on maternal health, pup weight & survival (Screening, Necropsy not performed)	LOAEL 720 mg/kg-dy, GD 7-16 (18)	Rib malformations; Reduced ossification; No effect on maternal health & fetal weight	LOAEL 50 mg/kg-dy, GD 7-16 (5)	Reduced maternal BW, All litters resorbed
Reproduction (Oral Gavage - rat) NOTE DIFFERENT EXPOSURE DAYS	NOAEL 625 mg/kg-dy, GD 6-15 (8)	LOAEL 1250 mg/kg-dy - Decreased food consumption & fetal weight; Delayed ossification; Skeletal variations	LOAEL 600 mg/kg-dy, GD 7-17 (19)	Visceral malformations; Delayed ossification	LOAEL 25 mg/kg-dy, GD 7-13 (28)	Increased gestation length; Decreased ornithine decarboxylase (ODC) activity in 3- day old rats (54% decrease)
Reproduction (Oral Gavage – rabbit)	NOAEL 500 mg/kg-dy, GD 6-18 (8)	LOAEL 1000 mg/kg-dy - Decreased dam body weight & food consumption; Delayed xiphoid ossification				

Study Type	TriEGME Dose	TriEGME Effects	DiEGME Dose	DiEGME Effects	EGME Dose	EGME Effects
Developmental Neurotoxicity Screen (rat)	Developmental NOAEL 300 mg/kg-dy Developmental Neurotoxicity LOAEL 3000 mg/kg-dy (highest dose), GD 6- PND 21 (9)	Systemic LOAEL 1650 mg/kg-dy - Decreased weight gain in male pups, Early testes descent Increased auditory startle amplitude				
Mutagenicity Assays						
Mutagenicity: Ames <i>Salmonella</i> Assay	Ames <i>Salmonella typhimurium</i> his- test (TA98, TA100, TA1535, & TA1537), with or without rat S9 metabolic activation (10)	No increase in mutagenic activity	Ames <i>Salmonella typhimurium</i> his- test (TA98, TA100, TA1535 & TA1537), with or without rat S9 metabolic activation (20)	No mutagenic activity	Ames <i>Salmonella typhimurium</i> his-test (TA97a, TA98, TA100 & TA102), with or without rat S9 metabolic activation (29, 26)	No mutagenic activity

Study Type	TriEGME Dose	TriEGME Effects	DiEGME Dose	DiEGME Effects	EGME Dose	EGME Effects
Mutagenicity: Chinese Hamster Ovary	2000 – 5000 µg/L (7)	Did not increase mutagenicity, with or without activation			EGME: 7.6×10^6 - 7.6×10^7 µg/L Metabolite - MALD (methoxy- acetaldehyde) 7.4×10^4 – 1.5×10^6 µg/L (30)	Did not increase mutagenicity with or without activation MALD induced deletion type mutations without S9 activation
					“very high concentrations” 3.17×10^6 µg/L (26)	Induced sister chromatid exchanges (SCEs) with & without S9; Induced chromosomal aberrations without S9 activation
Mutagenicity: Mammalian Bone Marrow Micronucleus Assay	0, 500, 1667, 5000 mg/kg-dy, single oral gavage in mice (7)	No evidence of clastogenicity				

References

1. IPCS INCHEM. 1996. Ethanol,2-(2-(2-methoxyethoxy)ethoxy- (Screening Information Data Set - SIDs). International Programme on Chemical Safety, Chemical Safety Information from Intergovernmental Organizations. <http://www.inchem.org/documents/sids/sids/112356.pdf>.
2. Sigma-Aldrich MSDS for Triethylene Glycol Monomethyl Ether, Product Number 90450. Sigma-Aldrich, St. Louis, MO. Updated 02-05-2006. Version 1.4.
3. RTECS, chemical # KL6390000. <http://www.cdc.gov/niosh/rtecs/k16180f0.html> Accessed 3-12-2007. (1958. Am. Ind. Hyg. J., 23, 95)
4. RTECS, chemical # KL6390000. <http://www.cdc.gov/niosh/rtecs/k16180f0.html> Accessed 3-12-2007. (1986. "Prehled Prumyslove Toxikologie; Organické Latky," Marhold J., Prague, Czechoslovakia, Avenicum, 634)
5. Leber, A. P., Scott, R. C., Hodge, M. C. E., Johnson, D., and Krasavage, W. J. 1990. Triethylene glycol ethers: Evaluations of in vitro absorption through human epidermis, 21-day dermal toxicity in rabbits, and a developmental toxicity screen in rats. J. Am. Coll. Toxicol. 9:507-515.
6. Gill, M. W., Fowler, E. H., Gingell, R., Lomax, L. G., and Corley, R. A. 1998. Subchronic dermal toxicity and oral neurotoxicity of triethylene glycol monomethyl ether in CD rats. Int. J. Toxicol. 17:1-22.
7. U.S. Environmental Protection Agency, Office of Prevention, Pesticides and Toxic Substances. 2007 (last updated 5 Oct 2007). Triethylene Glycol Ethers Test Results. <http://www.epa.gov/oppt/chemtest/pubs/triethgl.htm>.
8. Hoberman, A. M., Krasavage, W. J., Christian, M. S., and Stack, C. R. 1996. Developmental toxicity study with triethylene glycol given by gavage to CD rats and CD-1 mice. J. Am. Coll. Toxicol. 15:349-370.
9. Kimmel, C. A. 1996. Reproductive and developmental effects of diethylene and triethylene glycol (methyl-, ethyl-) ethers. Occup. Hyg. 2:131-151.
10. 55 FR 13956; 5/13/90, OTS0526547
11. Anon. 1993, "Methyldiglykol", Toxikologische Bewertung, Berufsgenossenschaft der chemischen Industrie, Heidelberg. (abstract)
12. Clayton, GD & FE Clayton, eds; 1994, Patty's Industrial Hygiene & Toxicology viID, John Wiley & Sons, New York, 2830-4. (Rowe VK. 1947. Unpublished data. Dow Chemical Co.)
13. Clayton, GD & FE Clayton, eds; 1994, Patty's Industrial Hygiene & Toxicology viID, John Wiley & Sons, New York, 2830-4. (Krasavage WJ & Terhaar CJ. 1981. Unpublished data. Eastman Kodak Co. Report No. TX-81-38.)
14. RTECS, 1995. (Marhold, J; 1986, Prehled Prumyslove Toxilogie; Organické Latky, Avicenum, Prague, Czech., 628.; Union Carbide Data Sheet, 4/21/67.)
15. McDougal, J. N., Pollard, D. L., Weisman, W., Garrett, C. M., and Miller, T. E. 2000. Assessment of skin absorption and penetration of JP-8 jet fuel and its components. Toxicol. Sci. 55:247-255.
16. Kawamoto, T., Matsuno, K., Kayama, F., Hirai, M., Arashidani, K., Yoshikawa, M., and Kodama, Y. 1990. Acute oral toxicity of ethylene glycol monomethyl ether and diethylene glycol monomethyl ether. Bull. Environ. Contam. Toxicol. 44:602-608.
17. Miller, R. R., Eisenbrandt, D. L., Gushow, T. S., and Weiss, S. K. 1985. Diethylene glycol monomethyl ether 13-week vapor inhalation toxicity study in rats. Fundam. Appl. Toxicol. 5:1174-1179.
18. Hardin, B. D., Goad, P. T., and Burg, J. R. 1986. Developmental toxicity of diethylene glycol monomethyl ether (diEGME). Fundam. Appl. Toxicol. 6:430-439.

19. Yamano, T., Noda, T., Shimizu, M., Morita, S., and Nagahama, M. 1993. Effects of diethylene glycol monomethyl ether on pregnancy and postnatal development in rats. *Arch. Environ. Contam. Toxicol.* 24:228-235.
20. EPA/OTS, 1989, #86-890000729. (abstract)
21. RTECS, 1995. (1974, Raw Material Data Handbook, v1, 57.)
22. Clayton, GD & FE Clayton, eds. 1994, Patty's Industrial Hygiene & Toxicology viID, John Wiley & Sons, New York, 2764-76. (Krasavage WJ & Terhaar CJ. 1981. Unpublished data. Eastman Kodak Co. Report No. TX-81-16).
23. Clayton, GD & FE Clayton, eds. 1994, Patty's Industrial Hygiene & Toxicology viID, John Wiley & Sons, New York, 2764-76. (Union Carbide Corp. Special report 8-3-38.)
24. RTECS, 1995. (Weil CS & Scala RA. 1971. Toxicol. Appl. Pharmacol., v19, 276.)
25. RTECS, 1995. (Marhold, J; 1986, Prehled Prumyslove Toxicologi.; Organické Latky, Avicenum, Prague, Czech., 623.)
26. Dieter, M. 1993. NTP Technical Report on Toxicity Studies of Ethylene Glycol Ethers, 2-Methoxyethanol, 2-Ethoxyethanol, 2-Butoxyethanol, Administered in Drinking Water to F344/N Rats and B6C3F1 Mice. National Toxicology Program, Research Triangle Park, NC. NIH Publication 93-3349, Toxicity Report Series Number 26.
27. Miller, R. R., Hermann, E. A., Young, J. T., Landry, T. D., and Calhoun, L. L. 1984. Ethylene glycol monomethyl ether and propylene glycol monomethyl ether: metabolism, disposition, and subchronic inhalation toxicity studies. *Environ. Health Perspect.* 57:233-239.
28. Toraason, M., Stringer, B., and Smith, R. 1986. Ornithine decarboxylase activity in the neonatal rat heart following prenatal exposure to ethylene glycol monomethyl ether. *Drug Chem. Toxicol.* 9:1-14.
29. Hoflack, JC; et al., 1995, *Mutat Res.* 341(4), 281-7. (abstract)
30. Ma, H., An, J., Hsie, A. W., and Au, W. W. 1993. Mutagenicity and cytotoxicity of 2-methoxyethanol and its metabolites in Chinese hamster cells (the CHO/HPRT and AS52/GPT assays). *Mutat. Res.* 298:219-225.

Appendix G. Hot Gas Path Evaluation of Compatibility with Turbine Engine Materials

INTENTIONALLY LEFT BLANK

Evaluation of TriEGME as a Replacement Fuel System Icing Inhibitor Additive for use in the TF33-PW-103 Engine

Hot Gas Path Test to Determine Compatibility of Triethylene Glycol Monomethyl Ether Fuel Additive with Turbine Engine Materials

Prepared for The Boeing Company

Boeing Purchase Contract No. 198866 / P&W P.O. No. 199477

United Technologies Corporation

Pratt & Whitney

400 Main Street
East Hartford, Connecticut 06108

April 27, 2009

Period of Performance: 20 February 2008 through 20 March 2010



Program Manager

Tedd Biddle

Fuels Technology Manager

Pratt & Whitney

Deputy Program Mgr.

Margaret Adamson

Fuels & Lubricants

Pratt & Whitney

Task Manager

Mark Ucasz

Advanced Coatings

Pratt & Whitney

Executive Summary

The objective of this program was to perform oxidation and corrosion hot gas-path testing to determine the compatibility of triethylene glycol monomethyl ether (TriEGME) fuel additive on turbine engine alloys and coatings.

The hot gas-path tests are part of the approval process set forth by jet engine manufacturers for the use of the TriEGME additive in fuels used by military and commercial aircraft. In this program the hot gas-path testing was accomplished using burner rigs. The 1850°F cyclic oxidation tests were carried out on six different alloy/coating combinations. The isothermal 1600°F, 3.5 ppm salt, hot corrosion tests were conducted on seven different alloy/coating combinations.

Oxidation and corrosion samples were tested using a TriEGME/Jet A additive blend and compared to a DiEGME/Jet A baseline blend. Test samples were evaluated by mass, dimensional and visual change. Only minor differences were found between the additive packages thus the TriEGME additive was deemed to be comparable to the DiEGME additive.

1.0 Program Objectives

The objective of this program was to perform oxidation and corrosion hot gas-path tests to determine the compatibility of triethylene glycol monomethyl ether fuel additive on turbine engine alloys and coatings.

2.0 Test Methodology

The paragraphs that follow describe the hot gas-path tests required to determine the effect of a triethylene glycol monomethyl ether fuel additive/Jet A fuel blend on turbine engine materials. Compatibility was based on testing two different burner rig regimes:

- 1850°F (1010°C) cyclic oxidation - 57 minutes heating and 3 minutes forced air cooling - 500 hrs
- 1600°F (871°C) isothermal hot corrosion with 3.5 ppm salt - 500 hrs

Oxidation & corrosion tests were performed concurrently on identical burner rigs using both a 0.15 volume percent (%) diethylene glycol monomethyl ether (DiEGME) fuel additive/Jet A fuel blended baseline and a 0.15 volume % triethylene glycol monomethyl ether (TriEGME) fuel additive/Jet A fuel blend. This approach provided a direct comparison of the TriEGME additive to that of the baseline containing the DiEGME additive.

Selection of the materials tested in each burner regime was based on anticipated exposure in the turbine. Both coated and uncoated alloys were tested. The turbine materials, shown in Table 2-1, were evaluated in burner rig tests at both 1850°F (1010°C) Cyclic Oxidation and at 1600°F (871°C) Isothermal Hot Corrosion which included 3.5 parts per million (ppm) salt.

Table 2-1. *Turbine materials and coatings evaluated in the DiEGME and TriEGME fuel additive program.*

1850°F (1010°C) Cyclic Oxidation Test		1600°F (871°C) Isothermal Hot Corrosion Test with 3.5 ppm Salt	
Alloy	Coating	Alloy	Coating
PWA 1484	PWA 275	PWA 1447	PWA 286
PWA 1447	PWA 73	PWA 1447	PWA 73
PWA 1447	PWA 286	PWA 663	PWA 73
PWA 655	Uncoated	PWA 655	PWA 73
PWA 1484	Uncoated	PWA 655	Uncoated
PWA 1447	Uncoated	PWA 1484	Uncoated
		PWA 1455	Uncoated

2.1 Test Apparatus

Ambient (~101 kPa) pressure isothermal and thermal-gradient burner rigs were used to evaluate a variety of turbine materials and coatings under simulated engine environment and temperature conditions. A typical isothermal burner rig setup is shown in Figure 2-1.

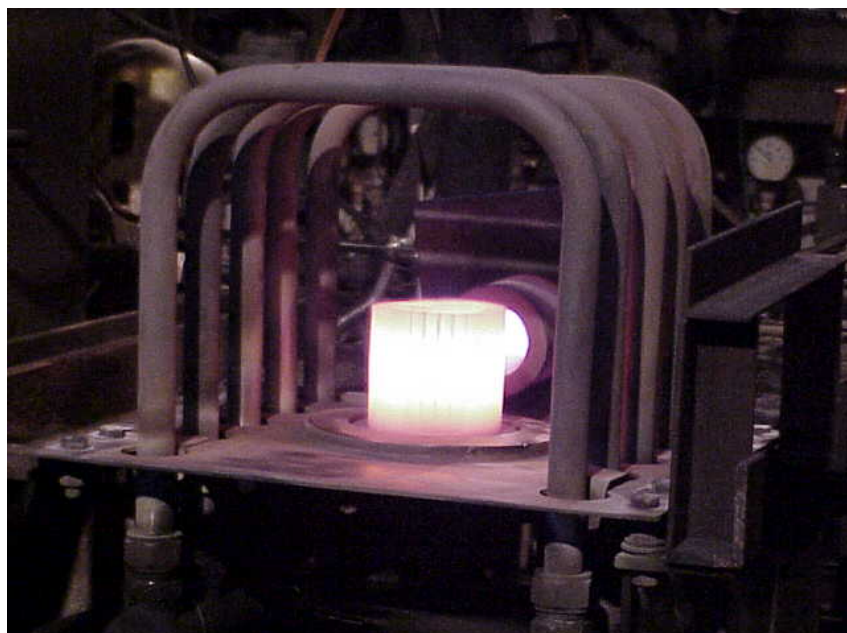


Figure 2-1. *Burner rig bars being tested in an isothermal burner rig with a Jet A fuel source.*

Up to twelve ½" x 4" (12 mm x 100 mm) cylindrical test specimens can be simultaneously exposed to the hot gas produced by a Jet A-fueled burner. Test specimen temperatures can range from 1350° to 2250°F (732° to 1232°C) with a hot-gas velocity of approximately 0.3 Mach (100 m/s). An optical pyrometer monitors and maintains specimen temperature automatically by interfacing with a computer control system that adjusts the fuel-valve output. Specimens rotate at approximately 500 rpm and move into and out of the burner flame for thermal cycling. Specimens are rapidly cooled by a high-pressure air blast applied during the cool-down portion of a cycle. The burner rigs are capable of operation in both oxidation and hot corrosion regimes. For hot corrosion testing, a salt solution is injected at the burner. In addition, fuel can be doped, and/or SO₂ gas can be injected into the combustion gases, to simulate various levels of sulfur or other types of contamination.

2.2 Test Matrix

Four 500-hour burner rig tests were performed according to the test matrices shown in Table 2-2 and Table 2-3.

Table 2-2. Oxidation test matrix for the 500-hour burner rig tests of the DiEGME additive/Jet A blended baseline and the TriEGME additive/Jet A blend.

Position	Alloy	Coating	Temperature °F (°C)	Cycle	Salt (ppm)	Additive (Vol%)	Specimen ID
Test 1: 1850°F (1010°C) Cyclic Oxidation – DiEGME Additive/Jet A Blended Baseline							
1A	PWA 1484	PWA 275	1850 (1010)	57/3	0	0.15	1740I
2A	PWA 1447	Uncoated	1850 (1010)	57/3	0	0.15	2042D
3A	PWA 655	Uncoated	1850 (1010)	57/3	0	0.15	2037L
4A	PWA 1447	PWA 73	1850 (1010)	57/3	0	0.15	2042F
5A	PWA 1484	Uncoated	1850 (1010)	57/3	0	0.15	1740E
6A	PWA 1447	PWA 286	1850 (1010)	57/3	0	0.15	2042E
7A	PWA 1484	PWA 275	1850 (1010)	57/3	0	0.15	1740T
8A	PWA 1447	Uncoated	1850 (1010)	57/3	0	0.15	2042B
9A	PWA 655	Uncoated	1850 (1010)	57/3	0	0.15	2037K
10A	PWA 1447	PWA 73	1850 (1010)	57/3	0	0.15	2042X
11A	PWA 1484	Uncoated	1850 (1010)	57/3	0	0.15	1740M
12A	PWA 1447	PWA 286	1850 (1010)	57/3	0	0.15	2042I
Test 2: 1850°F (1010°C) Cyclic Oxidation – TriEGME Additive/Jet A Blend							
1B	PWA 1484	PWA 275	1850 (1010)	57/3	0	0.15	1740H
2B	PWA 1447	Uncoated	1850 (1010)	57/3	0	0.15	2042Z
3B	PWA 655	Uncoated	1850 (1010)	57/3	0	0.15	2037A
4B	PWA 1447	PWA 73	1850 (1010)	57/3	0	0.15	2042S
5B	PWA 1484	Uncoated	1850 (1010)	57/3	0	0.15	1740S
6B	PWA 1447	PWA 286	1850 (1010)	57/3	0	0.15	2042Y
7B	PWA 1484	PWA 275	1850 (1010)	57/3	0	0.15	1740K
8B	PWA 1447	Uncoated	1850 (1010)	57/3	0	0.15	2042N
9B	PWA 655	Uncoated	1850 (1010)	57/3	0	0.15	2037Y
10B	PWA 1447	PWA 73	1850 (1010)	57/3	0	0.15	2042W
11B	PWA 1484	Uncoated	1850 (1010)	57/3	0	0.15	1740B
12B	PWA 1447	PWA 286	1850 (1010)	57/3	0	0.15	2042U

Table 2-3. Hot corrosion test matrix for the 500-hour burner rig tests of the DiEGME Additive/Jet A blended baseline and the TriEGME additive/Jet A blend.

Position	Alloy	Coating	Temperature °F (°C)	Cycle	Salt (ppm)	Additive (Vol%)	Specimen ID
Test 3: 1600°F (871°C) Isothermal Hot Corrosion - DiEGME Additive/Jet A Blend							
1C	PWA 1447	PWA 286	1600 (871)	Isothermal	3.5	0.15	2161Y
2C	PWA 663	PWA 73	1600 (871)	Isothermal	3.5	0.15	2160E
3C	PWA 655	PWA 73	1600 (871)	Isothermal	3.5	0.15	2158M
4C	PWA 1447	PWA 73	1600 (871)	Isothermal	3.5	0.15	2161H
5C	PWA 1484	Uncoated	1600 (871)	Isothermal	3.5	0.15	1641L
6C	PWA 655	PWA 73	1600 (871)	Isothermal	3.5	0.15	2158K
7C	PWA 1447	PWA 73	1600 (871)	Isothermal	3.5	0.15	2161R
8C	PWA 655	Uncoated	1600 (871)	Isothermal	3.5	0.15	2158I
9C	PWA 1455	Uncoated	1600 (871)	Isothermal	3.5	0.15	2043E
10C	PWA 1447	PWA 286	1600 (871)	Isothermal	3.5	0.15	2161H
11C	PWA 663	PWA 73	1600 (871)	Isothermal	3.5	0.15	2160H
12C	PWA 655	Uncoated	1600 (871)	Isothermal	3.5	0.15	2058P
Test 4: 1600°F (871°C) Isothermal Hot Corrosion - TriEGME Additive/Jet A Blend							
1D	PWA 1447	PWA 286	1600 (871)	Isothermal	3.5	0.15	2161S
2D	PWA 663	PWA 73	1600 (871)	Isothermal	3.5	0.15	2160A
3D	PWA 655	PWA 73	1600 (871)	Isothermal	3.5	0.15	2158L
4D	PWA 1447	PWA 73	1600 (871)	Isothermal	3.5	0.15	2161K
5D	PWA 1484	Uncoated	1600 (871)	Isothermal	3.5	0.15	1641D
6D	PWA 655	Uncoated	1600 (871)	Isothermal	3.5	0.15	2158A
7D	PWA 1447	PWA 73	1600 (871)	Isothermal	3.5	0.15	2161Q
8D	PWA 655	PWA 73	1600 (871)	Isothermal	3.5	0.15	2158J
9D	PWA 1455	Uncoated	1600 (871)	Isothermal	3.5	0.15	2043F
10D	PWA 1447	PWA 286	1600 (871)	Isothermal	3.5	0.15	2161J
11D	PWA 663	PWA 73	1600 (871)	Isothermal	3.5	0.15	2160C
12D	PWA 655	Uncoated	1600 (871)	Isothermal	3.5	0.15	2158G

3.0 Test Results

3.1 Oxidation

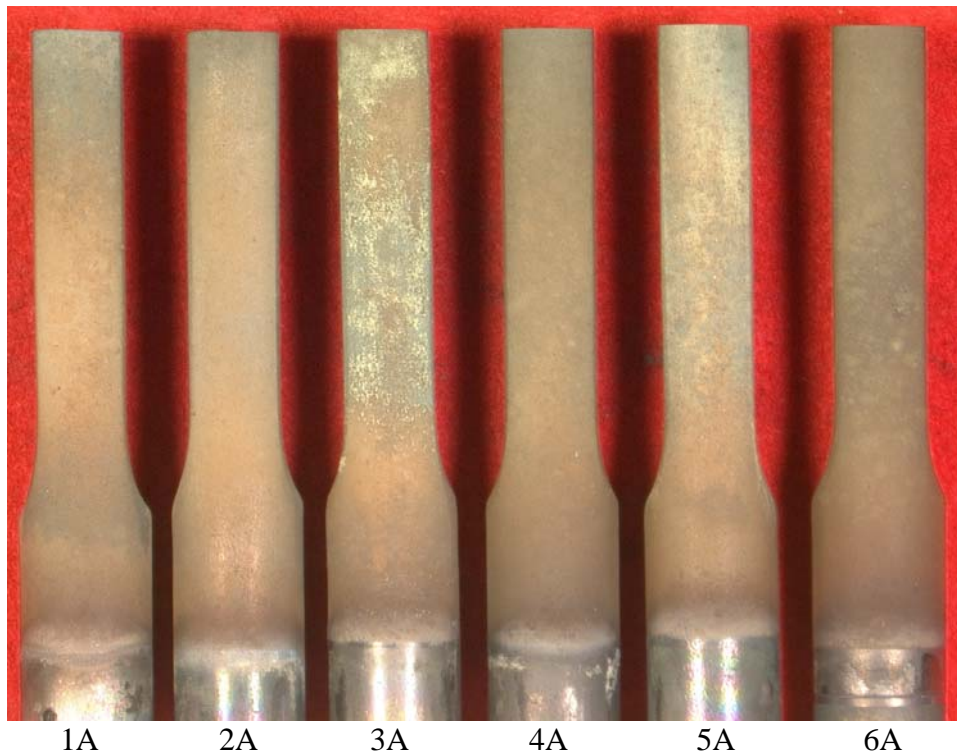
3.1.1 Cyclic Oxidation

Burner rig oxidation tests were run concurrently using both a TriEGME/Jet A blend and a DiEGME/Jet A blended baseline. Figures 3-1 to 3-4 show macro photos of the DiEGME/Jet A blended baseline specimens after running for 504.5 hours in cyclic oxidation testing. The DiEGME/Jet A test specimens show typical colors and surface conditions for these alloys and coatings after oxidation testing. The numbers superimposed on the bottom of the photos correspond to the sample numbers (specimen ID) given in Table 2-2.

Figures 3-5 to 3-8 show macro photos of the TriEGME/Jet A blend specimens after running for 502.5 hours in cyclic oxidation testing. The TriEGME/Jet A blend specimens also exhibit typical surface conditions, however, some test specimens exhibit colors which were slightly lighter/whiter than the baseline coloration. The numbers superimposed on the bottom of these photos also correspond to the sample numbers (specimen ID) given in Table 2-2.

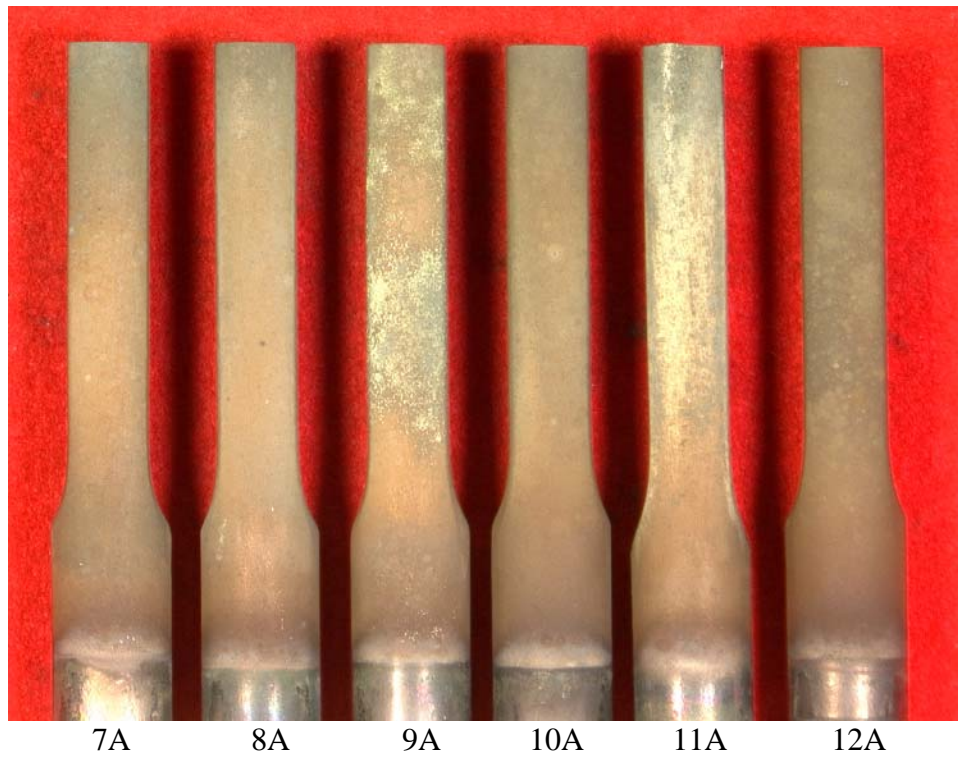
The differences in coloration between the two additives are further shown in Figures 10 & 11. It is clear from a comparison of the macro photos of the DiEGME/Jet A blended baseline (Figure 3-9) and the TriEGME/Jet A blended samples (Figure 3-10) that there is a brown deposit on the DiEGME samples, while there is a light brown/white deposit on the surface of the TriEGME/Jet A samples. The burner rig bar holders show additional evidence of the color differences between the fuel additives.

Energy dispersive spectroscopy (EDS) was used to characterize the deposit/oxide scale on the uncoated PWA1484 test bars that were oxidation tested using the DiEGME and TriEGME additives. The DiEGME burner rig test bar, 11A, was characterized by EDS on the bar shoulder and the spectra is shown in Figure 3-11. The EDS spectrum shows peaks of aluminum, tantalum, nickel, cobalt, oxygen, and iron with a minor amount of calcium. The EDS spectrum for the TriEGME burner rig specimen, 11B, was also conducted on the bar shoulder and is shown in Figure 3-12. The TriEGME spectrum contains the same elements as shown in the DiEGME spectrum with the exception of calcium. It is not known if the addition of calcium to the oxide/deposit would result in the color differences between the two test groups or if the difference in colors is related to oxide scale thickness. Additional x-ray characterization of the bar's surfaces would be needed to identify spinal phases present and oxide thickness differences.



1A.	1740 I	PWA 1484 / PWA 275
2A.	2042 D	PWA 1447 / Polished
3A.	2037 L	PWA 655 / Polished
4A.	2042 F	PWA 1447 / PWA 73
5A.	1740 E	PWA 1484 / Polished
6A.	2042 E	PWA 1447 / PWA 286

Figure 3-1. Test 1: DiEGME/Jet A blended fuel test bars (baseline) after 504.5 hours of 1850°F cyclic oxidation testing – Leading edge view.



7A.	1740 T	PWA 1484 / PWA 275
8A.	2042 B	PWA 1447 / Polished
9A.	2037 K	PWA 655 / Polished
10A.	2042 X	PWA 1447 / PWA 73
11A.	1740 M	PWA 1484 / Polished
12A.	2042 I	PWA 1447 / PWA 286

Figure 3-2. Test 1: DiEGME/Jet A blended fuel test bars (baseline) after 504.5 hours of 1850°F cyclic oxidation testing – Leading edge views.

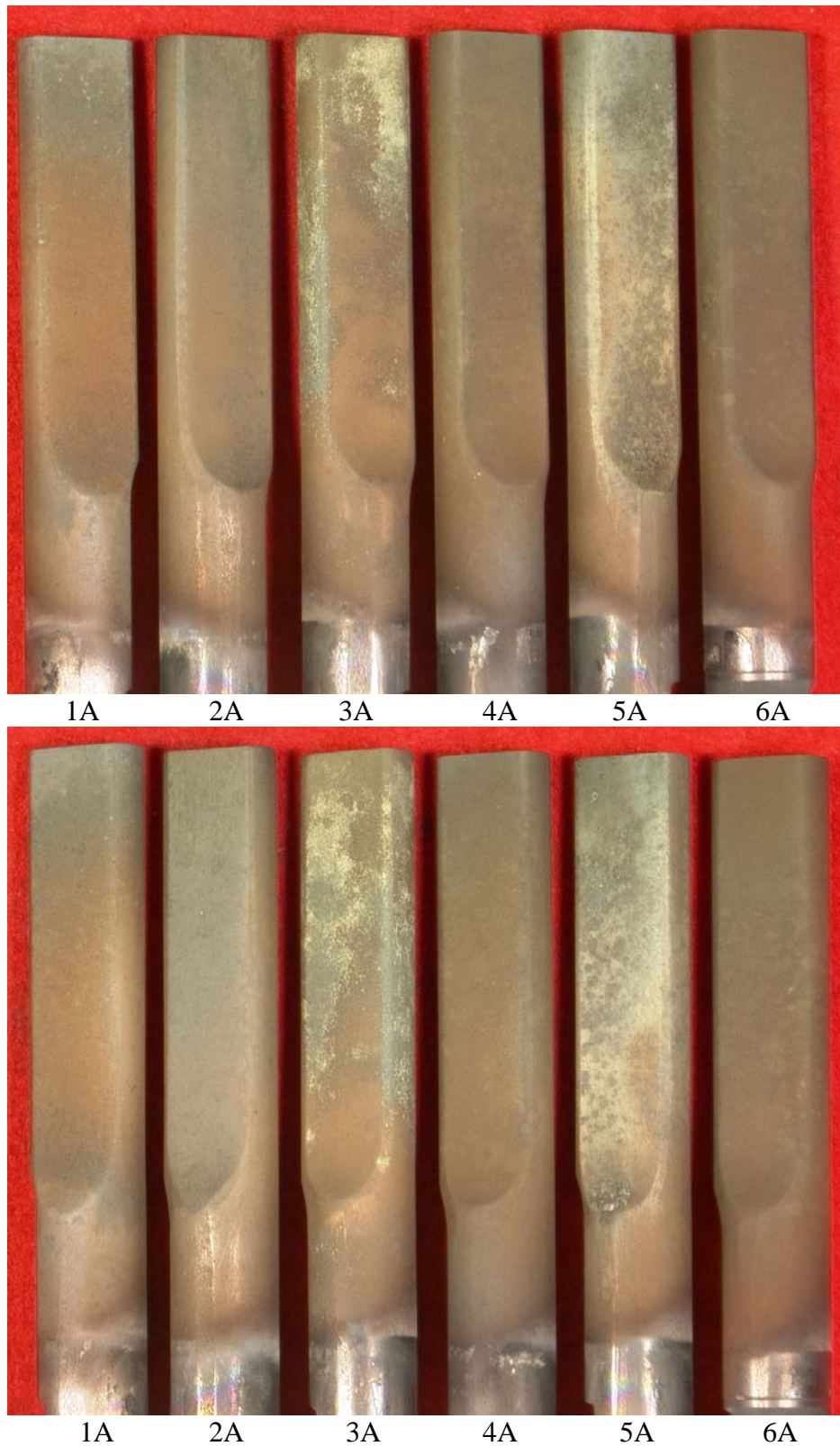


Figure 3-3. Test 1: DiEGME/Jet A blended fuel test bars (baseline) after 504.5 hours of 1850°F cyclic oxidation testing – Side views.

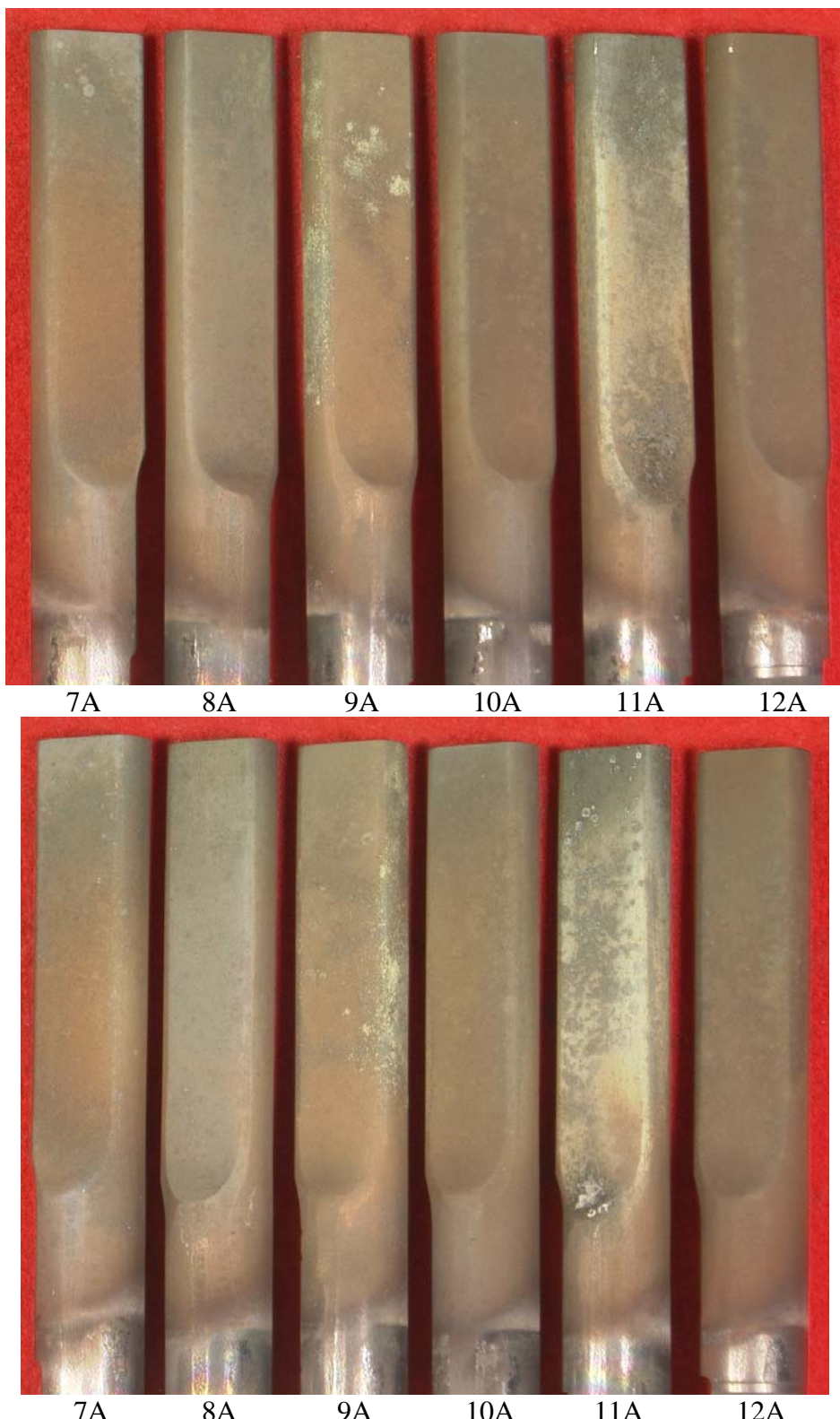
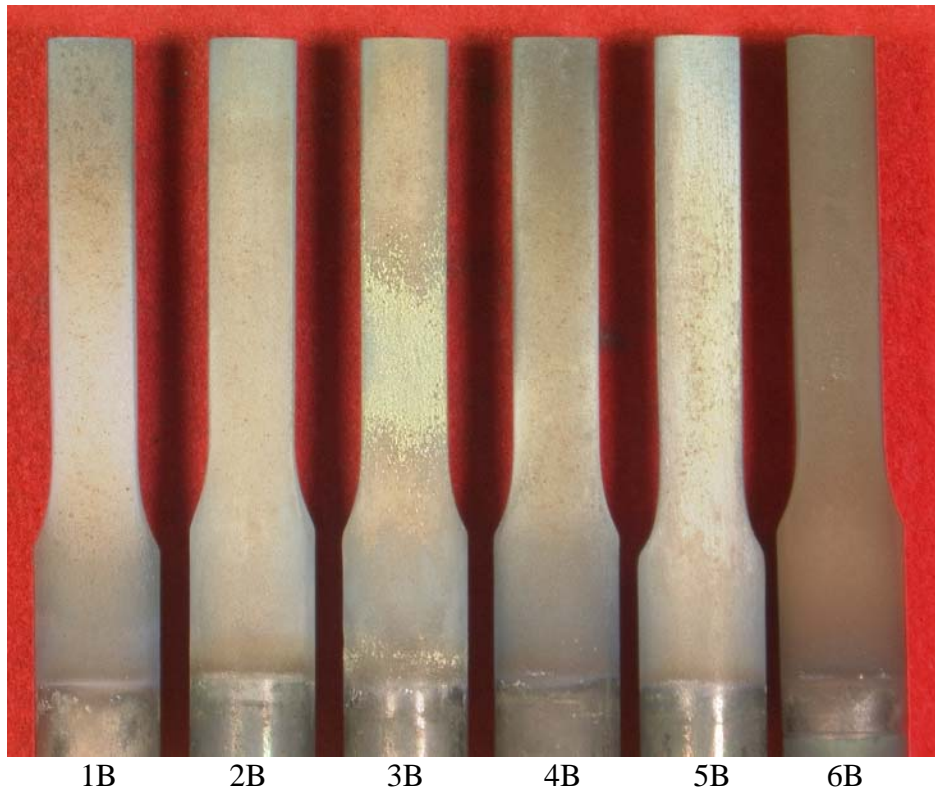
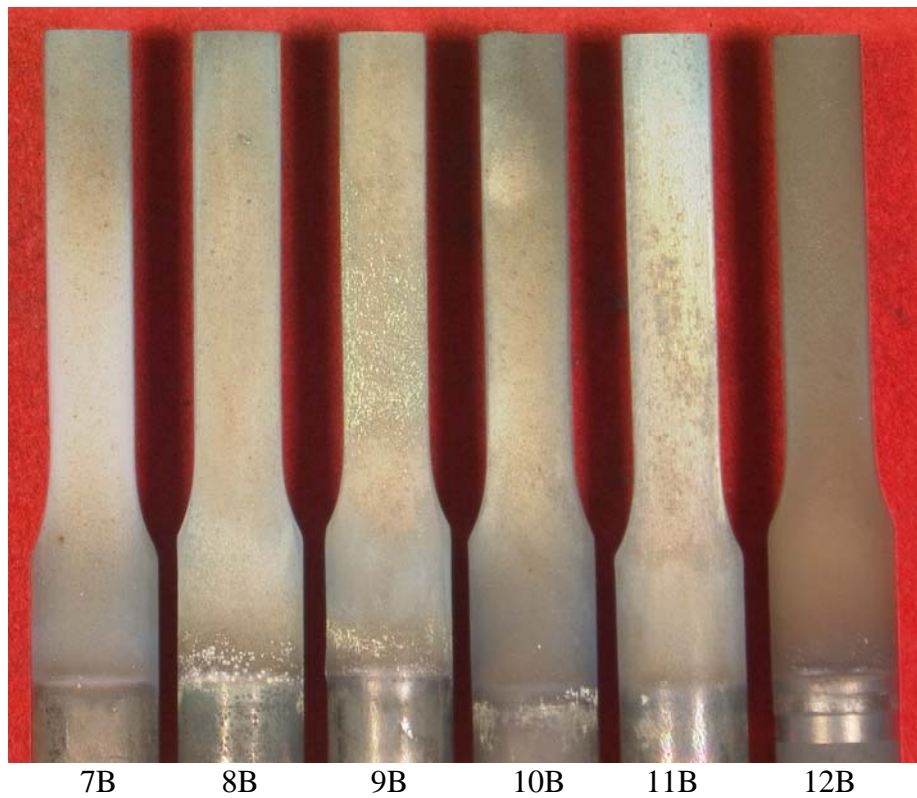


Figure 3-4. Test 1: DiEGME/Jet A blended fuel test bars (baseline) after 504.5 hours of 1850°F cyclic oxidation testing – Side views.



1B.	1740 H	PWA 1484 / PWA 275
2B.	2042 Z	PWA 1447 / Polished
3B.	2037 A	PWA 655 / Polished
4B.	2042 S	PWA 1447 / PWA 73 Sermatech
5B.	1740 S	PWA 1484 / Polished
6B.	2042 Y	PWA 1447 / PWA 286

Figure 3-5. Test 2: TriEGME/Jet A blended fuel test bars after 502.5 hours of 1850°F cyclic oxidation testing – Leading edge views.



7B.	1740 K	PWA 1484 / PWA 275
8B.	2042 N	PWA 1447 / Polished
9B.	2037 Y	PWA 655 / Polished
10B.	2042 W	PWA 1447 / PWA 73 Sermatech
11B.	1740 B	PWA 1484 / Polished
12B.	2042 U	PWA 1447 / PWA 286

Figure 3-6. Test 2: TriEGME/Jet A blended fuel test bars after 502.5 hours of 1850°F cyclic oxidation testing – Leading edge Views.

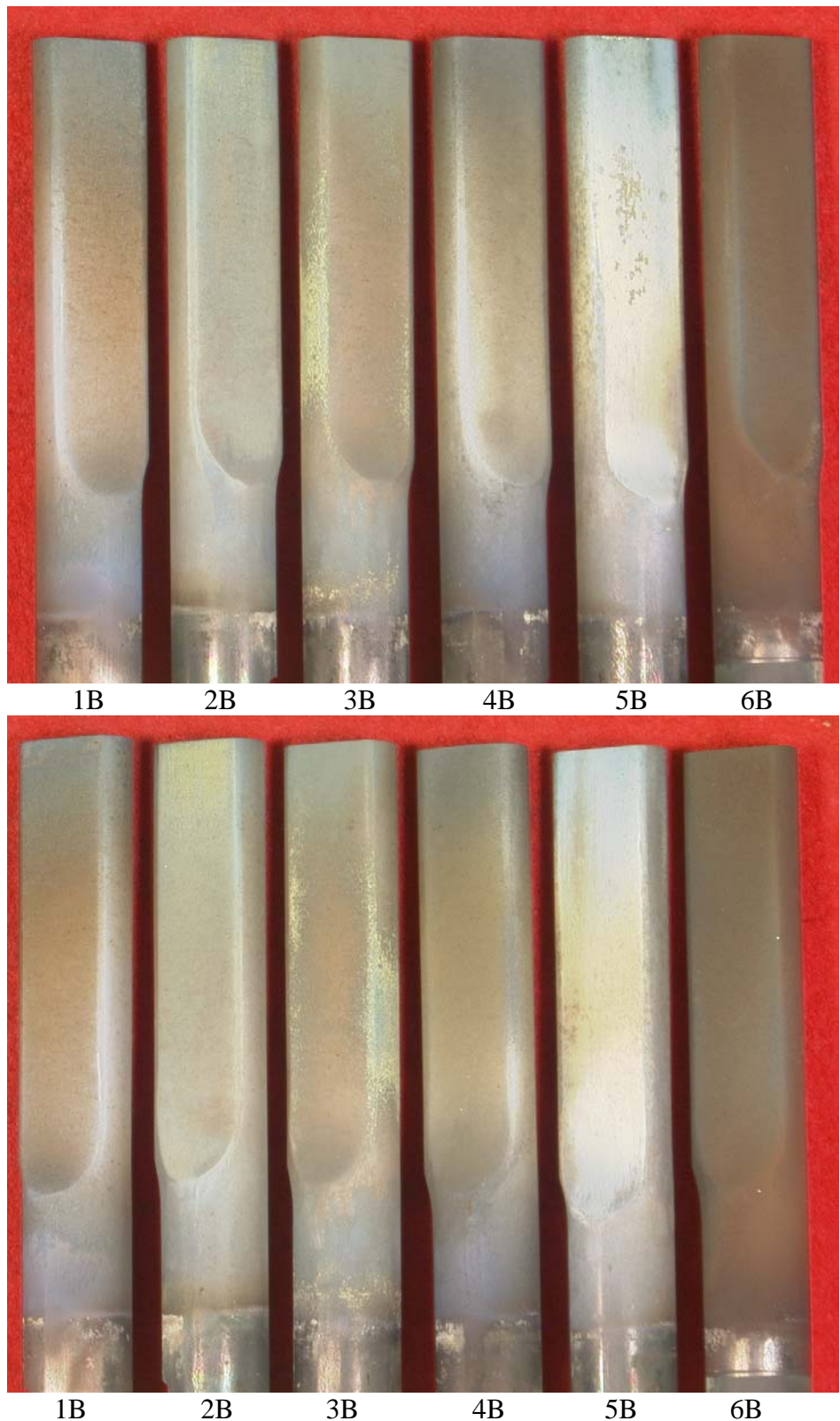


Figure 3-7. Test 2: TriEGME/Jet A blended fuel test bars after 502.5 hours of 1850°F cyclic oxidation testing – Side views.

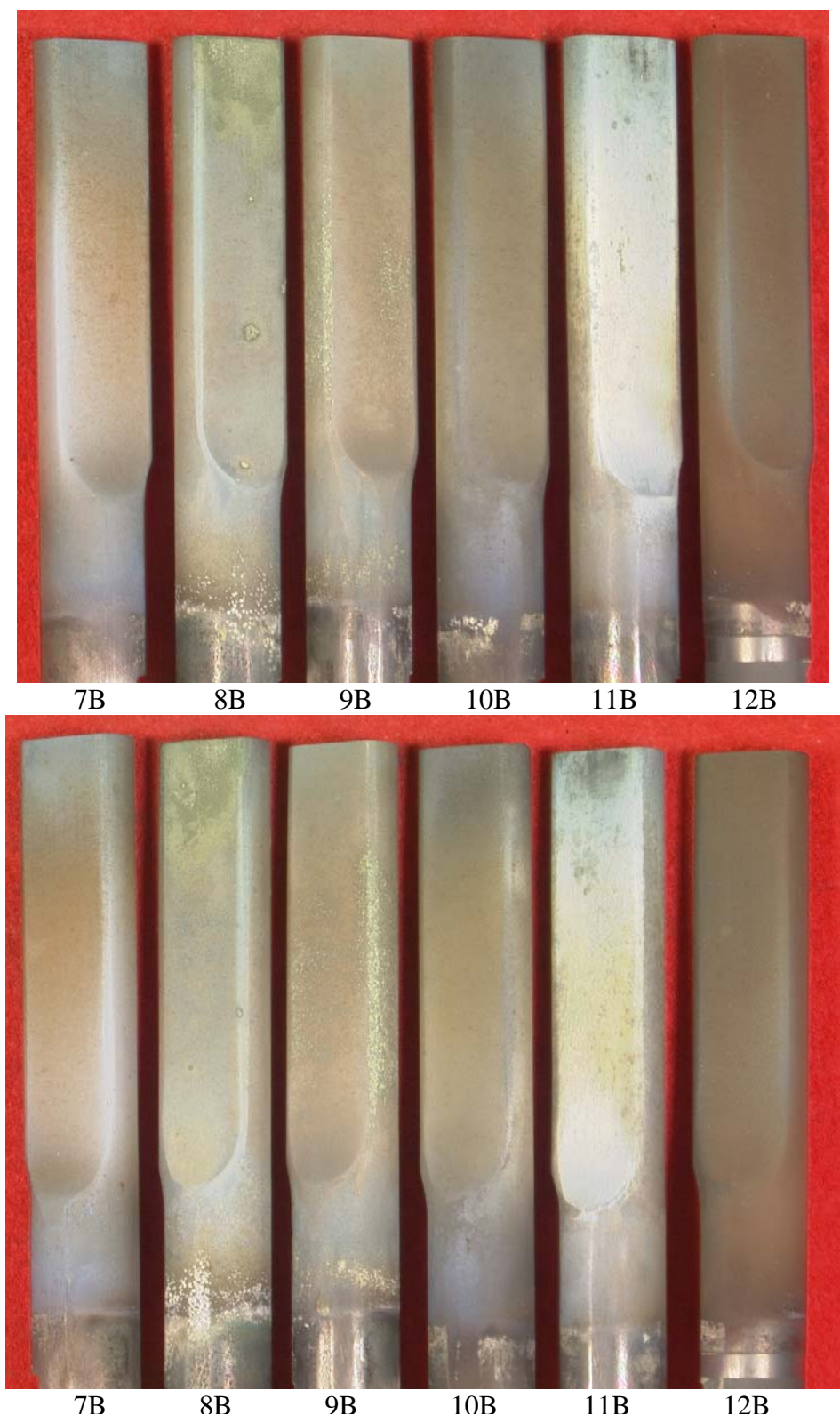


Figure 3-8. Test 2: TriEGME/Jet A blended fuel test bars after 502.5 hours of 1850°F cyclic oxidation testing – Side views.



Figure 3-9. Burner rig bar holder with test bars showing brown coloration after 504.5 hours of cyclic oxidation testing using a DiEGME/Jet A fuel blend.

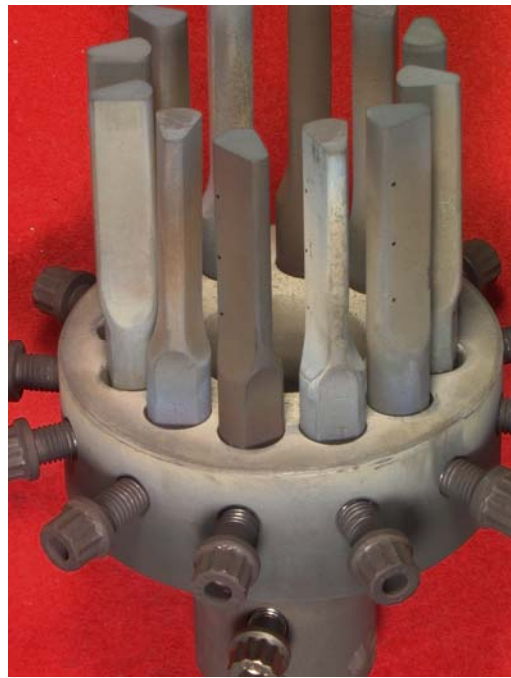


Figure 3-10. Burner rig bar holder with test bars showing light brown/white coloration after 502.5 hours of cyclic oxidation testing using a TriEGME/Jet A fuel blend.

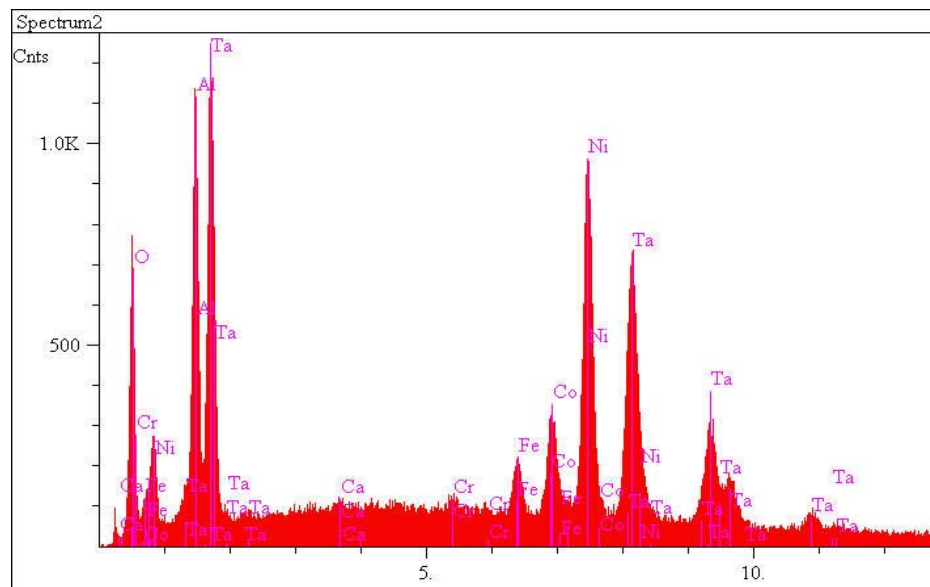


Figure 3-11. Energy Dispersive Spectrum of the deposit on test bar 11A (Uncoated PWA1484) after being oxidation tested for 504.5 hours using a DiEGME/Jet A blend.

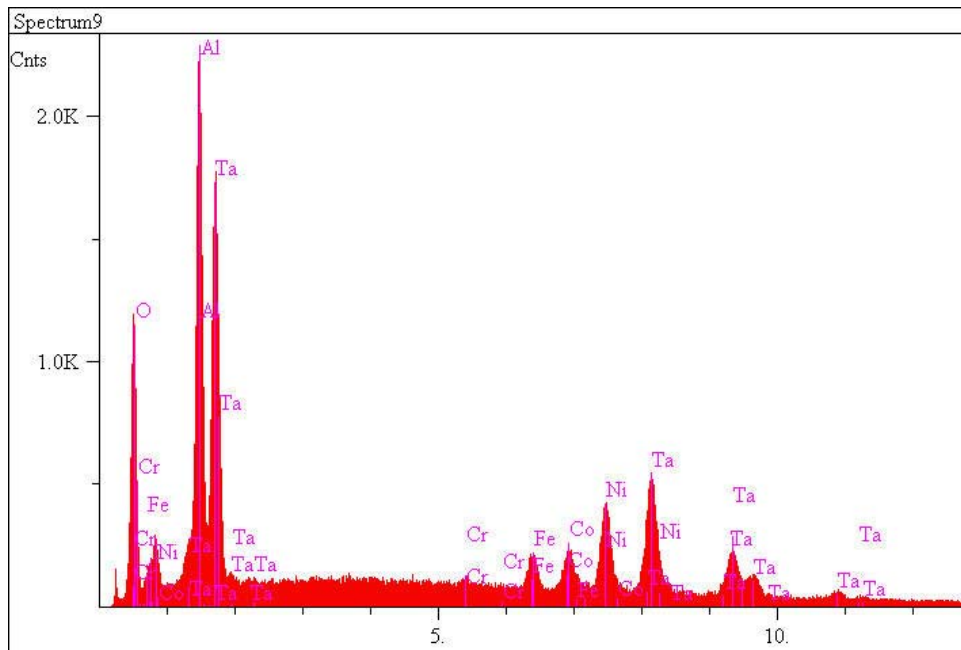


Figure 3-12. Energy Dispersive Spectrum of the deposit on test bar 11B (Uncoated PWA1484) after being oxidation tested for 502.5 hours using a TriEGME/Jet A blend.

3.1.2 Mass Change

Burner rig bars were weighed before and after the oxidation test. Table 3-1 and Figure 3-13 summarize the mass changes (grams) for the 1850°F (1010°C) cyclic oxidation tests.

Mass loss (negative weight change) was attributed to the metal oxide formation/exfoliation cycle on the surface of the test sample. Mass loss or mass loss per unit time can be used rank oxidation rate. A high oxidation rate (or mass loss) is undesirable due to metal loss.

Mass gain (positive weight change) was attributed to the formation of adherent oxides or the deposition of combustion by-products on the surface of the test samples. Large mass gains are undesirable in either case due to metal loss (conversion to oxide) or the build-up of foreign material on turbine surfaces.

Mass change results show that samples tested in the TriEGME/Jet A blend responded very similarly to samples tested using the DiEGME/Jet A blended baseline. Three test groups showed minor differences in mass loss between the two additive packages. Uncoated PWA 655 and uncoated PWA 1484 test samples showed slightly less mass loss for the TriEGME additive package, while the DiEGME additive was slightly better in mass loss for the PWA 275 coated PWA 1484 samples. These differences were considered minor and the additive blends were considered similar for this portion of the testing.

Table 3-1. Average percent mass change per oxidation hour for the DiEGME baseline (Test 1) and the TriEGME additive (Test 2) groups after 500 Hours of cyclic oxidation testing at 1850°F.

Average % Mass Change Per Oxidation Hour 1850°F Cyclic Oxidation Burner Rig Test			
Substrate	Coating	DiEGME	TriEGME
PWA 1484	PWA 275	1.12E-04	1.41E-04
PWA 1447	PWA 73	4.48E-05	5.24E-05
PWA 1447	PWA 286	9.99E-05	1.12E-04
PWA 655	Uncoated	-5.44E-05	-2.81E-05
PWA 1484	Uncoated	-1.31E-04	-7.72E-05
PWA 1447	Uncoated	-1.66E-05	-1.39E-05

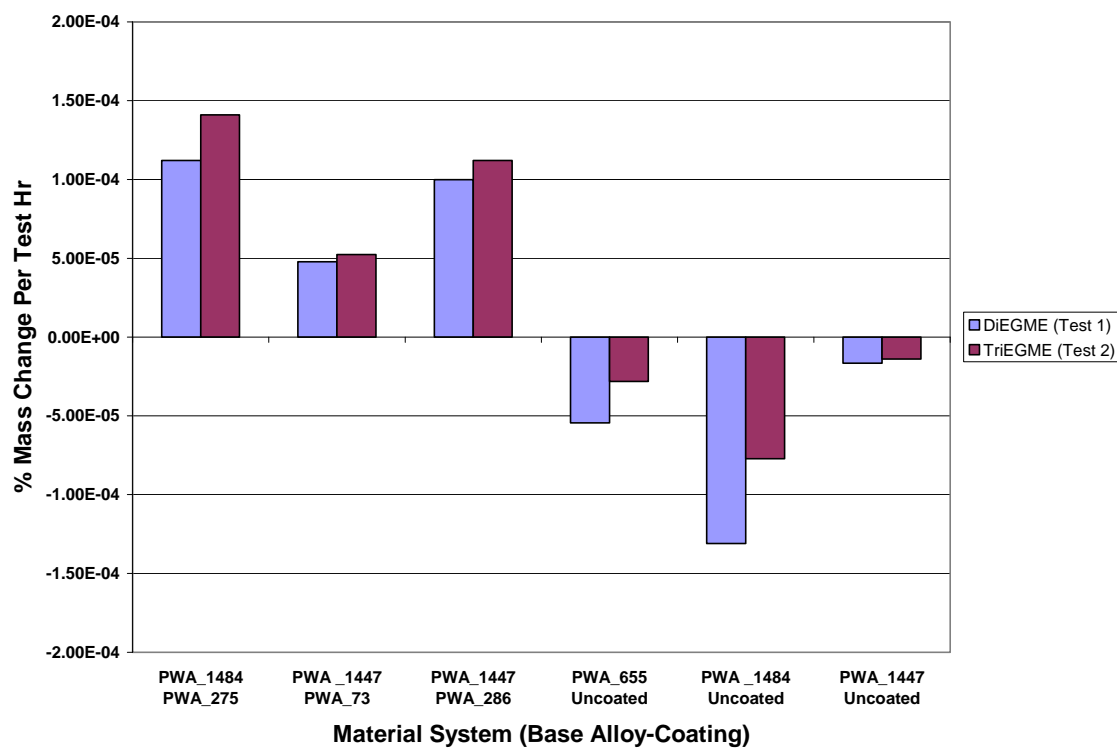


Figure 3-13. Average percent mass change per oxidation test hour for the DiEGME/Jet A blended baseline (Test 1) groups and the TriEGME/Jet A blended (Test 2) groups after 1850°F cyclic oxidation testing.

3.1.3 Dimensional Change

Burner Rig Bars were measured at three locations (2", 2½" and 3" from the bar base) across the leading edge (LE) and trailing edge (TE) dimension, before and after testing with vernier calipers. Figure 3-14 illustrates the measurement locations for the oxidation test bars.

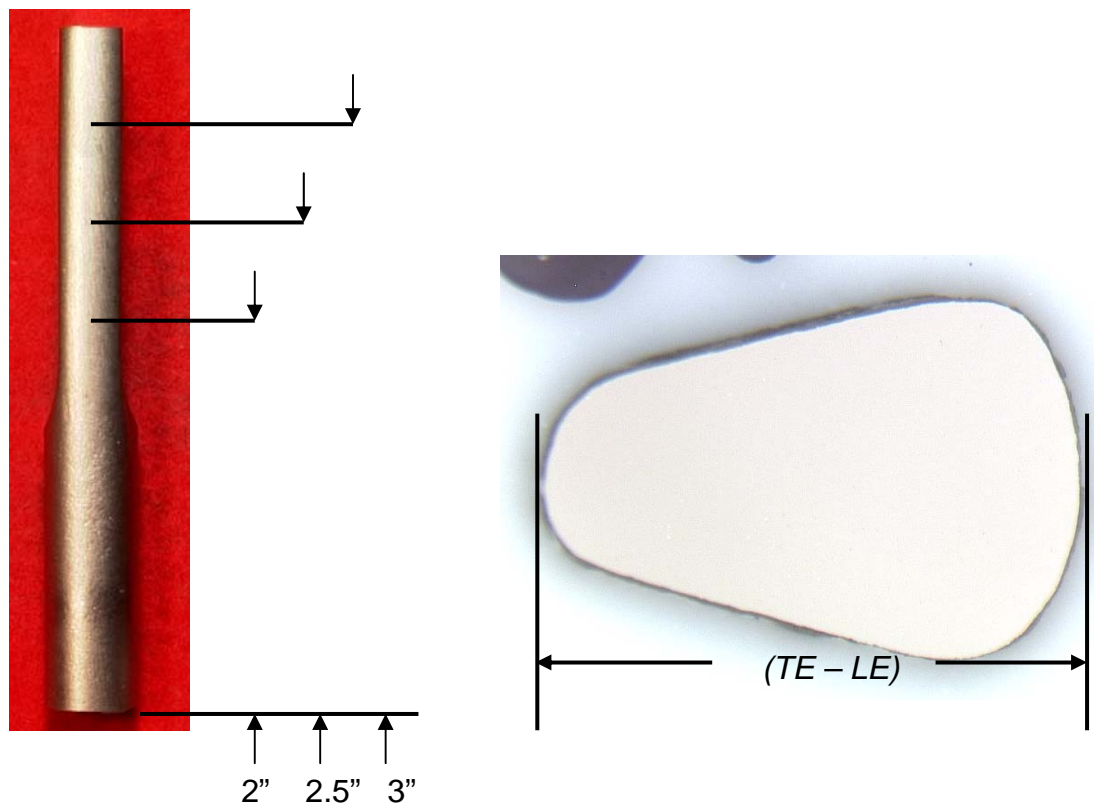


Figure 3-14. Burner rig bar measurement locations for the oxidation test bars.

As with mass loss, dimensional loss (negative dimensional change) was attributed to the metal oxide formation/exfoliation cycle on the surface of the test sample. Dimensional loss or dimensional loss per unit time can be used to rank oxidation rates. A high oxidation rate (or dimensional loss) is undesirable due to metal loss.

Again, as with mass gain, dimensional gain (positive dimensional change) was attributed to the formation of adherent oxides or the deposition of combustion by-products on the surface of the test samples. High dimensional gains are undesirable in either case due to metal loss (conversion to oxide) or the build-up of foreign material on turbine surfaces.

Dimensional changes were measured for each alloy/coating group tested with the DiEGME/Jet A blend and the TriEGME/Jet A blend. Table 3-2 and Figure 3-15 summarize the average dimensional changes for the 1850°F cyclic oxidation tests. Dimensional changes were considered similar if large differences were not found between the two test groups. Samples tested with the TriEGME additive blend were considered similar to samples tested with the DiEGME for the PWA 1484/PWA 275, PWA 1447/PWA 73, PWA 1447/PWA 286 and the uncoated PWA 655 samples. Minor differences were found for the uncoated PWA 1484 and uncoated PWA 1447 samples.

Table 3-2. Average percent dimensional change measured by vernier calibers for the DiEGME baseline (Test 1) and the TriEGME (Test 2) test groups after 500 Hours of cyclic oxidation testing at 1850°F.

Average % Dimensional Change Per Oxidation Test Hr 1850°F Cyclic Oxidation Burner Rig Test			
Substrate	Coating	DiEGME	TriEGME
PWA 1484	PWA 275	5.02e-04	4.36e-04
PWA 1447	PWA 73	3.70e-04	3.38e-04
PWA 1447	PWA 286	4.30e-04	4.32e-04
PWA 655	Uncoated	2.37e-04	2.37e-04
PWA 1484	Uncoated	4.37e-04	2.35e-04
PWA 1447	Uncoated	1.02e-04	2.38e-04

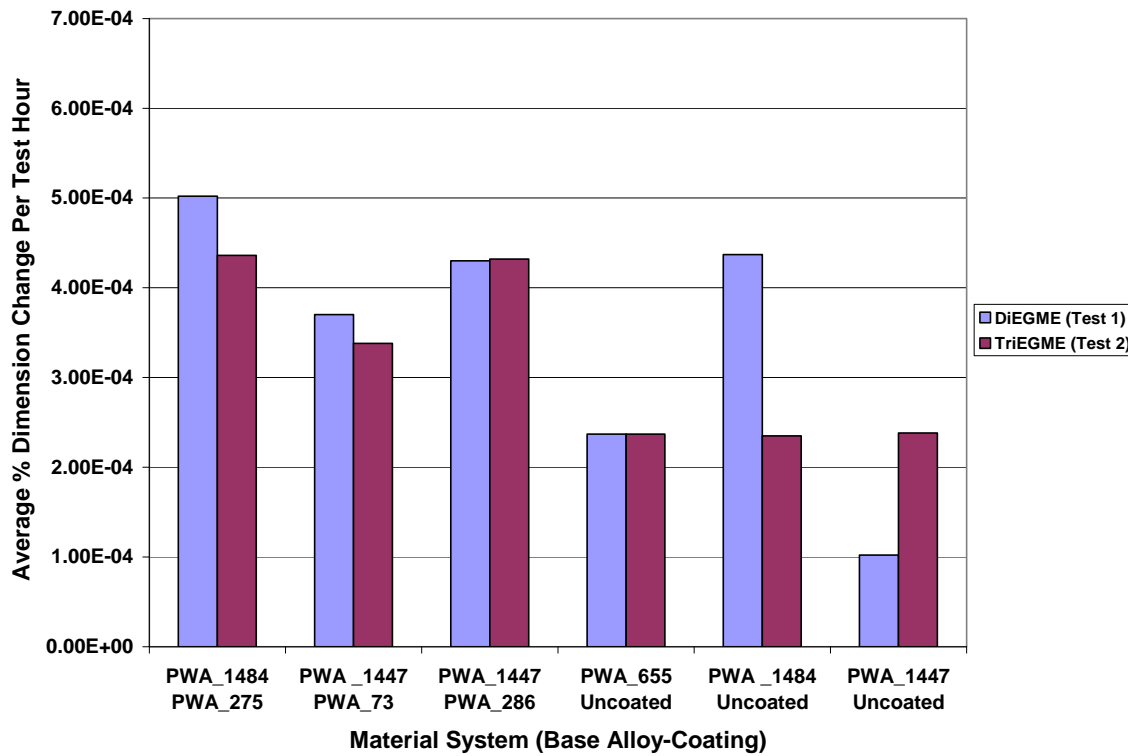


Figure 3-15. Average percent dimensional change per test hour for the DiEGME blended baseline (Test 1) and the TriEGME blended (Test 2) test groups after 500 hours of cyclic oxidation testing at 1850°F.

3.1.4 Microstructural Change

The effects of oxidation testing on dimensional change and weight change were minimal for both the DiEGME and TriEGME test pieces. Due to the minor oxidation changes found on the test samples, it was decided that the alloy/coating systems with the largest differences in dimensional change between the two additives would be sectioned through the hot zone and microstructurally evaluated. Two alloy groups, uncoated PWA 1484 and uncoated PWA 1447, were evaluated for both the DiEGME and TriEGME additives. Cross-sectional views comparing the microstructures of the etched test pieces are shown in Figures 3-16 to 3-19 with minimal differences found.

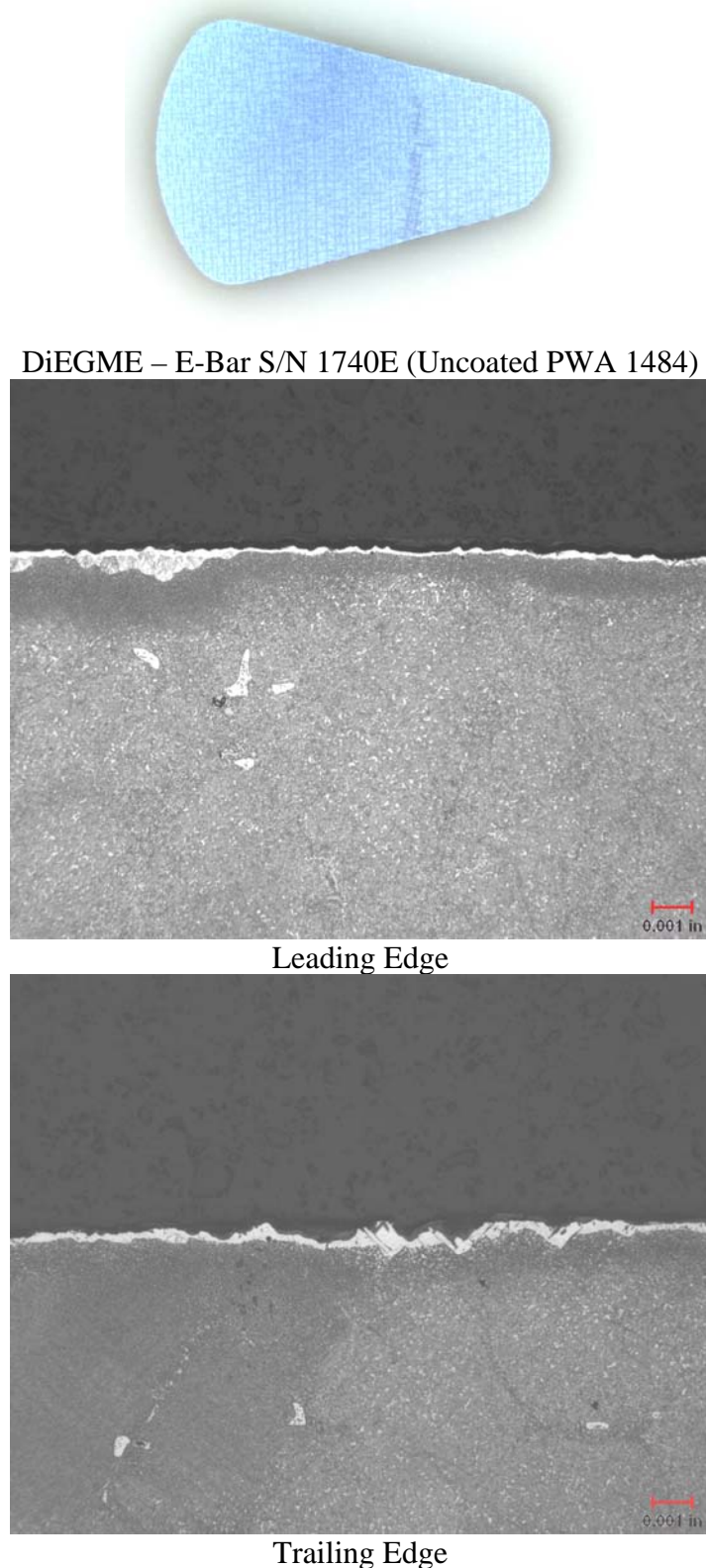


Figure 3-16. Cyclic oxidation photographs of specimen #5A (Uncoated PWA 1484), tested with a DiEGME/Jet A blend, after 504.5 Hours at 1850F.

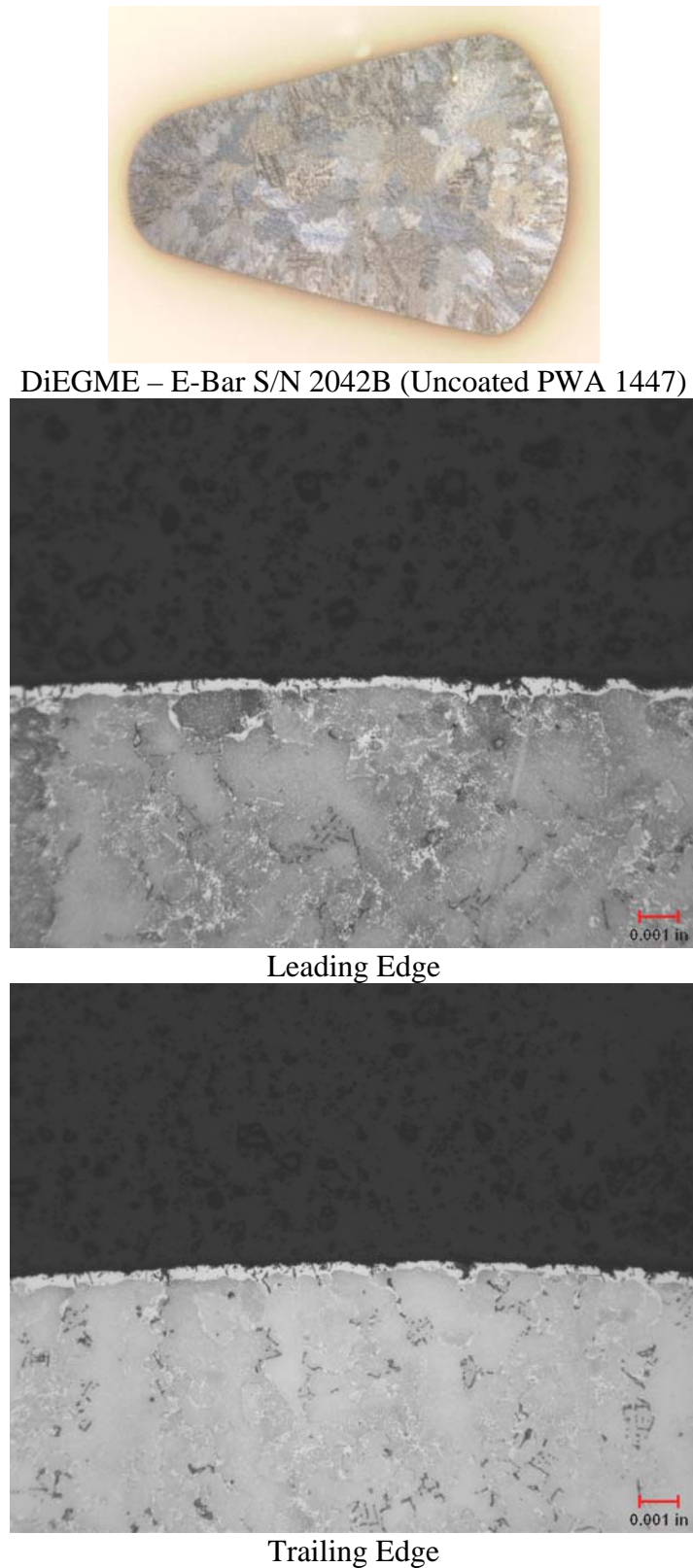


Figure 3-17. Cyclic oxidation photographs of specimen #8A (Uncoated PWA1447), tested with a DiEGME/Jet A blend, after 504.5 Hours at 1850F.

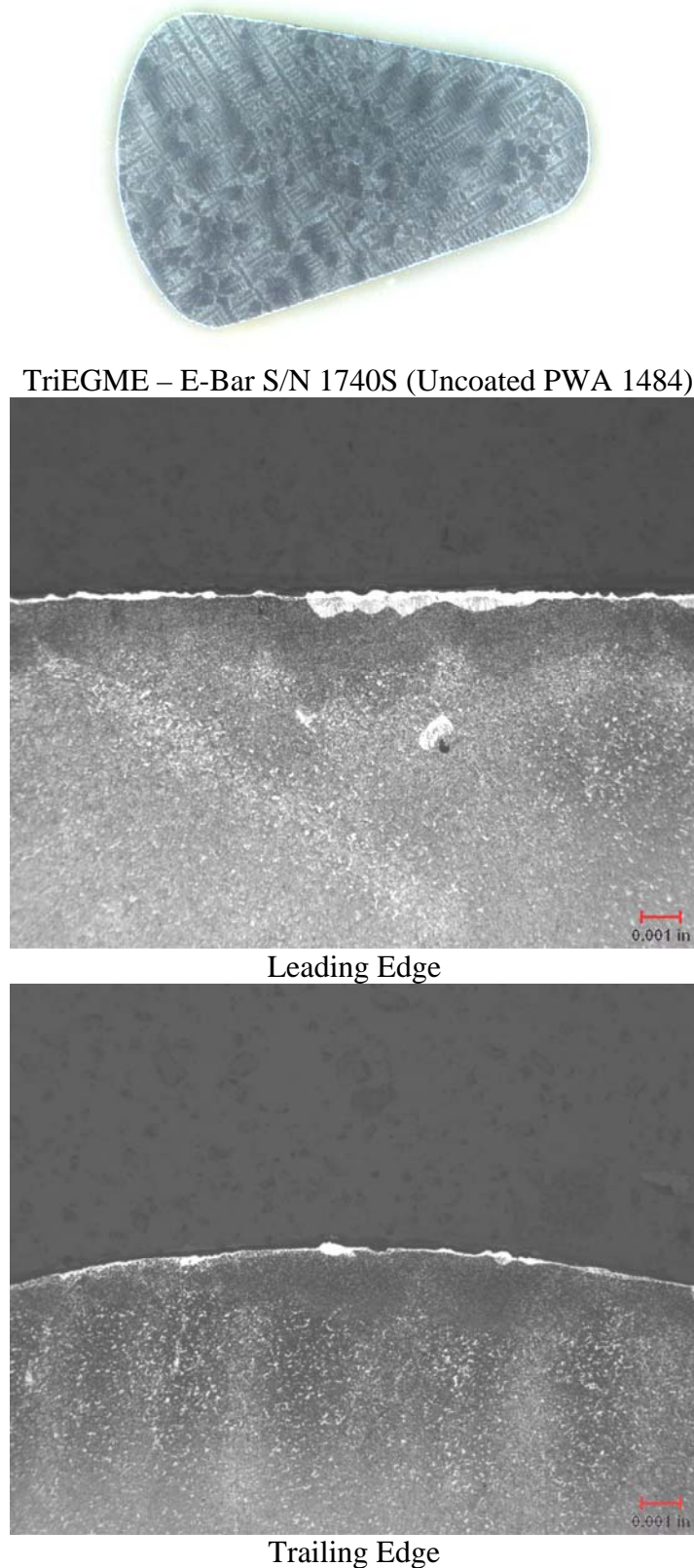


Figure 3-18. Cyclic oxidation photographs of specimen #5B (Uncoated PWA 1484), tested with a TriEGME/Jet A blend, after 502.5 Hours at 1850F.

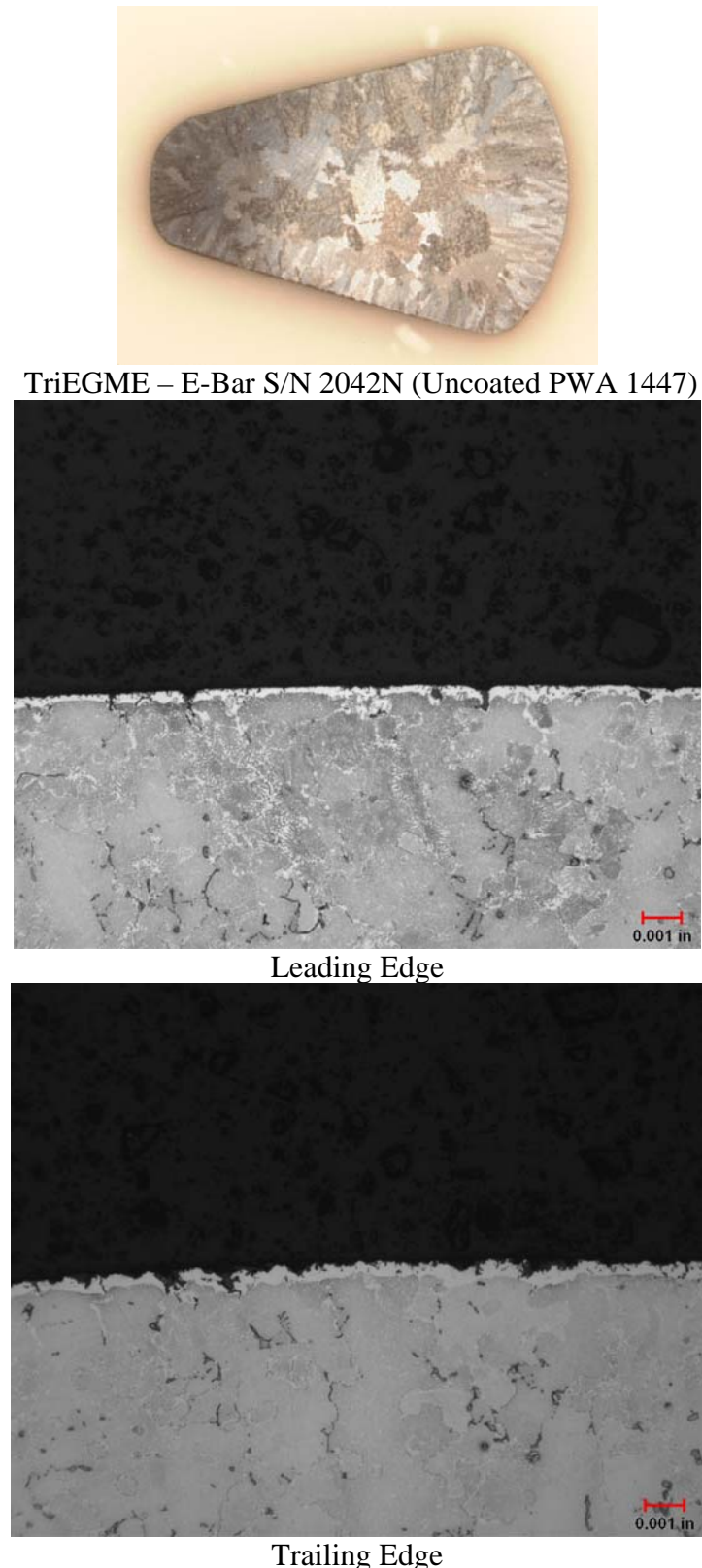


Figure 3-19. Cyclic oxidation photographs of specimen #8B (Uncoated PWA 1447), tested with a TriEGME/Jet A blend, after 502.5 Hours at 1850F.

3.1.5 Oxidation Conclusion

Oxidation test results showed that for the majority of alloy/coating combinations tested the TriEGME additive had minimal effect on sample mass change and thickness change when compared to the DiEGME baseline. The TriEGME test samples that showed slightly lower mass and thickness changes were for the uncoated PWA 1484 alloy. The uncoated PWA 1447 test samples showed minor increases in dimensional changes when tested with the TriEGME additive and compared to samples tested with the DiEGME additive; however the mass changes for this uncoated alloy were similar for both additives.

- PWA 1484 / PWA 275 – TriEGME Similar to DiEGME
- PWA 1447 / PWA 73 – TriEGME Similar to DiEGME
- PWA 1447 / PWA 286 – TriEGME Similar to DiEGME
- PWA 655 / Uncoated – TriEGME Similar to DiEGME
- PWA 1484 / Uncoated – TriEGME Slightly Better than DiEGME
- PWA 1447 / Uncoated – TriEGME Slightly Worse than DiEGME
- TriEGME Oxide/Deposit Lighter In Color Than DiEGME Oxide/Deposit

3.2 Hot Corrosion

3.2.1 Isothermal Hot Corrosion

Hot corrosion testing was performed concurrently on two identical burner rigs with the only difference being the fuel additive tested. The DiEGME/ Jet A blend was considered the test baseline and the TriEGME/Jet A blend the experimental mixture. Figures 3-20 to 3-23 show macro photos of the DiEGME/Jet A blended baseline specimens after 500 hours of hot corrosion testing. Figures 3-24 to 3-27 show macro photos of the TriEGME/Jet A blended specimens after 500.85 hours of hot corrosion testing. The numbers superimposed on the bottom of the photos correspond to the sample numbers (specimen ID) given in Table 2-3.

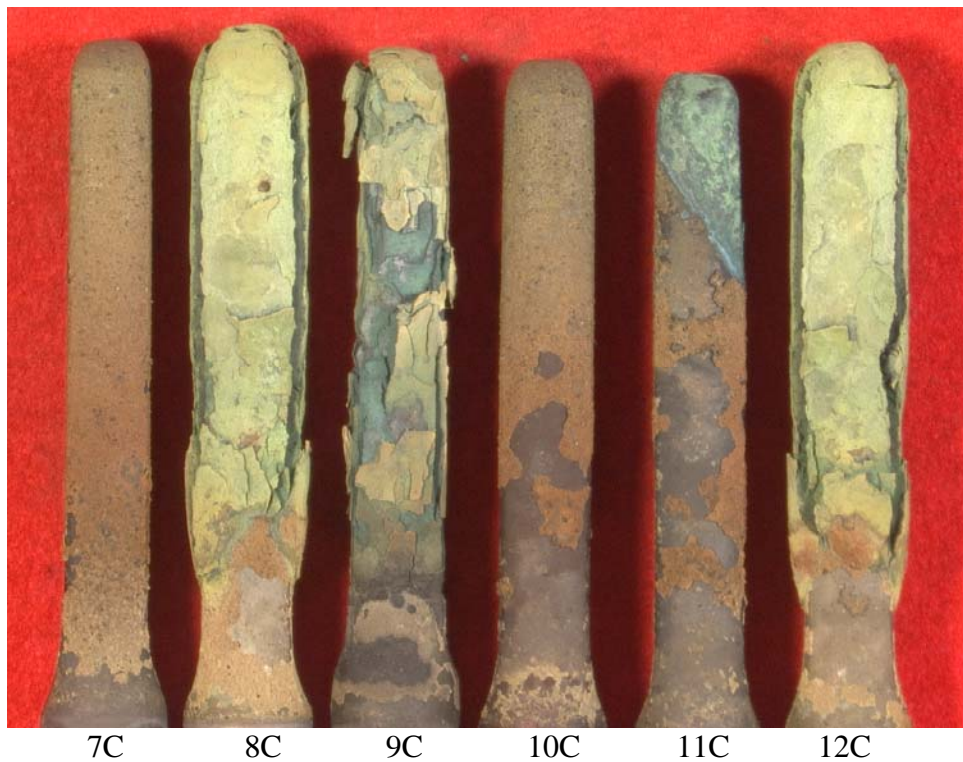
The hot corrosion tests resulted in the alloys/coatings changing colors and textures. The corrosion effects shown on both the DiEGME and TriEGME test samples were typical of the alloy and coating combinations tested. The voluminous growth of the outer alloy surface or the cracking and spallation of the outer corrodant zone was also typical of a hot corrosion test. Due to the large changes (measured thickness and mass) that occurred on the hot corrosion test samples, it is very important not to prematurely come to a conclusion based on either measured mass or thickness changes. A combination of mass change, dimension change, visual inspections and post-test cross sectional analysis of the remaining parent material is needed to provide an accurate comparison of the fuel additives.



1C 2C 3C 4C 5C 6C

1C.	2161 Y	PWA 1447/PWA 286
2C.	2160 E	PWA 663/PWA 73
3C.	2158 M	PWA 655/PWA 73
4C.	2161 H	PWA 1447/PWA 73
5C.	1641 L	PWA 1484/Polished
6C.	2158 K	PWA 655/PWA 73

Figure 3-20. Test 3: DiEGME/Jet A blended fuel test bars (baseline) after 500 hours of 1600°F isothermal hot corrosion testing with 3.5 ppm salt—Leading edge view.



7C.	2161R	PWA 1447/PWA 73
8C.	2158I	PWA 655/Polished
9C.	2043E	PWA 1455/Polished
10C.	2161H	PWA 1447/PWA 286
11C.	2160H	PWA 663/PWA 73
12C.	2058P	PWA 655/Polished

Figure 3-21. Test 3: DiEGME/Jet A blended fuel test bars (baseline) after 500 hours of 1600°F isothermal hot corrosion testing with 3.5 ppm salt – Leading edge view.

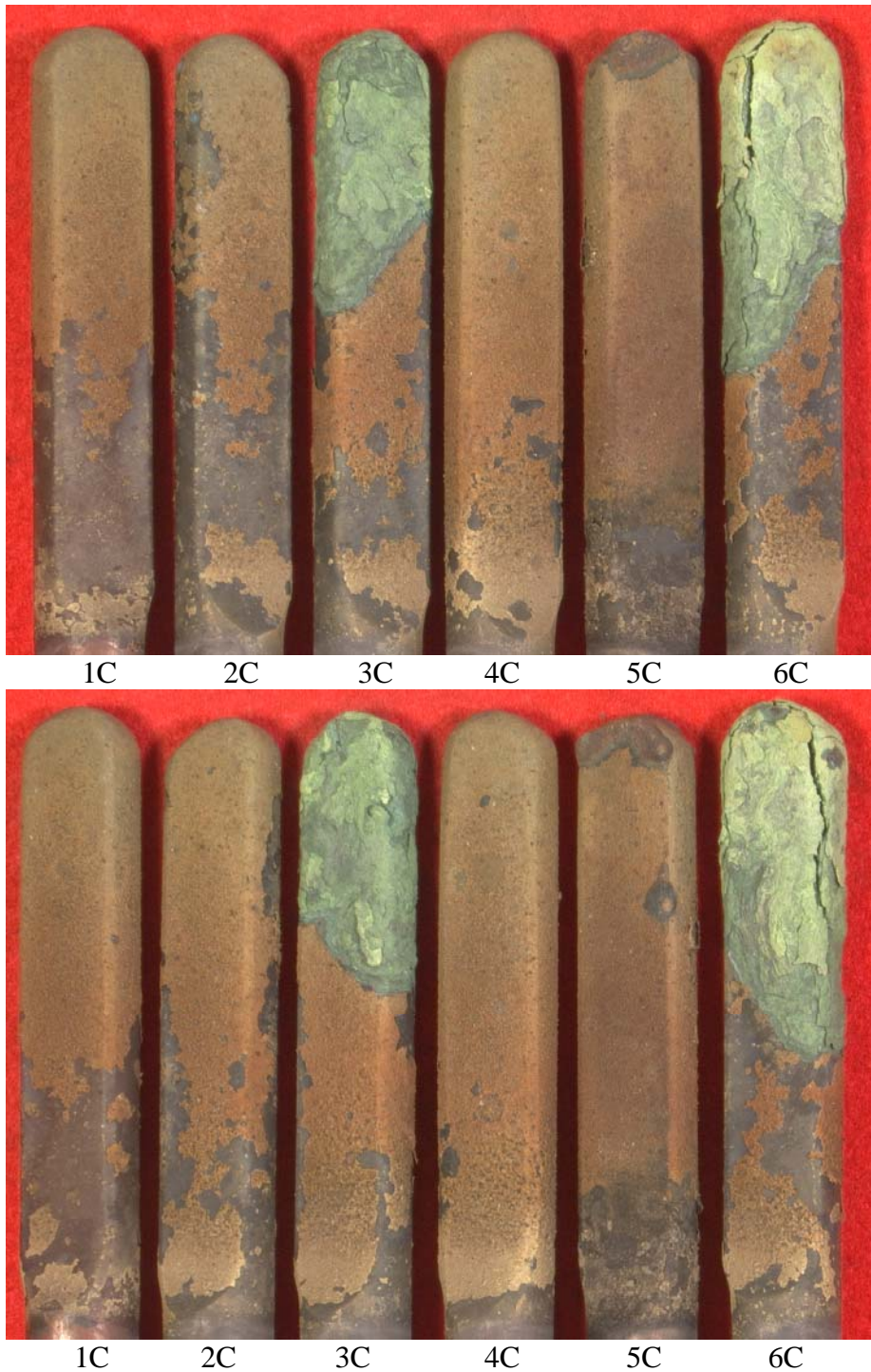


Figure 3-22. Test 3: DiEGME/Jet A blended fuel test bars (baseline) after 500 hours of 1600°F isothermal hot corrosion testing with 3.5 ppm salt – Side view.

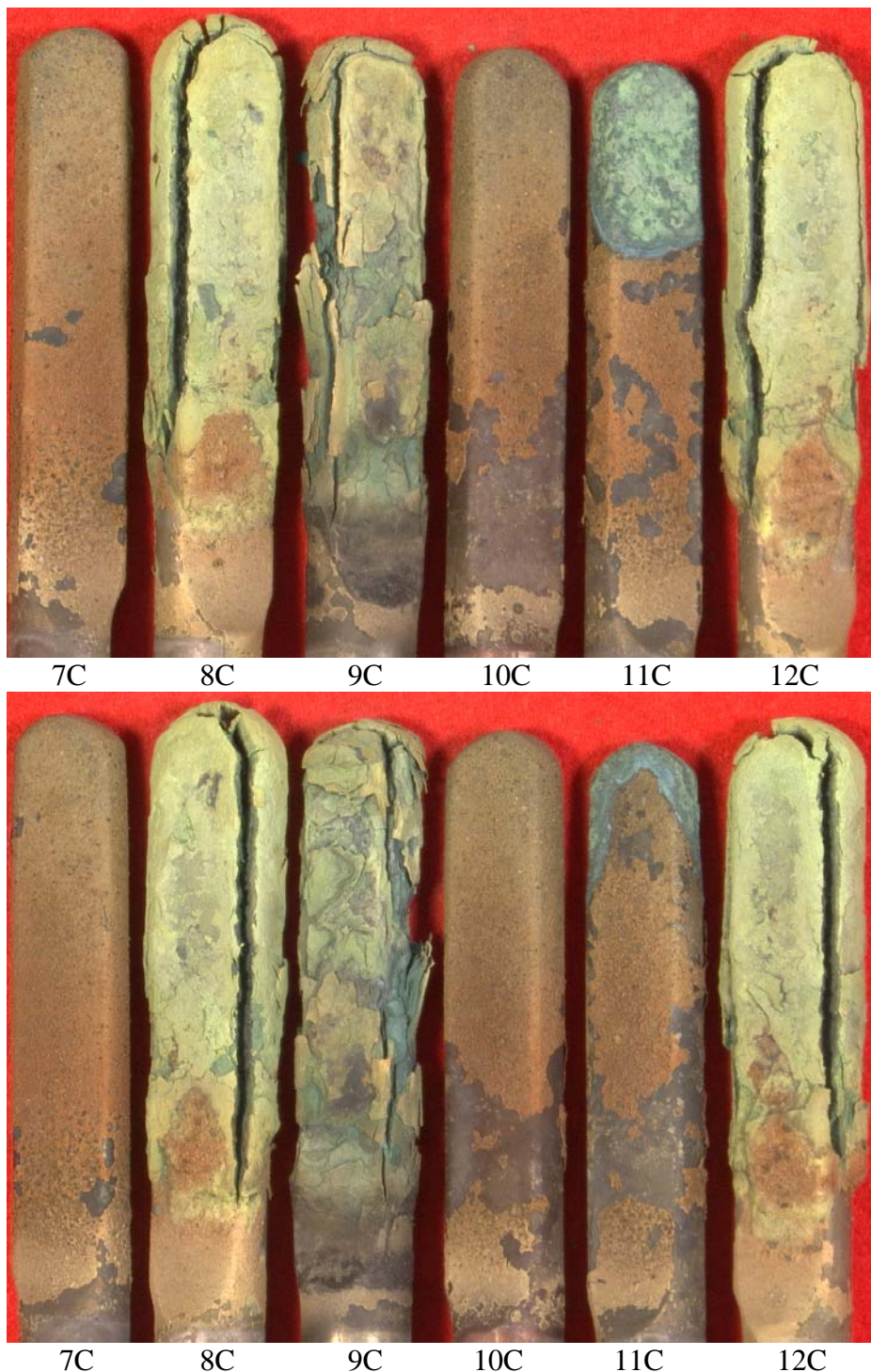
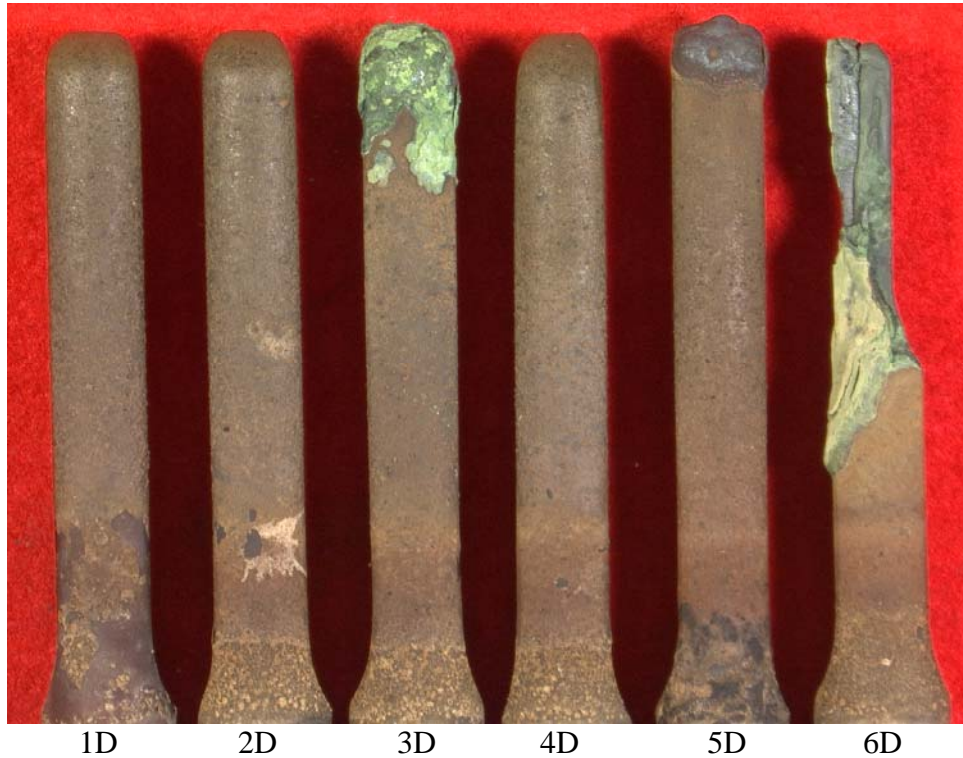


Figure 3-23. Test 3: DiEGME/Jet A blended fuel test bars (baseline) after 500 hours of 1600°F isothermal hot corrosion testing with 3.5 ppm salt – Side view.



1D.	2161 S	PWA 1447/PWA 286
2D.	2160 A	PWA 663/PWA 73
3D.	2158 L	PWA 655/PWA 73
4D.	2161 K	PWA 1447/PWA 73
5D.	1641 D	PWA 1484/Polished
6D.	2158 A	PWA 655/Polished

Figure 3-24. Test 4: TriEGME additive/Jet A blended fuel test bars after 500.85 hours of 1600°F isothermal hot corrosion testing with 3.5 ppm salt — Leading edge view.



7D 8D 9D 10D 11D 12D

7D.	2161 Q	PWA 1447/PWA 73
8D.	2158 J	PWA 655/PWA 73
9D.	2043 F	PWA 1455/Polished
10D.	2161 J	PWA 1447/PWA 286
11D.	2160 C	PWA 663/PWA 73
12D.	2058 G	PWA 655/Polished

Figure 3-25. Test 4: TriEGME additive/Jet A blended fuel test bars after 500.85 hours of 1600°F isothermal hot corrosion testing with 3.5 ppm salt – Leading edge view.

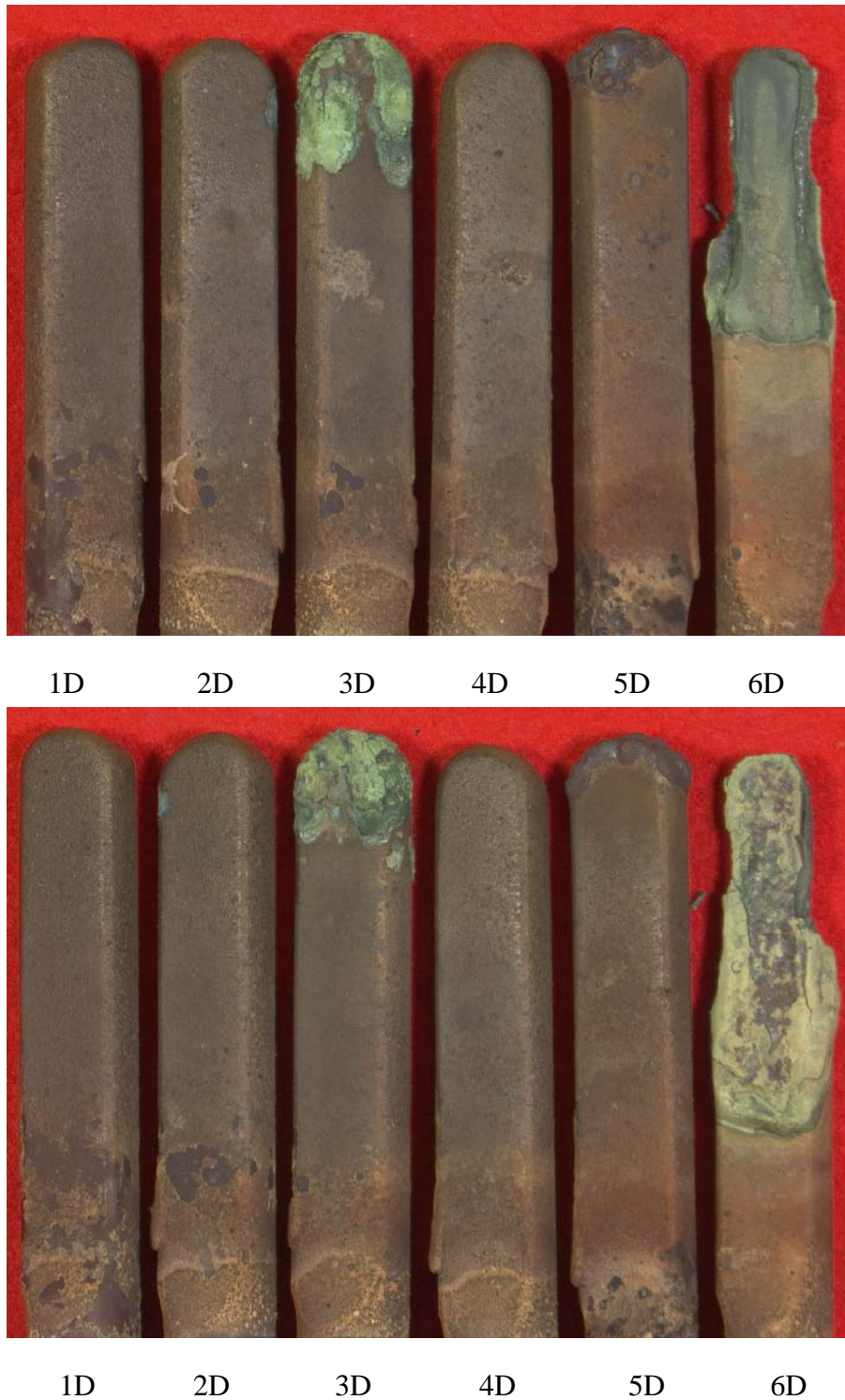


Figure 3-26. Test 4: TriEGME additive/Jet A blended fuel test bars after 500.85 hours of 1600°F isothermal hot corrosion testing with 3.5 ppm salt – Side view.

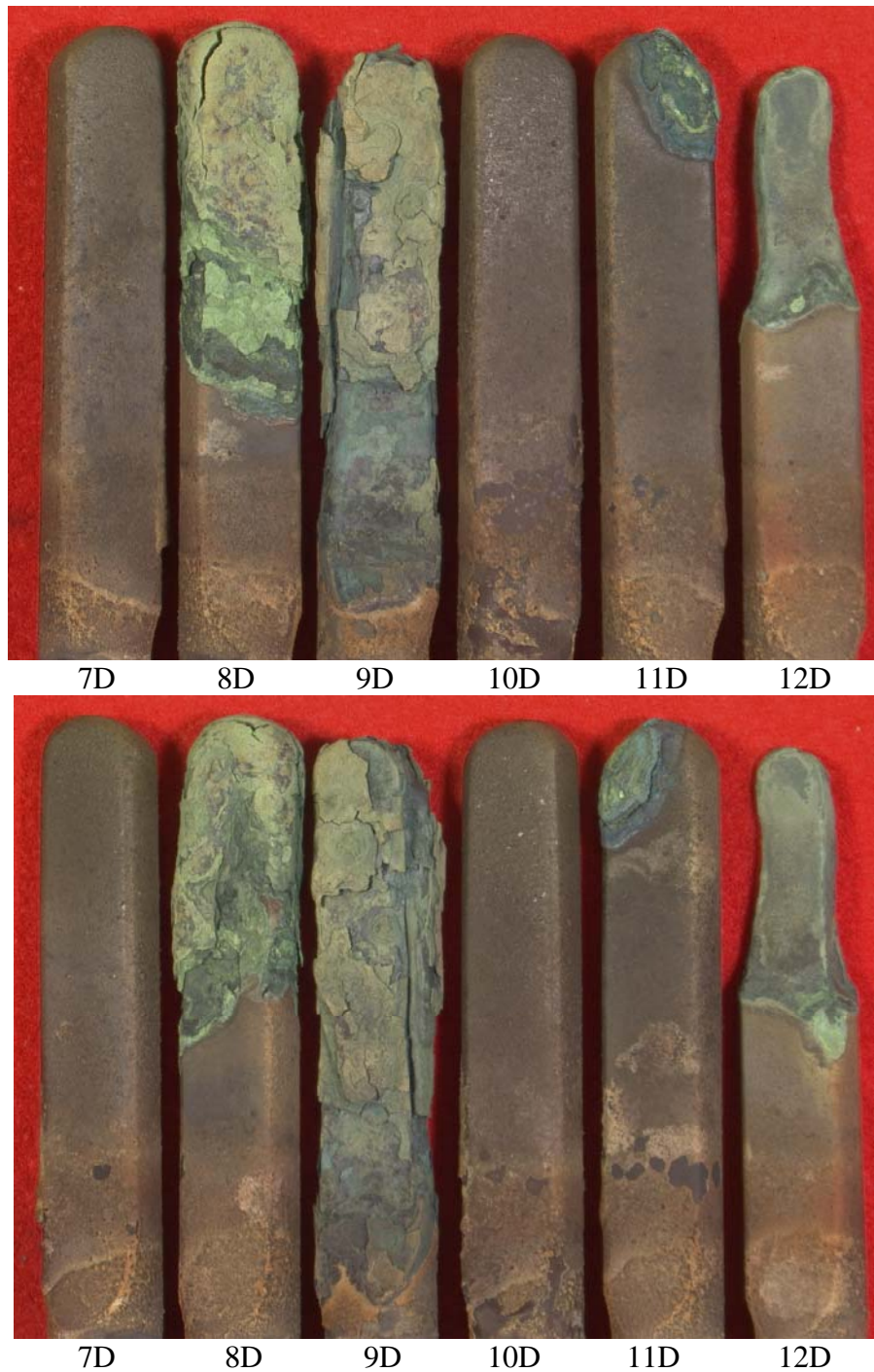


Figure 3-27. *Test 4: TriEGME additive/Jet A blended fuel test bars after 500.85 hours of 1600°F isothermal hot corrosion testing with 3.5 ppm salt – Side view.*

3.2.2 Mass Change

Burner rig bars were weighed before and after the corrosion test. Table 3-3 and Figure 3-28 summarize the mass change for the 1600°F isothermal hot corrosion tests with a 3.5 ppm salt addition after 500 hours. Mass loss (negative weight change) was attributed to the metal corrosion product formation/exfoliation cycle on the surface of the test sample. Mass loss or mass loss per unit time can be used to rank corrosion rate. A high corrosion rate (or mass loss) is undesirable due to metal loss.

Mass gain (positive weight change) was attributed to the formation of adherent corrosion products or the deposition of combustion by-products on the surface of the test samples. High mass gains are undesirable in either case due to metal loss (conversion to corrosion products) or the build-up of foreign material on turbine surfaces.

Burner rig bars tested in isothermal hot corrosion tests show vastly different appearances and greater mass changes than burner rig bars tested in oxidation. For corrosion testing of the DiEGME and TriEGME additives, the alloy/coating combinations that yielded similar mass change rates were for the following combinations: PWA 1447/PWA286, PWA 663/PWA 73, PWA655/PWA 73, PWA 1447/PWA 73 and uncoated PWA 1484. The substrate/coating systems that required additional investigation were the uncoated PWA 655 and uncoated PWA 1455 systems as these systems showed large differences in mass change rates between the two additive mixtures.

Table 3-3. The average percent mass change per corrosion hour for the DiEGME/Jet A blended baseline samples (Test 3) and the TriEGME/Jet A blended (Test 4) samples after 1600°F isothermal hot corrosion testing with 3.5 ppm salt.

Average % Mass Change Per Corrosion Hour 1600°F Isothermal Hot Corrosion Burner Rig Test			
Substrate	Coating	DiEGME	TriEGME
PWA 1447	PWA 286	7.56e-04	5.71e-04
PWA 663	PWA 73	-1.26e-03	6.28e-04
PWA 655	PWA 73	-1.45e-03	-9.84e-04
PWA 1447	PWA 73	1.14e-03	9.27e-04
PWA 1484	Uncoated	1.20e-03	1.12e-03
PWA 655	Uncoated	7.54e-03	-3.71e-02
PWA 1455	Uncoated	-1.53e-02	-2.55e-02

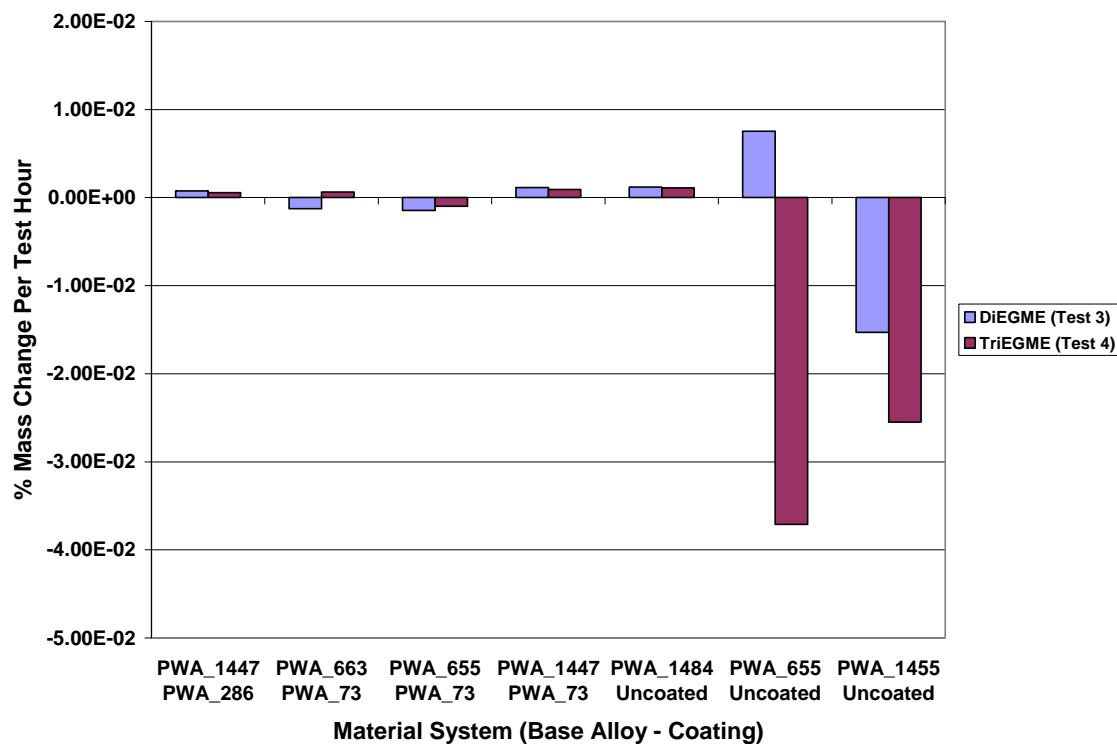


Figure 3-28. The average relative mass change per test hour for the DiEGME/Jet A blended baseline samples (Test 3) and the TriEGME/Jet A blended (Test 4) samples after 1600°F isothermal hot corrosion testing with 3.5 ppm salt.

3.2.3 Dimensional Change

Burner Rig Bars were measured with vernier calipers at three locations (1.87", 2.3", and 2.85" from the bar butt) across the leading edge (LE) trailing edge (TE) dimension, before and after testing. Figure 3-29 illustrates the measuring locations for the corrosion test samples.

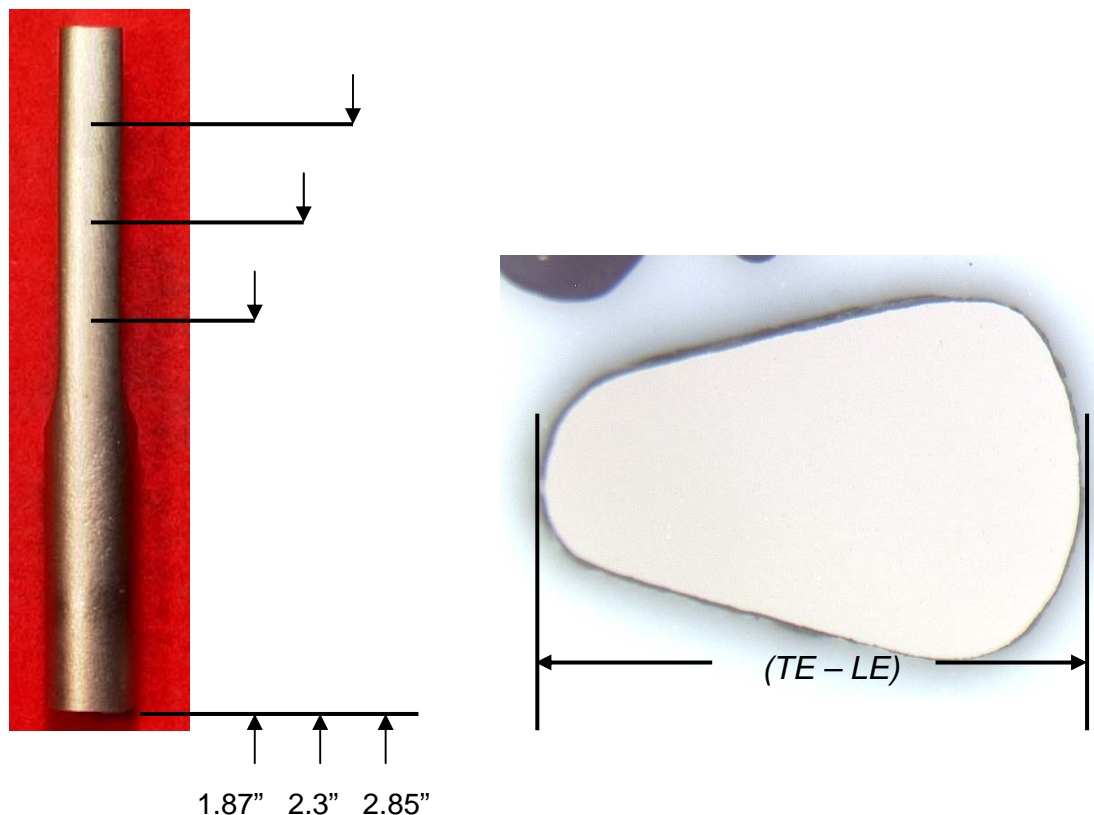


Figure 3-29. Burner rig bar measurement locations for the hot corrosion test bars.

Table 3-4 and Figure 3-30 summarize the average dimensional changes (mils) after 500 hours for the 1600°F isothermal hot corrosion 3.5 ppm salt burner rig test. Large dimensional changes that were the result of bars that had split and expanded, corroded unevenly or had chunks of material missing are not included in Table 3-4.

As with mass loss, dimensional loss (negative dimensional change) was attributed to the corrosion product formation/exfoliation cycle on the surface of the test sample. Dimensional loss or dimensional loss per unit time can be used rank corrosion rate. A high corrosion rate (or dimensional loss) is undesirable due to metal loss.

Again, as with mass gain, dimensional gain (positive dimensional change) was attributed to the formation of adherent corrosion products, the cracking and expansion of the alloy or the deposition of combustion by-products on the surface of the test samples. High dimensional gains are undesirable in either case due to metal loss (conversion to corrosion products) or the build-up of foreign material on turbine surfaces.

The test bars that were able to be measured showed that the dimensional changes associated with the TriEGME additive were similar or slightly better than the test bars run with the DiEGME additive. Due to the severity of damage done to the unmeasured samples, thickness changes should not be used to rank fuel additives. Mass changes, dimensional changes, visual observations and post test microstructural analysis should be used in combination to determine the effect of the TriEGME additive.

Table 3-4. Average percent dimensional change for the DiEGME/Jet A blended baseline (Test 3) and the TriEGME/Jet A blend (Test 4) after 500 hours of 1600°F hot isothermal corrosion testing with 3.5 ppm salt.

Average Percent Dimensional Change Per Test Hour - 1600°F Isothermal Hot Corrosion 3.5 ppm Salt Burner Rig Test - 500 Hours			
Base Alloy	Coating	DiEGME	TriEGME
PWA 1447	PWA 286	3.23e-03	3.72e-03
PWA 1447	PWA 73	4.82e-03	4.00e-03
PWA 663	PWA 73	NA	2.62e-03
PWA 655	PWA 73	NA	NA
PWA 655	Uncoated	NA	NA
PWA 1484	Uncoated	4.86e-03	3.36e-03
PWA 1455	Uncoated	NA	NA

Note: Only test bars that had not split/expanded, lost chunks or corroded heavily were included.

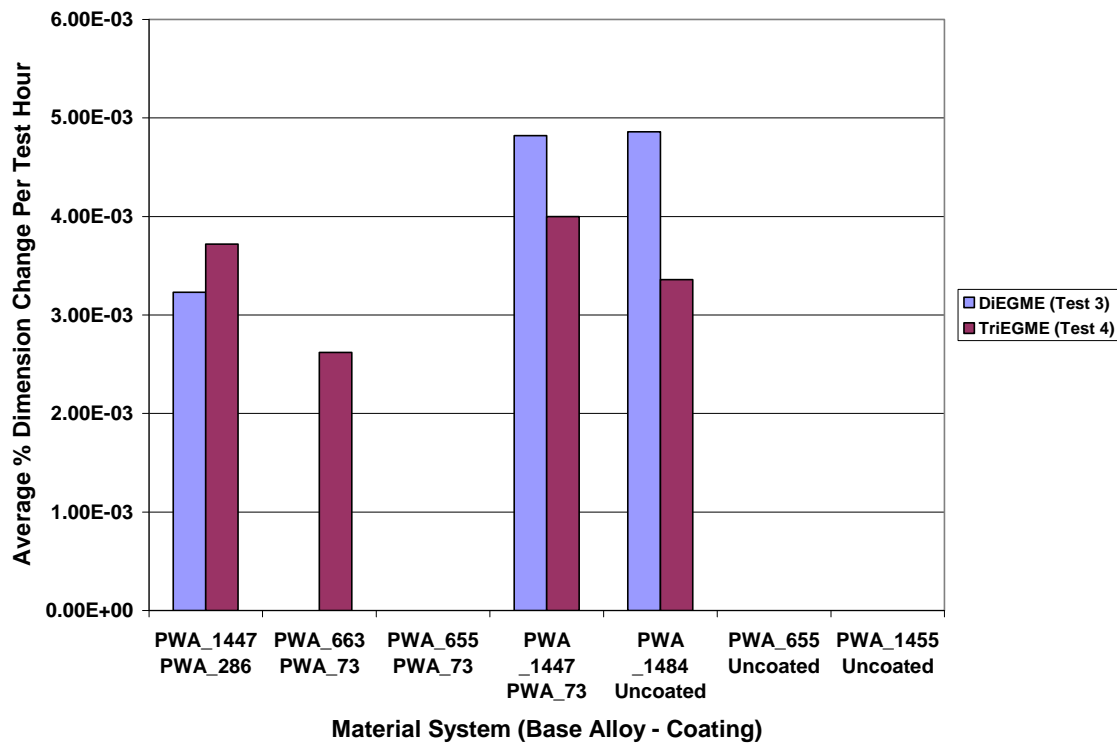


Figure 3-30. Average percent dimensional change per hot corrosion test hour measured by vernier calipers for the DiEGME/Jet A blended baseline (Test 3) and the TriEGME/Jet A blend (Test 4) after hot isothermal corrosion testing with 3.5 ppm salt. Note: Test bars that had split, lost chunks or corroded heavily were not included.

3.2.4 Visual Change

Burner rig groups (PWA 663/PWA 73, PWA 655/PWA 73, PWA 655/Uncoated & PWA 1455/Uncoated) that were not characterized by caliper measurements due to corrosion, severe expansion or non-uniform metal loss were compared by earlier test photographs. Test photographs were taken approximately every 100 hours for each of the additive groups and the photographs compared every 100 hours up to the 500 hour mark. Alloy/coating groups were considered failed when deep substrate cracks appeared. Figures 3-31 to 3-38 show the degradation of the coating/alloy systems as a function of hot corrosion test time.

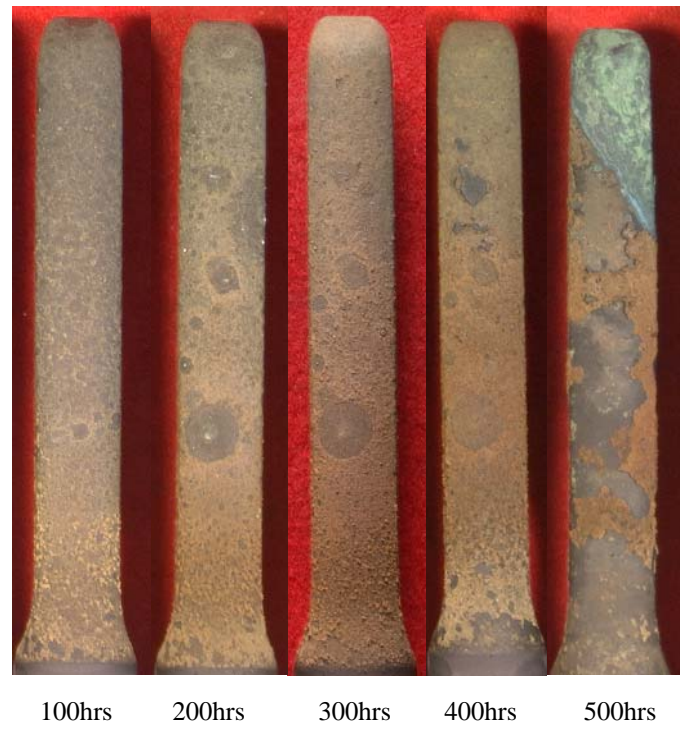


Figure 3-31. The effects of DiEGME/Jet A blended baseline on the leading edge of test bar 11C (PWA 663/PWA 73) after hot corrosion testing for 100, 200, 300, 400 and 500 hours at 1600°F with 3.5ppm salt.

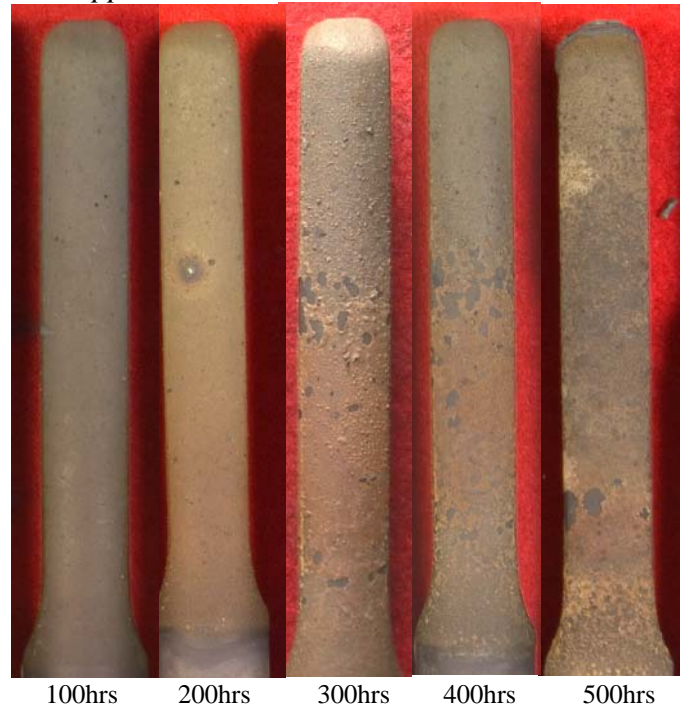


Figure 3-32. The effects of TriEGME/Jet A blended mixture on the leading edge of test bar 11D (PWA 663/PWA 73) after hot corrosion testing for 100, 200, 300, 400 and 500 hours at 1600°F with 3.5ppm salt.

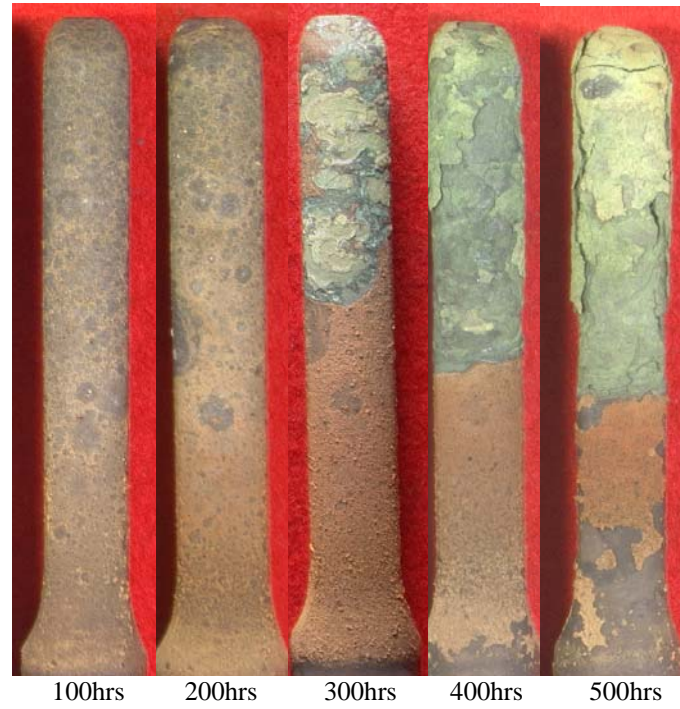


Figure 3-33. The effects of DiEGME/Jet A blended baseline on the leading edge of test bar 6C (PWA 655/PWA 73) after corrosion testing for 100, 200, 300, 400 and 500 hours at 1600°F with 3.5 ppm salt.

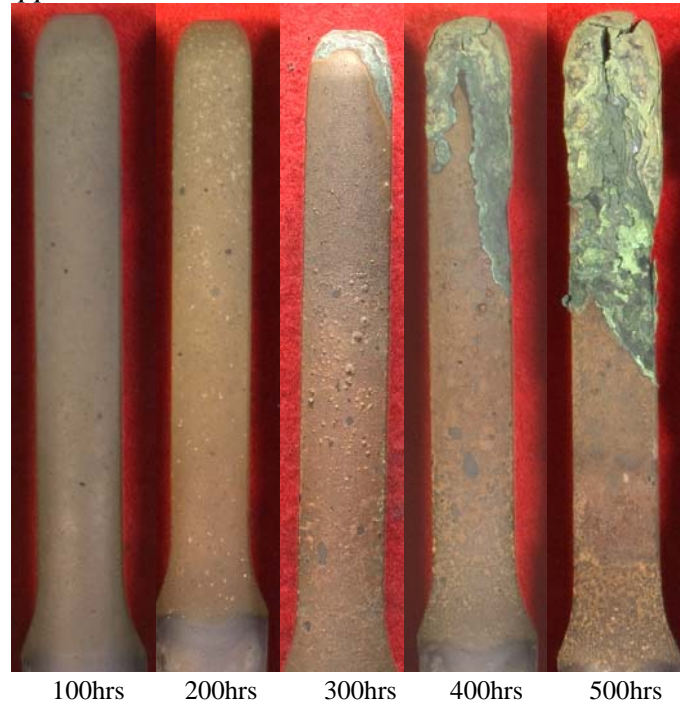


Figure 3-34. The effects of TriEGME/Jet A blended mixture on the leading edge of test bar 8D (PWA 655/PWA 73) after corrosion testing for 100, 200, 300, 400 and 500 hours at 1600°F with 3.5 ppm salt.

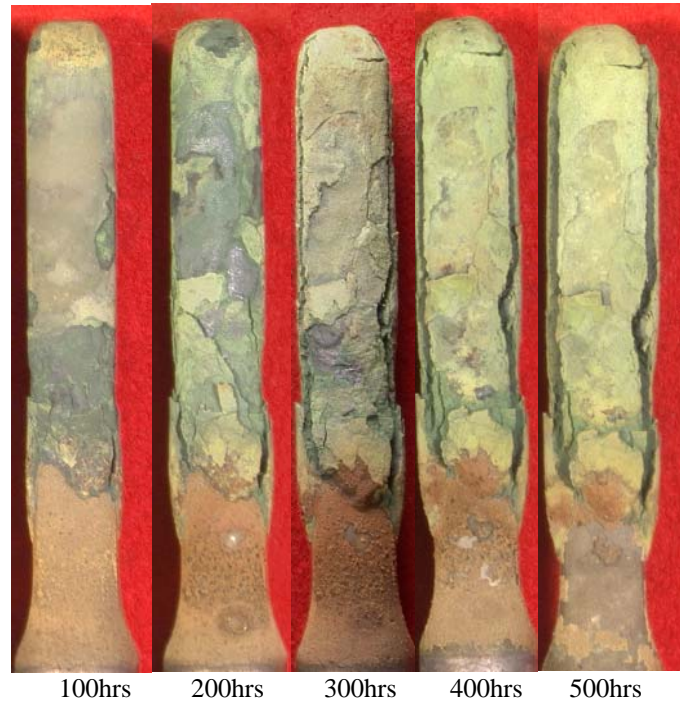


Figure 3-35. The effects of DiEGME/Jet A blended baseline on the leading edge of test bar 12C (PWA 655/Uncoated) after corrosion testing for 100, 200, 300, 400 and 500 hours at 1600°F with 3.5 ppm salt.

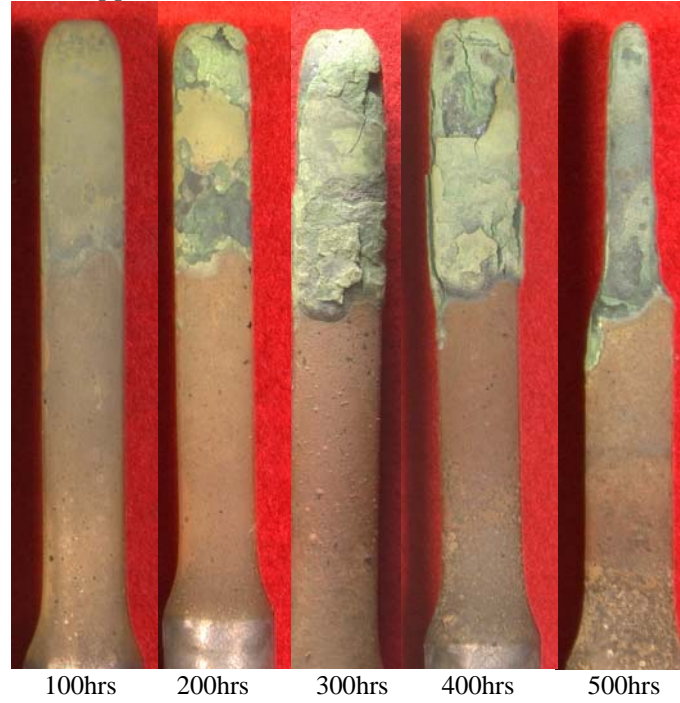


Figure 3-36. The effects of TriEGME/Jet A blended mixture on the leading edge of test bar 12D (PWA 655/Uncoated) after corrosion testing for 100, 200, 300, 400 and 500 hours at 1600°F with 3.5 ppm salt.

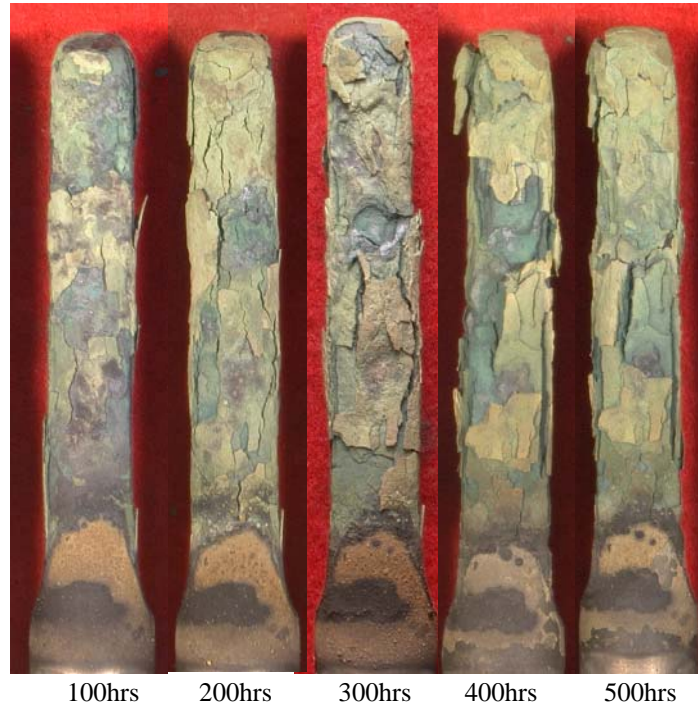


Figure 3-37. The effects of DiEGME/Jet A blended baseline on the leading edge of test bar 9C (PWA 1455/Uncoated) after corrosion testing for 100, 200, 300, 400 and 500 hours at 1600°F with 3.5 ppm salt.

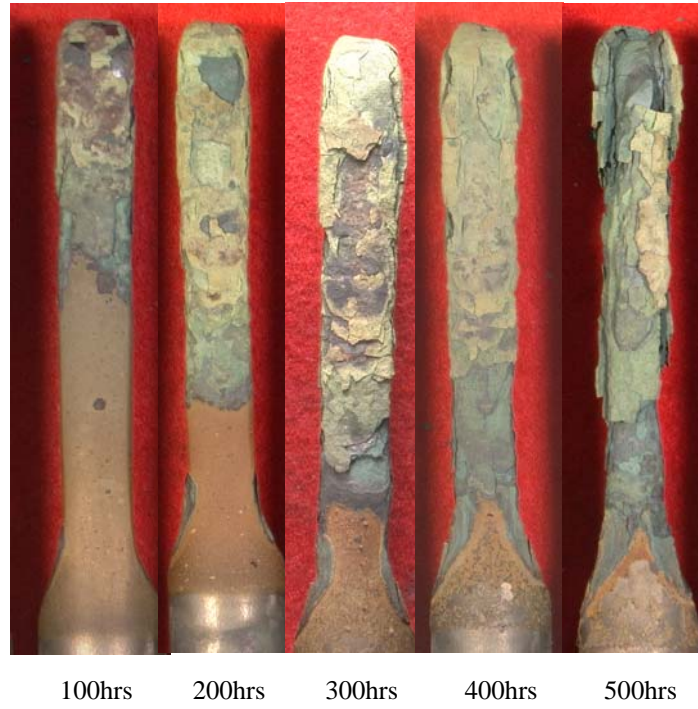


Figure 3-38. The effects of TriEGME/Jet A blended mixture on the leading edge of test bar 9D (PWA 1455/Uncoated) after corrosion testing for 100, 200, 300, 400 and 500 hours at 1600°F with 3.5 ppm salt.

Visual observations of the effects of fuel additives on PWA 663/PWA 73, PWA 655/PWA 73, PWA 655/Uncoated and PWA 1455/Uncoated are summarized in Table 3-5.

Table 3-5. Visual change observations for the DiEGME/Jet A baseline (Test 3) and the TriEGME/Jet A additive (Test 4) groups after 1600°F isothermal hot corrosion burner rig testing with 3.5 ppm salt for 500 hours.

Visual Change Observations - 1600°F Isothermal Hot Corrosion Burner Rig Test with 3.5 ppm Salt			
Base Alloy	Coating	DiEGME	TriEGME
PWA 663	PWA 73	Slight Corrosion at 500hrs	Start of Tip Corrosion at 500 hrs
PWA 655	PWA 73	Substrate Cracks at 500 hrs	Initial Substrate Tip Crack at 400 hrs
PWA 655	Uncoated	Initial Substrate Crack at 200 hrs	Initial Substrate Crack at 400 hrs
PWA 1455	Uncoated	Initial Substrate Crack ~100 hrs-200hrs	Initial Substrate Crack ~100 hrs-200hrs

3.2.5 Microstructural Change

Post-test microstructural analysis was performed on each alloy/coating combination for both the DiEGME and TriEGME corrosion test groups. Test bars were sectioned in representative areas, mounted in epoxy media, polished and photographed. Figures 3-39 to 3-52 show the locations of the cross section cut and the representative cross section after 500 hours of hot corrosion testing at 1600°F with additions of 3.5ppm salt. Alloy/coating groups PWA 1447/PWA 286, PWA 1447/PWA 73 and PWA 1484/Uncoated were examined and found to have minimal hot corrosion attack. Alloy/Coating groups PWA 663/PWA 73, PWA 655/PWA 73, PWA 655/Uncoated and PWA 1455/Uncoated were found to have significant hot corrosion attack. Post-test alloy

readings were taken to measure the parent material loss for these alloy/coating combinations.

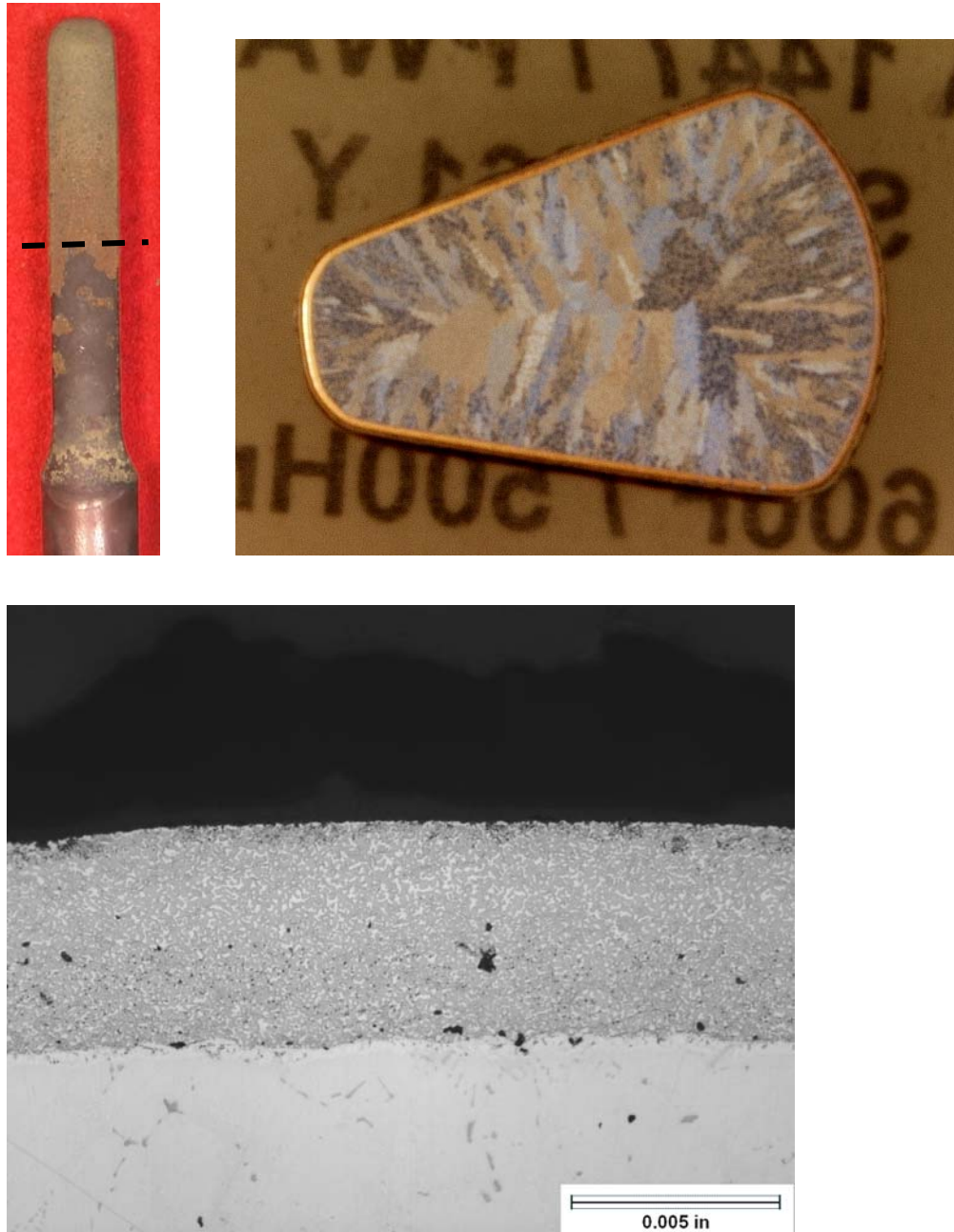


Figure 3-39. Test bar 1C (2161Y) showing the effects of the DiEGME/Jet A baseline blend on PWA 1447/PWA 286 after corrosion testing for 500 hours at 1600°F with 3.5 ppm salt.

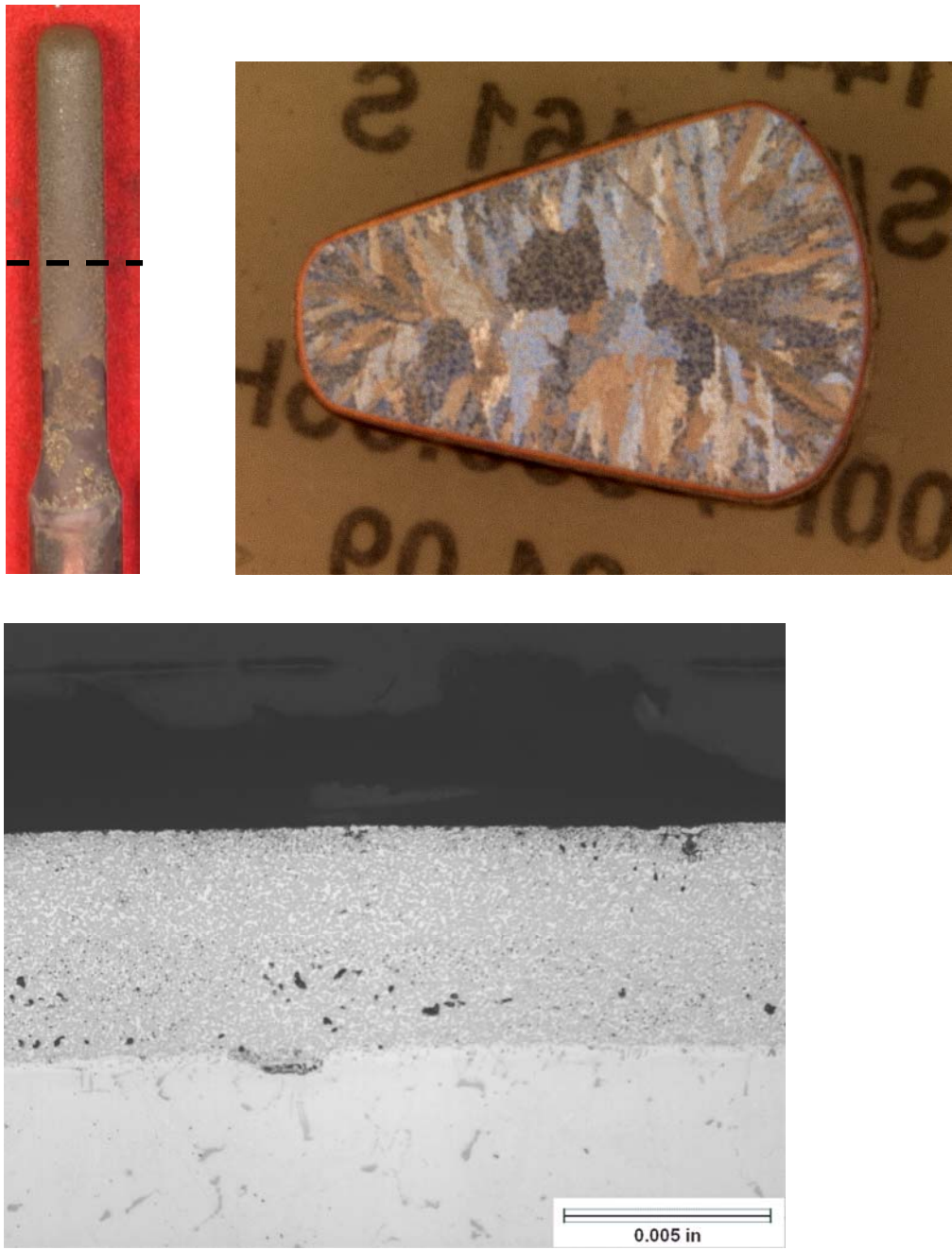


Figure 3-40. Test bar 1D (2161S) showing the effects of the TriEGME/Jet A blend on PWA 1447/PWA 286 after corrosion testing for 500.85 hours at 1600°F with 3.5 ppm salt.

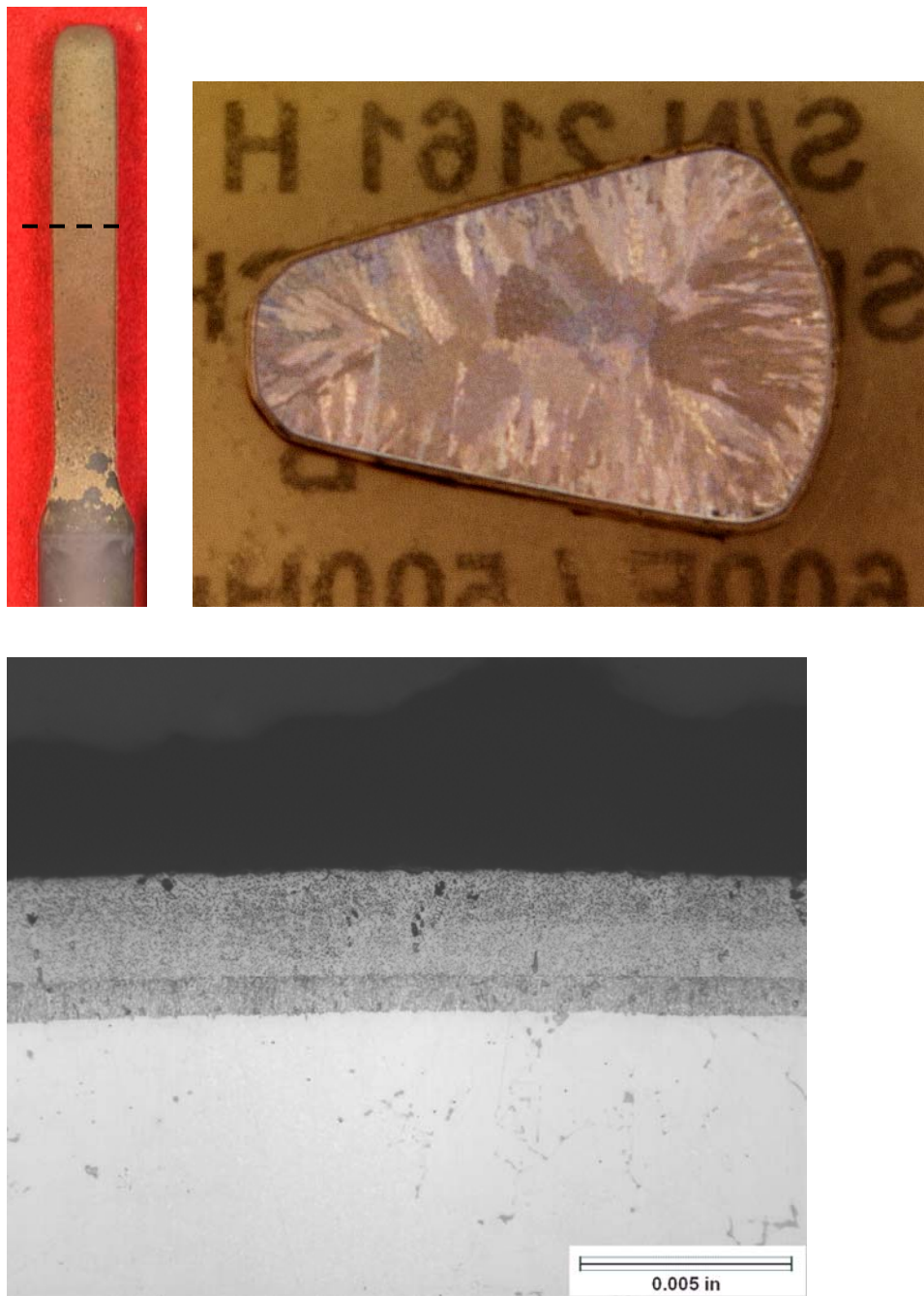


Figure 3-41. Test bar 4C (2161H) showing the effects of the DiEGME/Jet A baseline blend on PWA 1447/PWA 73 after corrosion testing for 500 hours at 1600°F with 3.5 ppm salt.

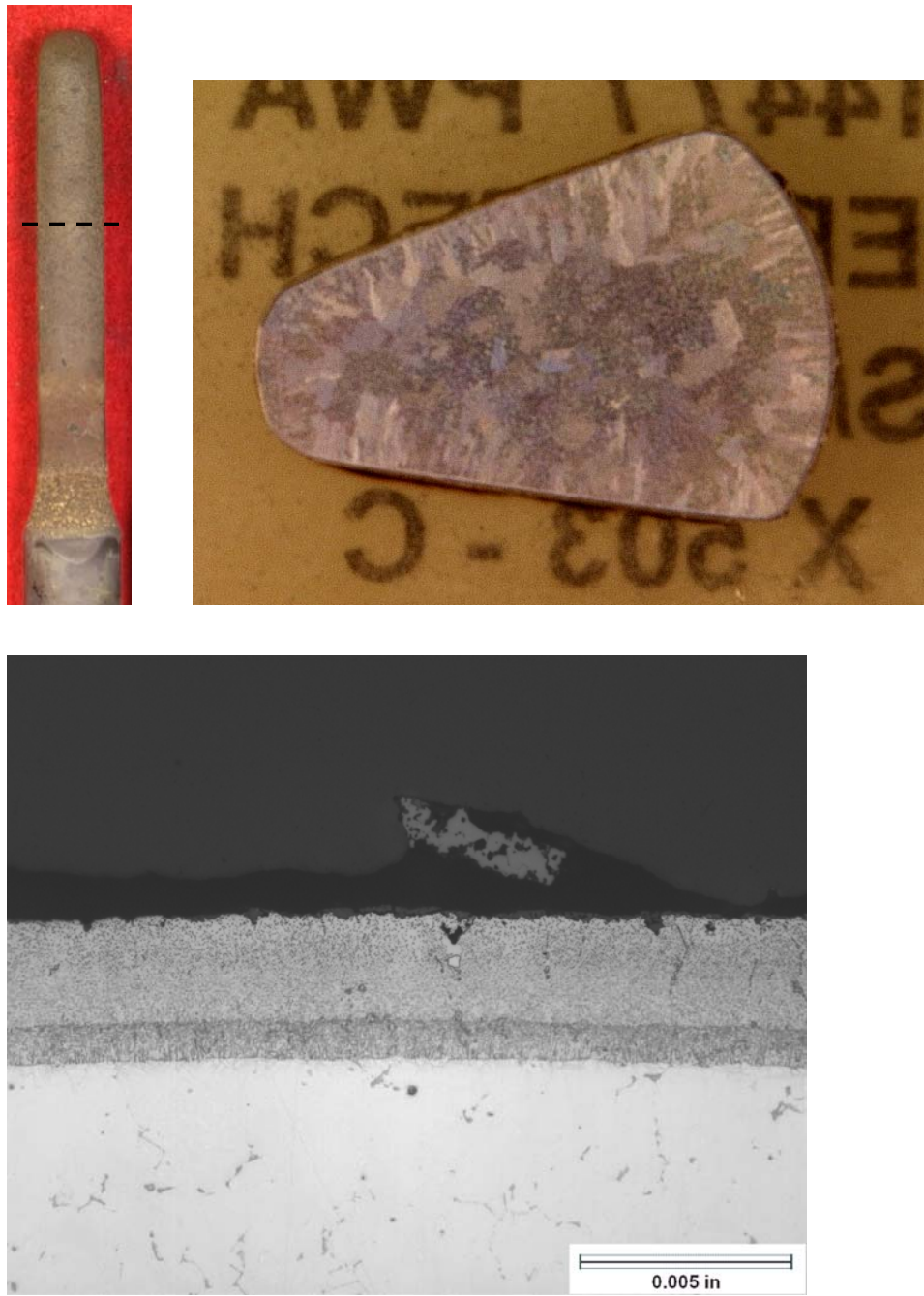


Figure 3-42. Test bar 4D (2161K) showing the effects of the TriEGME/Jet A blend on PWA 1447/PWA 73 after corrosion testing for 500.85 hours at 1600°F with 3.5 ppm salt.



Figure 3-43. Test bar 11C (2160H) showing the effects of the DiEGME/Jet A baseline blend on PWA 663/PWA 73 after corrosion testing for 500 hours at 1600°F with 3.5 ppm salt.

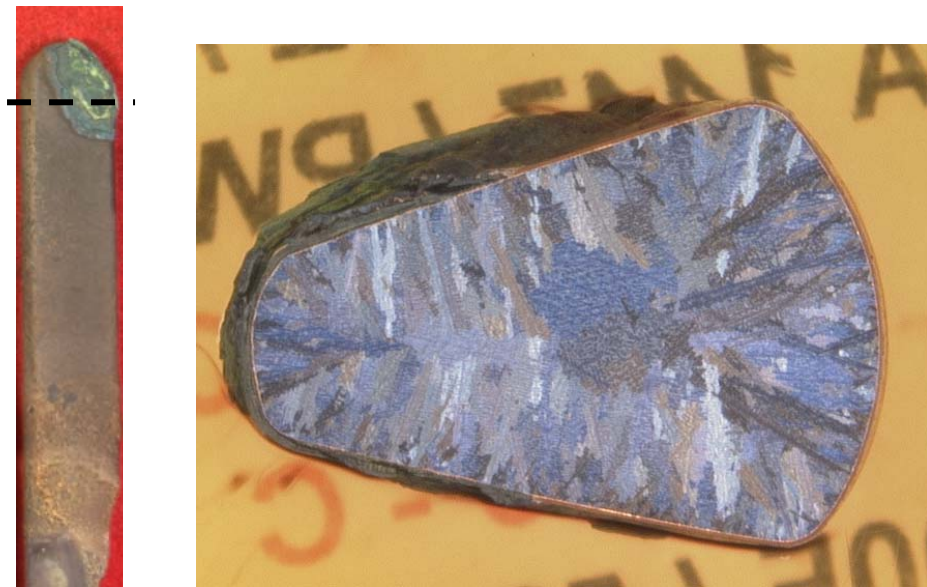


Figure 3-44. Test bar 11D (2160C) showing the effects of the TriEGME/Jet A blend on PWA 663/PWA 73 after corrosion testing for 500.85 hours at 1600°F with 3.5 ppm salt.



Figure 3-45. Test bar 6C (2158K) showing the effects of the DiEGME/Jet A baseline blend on PWA 655/PWA 73 after corrosion testing for 500 hours at 1600°F with 3.5 ppm salt.



Figure 3-46. Test bar 6D (2158J) showing the effects of the TriEGME/Jet A blend on PWA 655/PWA 73 after corrosion testing for 500.85 hours at 1600°F with 3.5 ppm salt.



Figure 3-47. Test bar 12C (2158P) showing the effects of the DiEGME/Jet A baseline blend on PWA 655/Uncoated after corrosion testing for 500 hours at 1600°F with 3.5 ppm salt.

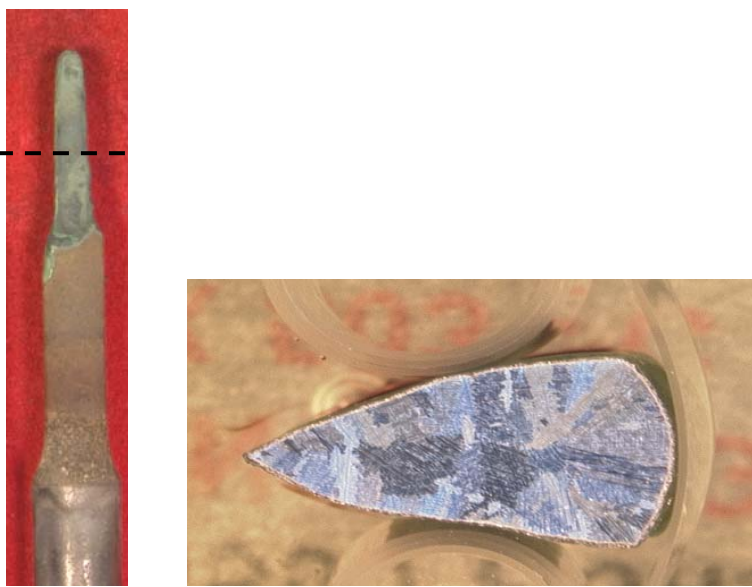


Figure 3-48. Test bar 12D (2158G) showing the effects of the TriEGME/Jet A blend on PWA 655/Uncoated after corrosion testing for 500.85 hours at 1600°F with 3.5 ppm salt.

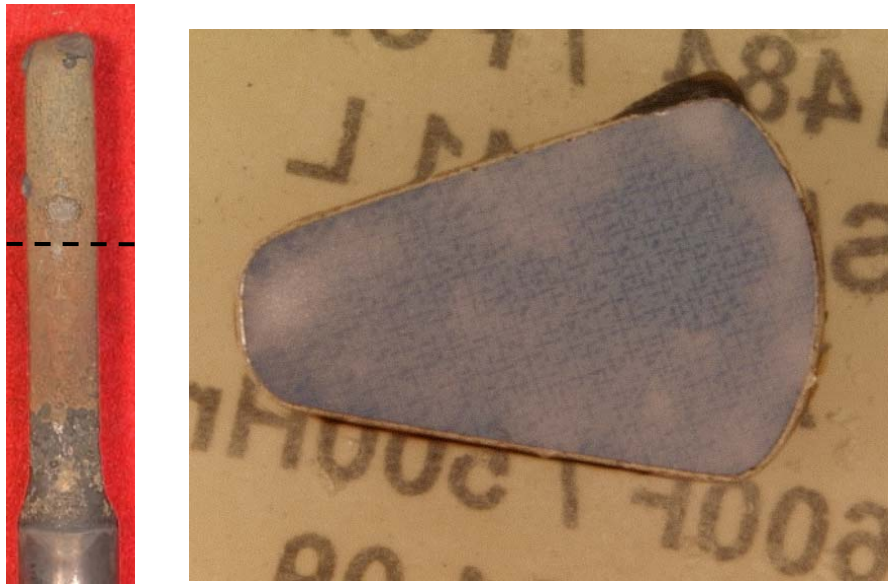


Figure 3-49. Test bar 5C (1641L) showing the effects of the DiEGME/Jet A baseline blend on PWA 1484/Uncoated after corrosion testing for 500 hours at 1600°F with 3.5 ppm salt.

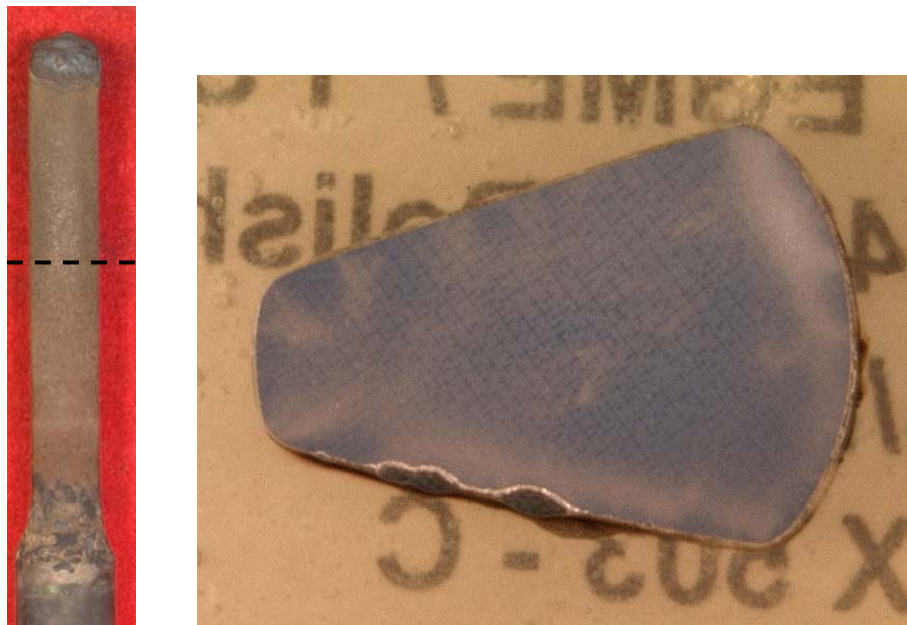


Figure 3-50. Test bar 5D (1641D) showing the effects of the TriEGME/Jet A blend on PWA 1484/Uncoated after corrosion testing for 500.85 hours at 1600°F with 3.5 ppm salt.

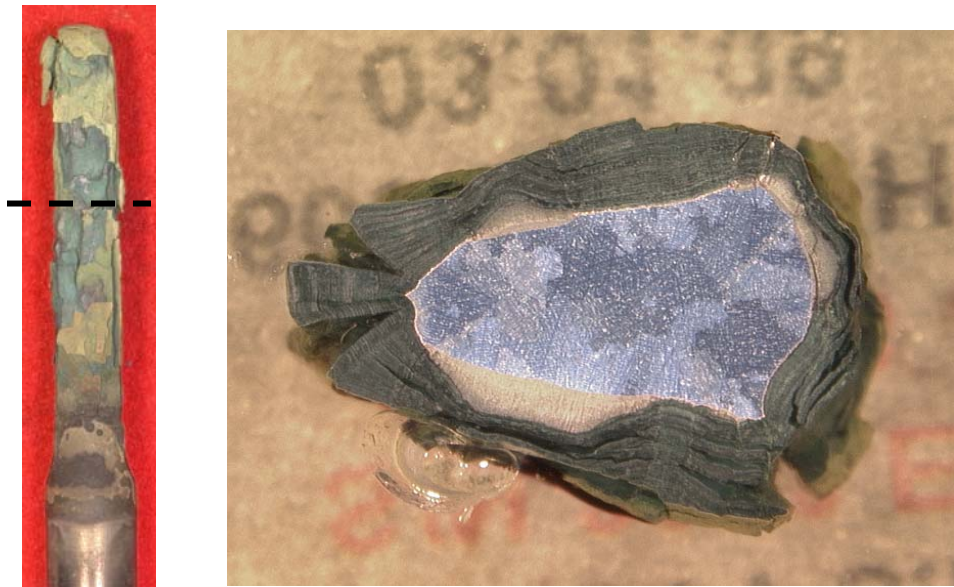


Figure 3-51. Test bar 9C (2043E) showing the effects of the DiEGME/Jet A baseline blend on PWA 1455/Uncoated after corrosion testing for 500 hours at 1600°F with 3.5 ppm salt.



Figure 3-52. Test bar 9D (2043F) showing the effects of the TriEGME/Jet A blend on PWA 1455/Uncoated after corrosion testing for 500.85 hours at 1600°F with 3.5 ppm salt.

The effects of fuel additives on hot corrosion base alloy degradation for alloy/coating systems PWA 663/PWA 73, PWA 655/PWA 73, PWA 655/Uncoated and PWA 1455/Uncoated are summarized in Table 3-6 and Figure 3-53. Dimensional changes are based on the difference between the initial alloy/coating measurement and the post test longitudinal measurement of the remaining alloy structure. The post-test alloy thickness does not take into account the green corrodant layer or the white/gray oxide layer as these layers indicate alloy defeat.

Table 3-6. Alloy dimensional change per test hour for test samples unable to be measured with calipers for the DiEGME/Jet A blended baseline (Test 3) and the TriEGME/Jet A blend (Test 4) after 500 hours of 1600°F isothermal hot corrosion burner rig test with 3.5 ppm salt.

Base Alloy Dimensional Changes in Inches per Test Hour 1600°F Isothermal Hot Corrosion Burner Rig Test with 3.5 ppm Salt			
Base Alloy	Coating	DiEGME	TriEGME
PWA 663	PWA 73	-4.27e-03	-3.67e-03
PWA 655	PWA 73	-1.04e-02	-1.81e-02
PWA 655	Uncoated	-7.08e-02	-6.70e-02
PWA 1455	Uncoated	-5.98e-02	-5.07e-02

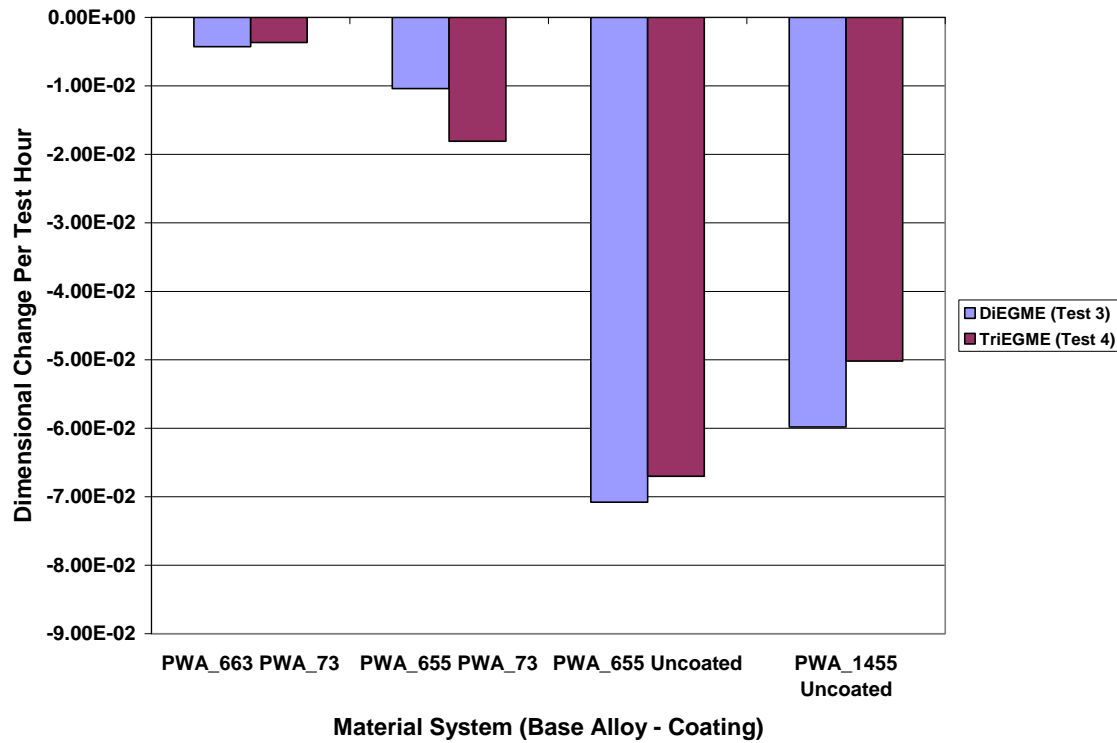


Figure 3-53. Base alloy dimensional changes per test hour for the heavily corroded alloy/coating groups that were not able to be measured with vernier calipers after 1600°F isothermal hot corrosion testing with 3.5 ppm salt for 500 hours.

The four alloy/coating groups that were unable to be measured with vernier calipers were found to have similar amounts of remaining base alloy after cross sectional microscopy was performed. Differences in remaining base alloy, between the DiEGME and TriEGME additives, were considered minor and the additives deemed similar.

3.2.6 Corrosion Conclusion

The TriEGME additive performed similar to the DiEGME additive for the majority of the test samples. The DiEGME and TriEGME additives did not perform the same for mass change of uncoated PWA 655 and uncoated PWA 1455 alloys. For these alloys, the TriEGME tested samples showed significantly greater mass loss due to spallation of the corroded alloy. The samples tested with the DiEGME additive did not show as large of a mass change due to reduced spallation of the outer surface. The TriEGME sample's weight loss might seem significant when compared to samples run with the DiEGME additive until the test samples were sectioned. The DiEGME samples did not spall however the uncoated PWA 655 and uncoated PWA 1455 samples did show large vertical cracks indicating that the base alloy was heavily corroded and the base alloy attacked. After comparing the remaining base alloy thickness measurements for the uncoated PWA 655 and uncoated PWA 1455 samples, it was concluded that there was not a difference between the DiEGME additive and TriEGME additives.

- PWA 1447 / PWA 286 – TriEGME Similar to DiEGME
- PWA 1447 / PWA 73 – TriEGME Similar to DiEGME
- PWA 663 / PWA 73 – TriEGME Similar to DiEGME
- PWA 655 / PWA 73 – TriEGME Similar to DiEGME
- PWA 655 / Uncoated - TriEGME Similar to DiEGME
- PWA 1484 / Uncoated – TriEGME Similar to DiEGME
- PWA 1455 / Uncoated- TriEGME Similar to DiEGME

4.0 Final Conclusions

Burner rig specimens tested with a TriEGME/Jet A additive blend were found to be comparable to burner rig specimens tested with a DiEGME/Jet A blended baseline. This conclusion was based on comparison of results from test specimens run in 1850°F cyclic oxidation tests and 1600°F isothermal hot corrosion tests, which included 3.5 ppm salt. Cyclic oxidation testing was performed on six different alloy/coating combinations. Hot corrosion testing was performed on seven different alloy/coating combinations. Oxidation and corrosion test samples were evaluated for mass changes, thickness changes, visual changes and remaining alloy dimensions. Minor differences were noted between the TriEGME and the DiEGME test samples thus the additives were deemed to perform similarly in the burner rig test.

Hot Gas Path Supplement.

The purpose of this supplement is to identify the alloys and coatings used for the Hot Gas Path tests performed at Pratt and Whitney.

Alloys:

- **PWA 655 – IN 713C, equiaxed alloy**
- **PWA 663 – B-1900, equiaxed alloy**
- **PWA 1447 – MAR-M-247 (similar to Rene 125), equiaxed alloy**
- **PWA 1455 – B-1900 + Hf, equiaxed alloy**
- **PWA 1484 – 2nd generation single-crystal alloy (similar to Rene N5, without the yttrium)**

Coatings:

- **PWA 73 – High aluminum activity, inward growing, pack aluminide coating**
- **PWA 275 – Low aluminum activity, outward growing, out-of-pack aluminide coating**
- **PWA 286 – NiCoCrAlY + HfSi, a low-pressure plasma spray overlay coating**

Alloy	Nominal Weight percent of constituents in alloy												
	Ni	Cr	Co	C	Ti	Al	Mo	W	B	Ta	Zr	Hf	Re
PWA 655	R*	13.5	-	0.14	0.9	6.0	4.5	-	0.01	2.1 (Cb/Ta)	0.08	-	-
PWA 663	R	8.0	10.0	0.11	1.0	6.0	6.0	-	0.015	4.3	0.07	-	-
PWA 1447	R	8.4	10.0	0.15	1.1	5.5	0.65	10.0	0.015	3.1	0.055	1.4	-
PWA 1455	R	8.0	10.0	0.11	1.0	6.0	6.0	-	0.015	4.25	0.08	1.15	-
PWA 1484	R	5.0	10.0	-	-	5.65	1.9	5.9	-	8.7	-	0.1	3.0

*R = Remainder

INTENTIONALLY LEFT BLANK

LIST OF ACRONYMS, ABBREVIATIONS, AND SYMBOLS

ACRONYM	DESCRIPTION
AFRL/RXSAC	Air Force Research Laboratory Adhesives, Composites, and Elastomers Section
AFRL/RZPF	Air Force Research Laboratory Fuels & Energy Branch
AFRL/RZTG	Air Force Research Laboratory Fuels & Energy Branch
AMS3283	Polysulfide noncuring groove sealant
AMS-C-27725	Polyurethane fuel tank coating
AMS-S-4383	Nitrile fuel tank coating
API	American Petroleum Institute
ARP	Aerospace Recommend Practice
ATCC	American Type Culture Collection
8Q462	GE JP-8+100 thermal stability additive package
BH	Bushnell-Haas solution
BMS 10-39	Topcoat material produced to Boeing Material Specification 10-39
cSt	centi-Stokes
CFU	Colony forming units
CI/LI	Corrosion inhibitor/lubricity improver
CTIO	Coatings Technology Integration Office
DoD	Department of Defense
DiEGEE	Diethylene glycol monoethyl ether
DPG	Dipropylene glycol
EDTST	Extended duration thermal stability test
EDS	Energy dispersive spectroscopy
EGME	Ethylene glycol monomethyl ether
EP	Endpoint
EPS	Extracellular polymeric substances
FSII	Fuel system icing inhibitor
FTTP	Fuel tank topcoat peeling
GC	Gas chromatography
GC-FID	Gas chromatograph-flame ionization detector
GC-MS	Gas chromatograph-mass spectrometer
GF	Glycerol formal
IP	Institute of Petroleum
JFTOT®	Jet Fuel Thermal Oxidation Test
L1120	fluorosilicone sample number
LB	Luria-Bertani agar plates
LE	Leading edge
mg/L	milligrams per liter
ml	milliter
mmHg	millimeters mercury
mol	mole
N0602	nitrile rubber sample number
OBIGGS	On-board inert gas generating system
OEM	Original equipment manufacturer
PC	Partition coefficient
ppm	part per million
pS/m	picoSiemens/meter
Pa-s	Pascal seconds

ACRONYM	DESCRIPTION
RTOC	DoD Reduction in ownership cost program
SDA	Static dissipating additive
SSIS	Small-scale icing inhibitor
TC	Topcoat
TE	Trailing edge
TNTC	Too numerous to count
TriEGEE	Triethylene glycol monoethyl ether
TriEGME	Triethylene glycol monomethyl ether
UDRI	University of Dayton Research Institute
vol%	Volume percent
V0747	Fluorocarbon sample number
v/v	volume to volume
WWT	Wetted wall temperature